ISSN 1232-5309

SOLTAN INSTITUTE FOR NUCLEAR STUDIES

INSTYTUT PROBLEMÓW JĄDROWYCH im. A. SOŁTANA

ANNUAL REPORT 1994

Otwock - Świerk

1995

PL9600346

ISSN 1232-5309

SOLTAN INSTITUTE FOR NUCLEAR STUDIES

ANNUAL REPORT

1994

Editors:

E. Infeld
M. Jaskóła
P. Żuprański

PL-05-400 OTWOCK-ŚWIERK, POLAND
Tel. 048-2-779 8948
TELEX 813244 IBJ swpl
FAX 048-2-779 3481

Otwock - Świerk
1 9 9 5

Technical Editor: Krystyna Traczyk

Technical Staff: Jolanta Falkowska
Danuta Szczepaniak

The Report was printed using a *Word Perfect 6.0* word processor on a *PC 486/40* and a *Hewlett Packard Laser Jet Series II*

A B S T R A C T :

This report surveys our activities in the following fields: nuclear, particle and cosmic ray physics, plasma and thermonuclear research and techniques, nuclear electronics, accelerator techniques and physics, as well as ionizing radiation detection and spectrometry techniques, developmental work and implementations resulting from chosen trends in nuclear physics*).

S T R E S Z C Z E N I E :

Raport roczny Instytutu Problemów Jądrowych im. A.Sołtana przedstawia zwięzły przegląd badań teoretycznych, doświadczalnych, technologicznych i technicznych z dziedziny fizyki jądrowej, promieniowania kosmicznego, fizyki cząstek elementarnych, fizyki plazmy, elektroniki jądrowej, detektorów gazowych i półprzewodnikowych, fizyki i techniki akceleratorów, fizyki osłon przed promieniowaniem i mikrodozymetrii**).

* This work was supported in part by the State Committee for Scientific Research in Poland, Decision Nr 621/E-78/S/94

** Badania były finansowane głównie przez Komitet Badań Naukowych w Polsce według Decyzji Nr 621/E-78/S/94

CONTENTS

FOREWORD

The Institute for Nuclear Studies was founded on January 1, 1983. It was previously a part of the former Institute of Nuclear Research which had been engaged in work on atomic physics since 1955. On October 10, 1987 the Institute was named the Soltan Institute for Nuclear Studies (SINS) in memory of Professor Andrzej SOŁTAN, a pioneer of nuclear science in Poland, who in 1958 (together with Leopold Infeld) also initiated plasma physics studies in Warsaw.

According to its statutes, the Institute is involved in basic research like: nuclear physics, particle and high energy physics, cosmic ray physics, plasma physics as well as developmental work and implementations resulting from chosen trends in nuclear physics, nuclear electronics, accelerator technology, radiation detection, radiation transport, instrumentation and plasma physics technology.

Many essential results have been obtained by the Institute scientific staff in fundamental research. Among them the most worthy of mention are:

- the long halflife predicted theoretically for isotopes of the elements with proton number Z=104-114 and neutron number around N = 162 by A.Sobiczewski's group of the SINS has been recently confirmed by experiments in GSI Darmstadt, GANIL Caen and JINR Dubna;
- the fundamental results important for the Standard Model obtained by a SINS group in the DELPHI experiment at CERN;
- diffractive production of vector mesons in deep inelastic scattering;
- high resolution measurements of KX-ray spectra following the collision with electron beam from the EAK-400 accelerator;
- soliton decay and interactions (in plasma physics);
- complex studies on temporal correlations of the emission of charged particles, neutrons and X-rays from PF-360 facility;

Several constructions and development projects showed considerable progress during the year:

- successful completion of the IGISOL system (Ion Guide Separator) and the first experimental results obtained at the 26 MeV proton beam of C-30 cyclotron;
- low-level neutron monitoring;
- pulse-shape discrimination for particle identification in "Silicon Balls";
- the method and results obtained in modification of the surface properties and structure of materials by using intense plasma-ion beam pulses;
- the long-time collaboration of the SINS staff with the Heavy Ion Laboratory of Warsaw University in construction, measurements of the RF accelerating system, sealing and conditioning the vacuum system. These groups succeeded in obtaining the ion beam in the U-200 cyclotron.

In our Experimental Establishment for Nuclear Equipment (ZDAJ) several construction and development projects showed considerable progress. Among them are:

- the therapeutical accelerator "Co-Line" 4 MeV was designed and constructed, the obtained X-ray beam parameters are close to Co - Unit beam parameters. The first Co-Line accelerator has been working since December 1994 in the Regional Oncological Centre in Łódź;

- the design and testing of a fully computerized system of medical accelerator parametrs control and steering;
- the design and completing of the modern air pollution monitoring mobile laboratory for controlling the content of SO_2, NO_x, CO_2, and hydrocarbons in air and in industrial flue gas with high precission.

In spite of financial difficulties, over the last years, we were able to publish about 300 scientific papers in 1994, more than half of them in international journals, and about 30% were presented at international conferences and published in conference preprints and proceedings. This is to a large extent the result of international cooperation. Our main international partners are: CERN, GSI Darmstadt, KVI Groningen, DESY Hamburg, PSI Villigen, IPN Orsay, INR Saclay, ICTP Triest, INR Kiev, KfK Karlsruhe, FA Jülich, Milan University, BNL USA, LBL USA, IPR Stuttgart, Uppsala University, INFN Frascati, JINR Dubna, the University of Durham, ISN Grenoble, ORNL, Notre Dame University USA, Warwick University, etc.

About 180 of our staff visited foreign scientific centres and universities, participated in international conferences and took part in international research programs. Also approximately 100 foreign visitors were received by the Institute and participated in several scientific meetings organized by SINS in collaboration with others Institutions. These include the Tempus Workshop and 17th Int. Conf. on Elementary Particle Physics.

In October 15-16,1994 during the "Days of open house" our Scientific Centre at Świerk was visited by about 1200 people, among them a lot of school pupils.

This report describes many of the activities which took place at SINS during the last 12 months in some detail. Credit for what was achieved during this time is due not only to SINS staff but also to our International and Polish collaborators and collegues.

The main problem of our Institute, as well as most research institutions in Poland, is insufficient recruitment of young graduates to its scientific and technical staff due to the small salaries offered. This results in a high average age and permanent reduction of the scientific staff.

Let me finally thank all contributors for their effort in presentation of results, and the "Annual Report 1994" Editional Staff for their hard and fruitful work.

Professor Wojciech Ratyński
Director

Otwock-Świerk, April 10, 1995

I. GENERAL INFORMATION

The Institute for Nuclear Studies was called into being on 1 January 1983. It was previously a part of the former Institute of Nuclear Research which had been engaged in work on atomic physics since 1955.

The Institute is subordinate to the National Atomic Energy Agency, PL-00-921 Warsaw, 36 Krucza street.

On 10 October 1987 the Institute was named the Soltan Institute for Nuclear Studies (SINS) in memory of Professor Andrzej SOLTAN, a pioneer of nuclear science in Poland.

Otwock-Świerk is the Institute's main site, but three of its departments (P-I, P-VI, P-VIII) are in Warsaw, PL-00-681 Warsaw, 69 Hoża street and one (P-VII) in the city of Łódź, PL-90-950 Łódź at 5 Uniwersytecka street.

According to its statutes, the Institute is involved in scientific research as well as developmental work and implementations resulting from chosen trends in nuclear physics, nuclear electronics, accelerator technology as well as ionizing radiation detection and spectrometry techniques.

II. MANAGEMENT OF THE INSTITUTE

Director	**Professor Wojciech RATYŃSKI**
Deputy Director, Scientific Research	Professor Marian JASKÓŁA
Deputy Director, Research and Development	Asst. Professor Zbigniew JANKOWICZ
Deputy Director, Administration and Economics	M.A. Marek JUSZCZYK
Accountant General	M.A. Helena DUDZIN
Institute Publications	Professor Eryk INFELD

The Scientific Council was elected on the 21st of May 1991 by the scientific, technical and administrative staff of the Institute. The Council has the right to confer PhD and DSc degrees in physics.

Chairman of the Scientific Council -	**Professor Jan ŻYLICZ**
Deputy Chairmen:	Assoc.Professor Michał NADACHOWSKI
	Professor Ryszard SOSNOWSKI
	Professor Sławomir WYCECH

The Institute is divided into the following departments and divisions:

- DEPARTMENT OF NUCLEAR REACTIONS (P-I)
  Head of Department - Professor Andrzej MARCINKOWSKI tel. fax 621-38-29

- DEPARTMENT OF NUCLEAR SPECTROSCOPY (P-II)
  Head of Department - Assoc.Professor Rościsław KACZAROWSKI tel. 779-86-18

- DEPARTMENT OF NUCLEAR ELECTRONICS (P-III)
  Head of Department - Assoc.Professor Michał NADACHOWSKI tel. 779-83-60

- DEPARTMENT OF RADIATION SHIELDING PHYS. AND DOSIMETRY (P-IV)
  Head of Department - Asst.Professor Stanisław PSZONA tel. 779-84-81

- DEPARTMENT OF THERMONUCLEAR RESEARCH (P-V)
  Head of Department - Professor Marek SADOWSKI tel. 779-86-78

- DEPARTMENT OF HIGH ENERGY PHYSICS (P-VI)
  Head of Department - Assoc.Professor Joanna STEPANIAK tel. 621-28-04
  fax 621-38-29

- DEPARTMENT OF COSMIC RADIATION PHYSICS (P-VII)
  Head od Department - Assoc.Professor Jerzy GAWIN tel.(0-42) 78-64-31

- DEPARTMENT OF ATOMIC NUCLEUS THEORY (P-VIII)
  Head of Department - Professor Sławomir WYCECH tel. 621-60-85
  fax 621-38-29

- DEPARTMENT OF RADIATION DETECTORS (P-IX)
  Head of Department - Assoc.Professor Jerzy PIEKOSZEWSKI tel. 779-86-43

- DEPARTMENT OF ACCELERATOR PHYSICS AND TECHNOLOGY (P-X)
  Head of Department - Asst.Professor Marian PACHAN tel. 779-86-33

- SECTION FOR STANDARDS AND QUALITY OF NUCLEAR APPARATUS
  Head of Section - Assoc.Professor Roman TRECHCIŃSKI tel. 779-98-52

- SERVICES AND TRANSPORT DIVISION (ZOIT)
  Director, Civ.Eng.Jerzy BABIK tel.779-82-03, Fax:0-028-2-779-82-44

- EXPERIMENTAL ESTABLISHMENT FOR NUCLEAR EQUIPMENT (ZDAJ)
  Director, MSc Jacek PRACZ tel.79-87-22, Fax:0-048-2-779-87-23

III. LIST OF PROFESSORS, ASSOCIATE PROFESSORS, ASSISTANT PROFESSORS AND SCIENTIFIC COUNCIL OF THE SOLTAN INSTITUTE FOR NUCLEAR STUDIES

a. PROFESSORS

1. DĄBROWSKI Janusz	Theoretical Nuclear Physics
2. INFELD Eryk	Plasma Physics and Nonlinear Dynamics
3. JASKÓŁA Marian	Nuclear Physics
4. ŁUKASZUK Leszek	Particle Physics
5. MARCINKOWSKI Andrzej	Nuclear Physics
6. MOSZYŃSKI Marek	Nuclear Electronics, Technical Physics
7. NASSALSKI Jan	Particle Physics
8. PIEKOSZEWSKI Jerzy	Solid State Physics
9. RATYŃSKI Wojciech	Nuclear Physics
10. RĄCZKA Ryszard	Theory of Field and Particle Physics
11. SADOWSKI Marek	Plasma Physics
12. SIEMIARCZUK Teodor	Particle Physics
13. SOBICZEWSKI Adam	Nuclear Theory
14. SOSNOWSKI Ryszard	Particle Physics, Member of the Polish Academy of Sciences
15. SUJKOWSKI Ziemowid	Nuclear Physics
16. SZEPTYCKA Maria	Particle Physics
17. TURKIEWICZ Jan	Nuclear Physics
18. TUROS Andrzej	Nuclear Solid State Physics
19. WDOWCZYK Jerzy (**)	Cosmic Ray Physics
20. WILCZYŃSKI Janusz	Nuclear Physics
21. WYCECH Sławomir	Nuclear and Particle Physics

b. ASSOCIATE PROFESSORS

1. DELOFF Andrzej	Particle Physics
2. FIRKOWSKI Ryszard (**)	Cosmic Ray Physics
3. GAWIN Jerzy	Cosmic Ray Physics
4. GRYZIŃSKI Michał	Plasma Physics and Atomic Physics
5. GUZIK Zbigniew	Nuclear Electronics
6. KACZAROWSKI Rościsław	Nuclear Physics
7. KAZIMIERSKI Adam (**)	Electron Technology
8. KIEŁSZNIA Robert (**)	Accelerator Techniques and Physics
9. KULIŃSKI Stanisław	Accelerator Techniques and Physics
10. MOROZ Zbigniew	Nuclear Physics
11. MRÓWCZYŃSKI Stanisław	Particle Physics
12. NADACHOWSKI Michał	Nuclear Electronics
13. PIOTROWSKI Antoni	Technical Physics
14. SŁAPA Mieczysław	Solid State Physics
15. SOWIŃSKI Mieczysław (**)	Nuclear Physics
16. STEPANIAK Joanna	Nuclear and Particle Physics
17. SURA Józef (*)	Accelerator Techniques and Physics
18. SZCZEKOWSKI Marek	Particle Physics
19. TRECHCIŃSKI Roman (**)	Nuclear Electronics
20. WERNER Zbigniew	Solid State Physics
21. WILK Grzegorz	Particle Physics
22. WÓJTOWICZ Stefan	Nuclear Electronics
23. WRZECIONKO Jerzy	Nuclear Theory
24. ZWIĘGLIŃSKI Bogusław	Nuclear Physics
25. ŻUPRAŃSKI Paweł	Nuclear Physics

c. ASSISTANT PROFESSORS

1. ADAMUS Marek PhD
2. APPELT Jacek (**) PhD
3. AUGUSTYNIAK Witold PhD
4. BIAŁKOWSKA Helena PhD
5. BIAŁKOWSKI Jacek (*) PhD
6. BIELIK Mirosław PhD
7. BIEŃKOWSKI Andrzej(*) PhD
8. BŁOCKI Jan PhD DSc
9. BOGDANOWICZ Jerzy (*) PhD
10. BOUŻYK Jacek PhD
11. BUDA Antoni (*) PhD
12. BURZYŃSKI Stanisław PhD
13. CZARNACKI Wiesław PhD
14. CHMIELEWSKA Danuta PhD
15. CZYŻEWSKI Tomasz PhD
16. DUDA-GŁOWACKA L. PhD.
17. DYGO Andrzej (*) PhD
18. FILIPKOWSKI Andrzej PhD
19. GOKIELI Ryszard PhD
20. GOLDSTEIN Piotr PhD
21. GÓRSKI Maciej PhD
22. HAHN Grzegorz PhD
23. ISKRA Włodzimierz PhD
24. JAKUBOWSKI Lech PhD
25. JANKOWICZ Zbigniew PhD
26. KORMAN Andrzej PhD
27. KOZŁOWSKI Tadeusz PhD
28. KUCIŃSKI Jacek PhD
29. KULKA Zbigniew PhD
30. KUPCZAK Radomir PhD
31. LANGNER Jerzy PhD
32. MARIAŃSKI Bogdan PhD
33. MYSŁEK-LAURIKAINEN B. PhD
34. PATYK Zygmunt PhD
35. PAWŁOWICZ Wiesław PhD
36. PIECHOCKI Włodzimierz PhD
37. PŁAWSKI Eugeniusz PhD
38. POCHRYBNIAK Cezary PhD
39. POLAŃSKI Aleksander PhD
40. PREIBISZ Zygmunt PhD
41. PSZONA Stanisław PhD
42. RABIŃSKI Marek PhD
43. RONDIO Ewa PhD
44. RONDIO Janusz PhD DSc
45. ROŻYNEK Jacek PhD
46. RURARZ Edward PhD
47. RUSEK Krzysztof PhD
48. RYMUZA Piotr PhD
49. RZYMKOWSKI Krzysztof (*) PhD
50. SANDACZ Andrzej PhD
51. SENATORSKI Andrzej PhD
52. SERNICKI Jan PhD
53. SKALSKI Janusz PhD
54. SKŁADNIK-SADOWSKA E. PhD
55. SKORUPSKI Andrzej PhD
56. SZABELSKA Barbara PhD
57. SZABELSKI Jacek PhD
58. SZYDŁOWSKI Adam PhD
59. SZYMANOWSKI Lech PhD
60. SZYMAŃSKI Piotr PhD
61. SZYMCZYK Władysław PhD
62. TRZCIŃSKI Andrzej PhD
63. TUCHOLSKI Andrzej PhD
64. WIŚLICKI Wojciech PhD
65. WOJTKOWSKA Jolanta PhD
66. WOLSKI Włodzimierz PhD
67. ZABIEROWSKI Janusz PhD
68. ZYCHOR Izabella PhD

(*) on leave of absence
(**) part-time employee

d. SCIENTIFIC COUNCIL OF SINS

	Name and degree	Discipline	Institution
A	**Scientists**		
1	J.Appelt, PhD	plasma physics	Institute for Nuclear Studies
2	H.Białkowska, PhD	particle physics	Institute for Nuclear Studies
3	A.Budzanowski, PhD., DSc., Professor Member of the Polish Academy of Sciences	nuclear physics	Institute of Nuclear Physics, Kraków
4	S.Gębalski, MSc	plasma physics	Institute for Nuclear Studies
5	A.Hilger, MSc	accelerator techniques	Institute for Nuclear Studies
6	A.Hrynkiewicz, PhD., DSc.,Professor Member of the Polish Academy of Sciences	nuclear physics	Institute of Nuclear Physics, Kraków
7	M.Jaskóła, PhD., DSc., Professor	nuclear physics	Institute for Nuclear Studies
8	Z.Komor, MSc	nuclear electronics	Institute for Nuclear Studies
9	J.Kownacki, PhD., DSc., Professor	nuclear physics	Institute of Experimental Physics Warsaw University
10	T.Kozłowski, PhD	nuclear physics	Institute for Nuclear Studies
11	[illegible]ólikowski, PhD., DSc., Professor Member of the Polish Academy of Sciences	particle physics	Institute of Theoretical Physics Warsaw University
12	S.[illegible]ski, PhD., DSc., Assoc.Professor	accelerator technique and physics	Institute for Nuclear Studies
13	L.Łukas[illegible]k, PhD., DSc., Professor	particle physics	Institute for Nuclear Studies
14	A.Marcinkowski, PhD., DSc., Professor	nuclear physics	Institute for Nuclear Studies
15	M.Moszyński, PhD., DSc., Professor	nuclear electronics technical physics	Institute for Nuclear Studies
16	M.Nadachowski, PhD., Assoc.Professor	nuclear electronics	Institute for Nuclear Studies
17	J.Piekoszewski, PhD., DSc., Assoc.Professor	solid state physics	Institute for Nuclear Studies
18	J.Pracz, MSc	accelerator technique	Institute for Nuclear Studies
19	W.Ratyński, PhD., DSc., Professor	nuclear physics	Institute for Nuclear Studies
20	M.Sadowski, PhD., DSc., Professor	plasma physics	Institute for Nuclear Studies
21	E.Skrzypczak, PhD., DSc., Professor	particle physics medical physics	Institute of Experimental Physics Warsaw University
22	A.Sobiczewski, PhD., DSc., Professor	nuclear physics	Institute for Nuclear Studies
23	R.Sosnowski, PhD., DSc., Professor Member of the Polish Academy of Sciences	particle physics	Institute for Nuclear Studies
24	Z.Sujkowski, Phd., DSc., Professor	nuclear physics	Institute for Nuclear Studies
25	M.Szeptycka, Phd., DSc., Professor	particle physics	Institute for Nuclear Studies
26	J.Tołwiński, PhD., DSc., Professor	medical physics	Institute of Oncology, Warsaw
27	A.Turos, PhD., DSc., Professor	nuclear/solid state physics	Institute for Nuclear Studies
28	J.Wdowczyk, PhD., DSc., Professor	cosmic ray physics	Institute for Nuclear Studies
29	Z.Wilhelmi, PhD., DSc., Professor	nuclear physics	Institute of Experimental Physics Warsaw University
30	G.Wilk, Phd., DSc	particle physics	Institute for Nuclear Studies
31	S.Wycech, PhD., DSc., Professor	nuclear and particle physics	Institute for Nuclear Studies
32	J.Żylicz, PhD., DSc., Professor	nuclear physics	Institute of Experimental Physics Warsaw University
B	**Technical and Administrative Staff Representatives**		
1	E.Fronczak, technician	mechanical engineering	Institute for Nuclear Studies
2	B.Gas, Eng.	mechanical engineering	Institute for Nuclear Studies
3	E.Jankowski, MSc Eng	electrical technology	Institute for Nuclear Studies
4	D.Jastrzębska, M.A.	book-keeping	Institute for Nuclear Studies
5	J.Kopeć, MSc Eng.	physical metallurgy	Institute for Nuclear Studies
6	J.Kuczyński, MSc Eng.	electrical engineering	Institute for Nuclear Studies
7	J.Mozdrzewska, M.A.	R & D planning	Institute for Nuclear Studies
8	E.Świątek, MSc	book-keeping	Institute for Nuclear Studies

IV. INTRODUCTION

This is the 7th Annual Report of our Institute. Areas covered include basic and applied research in: nuclear physics, particle and cosmic ray physics, plasma and thermonuclear research and techniques, nuclear electronics, accelerator techniques and physics, ionization radiation detection and spectrometry, and radiation shielding. These activities, supported by the Polish State Committee for Scientific Research, are carried out in the context of the following research and development programs:

A. Nuclear Physics and Applications: theory, experiment, instrumentation, applied nuclear physics and interdisciplinary activities

B. Particle and High Energy Physics, Cosmic Ray Physics

C. Accelerators: electron accelerators, proton and ion accelerators

D. Electronics and Detectors: nuclear electronics, semiconductor detectors, gaseous ionization detectors

E. Plasma Physics: theory and computational physics, experiment, instrumentation and technology.

Some departments of our Institute also participate in other research and developmental programs and contracts. The studies mentioned in the Annual Report are carried out within collaborations with other Polish and foreign institutes.

This Annual Report describes the most important results achieved in 1994, and also includes the important references, either as footnotes or in § VIa (the list in § VIa covers papers published in 1994).

V. PROGRESS REPORT BY DISCIPLINE

A. NUCLEAR PHYSICS AND APPLICATIONS

1. THEORY

1.1 Theory of Σ Hypernuclei
by J.Dąbrowski and J.Rożynek

Work on the single particle description of Σ hypernuclear states was continued. The cross section for the (K^-, π^+) reaction on the ^{16}O target calculated with a macroscopically estimated Σ optical potential agrees reasonably with the existing experimental data. [1-4]

[1] J.Dąbrowski, Acta Physica Polonica B25(1994)
[2] J.Dąbrowski, J.Rożynek, Phys. Lett. B323(1994)99-102
[3] J.Dąbrowski, J.Rożynek, Nucl. Phys., (in press)
[4] J.Dąbrowski, J.Rożynek, Izv.V.U.Z.Fizika, (in press)

1.2 The EMC effect in the relativistic mean field theory
by J.Rożynek

The role of the polarization process in the nucleon structure function in the medium is presented. The inclusion of the high momentum component of the distribution function is very important.

[1] J.Rożynek, Many Body Physics, World Scientific 1994

1.3 The QCD Based Hadronic Effective Lagrangians.
by J.Wrzecionko

The role of the multiple quark current contributions (generated by the self interaction of gluons) in the construction of the hadronic effective lagrangians is discussed. The corresponding multilocal effective fields built from quarks have been introduced. Using these fields a method to express the QCD effective action in terms of the hadronic effective fields has been developed. Applying the method of Functional Integration Calculus, one can select the effective lagrangians which involve both the mesonic and barionic parts and also the term which describes the interaction of mesons with barions. The parameters entering these lagrangian (the hadron masses and the coupling constants) are expressed by exact gluon propagators and by the vertices which characterize the self-interaction of gluons. These vertices have to be treated as a phenomenological input. [1]

[1] J.Wrzecionko, submitted to Int.J. of Mod. Phys. A

1.4 Properties of Radioactive Nuclei
by Z.Patyk, J.Skalski, R.Smolańczuk and A.Sobiczewski

Spontaneous-fission half-lives of heaviest nuclei have been analyzed in a multidimensional deformation space. They have been calculated in a dynamical approach, without any adjustable parameters. The potential energy has been obtained by the macroscopic-microscopic method and the inertia tensor by the cranking method. The action integral has been minimized by a variational procedure. Even-even nuclei with proton number Z=104-114 and neutron number N=142-176 have been considered. Alpha-decay half-lives have been also analyzed.

The results reproduce rather well the existing experimental data for the nuclei considered and predict relatively long half-lives for many nuclei not yet observed, sufficient to detect them if synthesized in a laboratory [1-5].

Masses of cesium and barium isotopes have been calculated in the macroscopic-microscopic approach. The calculations have been performed in close contact with the experimental group which measures these masses with the use of the electromagnetic Penning trap installed at ISOLDE-2 at CERN [6].

Extensive calculations of masses of spherical nuclei have been performed in the Hartree-Fock-Bogolubov approach, using various variants of the Skyrme force. The objective was to see how well experimental masses can be reproduced in this theoretical approach [7].

[1] R.Smolańczuk, J.Skalski, A.Sobiczewski, Proc. Int. Symp. on Nucl. Physics II, Tours (France) 1994, (in press)
[2] A.Sobiczewski, R.Smolańczuk, J.Skalski, Proc. Int. Conf. "Actinides-93", Santa Fe (USA) 1993, J.Alloys & Compounds 213/214 (1994)38
[3] R.Smolańczuk, J.Skalski, A.Sobiczewski, preprint GSI-94-77, submitted to Phys. Rev. C
[4] P.Rozmej, R.Smolańczuk, A.Sobiczewski, Proc. 4th Int.KINR School on Nuclear Physics, Kiev (Ukraine) 1994, (in press)
[5] R.Smolańczuk, J.Skalski, A.Sobiczewski, GSI Scientific Report 1994, (in press)
[6] H.Stolzenberg, G.Bollen, H.J.Kluge, T.Otto, G.Savard, L.Shweikhard, R.B.Moore, G.Rouleau, J.Szerypo, Z.Patyk, Nucl. Phys. A, (in press)
[7] Z.Patyk, J.Dobaczewski, R.Smolańczuk, A.Sobiczewski, GSI Scientific Report 1994, (in press)

1.5 Octupole Excitations in Light Xenon and Barium Nuclei

by J.Skalski, P.H.Heenen, P.Bonche and H.Flocard

The properties of light even and odd Xe and Ba isotopes (N and Z close to 56) with respect to octupole deformation have been studied by the Hartree-Fock+BCS and the generator coordinate (GCM) methods [1]. Although we do not find a stable static octupole deformation in the considered nuclei the octupole collectivity determined within the GCM is clearly enhanced, with sizable B(E3) values. Additional cranked shell model calculations indicate that octupole effects should persist at least up to spins around 10$\hbar$.

Calculated E1 transition rates are small but should be measurable. Recent experimental results on ^{114}Xe reported in [2] roughly agree with our calculations.

[1] P.-H.Heenen, J.Skalski, P.Bonche and H.Flocard, Phys. Rev. C50 (1994) 802
[2] S.L.Rugari et al., Phys. Rev. C49 (1993) 2078

1.6 Radial Pattern of Nuclear Decay Processes

by W.Iskra, M.Müller[1], I.Rotter[1]

At high level density of nuclear states, a separation of different time scales is observed (trapping effect). In the complex plane of the resonance widths versus energies a cloud of short lived (trapped) states is formed in the strong coupling regime together with a few long lived (broad) resonances.

We calculate [1] the radial profile of partial widths in the framework of the continuum shell model for some 1^- resonances with 2p-2h nuclear structure in ^{16}O as a function of the coupling strength to the continuum of decay (single nucleon) channels.

A strong correlation between the lifetime of a nuclear state and the radial profile of the corresponding decay amplitude is observed. In the short-time scale, most nucleons are emitted from the regions of small radii. The nucleons emitted from the surface region of the nucleus appear mainly in the long-time scale. The short-lived states form the structures in space and time. This result supports the recently proposed analogy [2] between nuclear trapping effect and selforganization.

[1] W.Iskra, M.Müller and I.Rotter, Preprint FZR-39 (Rossendorf, 1994)
[2] W.Iskra, M.Müller and I.Rotter, J.Phys. G19(1993)2045; G20(1994)775

1.7 Excitation of a Quantal and a Classical Gas in a Time-Dependent Potential

by J.Błocki, F.Brut[1], J.Skalski, and W.J.Świątecki[2]

We report on computer simulations of oscillating Woods-Saxon or cavity potentials filled with either a classical or quantal gas of independent particles. We have now available of the order of 600 excitation histories of such gases undergoing usually one period of oscillation (but sometimes several), classified according to frequency and multipolarity of the oscillation and of the degree of diffuseness of the potential. We are still in the process of displaying and interpreting some of the results, but certain important features are already apparent. A notable finding is that, contrary to concerns sometimes voiced in the literature, the classical wall formula [1] does not fail catastrophically when confronted with quantal calculations. This is true even for relatively small systems-in our case 112 neutrons in doubly degenerate eigenstates. On the contrary, the wall formula, in addition to reproducing accurately the classical computer simulations, gives also an approximate account of the quantal results in the regime where it in expected to be valid, namely for not too small oscillation frequencies and too large surface diffuseness. In those cases it is gratifying to observe that the deviations from the wall formula actually correlate (semi-quantitative) with the wave-mechanical corrections derived by Koonin et al. [2].

[1] J.Błocki, et al. Ann. Phys. 113(1978)330
[2] S.E.Koonin, et al. Phys. A283(19977)87

1) Institut des Sciencies Nucleaires, 38026 Grenoble-Cedex, France
2) Nuclear Science Division, Lawrence Berkeley Laboratory, University of California, Berekely, CA 94720

2. EXPERIMENT

2.1 Cluster-Folding Study of Polarized ^{7}Li Scattering from ^{208}Pb

by K.Rusek, J.Gomez-Camacho[1], I.Martel-Bravo[1] and G.Tungate[2]

A recent optical model study of ^{7}Li+^{208}Pb scattering at an energy range from 27 to 60 MeV revealed [1] that the real diagonal potential must be renormalized at energies around the Coulomb barrier in order to achieve a good description of the experimental data. This work is devoted to study the origin of this renormalization by taking into account projectile excitations to ^{7}Li resonant and non-resonant excited states.

The experimental data for polarized ^{7}Li elastic scattering from ^{208}Pb at 33 MeV were analysed by coupled-channel calculations. The diagonal and off-diagonal potentials used in the analysis were derived from empirical α+^{208}Pb [2] and t+^{208}Pb [3] optical model potentials by means of the cluster-folding method. The projectile was assumed to have ^{7}Li=α+t cluster structure. The ground and the 1st excited states of ^{7}Li were assumed to be pure 2P states with radial wave functions calculated in a potential well having a Woods-Saxon shape and the geometry parameters chosen so as to reproduce an experimental value of the reduced transition probability B(E2;$3/2^- \rightarrow 1/2^-$). The depths of the binding potentials were varied in order to reproduce the binding energies for these states. The resonant $7/2^-$ and $5/2^-$ states at excitation energies of 4.63 MeV and 6.68 MeV, respectively, were assumed to be pure 1F states.

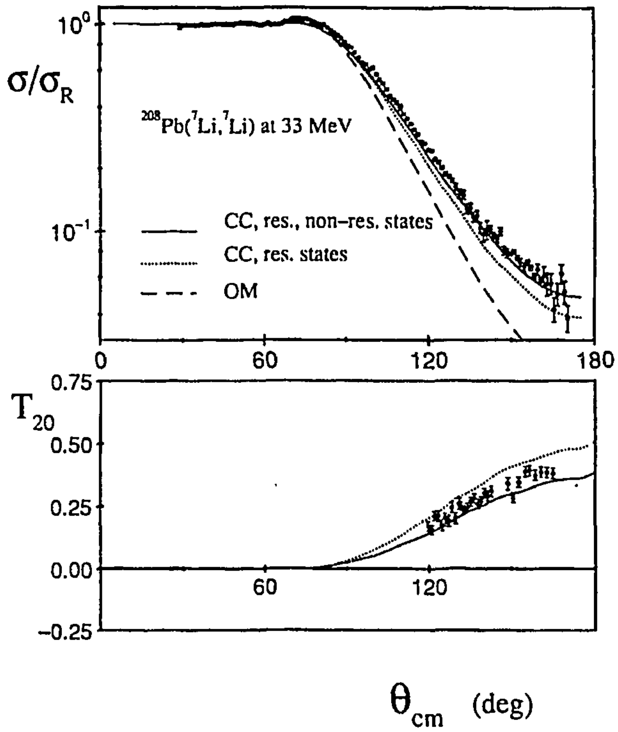

Fig.1. Results of the cluster-folding analysis. Experimental data from [1,5]

The α+t continuum above the ^{7}Li break-up threshold was discretized in line with [4] into a set of momentum bins with respect to the momentum $\hbar k$ of the α-t relative motion. The model momentum space was limited to the range $0.25 \leq k \leq 0.75$ fm^{-1} and the width of each bin was set to 0.25 fm^{-1}. The relative angular momentum of the α+t cluster system was limited to the values L=1,3.

The results of the calculations are shown in the figure. Calculations with the diagonal potential only (dashed curve) underestimate the experimental values of the differential cross section. Including ^{7}Li excitations to its bound 1st excited state and the two resonant excited states (dotted curves) one obtains an improvement for the description of the differential cross section and a substantial effect for the 2nd rank tensor analysing power T_{20}. Additional inclusion of ^{7}Li excitations to its non-resonant excited states (solid curves) yields further improvement for the description of the differential cross section and affects considerably the results for the 2nd rank tensor analysing power.

The present analysis shows that the ^{7}Li+^{208}Pb elastic scattering in the vicinity of the Coulomb barrier is strongly affected by projectile excitation effects. It also suggests that these effects are mainly responsible for the renormalization of the diagonal potential found previously in the optical model study [1].

[1] N.Keeley et al, Nucl. Phys. A 571 (1994) 326
[2] G.M.Hudson et al, Phys. Rev. C9 (1974) 1521
[3] F.D.Becchetti and G.W.Greenlees, Proc. of the 3rd Int. Symp., Madison 1970, ed. H.H.Barschall and W.Haeberli
[4] Y.Sakuragi et al, Nucl.Phys. A 480 (1988) 361
[5] I.Martel-Bravo et al, to be published

[1] Departamento de Fisica Atomica, Universidad de Sevilla, Spain
[2] School of Physics and Space Research, The University of Birmingham, UK

2.2 Gradual Absorption of Fast Neutrons in Niobium

by A.Marcinkowski and D.Kielan

Single- and double-differential neutron-scattering cross sections for niobium, at bombarding neutron energies of 7, 14, 20 and 26 MeV, have been consistently explained by statistical direct reactions accompanied by gradual absorption of neutrons into successive 2p1h, 3p2h, 4p3h etc. quasibound states, which evolve towards the compound nucleus [1].

It has been shown that in presence of collective isoscalar excitations direct processes prevail over preequilibrium compound reactions even at incident energies as low as 7 MeV. The contribution of direct reactions increases with bombarding energy from about 7% of the optical model absorption cross section at 14 MeV incident energy to 41% at 26 MeV. On the other hand, the multistep compound emission remains stagnant at a level of about 4-5%. This means that the old-fashioned division of nuclear-reaction mechanisms into the direct reactions and the compound nucleus reactions was not far from the present results. The latter however is not necessarily valid in charge exchange reactions, where collective excitations are weak [2,3].

[1] A. Marcinkowski, D. Kielan, Nucl. Phys. A 578 (1994) 168
[2] D. Kielan, A. Marcinkowski, Acta Phys. Pol. B 25 (1994) 1219
[3] A. Marcinkowski, in Proc. Int. Conf. on Nuclear Data for Science and Technology, Gatlinburg, Tennessee, May 9-13 1994, ed. by K. Dickens (published by the American Nuclear Society, 1994, p.45).

2.3 Deuteron Spectra from $^{27}Al(n,d)^{26}Mg$ Reaction

by A.Stonert, A.Korman, B.Mariański, J.Rondio

Deuteron spectra from reaction $^{27}Al(n,d)^{26}Mg$ at an incident neutron energy of 18.5 MeV were measured simultaneously with proton spectra. Measurements were performed with eight-telescope chamber [1]. Neutrons were produced in the $^{3}T(d,n)^{4}He$ reaction, the deuterons being accelerated to 2.3 MeV in the Van de Graaff accelerator. A self supporting aluminium foil (23 $\mu g/cm^2$) was used as a target. Deuteron spectra for 8 angles between 0° and 70° were measured. A deuteron spectrum obtained at 10° is shown in Fig. 1. Marked peaks correspond to transitions to the ground state and excited states at energies 1.8, 2.9 and 4.3 MeV. These transitions were observed recently in the same reaction at higher neutron energy of 22 MeV [2] .

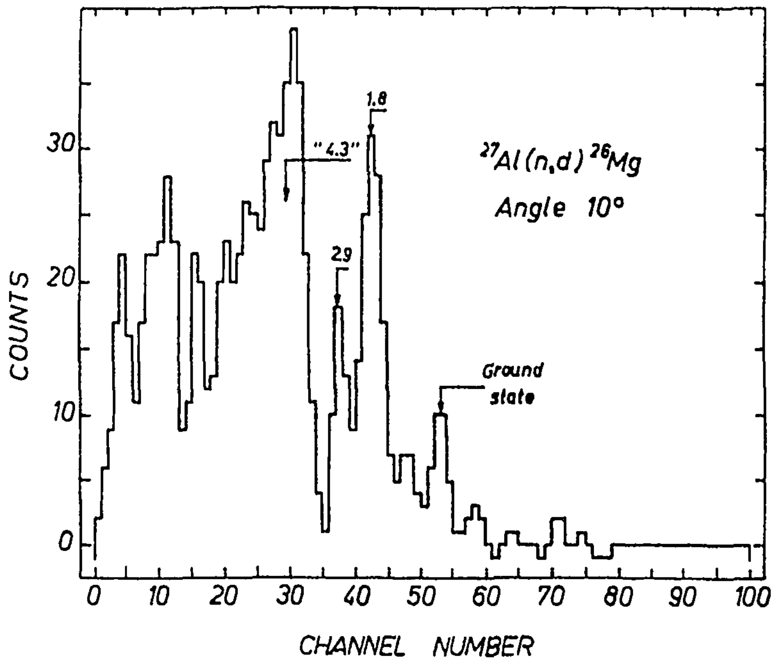

[1] B. Mariański, J. Rondio, A. Korman, Nucl. Inst. and Meth. 206 (1983) 421
[2] R.Y. Noidoo, K. B. Hanith-Ram, W. R. McMurray, Z. Phys. A. 336 (1990) 203

2.4 Studies of Nuclear Multifragmentation in the Relativistic Heavy Ion Collisions.

The ALADIN Collaboration at GSI-Darmstadt.
by A.Trzciński, B.Zwięgliński and the ALADIN Collaboration Staff.

The activities of the ALADIN Collaboration in 1994 concentrated on the three main issues:

i) Completion of the data analysis from the experiment S022,
ii) Continuation of the data analysis from the experiment S114,
iii) Preparation of the consecutive experiment S117, scheduled for running in the first half of 1995.

The data collected in the S022 experiment in which the fragments of projectile and target have been simultaneously detected for the Au + Au system at 100, 250 and 400 MeV/u with the aid of the ALADIN forward spectrometer and the MSU Miniball/Miniwall reveal two types of the collective flow effects. The collective radial flow of the intermediate mass fragments in the central collisions at 100 MeV/u [1] indicates that an essential part, typically one third to one half of the incoming center-of-mass energy is initially converted into the compressional energy. However the increase of $<E_r>$ with the fragment mass is not linear (see the attached figure), therefore the participation of heavier fragments in the flow progressively weakens. The exponential mass distribution of fragments in these central collisions as opposed to power-law in the peripheral ones at 1000 MeV/u, where multifragmentation is thermally driven, suggests that the radial expansion has a profound effect on the fragment formation mechanism [2]. The in-plane transverse flow of spectators in the semicentral and peripheral collisions at 400 MeV/u was analysed using two methods [3]. An orientation of the entrance-channel reaction plane is best determined $[\Delta\phi(FWHM) \approx 90^{\circ}]$ with the transverse - momentum vector method first proposed by Danielewicz et al.

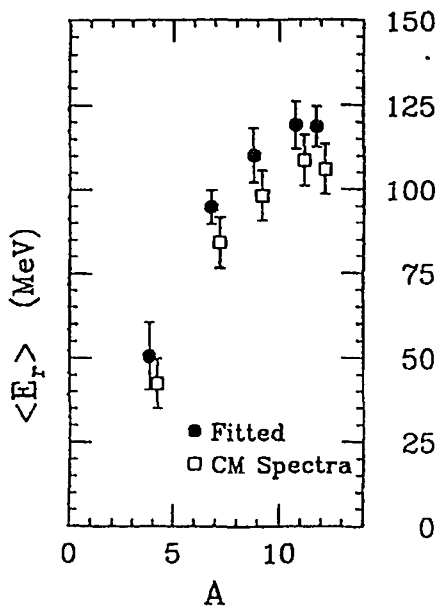

Fig. 1. Fragment mass dependence of $<E_r>$ - the mean radial kinetic energy

The experiment S114 studied the interactions of ^{129}Xe (600 and 1000 MeV/u), ^{197}Au (400, 600, 800 and 1000 MeV/u) and ^{238}U (600 and 1000 MeV/u) with a series of targets spanning the entire mass table. A review of the status of the data analysis at the Collaboration meeting at Rathen (near Dresden, Sept. 25-28, 1994) demonstrated that its results will shed light on the following aspects of the multifragmentation phenomenon:

- target and beam energy independence (universality) of the fragment production excitation curve,
- fragment emission time scale,
- correlation between the mass and excitation energy of the projectile residue,
- signals of the liquid-gas phase transition.

[1] W.C. Hsi, ..., B. Zwieglinski, Phys. Rev. Lett. 73(1994)3367
[2] G. J. Kunde, ..., B. Zwieglinski, Phys. Rev. Lett. (accepted for publication)
J. Pochodzalla, ..., B. Zwieglinski, Invited talk at the 5-th International Conference on Nucleus-Nucleus Collisions, Taormina, Italy (30.05.-04.06.1994) Nucl. Phys. A (to be published)
[3] G. J. Kunde, ..., B. Zwieglinski, Nucl. Phys. A (accepted for publication)

2.5 Interaction of the ^{14}N Ions with Light Nuclei at 124 MeV

by O.Yu.Goryunov[1], A.V.Mokhnach[1)], O.A.Ponkratenko[1)], A.A.Shvedov[1)], E.I.Koshchy[2)], Yu.G.Mashkarov[2)], L.Głowacka and J.Turkiewicz

Using the Kiev isochronous cyclotron U-240 charge, energy and angular distributions of reaction products from collisions of 124 MeV ^{14}N ions with ^{9}Be, ^{12}C, ^{24}Mg and ^{27}Al target nuclei have been measured [1]. The reaction products ($3<Z<15$) were identified by means of a ΔE-E telescope which consists of an ionization chamber (ΔE detector) and a semiconductor silicon detector (E-detector).

The experimental distributions have been analyzed in the framework of the statistical model using computer code EVRESD [2]. This code is of the Monte-Carlo type and allows us to calculate the isotopic yields and the energy and angular distributions of the evaporated particles and evaporation residues. The comparison of the experimental data with calculations shows that the main features of the energy and angular distributions are described by the model except the cases when isotopes of lithium and beryllium are emitted.

[1] O.Yu.Goryunov et al., Fifth Int. Conf. on Nucleus Nucleus Collisions, Taormina, Italy, 30 May - 4 June, 1994, p.183
[2] O.A.Ponkratenko and A.T.Rudchik, INR Report KIYaI-88-14, Kiev, 1988

1) Institute for Nuclear Research, Kiev, Ukraine
2) Kharkov State University, Kharkov, Ukraine

2.6 Study of Elastic α-Scattering from ^{2}H and ^{12}C at $E_\alpha = 4.2$ GeV. [1]

by P.Żuprański

The scattering of α-particles in the few GeV region has recently been used to investigate the properties of baryons related to their "scalar" (non spin flip and isoscalar) structure. Using a folding model approach scalar radii may be extracted from elastic scattering whereas spectroscopic information on dynamical properties of baryon may be deduced from excitation of baryon resonances. Using α-particles of an energy of 4.2 GeV from Saturne the differential elastic cross sections have been measured for ^{2}H on ^{12}C targets.

To test the validity of the folding model approach for nuclear systems we use this model for the α-α and α-^{12}C scattering. "Scalar" radii extracted from the data should be identified with the matter radii of these systems which in turn can be compared with the radii deduced from electron scattering unfolding isoscalar nucleon form factor.

The model yields for ^{2}H and ^{12}C the mean square radii of (3.6 ± 0.4) fm^2 and (5.4 ± 0.2) fm^2, respectively.

The corresponding values obtained from analysis of electron scattering are (3.77 ± 0.07) fm^2 and (5.43 ± 0.17)fm^2, respectively.

[1] H.P. Morsch et al and P. Zupranski, Zeitschrift für Physik

2.7 The Reconstructions of the Trajectories in the Forward Spectrometer

by W.Augustyniak and P.Żuprański

The forward spectrometer under construction is a part of an experimental arrangement called SPESIV-π which will form an additional detection arm for the existing magnetic spectrometer SPESIV at Laboratoire National Saturne. It consists of 2 subdetectors I and II placed after the magnet. Detector I is of the wire drift cell type while detector II is a scintillator hodoscope. The spectrometer will be used in experiments where the requirement of the missing mass - resolution is enough to distinguish between 1 and 2 pion decays. The aim of the reported code is to reconstruct the trajectories of particles passing through detector I. The code consists of three logical parts. The first one defines the spectrometer "geometry". The second one determines roughly trajectory parameters in order to improve these parameters in the third.

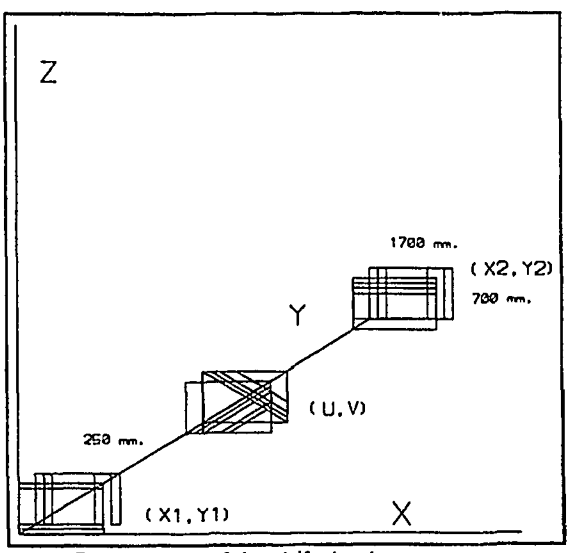

Fig.1. The geometry of the drift chamber set-up.

The "geometry" of the spectrometer constitutes the definitions of the lines corresponding to the anode wires that belong to the drift chambers called: X1, Y1, U, V, X2, Y2. (see figure 1) Each chamber contains two parallel layers of anode wires. The distance between two neighbouring wires is 8 mm.

The pairs of chambers are closely situated : X1 and Y1, U and V, as well as X2 and Y2. The distance between the pairs is 250 mm. Neither the distance between the chambers belonging to the same pair nor the dimensions of the holes for the beam to pass through are yet decided upon. The recorded signal will be proportional to the distance between the particle trajectories and the anode wire. From those proportional signals and the fired wire number the code reconstructs a particle trajectory:

$$x(t) = a_0 t + b_0.$$

As can be seen from Fig.1 $b_0^y=0$ and due to the fact that a_0 is a unit vector the four coordinates should be determined.

The simulations have proved that for the cases when a particle crosses all the chambers or misses one or two U and V chambers, the reconstruction of the coordinates of the **b** vector is better then 0.01 mm and better then 0.001 for the coordinates of the vector **a**.

2.8 M-Shell X-Ray Production by Carbon and Nitrogen Ions.

by J.Semaniak[1)], J.Braziewicz[1], M.Pajek[1)], T.Czyżewski, L.Głowacka, M.Jaskóła, M.Haller[2], R.Karschnik[2)], W.Kretschmer[2)], D.Trautmann[3)]

In the past few decades, inner shell ionization processes have received much attention both theoretically and experimentally. Initially, most experimental data were obtained for light ion impact for K-shell ionization [1,2]. Followed by increased availability of heavy ion beams, as well as, the development of high-resolution Si(Li)and HPGe detectors, the ionization measurements have been extended to heavier ions and L-[3] and M-shells [4]. Up to now, experimental data for the M-shell ionisation cross sections are scarce, which is connected with difficulties to measure the absolute cross sections for low - energy M x-rays, being typically below 3 keV. M-shell x-ray production cross sections have been measured for carbon ions with energies 6.0, 7.2, 9.6, 12.0, 14.4, 16.8, 19.2 and 25.25 MeV and nitrogen ions with energies 5.6, 7.0, 8.4, 9.8, 11.2, 12.6, 14.0, 16.8 and 19.6 MeV impinging on the Os, Ir, Au and Bi targets.

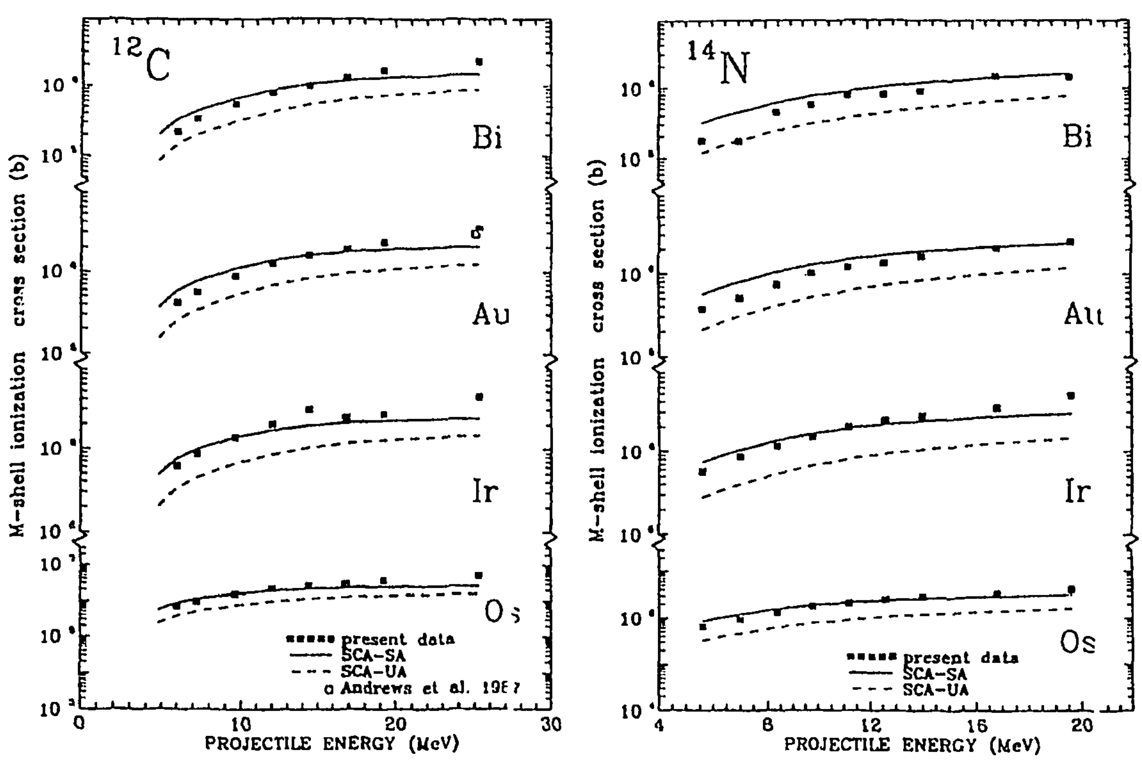

Fig.1. Measured M-shell ionization cross sections for the Os, Ir, Au and Bi versus the C^{3+} and N^{3+} ion energy. The data are compared with the prediction of the SCA calculation for separated (SA) and united atom (UA) limits.

The M-shell ionization cross sections obtained for the investigated targets bombarded by the C^{3+} and the N^{3+} ions are shown in fig. 1. These observations were compared with the predictions of the semiclassical approximation (SCA). Generally, the experimental data are systematically overestimated up to 30-40% in the low energy region, while the opposite tendency is observed for the highest energies, where the theoretical calculations are lower than the measured cross sections by up to 40%. The disagreement found at the low energies can be attributed to the binding effect. As one can see from fig. 1 the data tend rather to the SCA-UA cross sections for very low energies, what one physically expects. The discrepances observed for high energies are not fully understood, but can be related to the polarisation effect. Further theoretical studies are needed to explain observed discrepances.

[1] H.Paul and J.Muhr, Phys.Rev. 135 (1986) 47.
[2] G.Lapicki, J.Phys.Chem.Ref.Data 18 (1989) 111.
[3] I.Orlić, C.H.Sow and S.M.Tang, At. Data and Nucl. Data Tables 56 (1994) 59.
[4] R.Mehta, J.L.Duggan, J.L.Price, F.D.McDaniel and G.Lapicki, Phys.Rev. A28, 2770 (1983).
[5] M.C.Andrews et al., Phys.Rev. A36 (1987) 3699.
[6] D.Trautmann and T.Kauer, Nucl. Instr. and Meth. B42 (1989) 426.

1) Institute of Physics, Pedagogical University, Kielce, Poland
2) Institute of Physics, Erlangen-Nürnberg University, Germany
3) Institute of Physics, Basel University, Switzerland

2.9 Multiple N - Shell Ionization Induced by 0.4 - 2.0 MeV/amu Carbon and Nitrogen Ions

by J.Semaniak[1], J.Braziewicz[1], M.Pajek[1], T.Czyżewski, L.Głowacka, M.Jaskóła, M.Haller[2], R.Karschnik[2], W.Kretschmer[2], D.Trautmann[3]

Inner shell ionization cross-sections are studied by measuring x-rays emitted from the decay of inner shell vacancies. The probabilities of x - ray emission are determined for single vacancy configurations, i.e. when multiple ionization effects can be neglected. For heavier projectiles and higher energies, multiple ionization effect becomes important due to significant modification of atomic parameters (fluorescence yields and relative x - ray emission rates) describing the radiative transitions.

The standard technique used to study multiple ionization is high resolution x - ray spectrometry. In the present study we have adopted a different procedure suggested by Berinde et al. [1], which allows to extract ionization probabilities (p_{N_4}) for simultaneous ionization of L - shell and N_4 subshell from L x-ray spectra measured by medium - resolusion semiconductor detectors.

The measured data for probability of multiple N - shell ionization of the Au and the Bi atoms in central collisions with carbon and nitrogen ions in the energy range 0.4 - 2.0 MeV/amu were compared with N_4 - subshell ionization probability per electron for zero impact parameter, calculated using the SCA theory [2] and the "geometrical model" (GM) [3].

The experiment was performed at the Institute of Physics of Erlangen - Nürnberg University using beams of the $^{12}C^{3+}$ and the $^{14}N^{3+}$ ions from Tandem accelerator. The thickness of the Au and the Bi targets were 250 $\mu g/cm^2$ and 200 $\mu g/cm^2$, respectively, to assure good statistics.

The L x - ray spectra were also measured for 3 MeV protons to determine the L_η/L_{γ_1} intensity ratio in the case, when the multiple ionization effect is not expected to play an important role. For multiple ionization, the L_η/L_{γ_1} ratios are expected to be different for proton and heavy ion excitation. The intensity ratio of L_η and L_{γ_1} x-ray lines for heavy ions (HI) are related to that measured for protons (p) in the following way:

$$\left(\frac{I_\eta}{I_{\gamma 1}}\right)_{HI} = \left(\frac{1-p_{MI}}{1-p_{N4}}\right)\left(\frac{I_\eta}{I_{\gamma 1}}\right)_p$$

When additionaly $p_{M_I} < p_{N_4}$, this equation can be simplified by neglecting the p_{M_I} term. In fact the SCA calculations show that in our case $p_{M_I} \approx 0.01 - 0.02$, which is about 10 times smaller than p_{N_4}. The experimental uncertainties of ionisation probabilities measured in this way were estimated to be about 20-30%.

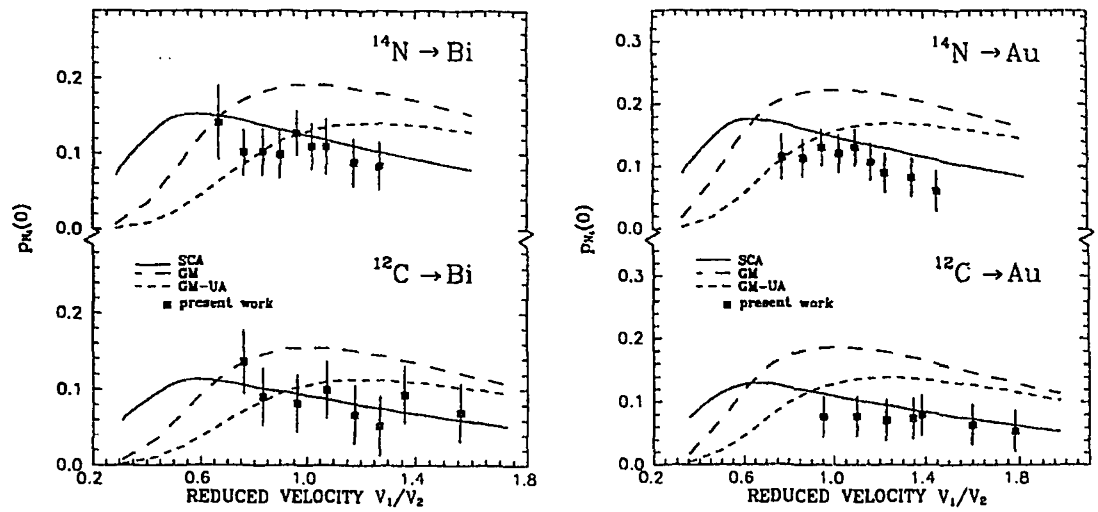

Fig.1. Measured ionization probabilities for N_4-subshell in central collisions of carbon and nitrogen ions with the Au and the Bi atoms versus reduced velocity V_1/V_2. The data are compared with the SCA theory and the "geometrical model".

The experimental data were compared with the ionization probabilities for N_4-subshell calculated for the zero impact parameter using the SCA theory [2] and the "geometrical model" and are shown in fig.1. The SCA theory describes the experimental data for Bi within the experimental uncertainties, while for Au the data are slightly smaller then the SCA predictions. For both elements, the experimental data are about 2.5 times smaller than the GM-SA (separated atom) predictions. These discrepancies can be reduced by taking into account the increased binding effect, simulated by the united atom (UA) limit, but also in this case GM-UA model gives quantitatively worse description than the SCA theory. We note that the UA approximation seems to be justified, because the adiabatic radius for L-shell ionization is much smaller than the radius of N-shell.

[1] A.Berinde, et al., J.Phys.B: At. Mol. Opt. Phys. 20 (1987) L481
[2] D.Trautmann and Rösel, Nucl. Instr. and Meth. B214 (1983) 21
[3] B.Sulik et al., Nucl. Instr. and Meth. B28 (1987) 509

1) Institute of Physics, Pedagogical University, Kielce, Poland
2) Institute of Physics, Erlangen-Nürnberg University, Germany
3) Institute of Physics, Basel University, Switzerland

2.10 Kβ_2 X-Ray Satellite Spectra Induced by Proton and Photon Impact on Zr, Mo and Pd Targets

by T.Ludziejewski, P.Rymuza, Z.Sujkowski, B.Boschung[1], J.-Cl.Dousse[1], B.Galley[1], Z.Halabuka[1], Ch.Herren[1], J.Hoszowska, J.Kern[1], Ch.Rheme[1], M.Polasik[2]

Precise diffraction spectroscopy has been used to measure the Kβ2 X-ray spectra of Zr, Mo, and Pd induced by photons and 16, 25, 45 MeV protons. Measurements of the Kβ2 line structures induced by proton beams were carried out at the Paul Scherrer Institute PSI (Villigen, Switzerland) with the use of a DuMond type curved crystal spectrometer. Photoionization measurements were performed with a similar spectrometer installation at the Fribourg University, with the same diffraction crystal and geometrical conditions.

The observed satelite structures were analysed by fitting the theoretical line profiles constructed on the basis of extensive MCDF calculations [1]. Assuming that the Kβ_2 satellite lines originate from the double K plus M shell ionization the average M-shell ionization probabilities were determined for proton and photon impact.

Photon data demonstrate an essential excess of the satellite line yields over those calculated within the Sudden Approximation model with the use of reliable SCF wavefunctions. The results are unexpected and surprising, since the assumed condition of a sudden change of the central potential is not fulfilled at least for the low energy part of the ejected photoelectron spectrum. Therefore, the theoretical results based on the SA model should be regarded as the upper limit of the shake-off plus shake-up probabilities. In addition, it was found that the M shell ionization probabilities (p_M) increase with the average energy of the photon beam. Two processes leading to the observed p_M energy dependence are possible, the direct knock-out of the M-shell electron by photoelectron, and the breakdown of Sudden Approximation for the low energy tail of photoelectrons and δ-electrons. The resulting p_M depend most likely on the interplay of both processes.

Results for protons show essentially the same behaviour of the total p_M as in the case of photoionization. Even if the direct Coulomb ionization is taken into account, the experimental p_M are systematically larger than sum of DI and shakeoff contributions.

The direct Coulomb ionization probabilities in near central collisions with protons are determined from the difference of the relative yields of $K\beta_2$ satellites in the proton and photon induced ionization. The underlying assumption is that the shake- and solid-state effects are independent of the ionizing agent, and that the secondary electron ionization is similar in the two processes. The overall dependence of the experimental p_M is rather well reproduced by the SCA theory. In view of large systematic and statistical errors the procedure does not allow for a critical discussion of dependency of the SCA calculations on the wavefunctions used.

Finally, it is suggested that observed enhancement of the satellite lines for both proton and photon impact is due to the contribution of the $K\beta_4$ ($4d_{3/2,5/2} \rightarrow 1s$) radiative transitions. For metals with $40 < Z < 48$, where the $4d_{3/2,5/2}$ states belong to the valence band, the quadrupole $K\beta_4$ transition can acquire dipole properties, which may results in a strong enhancement of its intensity [2].

Details of the experiment and the data analysis, as well as, the more detailed discussion of the results can be found in [3].

[1] M.Polasik, Phys. Rev. A40 (1989), 4361
[2] B.K.Agarwal "*X-ray Spectroscopy*" (Springer Series in Optical Sciences vol. 15; Springer-Verlag, Berlin, 1979 p. 116.
[3] T.Ludziejewski et al. submitted to Phys. Rev. A.

1) Physics Department, University of Fribourg,CH-1700 Fribourg, Switzerland
2) Institute of Chemistry, Nicholas Copernicus University, 87-100 Toruń, Poland

2.11 High resolution measurements of KX-ray spectra following the collisions with electron beams from the EAK-400 accelerator

by T.Ludziejewski, P.Rymuza, Z.Sujkowski

Recent systematic studies of the L and M-shell ionization probabilities induced by light charged particles showed that the use of realistic Dirac-Fock wavefunctions in the SCA calculations is of prime importance for the correct description of the inner shell ionization in fast ion-atom collisions [1]. The sensitivity of the theoretical cross sections to details of the wavefunctions has been found to increase with the reduced velocity of the projectile. Moreover, recent measurements of the KX-ray spectra of mid-Z atoms bombarded by photon and energetic proton beams revealed the existence of an unexpected enhancement of the $K\beta_2$ satellite line intensities with respect to the theoretical ones [2]. The latter have been obtained as being due to the contributions of the Direct Coulomb ionization calculated within the SCA-SCF approximation and the shake-off plus shake-up processes calculated within the Sudden Approximation model. To determine the M-shell ionization probabilities for very fast (relativistic) collisions and to investigate further the nature of the effects responsible for the $K\beta_2$ satellite line enhancement observed for elements $40 < Z < 46$ we decided to perform similar measurements of the $K\beta_2$satellites induced in collisions with the energetic electron beams.

The bent crystal diffraction spectrometer installed at the beam line of the EAK-400 electron accelerator at SINS Swierk has been described earlier [3]. The instrument allows the measurements of the X-ray spectra with the instrumental resolution comparable to the natural widths of emission lines. In order to perform the comparative studies of the $K\beta_2$ satellite spectra of the elements investigated in [2] the maximum Bragg angle of the spectrometer has been extended from 5° to 8.2° i.e. to the value needed for measurements of the $K\beta_2$ X-ray lines of elements with atomic number $Z \geq 40$. A new water cooled target holder permitting measurements of the KX-rays with the maximum beam intensity up to $300 \mu A$ has been installed.

Figure 1 presents the $K\alpha$ X-ray spectra of Pd target bombarded by 300 keV electron beam. The instrumental angular resolution extracted from the least square fit of the Voigt profiles to the experimental spectrum corresponds to the typical values measured for the rare-earth elements before the modification of the spectrometer. The $K\beta_2$ X-ray satellite spectra measured for the 25 μm Mo foil bombarded by 310 keV electrons is presented in fig.2. For elements with Z<50 the satellite structure of the $K\beta_2$ line partially overlaps with the K absorption edge leading to the step-like increase of the self-absorption in the target. The position of molybdenum absorption edge is marked in fig.2 by an arrow. The solid line represents the overall theoretical line shape fitted to the spectrum not corrected for the self absorption. The theoretical line profiles were calculated on the basis of the extensive multiconfiguration Dirac-Fock calculations carried out in the modified special average level scheme (MCDF-MSAL) version [4]. The dotted lines represent the decomposition of the experimental spectrum to the $K\beta_2M^0$ and $K\beta_2M^1$ components. Assuming that the yields in the $K\beta_2$ line region are due only to the M-shell ionization accompanying the removal of the K-shell electron, the M-shell ionization probability can be estimated to be p_M=10.0 (1.5)% i.e. the value comparable to the yields observed for proton impact. The observed high satellite line yields for electron impact suggest the existence of the similar mechanisms responsible for the $K\beta_2$ satellite line enhancement like those observed for proton and photon impact [2]. A more detailed, systematic investigation of the $K\beta_2$ satellite structure as a function of target atomic number and beam energy will be performed in 1995.

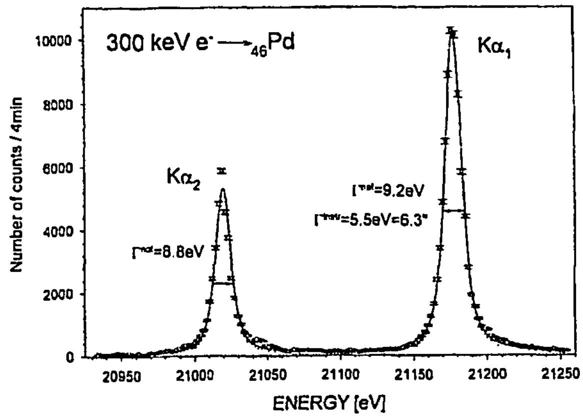

Fig.1. The $K\alpha_{1,2}$ X-ray spectrum of Pd excited by 300 keV electron impact.

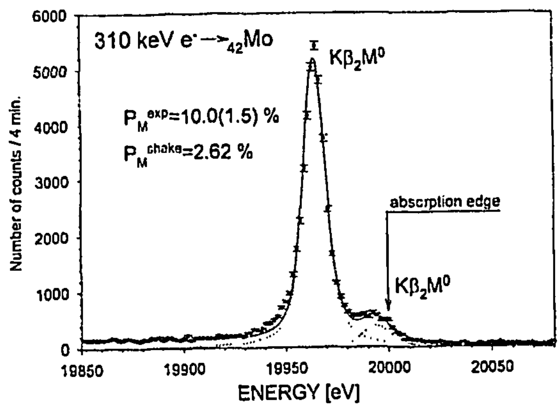

Fig.2. High resolution crystal spectrometer $K\beta_2$ X-ray spectrum of Mo induced by 310 keV e- beam.

[1] Z.Halabuka, et al., Z.Phys.D 29 (1994) 151, (see also D.F.Anagnostopoulos et al., J.Phys.B 25 (1992), 2771)

[2] T.Ludziejewski et al., submitted to Phys. Rev. A. (see also preceding contribution).

[3] T.Ludziejewski et al., SINS Annual Report 1993 p. 25 and references therein.

[4] M.Polasik, Phys.Rev. A40 (1989), 4361

2.12 Breathing mode in finite nuclei and the equation - of - state of nuclear matter
by Z.Sujkowski

The present empirical information on the Equation - Of - State of nuclear matter, EOS, is practically limited to the values of the coordinates of one point on the function of the energy per nucleon, E/A, versus the density, ρ, that is the binding energy at the saturation density: E_0 = 16MeV, ρ_o = 0.16fm^{-3}. These are obtained from a fit to the nuclear masses. A similar fit to the measured incompressibility moduli of finite nuclei, $K_{A,Z}$, should in principle give the second derivative at this point, or the incompressibility modulus of the infinite, symmetric nuclear matter, K_∞.

Most of the predictions of the properties of dense and often hot stellar and nuclear objects (e.g. the neutron stars, the supernovae explosions or the systems of colliding heavy nuclei) use these data as the starting information for extrapolations. The quality of and the confidence in this information is therefore of primary importance.

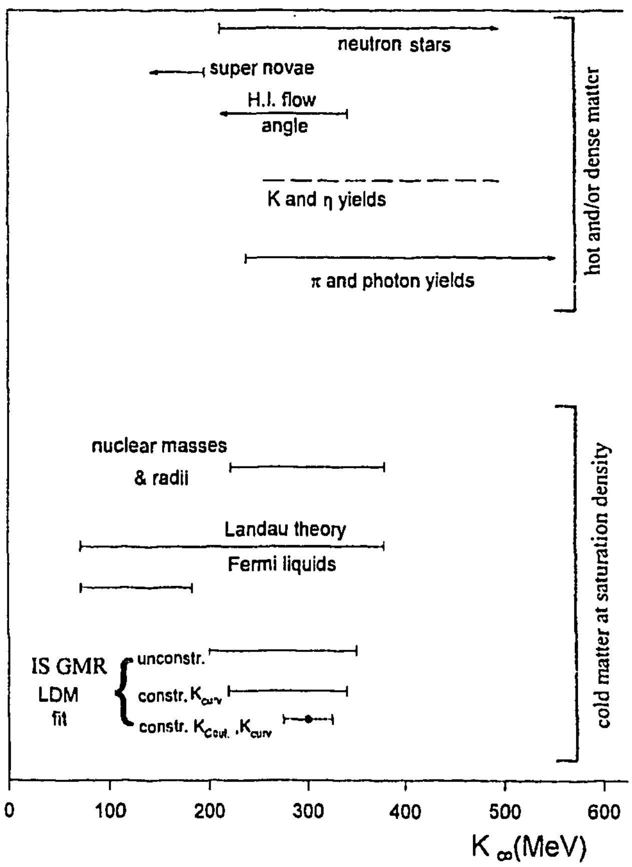

Fig.1. Ranges of values of the incompressibility modulus, K_∞, deduced from or compatible with various nuclear and astrophysical observations.

The $K_{A,Z}$ values can be obtained from the energies of the Iso-Scalar Giant Monopole Resonances, ISGMR. For a review of the experimental information on the electric giant resonances see [1]. Recent developments in the studies of the ISGMR are discussed in [2]. The present work attempts to assess the status of the ISGMR data and the reliability of the $K_{A,Z} \rightarrow K_\infty$ transformation. It is shown that neither the quality of the data nor the state - of -the- art theory permit to determine the K_∞ value to better than within an interval of 200 MeV < K_∞ < 350 MeV.

The K_∞ value determined for the "normal" nuclear matter ($T = 0$, $N \approx Z$, $\rho \approx \rho_0$) are used as a starting point in various extrapolations, e.g. in order to deduce the properties of dense, asymmetric matter in neutron stars (ρ ranging up to $5\rho_0$) or in hot and dense matter in supernova collapse. The EOS needed for these extrapolations in sensitively dependent on the initial K_∞ value. Changing this value from about 210 MeV (the value often quoted in astrophysical calculations as "the experimental nuclear physics value") to about 300 MeV results in going from a "moderately soft" to "stiff" EOS. This makes the plea for new precise data on Giant Monopole Resonances a very urgent one.

Several nuclear and astrophysical phenomena depend on the compressibility of nuclear matter. Reversing the argument, one might determine ranges of the K_∞ values compatible with the corresponding diverse observations. A collection of such ranges, applicable to or deduced from several different physical objects and/or phenomena, is displayed in fig.1. In composing this figure we have followed ref.[3], though the selection of observables is slightly different and some more recent observations and analyses are made use of.

The entries in fig.1 are arranged separately for processes and objects related to cold nuclear matter at saturation density and for those pertaining to hot and/or very dense matter, for which the condition of being at thermodynamical equilibrium most likely is not satisfied. We note that this condition is by definition a necessary one for the concept of EOS to be valid.

The large differences among the ranges shown in fig.1. may reflect either the shortcomings in the analysis or the different physics underlying the phenomena.

The three different entries referring to the ISGMR data are obtained from the fits to the liquid drop model expansion under different simplifying assumptions: (i) the three parameter fit, assuming an analytical form for the Coulomb term and putting the curvature term equal to zero, [5]; (ii) the four parameter fit including the Coulomb term (the present work); and (iii) the unconstrained fit, [4].

Details of these analyses as well as a discussion of the entries stemming from the nucleus-nucleus collision data and from astrophysical observations can be found in [6] and [7].

[1] A van der Woude, in "Electric and magnetic giant resonances in nuclei", J.Speth, Ed., World Scientific Publ. Co., 1991, p99
[2] Z.Sujkowski, invited talk, Proc. 7th Int. Conf. on Nuclear Reaction Mechanisms, Varenna, June 1994, p.300
[3] N.K.Glendenning, Phys. Rev. C37(1988)2733
[4] S.Shlomo and D.H.Youngblood, Phys. Rev. C47(1993)529
[5] M.M.Sharma et al., Phys. Rev. C38(1988)2562, Nucl. Phys. A504(1989)337
[6] Z.Sujkowski,Physica Scripta, (in press).
[7] Z.Sujkowski, invited talk, Guardamar 1993, in "Gamma Ray and Particle Production in Heavy Ion Reactions" p.50-71, J.Diaz, G.Martinez and Y.Schutz, Eds., World Scientific Publ. Co., 1994.

2.13 Test of lepton flavour conservation in nuclear $\mu \rightarrow$ e conversion (SINDRUM Coll.)

by T.Kozłowski

In the Standard Model lepton flavours are strictly conserved. This is not true for most of its extensions and experimental searches of lepton flavour violation provide very powerful constraints of their parameters - masses of new postulated particles. Due to the enhancement by the coherent contribution of all the nucleons in the nucleus the nuclear $\mu \rightarrow$ e conversion

$$\mu^- + (A,Z) \rightarrow e^- + (A,Z)$$

gives more stringent limits than the ones obtained from the purely leptonic decays $\mu \rightarrow$ eee, $\mu \rightarrow e\gamma$ or decays of kaons, leptons τ, bosons Z^0 etc.

The goal of the SINDRUM II experiment, which was proposed in 1987 at PSI Villigen, Switzerland (see [1] for details) is to search for coherent $\mu \rightarrow$ e conversion with the sensitivity of the order of 10^{-14}. In the first run in 1989 the following upper limits (90% C.L. - confidence level) for the ground state transitions have been obtained [2]:

$$\Gamma(\mu^- Ti \rightarrow e^- Ti^{g.s})/\Gamma(\mu^- Ti_{capture}) < 4.3 \cdot 10^{-12}$$
$$\Gamma(\mu^- Ti \rightarrow e^+ Ca^{g.s})/\Gamma(\mu^- Ti_{capture}) < 4.3 \cdot 10^{-12}$$

These limits were slightly lower than those obtained before.

In 1992 a measurement was done on Pb, what is of interest since it gives an increased sensitivity to the isovector part of the interaction, i.e. to the contribution which is dependent on the neutron (d quark) excess. In 1993 a second data set on Ti was obtained with some improvements in passive and active cosmic ray background suppression and much higher muon stop number. These data are presently being evaluated and the results (still preliminary) are the following ones:

$$\Gamma(\mu^- Ti \rightarrow e^- Ti^{g.s})/\Gamma(\mu^- Ti_{capture}) < 7.3 \cdot 10^{-13}$$
$$\Gamma(\mu^- Pb \rightarrow e^- Pb^{g.s})/\Gamma(\mu^- Pb_{capture}) < 4.4 \cdot 10^{-11}$$

These new limits are much lower (factor of six for Ti and ten for Pb) than those known before and they are close to the branching ratios expected in the minimal supersymmetric model [3]. In the case of Ti this limit is seven orders of magnitude better than in direct $Z^0 \rightarrow \mu e$ searches at LEP.

Presently a dedicated beamline for this experiment is under construction. This is a superconducting solenoid with a length of 8.5 m and an inner diameter of 0.4 m connected axially to the SINDRUM II spectrometer. The expected stop rate of $10^8 \mu^- s^{-1}$ is 20 times higher than presently available and will allow to achieve the sensitivity of 10^{-14}. The first data taking is planned for fall 1995.

[1] T.Kozłowski, SINS Annual Report 1990, p.27
[2] C.Dohmen,..., T.Kozlowski et al, Phys. Lett. B317(1993)631
[3] R.Barbieri, L.J.Hall, Phys. Lett. B338(1994)212

2.14 Systematics of Fusion-Fission Time Scales Deduced From a Dynamical-Model Analysis of Prescission Neutron Multiplicities

by J.Wilczyński, K.Siwek-Wilczyńska[1], R.H.Siemssen[2], H.W.Wilschut[2]

In the Annual Report 1993 we described a new method of determination of the time scale of fusion-fission reactions from measured prescission neutron multiplicities. In this method, the time dependent statistical-cascade calculations are coupled to the Feldmeier's model [1] of nucleus-nucleus collisions. The inclusion of the dynamical model calculations makes it possible to correctly evaluate the excitation energy of the composite system in consecutive stages of the nucleus-nucleus collision---from touching spheres to fusion, then to the saddle and finally to scission. The deexcitation of the dynamically evolving composite system is traced in time along the statistical decay cascade, calculated with a simple Monte Carlo code. The event-averaged results of the calculations give the relation between time and neutron- or other light particle multiplicity accumulated till that time. By using this relation, the experimental prescission-neutron multiplicity data can be used for determination of the fusion-fission time scale.

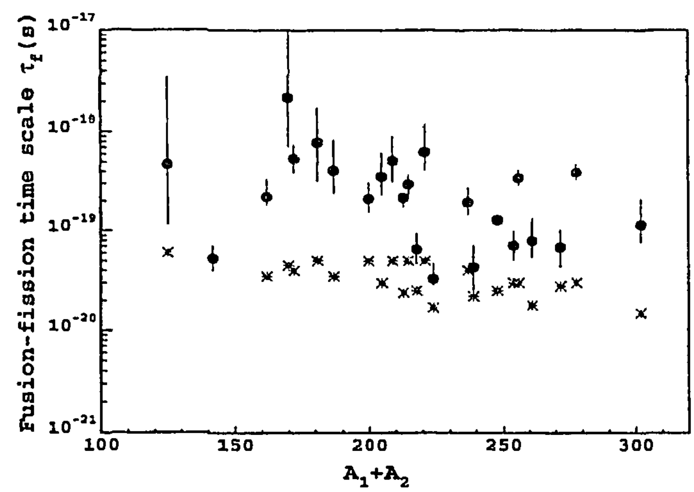

Fig.1.

We have analysed the complete set of data on prescission neutron multiplicities reported by Hinde et al. [2]. The deduced fusion-fission times τ_f (full circles) are displayed in the figure above as a function of the combined mass number of the composite system A_1+A_2. Results of "static" calculations of Hinde et al. [2] are shown by asterisks. It is seen from the figure that taking the dynamic evolution of the composite system into account leads to a considerably longer fusion-fission time scale (on the average by a factor of 10) than that deduced in the static approach.

It should be noted that the results of our analysis of the prescission neutron multiplicities agree with results of an essentially different analysis of the prescission GDR γ-multiplicities [3]. The very long times τ_f obtained independently in both types of experiments can be interpreted [3] as evidence of an unexpectedly large value of the dissipation coefficient in hot composite systems.

[1] H. Feldmeier, Rep. Prog. Phys. 50 (1987) 915
[2] D.J. Hinde, et al., Phys. Rev. C45 (1992) 1229
[3] P. Paul and M. Thoennessen, Ann. Rev. Part. Nuc. Sci. 1994 ((in press))

1) Institute of Experimental Physics, Warsaw University, 00-681 Warsaw, Poland
2) Kernfysisch Versneller Instituut, 9747 AA Groningen, The Netherlands

2.15 Lifetime Measurements of the High-spin States in the N=106 Nuclei: ^{183}Ir and ^{182}Os

by R.Kaczarowski, U.Garg[1], S.Naguleswaran[1], J.C.Walpe[1], I.Ahmad[2], D.Blumenthal[2], M.P.Carpenter[2], B.Crowell[2], R.V.F.Janssens[2], T.L.Khoo[2], T.Lauritsen[2], D.Nissius[2]

Lifetimes in the pair of the N=106 isotones, ^{183}Ir and ^{182}Os, have been measured using the Notre Dame "plunger" device, in conjunction with the Argonne-Notre Dame Gamma-ray Facility. The ^{150}Nd (^{37}Cl,4n) ^{183}Ir and ^{150}Nd (^{36}S,4n) ^{182}Os reactions were used at beam energies of 169 MeV and 164 MeV, respectively. The target was enriched ^{150}Nd (0.9 mg/cm^2 thick) evaporated onto a stretched 1.5 mg/cm^2 Au foil and covered by thin layer (0.06 mg/cm^2) Au to prevent oxidation. Runs of approximately 4 hours were taken at about 20 target-stopper distances, ranging from 16 μm to 10400 μm, for both final nuclei. The primary reason of these measurements is to study deformation-driving properties of the $h_{9/2}$ proton intruder state by comparing the values of the deduced quadrupole moments, Q_t, in the ground state rotational bands in the odd-A Ir nucleus and the even-even Os core. Preliminary results show that it will be possible to extract the lifetimes of the yrast bands up to and including part of the backbending region with sufficient accuracy.

The measured Q_t values impose strong restrictions on sets of β_2, β_4 and γ parameters available for model calculations. Our previous work [1] and these preliminary results effectively ruled out very different β_2 deformations as the cause of the different backbending behaviour of the GSB in Os and the $h_{9/2}$ proton band in Ir nuclei with N=104 and N=106 (see Table 1). However, it is still possible that observed small differences in β_2 deformations an/or very different γ deformations and γ-softness may be the cause. In addition, the results confirm also earlier conclusion of Walpe *et al.* [2] that $\pi i_{13/2}$ orbital (far from the Fermi level) is much more deformation driving in relation to the $\pi h_{9/2}$ orbital (at or close to the Fermi level) than predicted by the TRS calculations [2] for the N=104 and N=106, Os and Ir nuclei (see Table 2).

Table 1

N = 104	^{180}Os			^{181}Ir ($h_{9/2}$, $i_{13/2}$)			^{182}Pt		
	Q_0	β_2	β_4	Q_0	β_2	β_4	Q_0	β_2	β_4
Exp.:	6.1(4)	0.221(13)	-0.028	6.04(16) 8.99(26)	0.213(5) 0.304(8)	-0.017 0.0	5.77(17) 6.9(2)* 2.6(2)*	0.201(5) 0.238(8) 0.20(2)	-0.017 -0.017 0.001
Calc.:	6.20	0.224	-0.028	6.80 7.91	0.238 0.270	-0.017 0.0	6.66 2.06	0.23 0.16	-0.017 0.001
N = 106	^{182}Os			^{183}Ir ($h_{9/2}$, $i_{13/2}$)			^{184}Pt		
	Q_0	β_2	β_4	Q_0	β_2	β_4	Q_0	β_2	β_4
Exp.:	5.69(18)	0.203(6)	-0.018	6.07(10) 8.8(2)	0.214(4) 0.296(6)	-0.026 0.0	5.99(11) 7.3(3)** 2.4(3)**	0.209(3) 0.252(10) 0.19(2)	-0.017 -0.017 -0.004
Calc.:	6.10	2.17	-0.018	6.79	2.38	-0.026	6.33 2.06	0.22 0.16	-0.029 -0.004

*) Prolate - oblate band mixing calculations: **) the same, preliminary results Exp. data from this work and ref. [1-4]

Table 2: Ratios of quadrupole transition moments

	N=104 (^{181}Ir)	N=106 (^{183}Ir)	N=108 (^{187}Au)
$Q_t(h_{9/2})/Q_t$(core) exp.:	0.98(7)	1.07(4)	
$Q_t(h_{9/2})/Q_t$(core) calc.:	1.10	1.11	
$Q_t(i_{13/2})/Q_t(h_{9/2})$ exp.:	1.49(6)	1.45(4)	1.33(6)
$Q_t(i_{13/2})/Q_t(h_{9/2})$ calc.:	1.19		1.21

[1] R.Kaczarowski et al., Phys. Rev. C41 (1990) 2069
[2] J.C.Walpe et al., to be published,
[3] J.C.Walpe et al., BAPS 39 (1994) 1419
[4] U.Garg et al., Phys. Lett. B180 (1986) 319

[1] Physics Department, University of Notre Dame, Notre Dame, IN 46556, USA
[2] Physics Division, Argonne National Laboratory, Argonne, IL 60439, USA

2.16 Study of High Spin States in the ^{183}Ir and ^{182}Ir Nuclei

by R.Kaczarowski, U.Garg[1], S.Ghugre[1], S.Naguleswaran[1], D.Blumenthal[2], M.P.Carpenter[2], B.Crowell[2], R.V.F.Janssens[2], B.Glagola[2], T.L.Khoo[2], T.Lauritsen[2], D.Nissius[2]

The region of neutron-deficient Os - Pt nuclei presents a variety of shape evolution and shape coexistence phenomena. Especially interesting is a role of the $i_{13/2}$ proton intruder state in these phenomena. To gain further insight into this region, an experiment was carried-out at the Argonne National Laboratory using Argonne Tandem Superconducting Linear Accelerator system (ATLAS). High spin states of the ^{183}Ir and ^{182}Ir nuclei were populated with the ^{150}Nd (^{37}Cl, 4n) ^{183}Ir and ^{150}Nd (^{37}Cl, 5n) ^{182}Ir reactions, respectively, at a beam energy of 170 MeV. The Argonne-Notre Dame Gamma-ray Facility (an array of 12 high-efficiency Compton-suppressed HP Ge spectrometers surrounding (nearly) 4π, 50-element BGO-detector multiplicity array) was used to measure the emitted γ-radiation. The target was enriched ^{150}Nd (1.7 mg/cm^2 thick) evaporated onto a stretched 20 mg/cm^2 Au foil and covered by thin layer (0.27 mg/cm^2) Au to prevent oxidation. About 114 million γ-γ and higher fold coincidence events were recorded on 23 magnetic tapes (6250 bpi) during 128 hours of the beam time. Only events with multiplicity higher or equal to 5, as registered by the BGO array, and with Ge-multiplicity higher or equal to 2 were collected. The events were unfolded and sorted into eight γ-γ, 2K matrices (in-beam and out-of-beam prompt and delayed coincidences) with different conditions set on the BGO multiplicity to enhance the reaction channels of interest. The events have been also sorted into a γ-t, 2Kx256 matrix for determination of the half-lives of the excited levels. Additional sorting into six γ-γ matrices, where γ-rays were selected according to the respective detector - beam angle, was also made for further extraction of the DCO ratios for individual γ-transitions.

Already on-line analysis has allowed us to extend considerably the previously known level schemes of both nuclei of interest. Several new isomers in the $T_{1/2}$ range of 10 - 1000 ns have been identified for the first time. Off-line analysis is in progress.

[1] Physics Department, University of Notre Dame, Notre Dame, IN 46556, USA
[2] Physics Division, Argonne National Laboratory, Argonne, IL 60439, USA

2.17 Study of Band Structures in ^{180}Os

by S.Utzelmann[1], R.M.Lieder[1], P.Hoernes[1], A.Georgiev[1], D.Bazzacco[2], R.Menegazzo[2], C.Rossi-Alvarez[2], G.deAngelis[3], Ts.Venkova[4], R.Kaczarowski, T.Rząca-Urban[5]

In continuation of our investigation of structural and shape changes in the neutron-deficient Os nuclei, study of high spin states in ^{180}Os have been performed using the ^{150}Nd (^{36}S, 6n) ^{180}Os reaction. The ^{36}S-beam of 177 MeV was supplied by the Tandem-XTU accelerator at the LNL, Legnaro and the emitted γ-radiation was measured with the γ-spectrometer GASP which consists of 40 high-efficiency Ge-detectors and an inner ball of 80 BGO scintillators. We used a stack of two thin targets with thicknesses of 0.5 and 0.6 mg/cm^2. In the experiment a total of about 10^9 triple or higher fold events were collected.

In the energy correlation matrices a ridge-structure formed like a trumpet is observed which indicates a decrease of the dynamic moment of inertia. The previously known rotational bands in ^{180}Os [1] have been extended to higher spins. On the aligned spin vs. the rotational frequency plot one can notice a decrease of the alignment at higher frequencies for several rotational bands. This decrease of the alignment reflects a decrease of the dynamic moment of inertia. Such behaviour of the rotational bands at high spins can explain the observation of the "'trumpet ridge"'. It is probably due to a change from a prolate to a strongly triaxial deformation as predicted by Wyss et al. [2].

Work supported in the framework of the German-Polish Scientific & Technological Cooperation under contract nr. X081.71 and by the DFG under contract nr. 436 BUL 113/75/0 S.

[1] R.M.Lieder et al., Nucl.Phys. A476 (1988) 545
[2] R.Wyss et al., Nucl.Phys. A511 (1990) 324

[1] IKP, KFA Jülich, Jülich, Germany,
[2] INFN, Sezione di Padova, Padova, Italy,
[3] INFN, LNL, Legnaro, Italy,
[4] BAS, INRNE, Sofia, Bulgaria,
[5] UW, Warsaw, Poland

2.18 An Attempt to Evaluate Cross Sections for the ^{68}Zn(p,2p)^{67}Cu Reaction Using Model Calculations.

by J.Tys[1], E.Rurarz, S.Mikołajewski

The excitation functions for the ^{68}Zn(p,2p)^{67}Cu reaction have been calculated (from threshold up to 120 MeV) by using hybrid model based computer codes Overlaid Alice and Alice 85/300. The nucleon-nucleus interaction in this model is treated as proceeding through a preequilibrium phase followed by nuclear evaporation. Applying this model we hoped that below 100 MeV proton energy in the reaction (p,2p) both protons were emitted in the preequilibrium stage. The calculated excitation functions for the ^{68}Zn(p,2p)^{67}Cu reaction have been compared with their literature values (E^p = 20 - 430 MeV). Unfortunately both codes completely fail (See Fig 1) to explain discrepancies between experiment and calculations. The disagreement seems to indicate that the calculation does not account for the contribution of direct processes.

[1] Heavy Ion Laboratory, Warsaw University

3. APPLIED NUCLEAR PHYSICS AND INTERDISCIPLINARY ACTIVITIES

3.1 Channeling on Rough Surfaces

by S.Kwiatkowski, R.Sidor, A.Turos

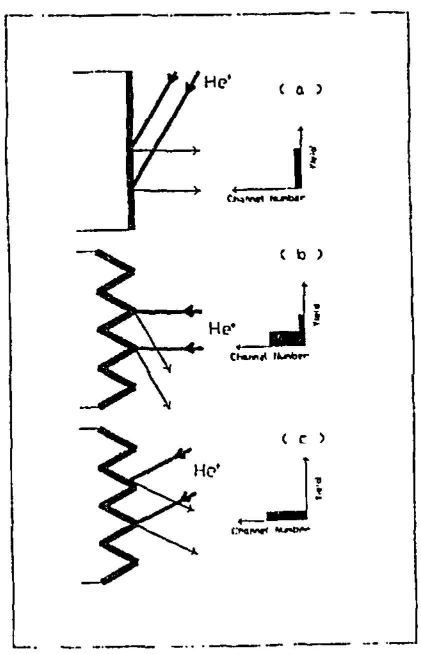

Fig.1. Schematic of different surface morphology and experimental geometry leading to the modification of the damage peak:
a - flat surface, "classical" surface peak
b - triangle-patterned surface, low-energy tail appearing
c - in- and out-going trajectories parallel to triangle sides, no surface peak forms

Surface morphology of solids was studied by means of the Reflected Beam Scattering Experiments (RBS)using 2 MeV ^4He ions.

In the energy spectra recorded in the channeling configuration peaks appear similar to those observed for single crystals containing radiation defects. Such a quasi "damage peaks" depend critically on surface roughness [1]. Moreover, they exhibit tails reaching towards the greater depths that can be easily misinterpreted as defect depth distribution. Fig. 1 shows the simplified representation of a rough surface. Due to the different trajectories of particles scattered from such a surface energy spectra are created also as shown in Fig. 1. One can conclude that the formation of a quasi "damage peak" is of purely geometrical nature . This effect becomes significant when dimensions of the surface features exceed the depth resolution. Experiments illustrating the above findings were performed on (100) InP sputter-etched with Ar ions at energies 0.5-4.0 keV. Correlation between the population of the conical features which develop upon ion milling and the corresponding distortion of the channeling spectrum is demonstrated.

[1] A.R.Knudsen, Nucl. Instr. and Meth., **168**, 163 (1980)

3.2 Structural Transformations in Leached Uranium Dioxide

by A.Turos, R.Falcone[1], A.Drigo[2], A.Sambo[2] and Hj.Matzke[3]

The stoichiometric UO_2 is today's nuclear fuel. After a few years utilization in a nuclear power station the fuel is either reprocessed or stored in a specially designed safe repository in a deep geological formation (e.g.granite or salt). Though the access of water to such a repository is quite unlikely, the effects of ground water interaction with UO_2 must be studied. Hence basic data on the mechanisms of leaching are necessary. From our previous study [1] it is known that interaction of UO_2 with water leads to the formation of higher uranium oxides of compositions between U_2O_7 and U_2O_5. The transformed surface layers are essentially water-free and grow by oxygen diffusion through the oxidized layer.

The samples used were single-crystalline UO_2 wafers of <110> orientation. Leaching was performed in water of different pH value in autoclaves at temperatures up to 200°C. The leached samples were analyzed by means of the RBS/channeling technique using a 7.53 MeV ^4He beam from the CN accelerator as described in our another contribution to this Report.

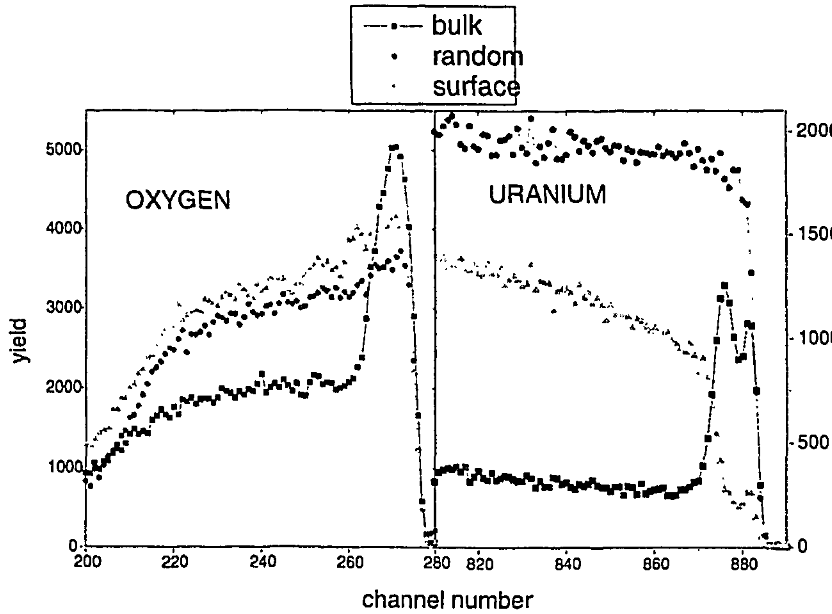

Fig.1. Random and aligned spectra for the UO_2 single crystal leached at 180°C for 24 hrs. The spectra labelled *bulk* and *surface* are taken for the crystal aligned with the <110> axis of the bulk and transformed region, respectively.

Fig.1 shows the channeling spectra for uranium and oxygen sublattices. One notes that the oxygen spectrum is plotted after the due subtraction of the uranium background. Let us first discuss the spectra labelled *random* and *bulk*. In the uranium portion of the spectra a peak appears, similar to a damage peak usually formed by ion implantation. It is apparently produced by displacements of uranium atoms due to the incorporation of additional oxygen atoms. The presence of the latter is clearly visible in the oxygen portion of the spectra. A strong peak in the transformed surface region can be seen that is higher than the random spectrum. This flux peaking effect indicates that excess oxygen atoms are distributed along the <110> rows, preferentially occupying positions close to the center of that channel.

Angular scans performed for the leached sample provide additional information on the nature of the transformed layer. Fig.2 shows the angular scans performed along the (100) plane with two different energy windows. The first one covered only the transformed layer (labelled *surface*) whereas the second one was set beneath the distorted region (labelled *bulk*)

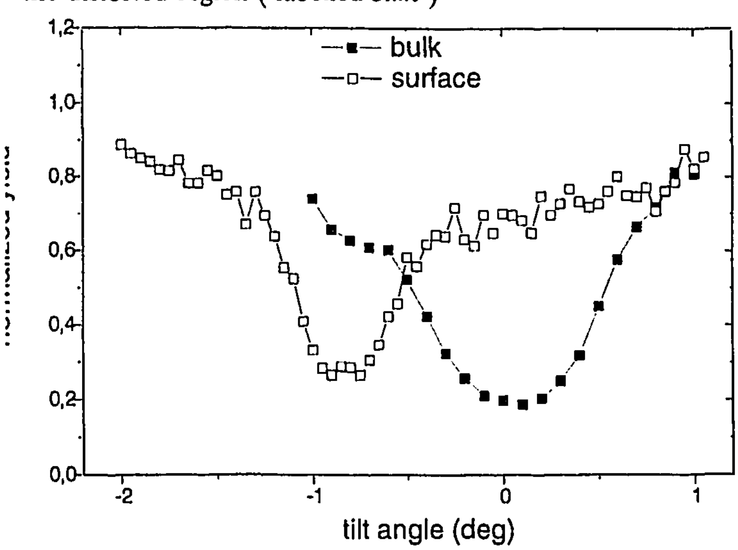

Fig.2. Angular scans across the <110> axis in the (100) plane for the uranium sublattice of the leached UO_2 single crystal.

The minimum in the scan for the transformed region is shifted by about 1° with respect to the scan for the bulk crystal. The surface region is thus slightly misaligned with respect to the bulk. The measured stereogram clearly indicates that the surface region is inclined in the (100) plane and is composed of some twins i.e. the misalignment can be either positive or negative.

Let us come back to Fig.1. As can be seen dramatic changes can be observed in the energy spectra labelled *surface* i.e. taken for the sample aligned with transformed layer in the (100) plane of the bulk. One notes almost perfect channeling in the surface region of uranium whereas no channeling features can be observed for the oxygen sublattice. The detailed structure of the transformed layer that preserves the long range order in the uranium sublattice and almost completely destroys it in the oxygen sublattice is at the moment not known.

[1] Hj.Matzke and A.Turos, Solid State Ionics, 49,189(1991).

1) Centro Nazionale per la Ricerca e lo Sviluppo dei Materiali,CNRSM, Brindisi, Italy
2) Università degli Studi di Padova, Padova, Italy
3) European Institute for Transuranium Elements, Karlsruhe, Germany

3.3 Channeling Analysis of the Oxygen Sublattice in UO_2 Single Crystals

by A.Turos, R.Falcone[1], A.Drigo[2], A.Sambo[2] and Hj.Matzke[3]

Uranium dioxide is a calcium fluorite (CaF_2) type ceramic oxide. Binary metal oxides are composed of two sublattices: cation (metal) and anion (oxygen) and are usually highly ionic. The diffusion and defect transformations proceed differently for anions and cations though some coupling between the two sublattices exists. Because of the high complexity of these processes one expects that only the separate analysis of each sublattice can elucidate the problem [1]. In the case of uranium oxide it is a particularly difficult task because of the extremely great mass and atomic number differences between component atoms. Since for the classical RBS/channeling the oxygen yield is less than 1% of that for uranium only the resonant $^{16}O(^4He,^4He)^{16}O$ scattering can be used for the purpose.

UO_2 single crystals of good quality were prepared at EITU, Karlsruhe [2]. The channeling experiments were performed at LNL using the CN Van de Graaff accelerator. The samples were mounted on the three axis goniometer and analyzed using a 7.53 MeV ^4He beam. Scattered ions were detected at 160°.

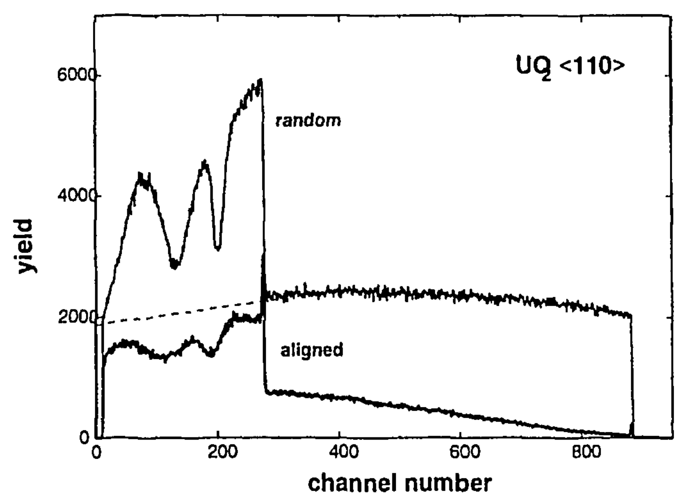

Fig.1. Random and aligned spectra for a virgin UO_2 single crystal.

Fig.1 shows random and aligned spectra for a <110> UO_2 single crystal. The three broad peaks appearing below channel number 300 are due to the resonant scattering by oxygen atoms and reflect the energy dependence of the scattering cross section [3]. Since the O-peaks appear over the continuous spectrum due to the scattering by uranium atoms, the O portion of the spectrum has to be separated by subtracting the U-background as indicated by a dotted line in Fig.1.

Fig.2 shows the measured channeling angular scans for <110> and <111> directions. As expected the oxygen dip for the <110> direction was much narrower than the uranium one. In contrast, only a very small difference in critical angles was observed for the <111> direction. In the fluorite type structure of UO_2 atomic rows of uranium and oxygen are separated for <100> and <110> directions, whereas along <111> direction only mixed rows with equidistant O and U atoms can be found. The difference of the dip widths for the <110> direction (0.18° vs. 0.61°)reflects the profound effect of the extremely large difference of atomic numbers on the steering force of O- and U-rows. For the <111> direction the much higher potential of U atoms governs the particle motion along mixed rows. The role of oxygen atoms is much less important but not negligible. One notes the small narrowing of the O-dip with respect to the U-dip (0.39° vs. 0.47°) and also slightly higher minimum yield for oxygen. These effects can be attributed to the much higher amplitude of oxygen atom thermal vibrations: 10 pm as compared to 7 pm for U-atoms.

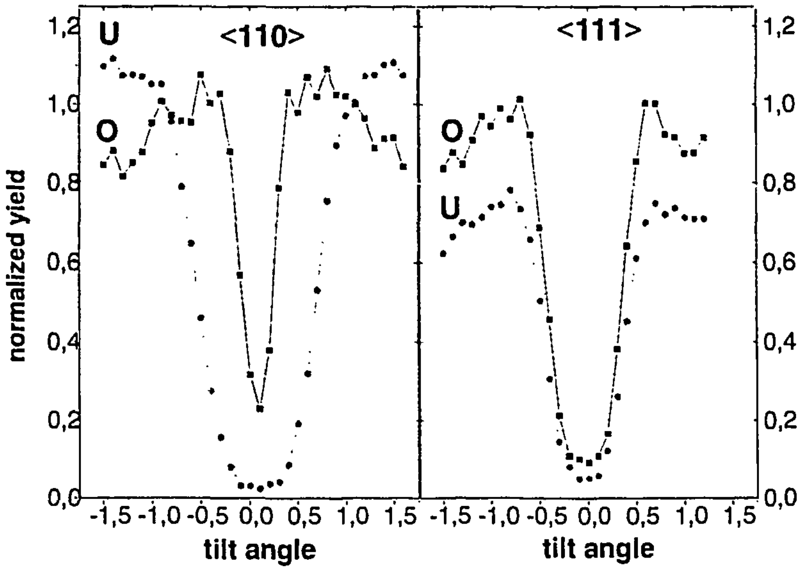

Fig.2. Angular scans for two principal directions of a UO_2 single crystal for O and U sublattices.

The effect of the dominant role of the U-atoms steering can also be observed for planar channeling: only for mixed planes, like (110) or (112) oxygen dips of the same shape as for uranium were observed. For the other major planes only very small oxygen minima, if any, could be noticed. The (100) plane is a very special case for channeling in the O sublattice. Since in this direction oxygen atoms are located in the midplane between two U planes the O peak instead of a dip was observed. The maximum of oxygen normalized yield amounts to 1.25 thus reflecting the strong flux peaking effect. This results confirm and extend previous data obtained with the use of RBS and the $^{16}O(d,p)^{17}O$ nuclear reaction [4].

[1] A.Turos, O.Meyer, L.Nowicki, J.Remmel and M.Wielunski, Nucl. Instr. and Meth. B (in press, 1994) Proc. IBA - 11.
[2] Hj.Matzke and A.Turos, J. Nucl. Mat., **114**,349(1983)
[3] J.John, J.P.Aldridge and R.H.Davis, Phys. Rev. **181**,1455(1969)
[4] Hj.Matzke, J.A.Davies, N.G.E.Johannson, Can. J. Phys. **49**,2215(1971)

[1] Centro Nazionale per la Ricerca e lo Sviluppo dei Materiali,CNRSM, Brindisi, Italy
[2] Università degli Studi di Padova, Padova, Italy
[3] European Institute for Transuranium Elements, Karlsruhe, Germany

3.4 Ion Cin Spinel Single Crystals

by A.Turos, R.Falcone[1], A.Drigo[2], A.Sambo[2] and Hj.Matzke[3]

Spinels are materials which crystallize with a structure similar to that of the mineral having this name. The characteristic feature of the spinel family of materials is the enormous variation in chemical composition which is reflected in the broad range of their physical properties [1]. Recently, a very low sensitivity of the $MgAl_2O_4$ spinel to the ionizing radiation led to its application as a window material in nuclear fusion devices and as inert matrix for reactor irradiation of higher actinides. In spite to its important applications, the detailed response of spinel to the ion bombardment and its annealing behavior are only poorly known. The aim of the reported project is to perform such a study using the RBS/channeling technique. As a first milestone the investigation of the channeling properties of $MgAl_2O_4$ single crystals was envisaged.

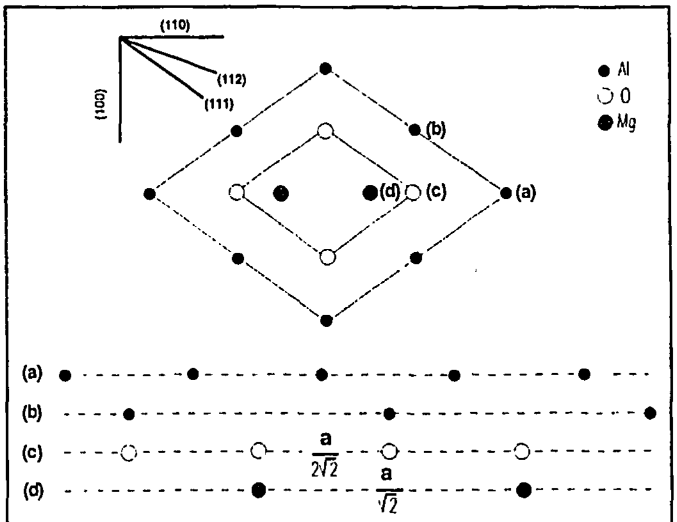

Fig.1. View along the <110> direction of $MgAl_2O_4$ spinel single crystal and the structure of atomic rows (a), (b), (c) and (d).

The crystal structure of spinel, though cubic, is quite complex. There are 56 atoms in a unit cell: Mg atoms are occupying a diamond cubic structure, one half of the unit cell octants is occupied by Al atoms in a tetrahedral arrangement, whereas O atoms are located in all octants forming complementary oriented tetrahedra.

Spinel single crystals of <110> orientation were polished with diamond paste down to 0.25 μm and subsequently heated at 1400°C in Ar/H^2 to anneal the polishing damage. The channeling experiments were performed at the LNL using the AN2000 Van de Graaff accelerator. The samples were mounted on the 2-axis goniometer and analyzed with the 2 MeV ^4He beam.

Channeling spectra for principal directions of a spinel single crystal are shown in Fig.2. The shape of the spectra reflects clearly the structure of atomic planes and rows (cf. Fig.1). Taking as a reference the relative height of steps in the random spectrum, characteristic for each atomic species, one can deduce which kind of atoms is mostly exposed to the channeled beam. The channeling spectrum for the (111) plane shows similar features as the random one, thus indicating that no atomic component is shielded. In contrast, the increase of scattering intensity for Mg and the reduction for O can be observed in the (100) planar direction. Some shielding of Mg atoms was noted for the (110) plane. The <110> axial spectrum does not show any peculiarities which is in accordance with the channel structure shown in Fig.1. It is worth mentioning, that a largely enhanced scattering yield for Al and O was observed in the <111> axial channeling spectrum (not shown here). This is apparently due to the location of a mixed Al-O row in the middle of that channel.

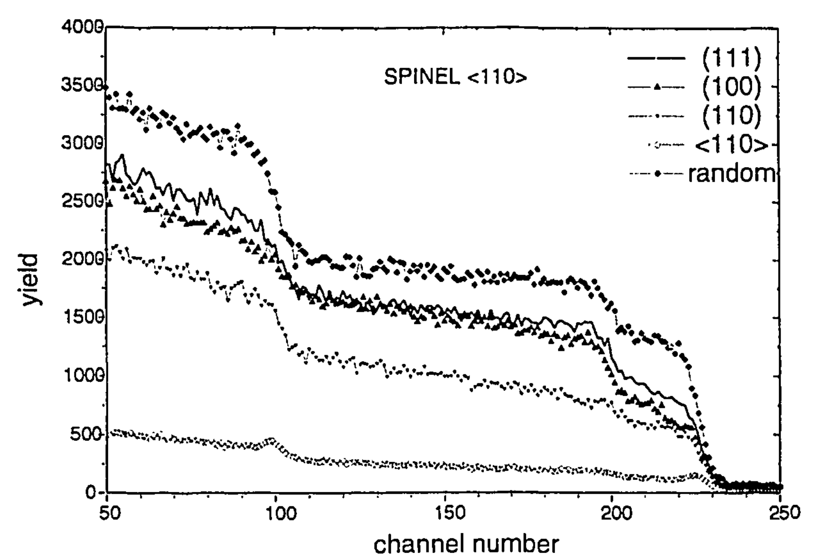

Fig.2. Random and aligned spectra for the <110> principal axis and three major planes of a spinel single crystal.

The basic work on radiation damage behavior in compound materials demands the separate analysis of lattice defects in each sublattice. We have demonstrated that ion channeling is a suitable technique for this purpose. By the judicious choice of the channeling direction the sensitivity to the atomic displacements in the chosen sublattice can be significantly enhanced.

[1] Encyclopedia of Materials Sc. and Engineering, Vol.6, M.B.Bever Ed., (Pergamon Press, 1986) p.4543.

[1] Centro Nazionale per la Ricerca e lo Sviluppo dei Materiali,CNRSM, Brindisi, Italy
[2] Università degli Studi di Padova, Padova, Italy
[3] European Institute for Transuranium Elements, Karlsruhe, Germany

3.5 AES Investigations of Al-Mo Glassy Metals (joint effort with the Institute of Physical Chemistry of the Polish Academy of Sciences, Warszawa)

by M.Janik-Czachor[1], A.Wołowik[1], Z.Werner

The passive properties of Al-Mo metallic glasses obtained by sputter deposition have been studied. A stable passivity of these alloys has been found over a wide range of potential. The value of E'_{np} has increased by about 1200 mV with respect to pure Al. The AES measurements revealed the presence of Al^{ox}, Mo and O in the passive film. The advantageous effect of Mo is attributed to its presence in the passive film (which increases the film stability) and possibility of formation of insoluble chlorides which reduce the concentration of active Cl^- ions at the surface.

[1] The Institute of Physical Chemistry, Polish Academy of Sciences, Warsaw

3.6 Dosimetry for Radiotherapy

by J.Kula, S.Marjańska and S.Pszona

The DM90 model therapy dosemeter is designed for use in medical physics departments for calibration dosimetry and quality assurance purposes. Two channel system, rich in measuring algorithms, provides accurate and fast measurements of the basic dosimetric data. The statistic algorithms for variance and covariance determination are very useful in quality assurance in dosimetry.

Owing to the use of a microcomputer and internal, high quality charge digitizer, the type DM90 dosemeter has excellent instant and long term stability. The ionization chambers calibration factors are read by a microcomputer through an easy coded plug on the front panel of DM90 and displayed on CRT. This plug is constantly controlled by the system and then it is taken out the dose/dose rate measurements stop.

The DM90 realizes measurement of charge dose, dose rate and time, simultaneously in two channels with independent time, temperature, pressure and free correction factor settings. It can be also used for two channel measurements: when the ratio of currents is indicated or when dose from one channel is normalized to the charge of the second.

The two channel system enables the DM90 to provide specialized programs for automatization of the saturation correction factors and polarization factors measurements. With these algorithms the correction factors are determined within 90s, as compared with hours, with the conventional methods.

Finally, the statistical programs for variance-covariance determination, are the very powerful tools for quality assurance in dosimetry.

Specifications

channel A			channel B		
for N_K = 0.1 Gy/nC			for N_K = 0.1 Gy/nC		
dose	0.0001	- 999.9 Gy	dose	0.0001	- 999.9 Gy
dose rate	0.0001	- 15 Gy/min	dose rate	0.0001	- 6 Gy/min
charge	0.05 pC	- 9999 nC	charge	0.02pC	- 999 nC
current	0.0001	- 2499 pA	current	0.0001	- 999.9 pA

Resolution

channel A		channel B	
charge	0.05 pC	charge	0.02 pC

Accuracy

dose	0.5% plus calibration accuracy
charge	0.5% in the range 0.2 - 9999 nC
Input leakage	< 0.05 pA
Linearity	< 0.1%
Temp. stability	< 0.01%/ °C
Internal high voltage	± 250 V, programmable changed during polarization and saturation correction factors determinations.

Accessories

Therapy level ionization chambers:
- Air equivalent, 0.3ccm, cylindrical, general purposes, model KP03C for medium and high energy photons.
- Water equivalent, 0.3ccm, cylindrical, for medium and high energy gamma radiation, model KRT03C.
- Water equivalent, 0.2ccm, flat, for electrons, model KRT03P.

Radiation protection level ionization chambers:
- Tissue equivalent 80ccm, cylindrical, model KRT80C.
- Tissue equivalent 160ccm, cylindrical, model KRT160C.

Check sources

Two types check sources containing radioactive - Sr90-Y90, 150 MBq, are available, i.e. type C for cylindrical chambers and type U for flat and cylindrical chambers.

Phantoms
- **Solid phantom** made of PMMA, model FSG, for comparative measurements in X-ray and gamma ray beams.
- **Solid phantom** made of PMMA, model FSE, 300x300mm flat plates of different thicknesses, for measurements in electron and photon beams.
- **Water phantom,** model FW, with a detector in fixed horizontal position.

3.7 Nanodosimetry*)

by S.Pszona

The experimental set up "JET COUNTER" [1] is under reconstruction toward the new experiment in which the relative frequency of creation of different number of ions created by low energy electrons in the simulated nanometer sites will be investigated. At present the shape of a gas jet is studied by the attenuation method using monoenergetic electrons in the range of 700eV. For this purpose the electron gun EG and a channeltron CH were installed inside the interaction chamber as is shown in Fig.1. The operation of JC in this experiments is as follows: when a pencil beam of electrons is switched on, the channeltron CH is detecting them and the signals are counted on a multiscaler, then the valve PZ is opened for 600 μs which is seen on multiscaler by its attenuation effect. By deflecting the electron beam and corresponding moving of a channeltron the shape of the pulsed gas jet is investigated.

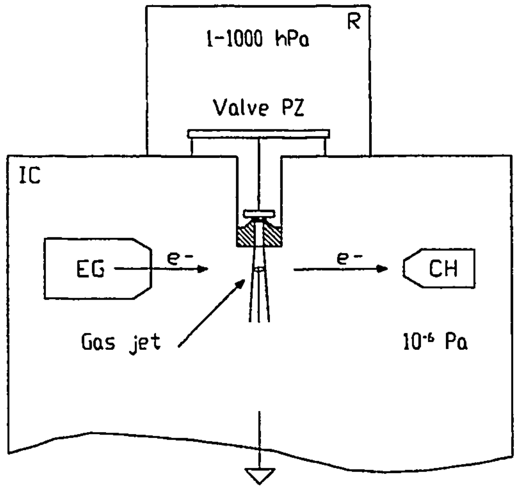

Fig.1. Schematic view of the Jet Counter.

[1] S.Pszona, Rad.Prot.Dos. 52, No 1-4, p.427, (1994)

*) Work supported by CEC under subcontract ERBCIPD CT 930407.

3.8 Photon Fields Above an Air-Ground Interface

by K.Wincel and B.Zaręba

Data file with gamma-ray energy distributions in air was generated based on results of one dimensional transport calculations. It contains energy distributions of the photon density flux above infinite plane isotropic sources of monoenergetic gamma-ray with energies of 0.30 MeV, 0.65 MeV, 1.25 MeV, 3.5 MeV and 4.5 MeV.

The numerical code WIDMA was written to convert the output from code ANISN (Multigroup One Dimensional Discrete Ordinates Transport Code with Anisotropic Scattering) into simple form. This form can be directly used as an input of graphics codes such as Harvard Graphics or Quatro Pro. Code WIDMA was written in Turbo Pascal 6.0 for DOS operating system.

3.9 Nuclear Cross Sections for Radiation Transport

by V.S.Barashenkov[1] and A.Polański

In order to calculate the constants for high energy particles transport, a standard program calculating hadron and nucleus-nucleus cross-sections at energies exceeding 14 MeV/nucleon has been developed [1, 2].

The hadron-nucleus (pion-nucleus, nucleon-nucleus) cross-sections are obtained, by means of interpolation between evaluated experimental data at target charge numbers Z>3 and energies from 14 MeV up to 1 TeV. The nucleus-nucleus cross sections are calculated with the help of an approximation formula with fitted coefficients at energies above several MeV/nucleon. A set of all available experimental total hadron-nucleus cross-sections at energies exceeding 14 MeV and plots of evaluated total, inelastic and elastic cross sections for pion and nucleon interactions are presented in [3]. Two methods have been employed to calculate the energy dependence of cross-sections. At high energies, where the projectile de Broglie wave length is significantly smaller then the size of the target nucleus the quasioptical model is used. The parameters of the model have been fitted to obtain the best agreement of calculations with experimental data. The high-energy region has been divided into separate intervals with a characteristic behaviour of cross sections. A set of parameters has been defined for each interval. Phenomenological approximation of cross sections was used at lower energies [3].

[1] V.S.Barashenkov, A.Polański, Electronic Guide for Nuclear Cross Sections, JINR Preprint E2-94-417 Dubna, 1994 (in Russian).
[2] V.S.Barashenkov, G.F.Gareeva, A.Polański, JINR Preprint P10-92-214, Dubna, 1992, (in Russian).
[3] V.S.Barashenkov, Cross-Section of Particle and Nucleus Interactions with Nuclei, JINR, Dubna, 1993 (in Russian)

[1] Joint Institute for Nuclear Research, Dubna, Russia.

3.10 Low-level neutron monitoring[*]
by S.Pszona

There are number of tasks of practical radiation protection where low-level neutron radiation fields in have to be monitored, the main of them being:
- neutron monitoring of the workplace where the sensitivity of personal monitoring is inadequate and where the personal exposures have to be evaluated based on the field measurements;
- neutron monitoring around large radiation facilities where estimation of doses received by workers outside of the controlled areas at level comparable to natural neutron background has to be evaluated;
- neutron monitoring on board of the passenger airliners to monitor the exposure of the air crews to galactic and solar cosmic radiation interacting with the atmosphere.

Three detectors, two spherical proportional counters and ionization chamber, all filled with ^{3}He to pressures of 160kPa, 325kPa and 1 MPa, respectively have been experimentally studied with respect to using them for low-level neutron monitoring. A summary of technical data is shown in Table 1. The responses and energy resolutions of these detectors are summarized in Table 2.

Data for a conventional rem counter of the type NM2 monitor (NE) have been included for comparison. It has been shown that spectrometrical treatment of the signals from these detectors gives not only high sensitivity readings with regard to the ambient dose equivalent but also improves the quality of the measurements. The results of these measurements are summarized in Table 3. The background pulse rates were expressed in readings of the ambient dose equivalent rates when the system was calibrated with a Pu-Be neutron source.

For comparison of the studied detectors the ratio n^2/b has been calculated as a factor of merit; where n is the number of counts corresponding to $10nSv\,h^{-1}$ and b is the number of the background pulses per hour. As shown in Table 3 the background readings of the proportional counters and ionization chamber are extremely low.

The sensitivity of the detectors, numerically equal to lower detection limit, have been here defined as equal to the background readings are better than satisfactory, as seen in Table 3. This is also indicated by the calculated the so called Factor of Merit (which is used for comparison of low-level counting equipment). Finally, the question of the selection of a detector for application with a prototype of an instrument for low-level neutron monitoring has been solved by choosing 160kPa counter as sufficiently sensitive but also having lowest high voltage bias. As seen from Table 3. the lower detection limit in terms of the ambient dose equivalent rate is 1.7nSv per 24h.

A special instrumentation for low-level neutron monitoring is devised. A prototype of the instrument, ordered specially for this work, is able of pre-amplifying signals from proportional counters, shaping them for accurate peak detection, digitizing peak amplitude and maintaining a 256 channel histogram on 64x256 LCD graphic screen. This histograms together with other parameters as HV bias of a detector, astronomical time and measurement time can be stored on a battery powered 64kB SRAM Card (PCMCIA) which makes all saved data non-volatile. Steering and control functions are performed by a H8/532 microprocessor programmed with Forth language. Data processing function allows: viewing of the stored data as number of counts per channel or as a pulse height spectrum, finally send a selected data stored in 120 bank SRAM Card to a printer or PC computer by an RS-232 communication interface. The measuring time can be selected in 1s steps up to 24 hours and up to 120 cycles.

Table 1. Characteristics of the detectors under study.

Detector	Technical data
240 G	160kPa ^{3}He, 53kPa Xe, spherical 40mm dia.
440 G	325kPa ^{3}He, 170kPa Xe, spherical 40 mm dia.
FNS-1	1MPa ^{3}He, cylindrical 50mm diax150mm

Table 2. Resolution and response data for the detectors.

Detector	Response Sv^{-1}	Resolution %
240 G	$9.3 \cdot 10^9$	17
440 G	$15.4 \cdot 10^9$	40
FNS-1	$77.5 \cdot 10^9$	2.7

Response of a NM2(NE) neutron remmeter: $0.9 \cdot 10^9 Sv^{-1}$

Table 3. Comparative data of the detectors.

Detector	Background rate [nSv/24h]	Factor of Merit [n^2/b]
240 G	1.7 ± 0.5	86
440 G	1.6 ± 0.3	237
FNS-1	0.6 ± 0.1	3000

*Supported by State Committee for Scientific Research (Grant No 2 0951 9101)

3.11 Radioactive Fallout Analysis*)

by K.Wincel

Radioactive fallout resulting from radionuclide release from severe accidents at nuclear power plants and nuclear detonation has been analyzed. Also methods of aircraft measurements of radioactive fallout have been studied. To better understand aircraft measurements photon spectra in air were calculated and analyzed for three fallout patterns. Values of height above which mean energy of spectra becomes constant, were found.

*) Supported by State Committee for Scientific Research (Grant No O S001 013 04)

3.12 Flue Gas Treatment by Electron Beam: Internal Electron Beam Monitor and Calculation of the Spatial Dose Distribution in the Reaction Chamber.*)

by E.Kulczycka, M.Kisieliński, Z.Moroz, T.Pławski, M.Sowiński, J.Wojtkowska

A prototype of the internal electron beam monitor for the irradiation chamber was constructed and preliminary tested at EB flue gas treatment pilot plant in Kawęczyn power station. The schematic view of the reaction chamber with the monitor installed as well as the construction of the beam monitor are shown in Fig.1 and its insert, respectively.

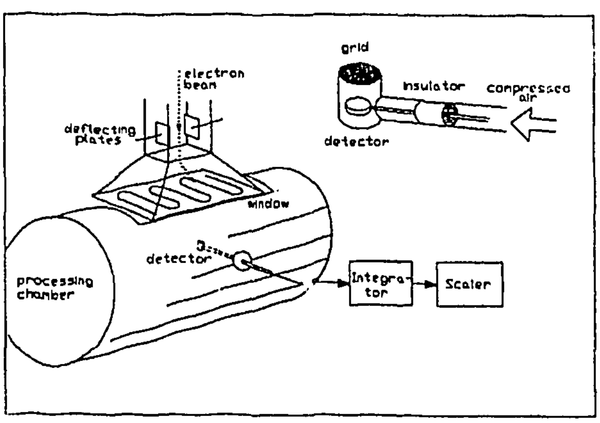

Fig.1. General view of the reaction chamber

The prototype monitor consists of a metal probe collecting the beam charge which is further electronically converted to the signal frequency and then integrated by a standard scaler. The probe is shielded by a metal tube and sees the electron beam only through a brass mesh window. To shield the probe from heavy dust present in the reaction chamber an air stream under a pressure of 2 atm is blown through the metal tube.

The monitor was tested in two runs. In the first one, seven days long, the monitor was the flue gas inside the reaction chamber treated by water and ammonia, irradiated by 25 mA 800 keV electron beam. The aim was to study the resistance of the monitor for long term irradiation in the reaction chamber. In the second one, with the chamber filled with the atmospheric air only and irradiated by 500 - 750 keV electrons (0-30 mA), the aim was to study the performance of the electronics.

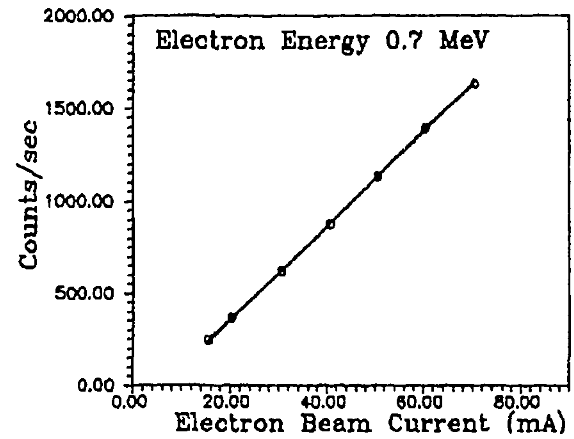

Fig.2. The dependence of signal frequency on electron beam current.

After the 1-st run, within 10% accuracy, no signifficant change of the electric signal from monitor was found. In Fig.2 the linearity of the signal frequency from the monitor vs. electron beam current at 700 keV is presented.

These preliminary experimental results are considered by us as quite satistactory.

To calculate the spatial dose distribution in the reaction chamber when irradiated by the electron beam, the suitable Monte Carlo program DSHAPE was written. It includes effects of the energy absorption by the titanium entrance windows, backscattering of the electrons from the entrance windows, electron energy loss in the gas inside the chamber and multiple scattering of electrons in the windows and the gas medium.

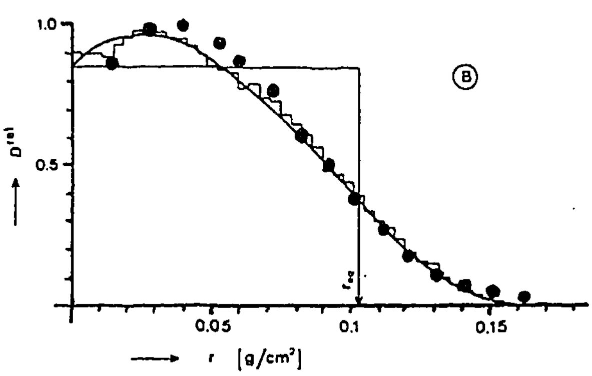

Fig.3. Dose depth distribution

The results of the calculations were compared with experimental data published by Proksch et al [1] for 500 keV electron beam. The corresponding depth profile of the dose is shown in Fig.3. The histogram presents the experimental data while full black circles are our calculated values normalized to unity at r=0.02 g/cm^2.

It is seen that in this approximation an agreement of experimental and calculated values is very good.

[1] E.Proksch et. al. Int. Journ. Appl. Radiation and Isotopes, vol 30, p 279 (1979)

*) This work was supported by State Commitee for Scintific Research (Grant No 209859101/po3)

3.13 Modelling and Control of the e-Beam Process in Flue Industrial Gases.*)

by J.Boużyk, M.Sowiński

The monitoring and control system for a e-beam flue gas treatment pilot plant was presented in the previously published papers [1,2]. The developed system is coupled with automatized industrial process and is used for collecting readings from the analytical units of the plant. Having information on the process variables at the input and output of the process vessel an optimization of the quality coefficient reflecting costs of the e-beam process is actually developed. The analysis of the e-beam process shows that the process variables such as temperature of gases and their humidity, ammonia stechiometry addition, inlet concentrations of SO_2 and NO_x removal efficiencies are in some cases acting against each other. Especially "thermal phase" of SO_2 removal and ammonium salts formation are sensitive to the e-beam process parameters and their variations should be controlled by an optimized process function based on the process model of an accessible accuracy. The first approximation of the real e-beam process was done by the elaborated simplified model [3]. Assuming in the time range most affective for NO_x and SO_2 degradation in the e-beam process:

- a quasi-stationary level, of the radical concentrations,
- an amount of main components of flue gases to be nearly constant in respect to fast changes of a small concentration of NO_x and SO_2,
- chemical reactions with NO and NO_2 as the essential link between the primary species and the nitric acid conversion to ammonium salts,
- SO_2 oxidation (without "thermal phase") to be main, quasi-one-molecular chemical reaction chain in SO_2 removal process

the algorithms describing NO, NO_2 and SO_2 concentration changes in the homogeneous gas-phase of the e-beam process have been elaborated. In Fig.1, the compiled results of test calculations are shown. Relatively simple and flexible relationships obtained in this approach are designed for the preliminary estimation and diagnostics in an on-line control of radiation cleaning of flue gases. The elaborated model represents a class of models assisting a control process. The controlled parameters are time constants of the e-beam process. These lumped parameters will be estimated using data from pilot plants to approximate better the simplified model to the real e-beam process. Generalized simplified model will be used for simulating the e-beam process in a computer control system. In Fig 2 the example of a possible use of the simplified model in such a control system is shown.

[1] J.Szlachciak et at., Radiat.,Phys.Chem. 40,341,1992
[2] T.Pławski,M.Sowiński, SINS Annual Report 34,1993
[3] J.Boużyk,M.Sowiński, SINS Report No 7/II/1994
[4] J.Boużyk,M.Sowiński,to be published in SINS Report

*) This work is supported by State Committee for Scientific Research (No 209859101/p03)

3.14 Emission of Negative Ions from the Tubular Ioniser

by T.Kozlowski, M.Laskus and A.Piotrowski

Since the tubular ioniser was developed at Dubna and Livermore the high temperature cavity has been known as an efficient positive ion source for radioactive elements. Certain efficiency of this kind of the ion source is expected for negative ions and the aim of this work was to study this possibility.

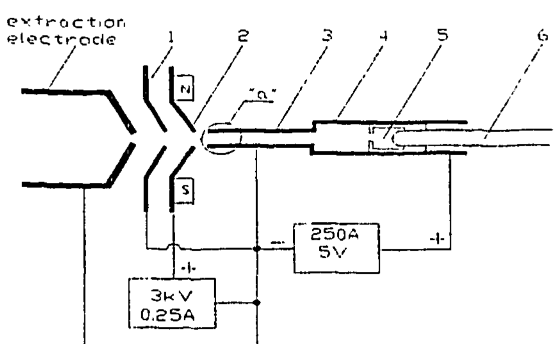

Fig.1. Schematic diagram of the ion source. 1 - ground electrode, 2 - electron filter, 3 - ioniser, 4 - transfer line, 5 - Knudsen cell, 6 - thermocouple.

The principle and construction of the ion source is schematically shown in Fig.1. A tubular emitter made of tungsten or tantalum (in which a LaB_6 cylinder can be inserted in place "a") is mounted on one end of a tantalum transfer line and is heated by an AC current up to 250 A. The ioniser temperature was measured using an optical pyrometer. The ionised material is loaded in the Knudsen cell to evaporate at controlled temperatures measured by a thermocouple. The negative ions and electrons are extracted by means of two extracting electrodes and electrons are deflected by an magnetic electron filter. The perpendicular magnetic field of 40 mT was obtained by permanent magnets.

This source was installed on a versatile low energy mass separator [1] and the negative ions were accelerated up to 30 keV and mass analysed with the resolving power of 700 (FWHM). The collector chamber contained a beam diagnostic system: a mechanical scanner and a Faraday cup with the sensitivity better than 1 pA. The measurements were carried out in a vacuum of 7×10^{-7} Torr and the transmission efficiency was close to100% for 30 keV ions.

A standard ISOLDE type tung sten emitter was applied with an inner diameter of 3 mm and a length of 30 mm heated up to 2500^0 K. First tests were performed with a pure NaCl powder in the Knudsen cell and the negative ions of H^-, O^-, Na^-, Na_2^- and Cl^- were observed. The efficiency of the source for Na^- and Cl^- defined as the ratios of the measured currents to the number of molecules emitted from the Knudsen cell is shown on Fig.2 and compared to the efficiencies on the hot surface given by the Saha - Langmuir formula.

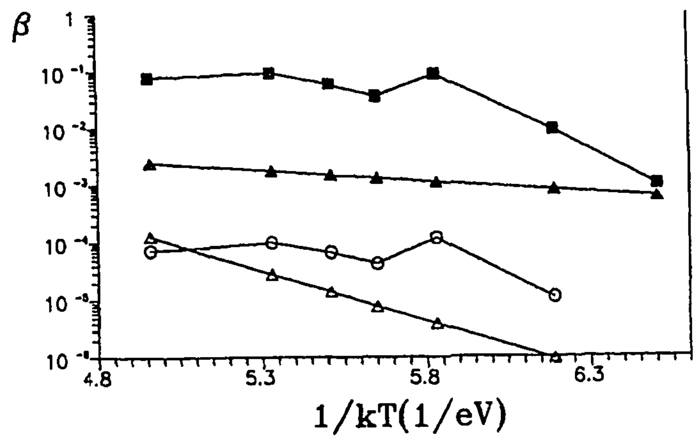

Fig.2. The experimental (■ - for Cl, o - for Na) and the theoretical (▲ - for Cl and △ - for Na multiplied by 10^5) efficiencies of the tungsten ioniser.

The experimental efficiency for Cl^- is by one order and for Na^- by five orders of magnitude higher than expected for the temperatures above 1800^0 K. It shows clearly that in the tubular ioniser the production of negative ions is strongly enhanced but a definite explanation requires further studies.

By adding a small amount of barium to the salt it was possible to check the effect of lowering of the ioniser work function. For the number of evaporated Ba atoms roughly equal to the number of NaCl molecules the efficiency for Cl^- reached 100% and currents of these ions up to 30 μA were observed.

[1] T. Kozłowski,M.Laskus,A.Piotrowski and A.Sulik, SINS Ann.Rep. 1993 p.33

3.15 Radioactive ground-level air pollution in the vicinity of Świerk in 1994

by E.Droste, M.Matul, S.Mikołajewski, B.Mysłek-Laurikainen, H.Trzaskowska

In 1994 the routine environmental air monitoring using a high volume air sampler ASS-500 was performed as a continuation of the systematic measurements started in 1991 (see Annual Report 1992, 1993). The aerosol sampling station ASS-500 is placed 6 km West from Świerk at the Geophysical Observatory of the Polish Academy of Sciences, Świder near Otwock, where the study of air properties are done since 70 years.

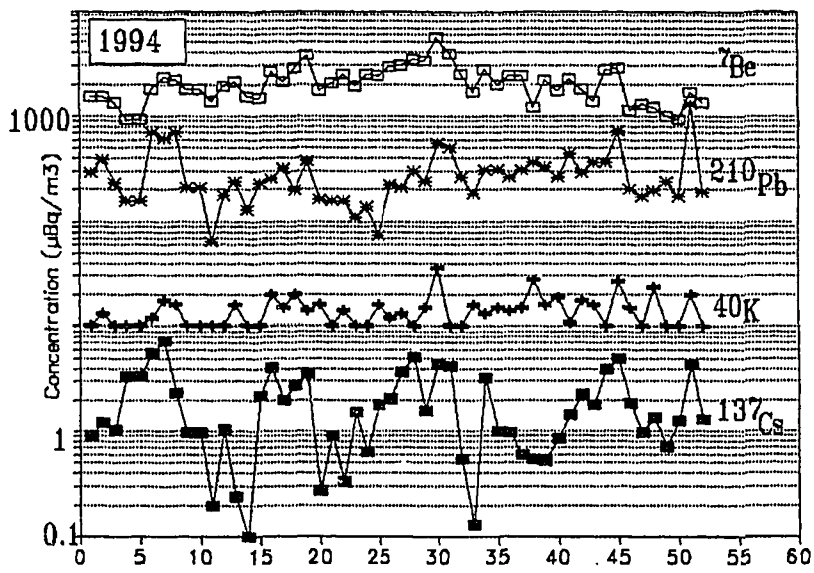

Fig.1. The weekly changes of 7-Be, 210-Pb, 40-K, 137-Cs concentration in air in 1994 at Świder

This station belongs to the aerosol sampling station network supervised by Central Laboratory for Radiological Protection. Air aerosols with size > 0.3 μm are collected on Petrianov filter type FPP 15-1.7.

The average air flowrate ~350 m^3/h collects the dust from about 60000 m^3 of air in a week. The amount of air dust is determined by weighting filter before and after sampling expose.

Fig.1 presents the concentration of 7-Be, 210-Pb, 40-K, 137-Cs in collected aerosols in 1994. The amount of dust collected of Świder depends strongly on seasons changes and is lower than in Warsaw. Fig 2. shows the dust concentration for Warsaw-Żerań and Świder.

The corellation between heatingseason and the amount of dust collected on the filter is visible. On the basis of this measurements one can see that the contribution of radioactivity of post-Charnobyl origin to the total inhalated dose is negligible small, but the role of 210-Pb becomes most important. In order to determine the 210-Pb circulation the measurements of its content in water, soil and plants were performed, and the more extensive study are in progress.

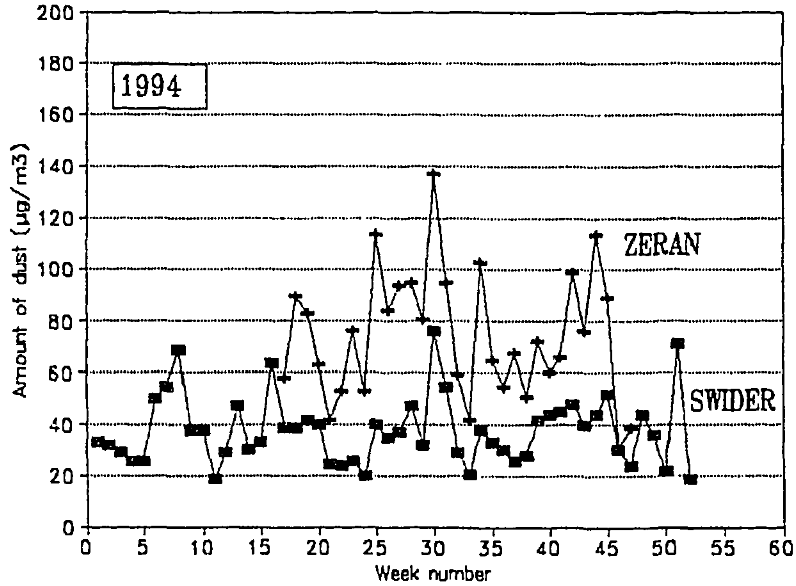

Fig.2. The comparison of the weekly changes of dust concentration at Świder ASS-500 station located in the forest with the data of Warsaw-Żerań station placed near to coal electric power station.

3.16 Mobile Laboratory for Controlling and Monitoring Atmospheric Pollution

by A.Kazimierski, J.Pracz, Z.Sienkiewicz

A set of 9 Mobile Laboratories was made by Experimental Establishment for Nuclear Equipment (ZDAJ) in cooperation with the Italian firm Strumentatione Elettronica Avanzata (SEA). The laboratory is destined for air pollution monitoring both in imission and emission mode. It consists of SO_2, NO_x, CO, CO_2, TNMH, and O_2 analyzers, gas chromatograph, METEO Sensors and additional equipment necessary for measuring procedure, data processing, acquisition and recording [1].

The 1994 was the first year of Mobile Laboratories' exploitation. A lot of measurements have been done covering the distance of about 10.000 km.

The Mobile Laboratories appeared to be very useful to perform a lot of specific tasks; some of them are summarized below:

- **Area Monitoring** - periodic analysis of select location in order to produce data on the concentration and diffusion of pollutants
- **Environmental Impact Verification**
- **Emergency Management** - pollution resulting from industrial accidents can be monitored, particularly during the evolution phase
- **Site Selection for Fixed Monitoring Stations** - data produced by a-priori surveillance of specific sites are an indispensable support for the planning and locating of fixed stations.

Some results of the air pollution concentration measurements are shown in the figures below. The measurements have been corried out in various places of the city of Warsaw on April 20-24, 1994.

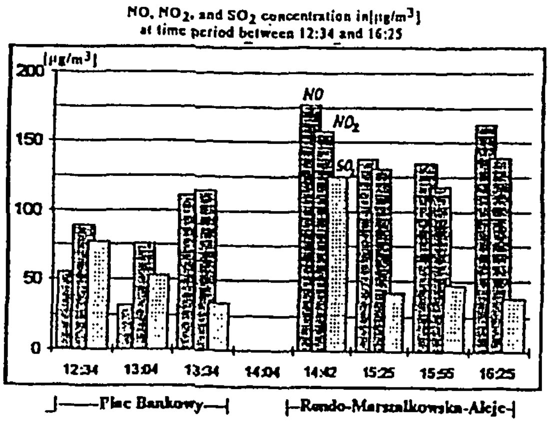

Fig.1.

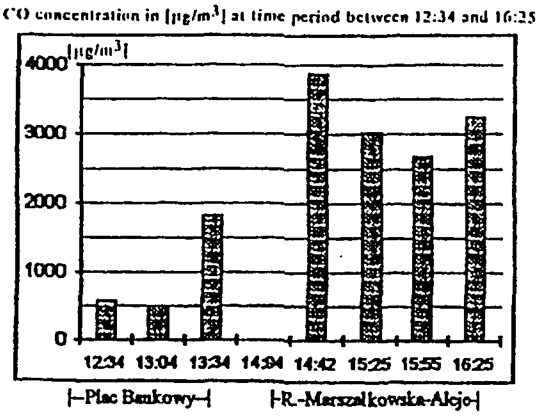

Fig.2.

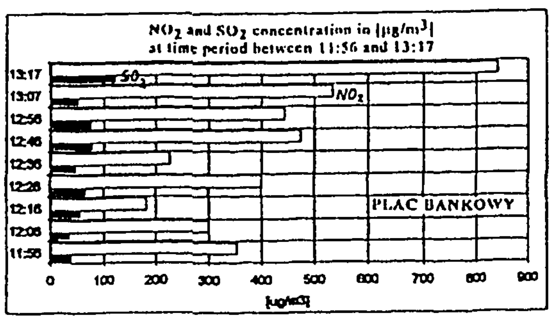

Fig.3.

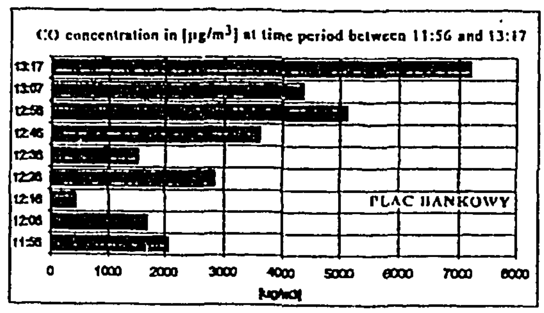

Fig.4.

[1] A.Kazimierski, J.Pracz. A Mobile Laboratory for Air Pollution Monitoring, SINS Annual Report, Otwock-Świerk 1993 pp 39-44

B. PARTICLE PHYSICS AND COSMIC RAY PHYSICS

1. PARTICLE AND HIGH ENERGY PHYSICS (THEORY AND EXPERIMENT)

1.1 Neutron Haloes in Heavy Nuclei

by J.Skalski, R.Smolańczuk, S.Wycech

A Warsaw-Münich experiment at CERN (PS203) was completed. The aim was to analyse and identify nuclei formed in antiproton nuclear absorption from antiproton atomic states. This allows us to determine the neutron/proton ratios at extreme nuclear peripheries. Several examples of neutron haloes were found [1]. Theoretical aspects of this reaction were analysed.

New CERN proposal (PS209) to measure additional X rays in the atoms of interest was accepted [2].

[1] P.Lubiński, J.Jastrzębski, A.Grochulska, A.Stolarz. A.Trzcińska, W.Kurcewicz, F.J. Hartmann, W.Schmid, T.von Egidy, J.Skalski, S.Smolańczuk, S.Wycech, D.Hilscher, D.Polster and H.Rossner, Phys. Rev. Lett. 73(1994)3199

[2] Letter of Intent CERN, Proposal, CERN 1994 - X ray transition in antiprotonic atoms Spokesman, J.Jastrzębski

1.2 Collinear Asymptotic Dynamics for Massive Particles

by J.Boguszyński, L.Łukaszuk, L.Szymanowski

The dynamics of massive particles in the collinear high momentum regime has been investigated. Methods hitherto exploiting large time asymptotic Hamiltonians in the Dirac picture for the treatment of infrared divergences have been adapted to the collinear asymptotic dynamics. [1]

[1] J.Boguszyński, H.D.Dahmen, R.Kretschmer, L.Łukaszuk, L.Szymanowski, submitted to Zeit. für Physik C

1.3 A Higgs-Free Model for Fundamental Interactions and its Implications

by M.Pawłowski and R.Rączka

A model for strong, electroweak and gravitational interactions based on the local symmetry group $G=SU(3) \times SU(2)_L \times U(1) \times C$ where C is the local conformal symmetry group is proposed. The natural minimal G-invariant form of total lagrangian is postulated. It contains all Standard Model fields and the gravitational interaction. Using the unitary gauge and the conformal scale fixing conditions we can eliminate all four real components of the Higgs field in this model. In spite of that, the tree level masses are automatically generated and are given by the same formulas as in the conventional Standard Model. In this manner one gets mass generation without the mechanism of spontaneous symmetry breaking. We calculated in this model the predictions for a series of electroweak observables and we show that they are in agreement with experimental data. The gravitational sector of the model is also analyzed and it is shown that the model admits in the classical limit the Einsteinian form of gravitational interactions.

[1] M.Pawłowski and R.Rączka, Found. of Phys. 24 (1994) 1305; M.Pawłowski and R.Rączka, Bull. Boarad: hep-ph 9403303

1.4 Conformal Space-Times - the Arenas of Physics and cosmology
by A.O.Barut, P.Budinich, J.Niederle and R.Rączka

The problem of properties of conformal space-time was analysed in detail. The group - theoretical classification of conformal space-times was considered and non-trivial geometrical and topological structures were investigated in detail. The very interesting application of global compactified conformal space-time in cosmology was found. In particular it was shown that the periodic structure in matter distribution observed in the pencil beam experiment can be explained by the inflationary model considered in compactified conformal space time.

[1] A.O.Barut, P.Budinich, J.Niederle and R.Rączka, Foundation of Physics 24, No 11 (1994)

1.5 An Analysis of Mean Life and Life Time of Unstable Elementary Particles
by J.Bogdanowicz, M.Pindor and R.Rączka

The new analysis of a concept of life time and mean life was found. The new analytic formulas for mean life as the function of the decay width Γ and the mean mass m was derived for Breit-Wigner and Matthews-Salam energy distributions. It was shown that for unstable particles with larger width like ρ-meson the deviation of the exact formula from the generally accepted mean life $\tau=\Gamma^{-1}$ is significant.

[1] J.Bogdanowicz, M.Pindor and R.Rączka, Foundation of Physics 25, No 6 (1995)

1.6 Effective Action for Multi-Regge Processes in QCD
by R.Kirschner, L.N.Lipatov, L.Szymanowski

We construct the effective Lagrangian describing QCD in the multi-Regge kinematics. It is obtained from the original QCD Lagrangian by eliminating modes of gluon and quark fields not appearing in this moderlying kinematics.

[1] R.Kirschner, L.N.Lipatov, L.Szymanowski, Nucl. Phys. B425(1994)579

1.7 Symmetry Properties of the Effective Action for High-Energy Scattering in QCD
by R.Kirschner, L.N.Lipatov, L.Szymanowski

We study the effective action describing high-energy scattering processes in the multi-Regge limit of QCD which should provide the starting point for a new attempt to overcome the limitations of the leading logarithmic and the eikonal approximations. The action can be obtained via simple graphical rules or by integrating in the QCD functional integral over momentum modes of gluon and quark fields that do not appear explicitly as scattering or exchanged particles in the processes considered. The supersymmetry is used to obtain the terms in the action involving the quark field from the pure gluonic ones. We observe a Weizsäcker-Williams type relation between terms describing scattering and production of particles.

[1] R.Kirschner, L.N.Lipatov, L.Szymanowski, Phys. Rev. D, January 15, 1995

1.8 Beam Jets and Central Fireballs
by G.Wilk

We have constructed a new Monte Carlo event generator for high energy multiparticle collisions of hadrons and nuclei with special emphasis on distinguishing between the production (and hadronization) of the so called *beam jets* and central "mini-fireballs". The first are carrying all quantum numbers of projectiles and produce secondaries in *a coherent* way whereas the second emerge as a result of strong interaction of gluonic clouds of colliding hadrons and produce secondaries in a *chaotic* way. [1] The resulting event generator thus provides, for the first time, a description of both *coherent* and *chaotic* features of high energy multiparticle production processes [1].

[1] U.Ornik, R.M.Weiner and G.Wilk, Nucl. Phys. A566 (1994) 469c-472c

1.9 Fluctuations in Cosmic Rays Continued
by G.Wilk

We have demonstrated that unexpected non-exponential behaviour of some cosmic ray data are just manifestation of cross section fluctuations discussed recently in the literature and observed in nuclear *collisions and in the diffraction dissociation experiments on accelerators [1].*

[1] G.Wilk and Z.Włodarczyk, Phys. Rev. D50 (1994) 2318-2320

1.10 Interacting Gluon Model with Hadronization
by G.Wilk

We extend our previous analysis concerning the behaviour of inelasticity (with production of mini-jets included) at high energies and discuss the effects of the hadronization process on this quantity. We analyze also the UA5 and UA7 data on rapidity distributions [1].

[1] F.O.Durães, F.S.Navarra and G.Wilk, Phys. Rev. D50 (1994) 6804-6810

1.11 Bose-Einstein Correlations
by G.Wilk

The (so called: Bose-Einstein) correlation data for identical K-mesons production in S + Pb collisions at 200 GeV/c were analysed with special emphasis on the corrections due to the long-range *corresponding interaction ranges* (as given by the mean square roots R_{rms} are respectively: $R_{rms}(K^-K^-) \simeq (5.2 \sim 6\text{ fm}) \leq R_{rms}(K^+K^+) \approx (7 \sim 7.5\text{ fm})$. This suggests that in nuclear collisions the anti u-quarks are produced in smaller space regions that the u-quarks [1].

[1] M.Biyajima, T.Mizoguchi, Y.Nakata and G.Wilk, accepted by Prog. Theor. Phys. (December 1994)

1.12 Experiments with Relativistic Heavy Ions at CERN
by H.Białkowska

The analysis of data from the NA-35 experiment, using both a streamer chamber and a Time Projection Chamber concentrated on the following topics:

1. A comprehensive study of energy distribution between various particles produced in central nuclear collisions [1]. The energy balance is consistent with strange particle and anti-baryon production enhancement.
2. A comparative investigation of strange particle production in central SS, SAg and SAu collisions [2]. Data from various target and magnetic field configurations enable a wide coverage of phase space available for particle production. The observed strangeness enhancement, observed both in SS and SAg collisions is analysed in terms of extra produced ss pairs. About 30 and 28 additional ss quark pairs are produced in SS and SAg collisions respectively. Fig. 1 shows the rapidity distibution of extra produced Λ and K^0 particles.
3. The transverse source size has been studied for SS, SCu, SAg and SAu collisions as a function of transverse momentum [3].
4. Antiproton production is studied by means of deconvolution of the dE/dx signal from Time Projection Chamber. The information will be of crucial importance for the study of dense hadronic matter.

A large part of our activities was directed at the preparation for the autumn 1994 run of 160 GeV/N Pb ions in the NA-49 experiment, both in detector construction and software [4]. The run was carried out in November/December 1994.

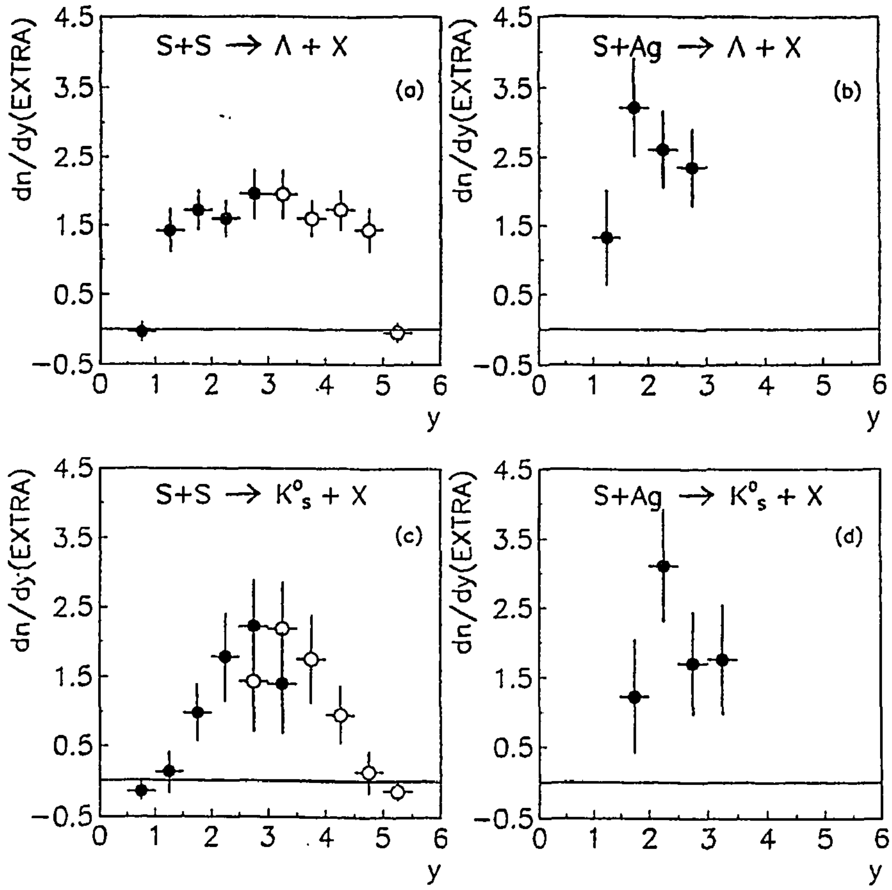

Fig.1. Rapidity distributions of extra strange particles produced in central nuclear collisions.

[1] J.Bächler, H.Białkowska et al., Phys. Rev. Letters 72(1994)1419
[2] T.Alber,H.Białkowska et al., Z. Phys. C64(1994)195
[3] R.Morse, H.Białkowska et al., Submitted to Phys. Rev. Letters
[4] T.Alber, H.Białkowska et al., JEEE Transactions on Nuclear Science 41(1994)30

1.13 DELPHI Experiment in 1994

by R.Gokieli, M.Górski, R.Sosnowski, M.Szczekowski, M.Szeptycka, P.Szymański, P.Zalewski

In 1994 the luminosity of the LEP e^+e^- accelerator at CERN increased substantially. Effective running of the accelerator and the DELPHI detector allowed accumulation of about 1.5 million of e^+e^- annihilation events with Z^0 boson production. All the components of the detector worked efficiently, and in particular the barrel electromagnetic calorimeter - HPC maintained by, among others, the Warsaw group.

The physics analysis performed in 94 on the data from the previous years can be grouped into six subjects:

1. Precise tests of the Standard Model of electroweak interactions,
2. Tests of Quantum Chromodynamics,
3. Properties of hadron production in e^+e^- annihilations,
4. Properties of hadrons with charm or beauty quarks,
5. γ - γ scattering,
6. Search for new particles,

with contributions from the Warsaw group mainly to points 3,4 and 5.

One of the most interesting results achieved in 94 is the further increase in the precision of measurements of the electroweak Standard Model parameters. The mass and width of the Z^0 boson measured from the shape of e^+e^- annihilation cross-section is shown in Fig.1 as a function of the center of mass energy reach the relative precision of $5x10^{-5}$ and $1,5x10^{-3}$, respectively.

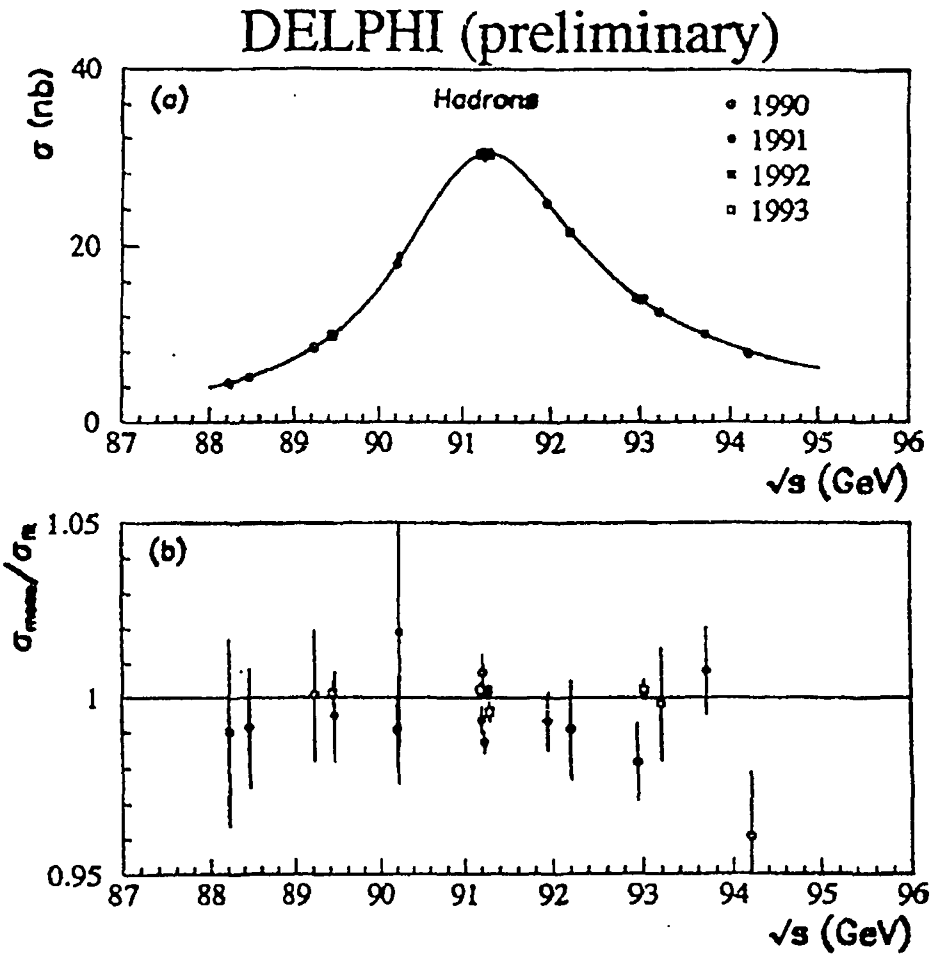

Fig.1. (a) e^+e^- annihilation cross-section as function of the center of mass energy $\sqrt{s}$.
(b) the ratio of the measured and the predicted by the Standard Model cross-sections.

Such precision allows the detailed tests of the Standard Model radiative corrections. The unknown parameters of the model - the strong interactions coupling constant, α_s and the mass of the top quark, m_t can be calculated indirectly:

$$\alpha_s = 0{,}125 \pm 0{,}005 \pm 0{,}002,$$
$$m_t = 178 \pm 11 \pm {}^{18}_{19}\ \text{GeV},$$

where the second errors reflect uncertainties due to the variation of the unknown Higgs boson mass, m_H between 60 and 1000 GeV, with the central value for the calculations m_H = 300 GeV. These results can be compared with the direct measurements of α_s (also done at LEP in the DELPHI collaboration) and with the mass of the recently discovered top quark:

$$\alpha_s = 0{,}123 \pm 0{,}006,$$
$$m_t = 174 \pm 10 \pm {}^{13}_{12}\ \text{GeV}.$$

Good agreement of indirect and direct measurements (with comparable precision) is a success of the Standard Model of elementary particles.

1.14 Observation of Two Enhancements in M(π^- pp) in the Reaction pd → π^-ppp at 1 GeV

by A.Deloff, T.Siemiarczuk

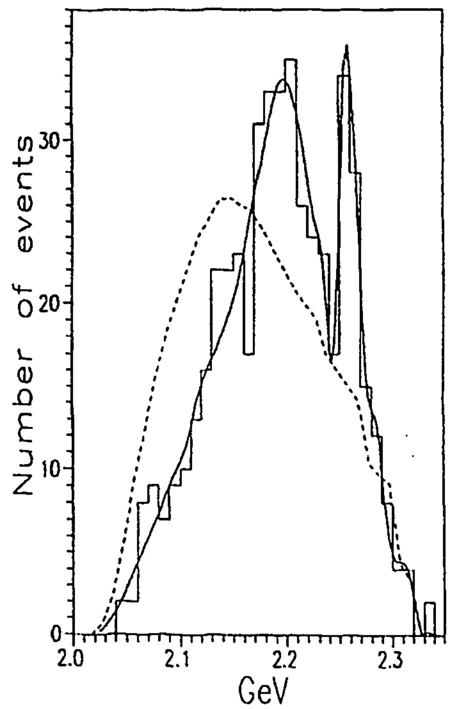

Fig.1.

The reaction pd → π^-ppp has been investigated in a line reversed hydrogen bubble chamber experiment using 3.3 GeV/c deuteron beam. The observed spectra are very well reproduced by a parameter free model based on the impulse approximation. When kinematic cuts are introduced, the effective mass distribution of the pion and the two slowest protons M(π^-pp) exhibits two narrow enhancements at 2199 MeV/c^2 (fig.1) which are not accounted for by our model and might be considered as candidates for dibaryonic resonances.

1.15 Diffractive Production of Vector Mesons in Deep Inelastic Scattering

by J.Nassalski, E.Rondio, A.Sandacz, M.Szleper

Data on diffractive production of ϱ^0, ϕ and J/ψ mesons in Deep Inelastic Scattering of muons has been published [1,2]. The experiment was carried out at CERN by the New Muon Collaboration (NMC). The ϱ^0 and ϕ data cover the range of large Q^2 (> 2 GeV^2) and were obtained with deuterinum, carbon and calcium targets. The J/ψ data extends into the lower Q^2 range (down to 0.5 GeV^2) and were collected with hydrogen, deuterium, carbon and tin.

For ϱ^0 production, the large slopes of the p_t^2 distributions for the incoherent cross sections, the approximate s-channel helicity conservation and the weak ν dependence observed in this experiment are characteristic features of diffractive processes.

In Fig. 1, the Q^2 dependence of the cross section for exclusive ϱ^0 virtual photoproduction is shown. Also shown are the EMC data on protons [3]. The errors are statistical; systematic errors are about 20%.

The solid curve represents the prediction of a model by Donnachie and Landshoff [4], in which an exchange of two nonperturbative gluons is assumed. It was calculated for the reaction γ^* p → ϱ^0p assuming the values of the virtual photon polarisation as in Ref. [3]. The dashed curve (normalised arbitrarily) represents a dependence $\propto 1/Q^6$ predicted by the models [5]

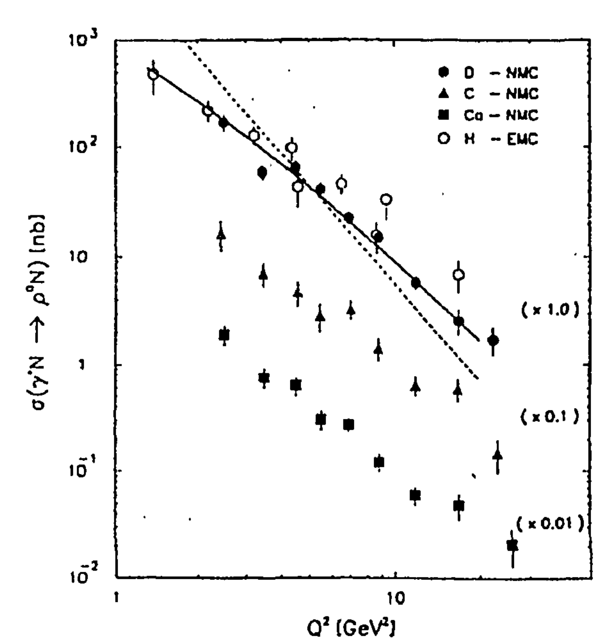

Fig.1.

for large Q^2. The measured total cross sections for the process $\gamma^* N \rightarrow \varrho^0 N$ as a function of Q^2 can be parametrised by a function $\propto 1/(Q^2)^\beta$ with β close to 2.

The total cross sections per nucleon for ϱ^0 virtual photoproduction are consistent with no A dependence. Nuclear effects are seen in the nuclear transparencies for carbon and calcium (for the ϱ channel), which are significantly below unity.

The nuclear transparencies are shown in Fig.2 in which the preliminary results of the experiment E665 [6] are also displayed. The curves are predictions of the colour transparency model of Ref. [7].

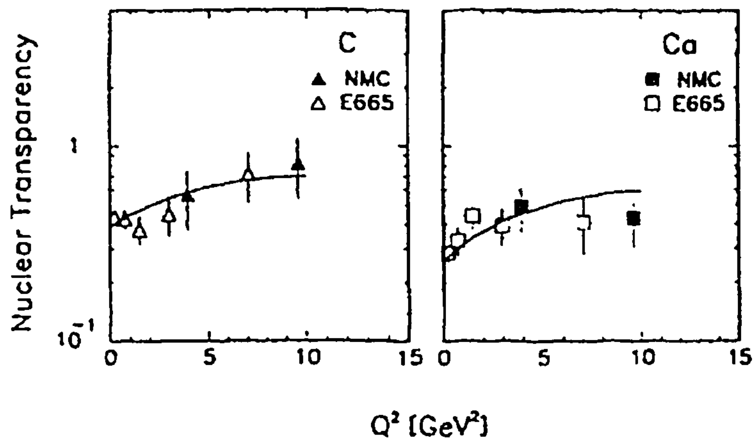

Fig.2.

The distinct features of ϕ production are a smaller cross section and less steep p_t^2 distributions than those for the ϱ^0 mesons. For the diffractive incoherent J/ψ production the p_t^2 slopes are comparable to those for ϕ and the ratio of cross sections from tin to carbon is consistant with the colour transparency model of Nikolaev and coauthors.

[1] NMC, M.Arneodo et al., Nucl. Phys. B429 (1994) 503

[2] NMC, P.Amandruz et al., Phys. Lett. B332 (1994) 195

[3] EMC, J.J.Aubert et al., Phys. Lett. B161 (1985) 203

[4] P.V.Landshoff, Proc.of Joint Lepton-Photon Symposium and Europhysics Conf. on HEP, Geneva 1991, vol.2, p.363; Eds. S.Hegarty, K.Potter and E.Quercigh (World Scientific 1992)

[5] for example see: S.J.Brodsky et al., preprint: SLAC-PUB-6412 (1994), submitted to Phys. Rev. D

[6] E665, G.Y.Fang, preprint: FERMILAB-Conf. 93/305 (1993); private communication

[7] B.Z.Kopeliovich et al., Phys. Lett. B324 (1994) 469

1.16 Participation in CMS and RD5 Experiments at CERN

by M.Szeptycka, M.Górski

The activity in the preparation of the CMS experiment is a continuation of last year's work.

Partcipation in the CMS and RD5 experiments at CERN consisted of two parts. The first one consisted of the building and testing in Warsaw of a prototype of the Resistive Plate Chamber (RPC) which was subsequently tested at CERN in the framework of the RD5 experiment. The aim is to obtain RPC a chamber operating with good efficiency at high incident fluxes. The second part was devoted to further studies of the behaviour of a prototype device meant to provide the fast trigger for high energy muons.

1. The construction and testing of the RPC prototype.

Several prototypes of RPC chambers were built in collaboration with the Institute of Experimental Physics of Warsaw University. The chambers consist of a gas gap of two millimeters width and a readout plane of 20*1-cm strips. They were first tested in Warsaw with a radioactive source and with cosmic rays. During May they were installed in the RD5 experiment at CERN. Tests included the determination of the chamber efficiency as a function of the high voltage and of the beam intensity for various gases. It was found that the efficiency remains high (above 90%) for incoming rates up to about 500 Hz/cm^2 (last year - only up to 30 Hz/cm^2). These results were obtained when the chamber was operated in the so-called proportional mode, that is with relatively low gas amplification. The chamber efficiency as a function of beam intensity is shown in Fig.1.

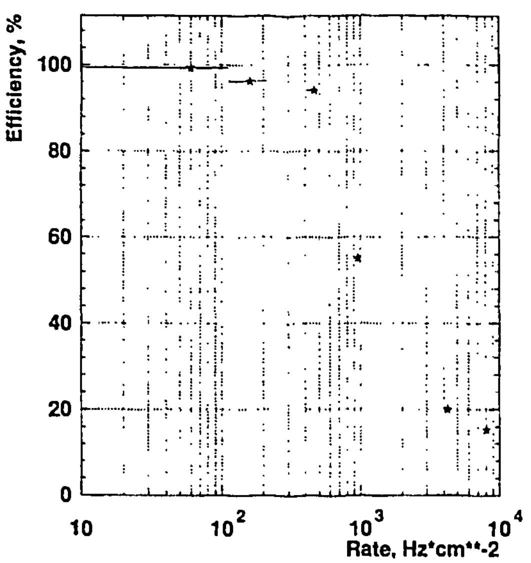

Fig.1. Chamber efficiency vs rate

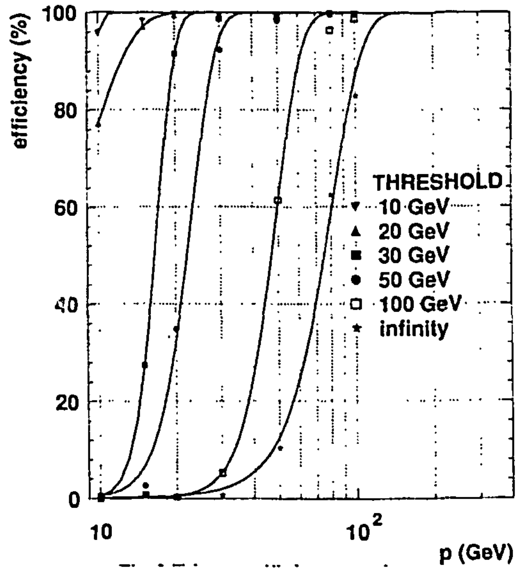

Fig.2. Trigger efficiency vs beam momentum

The timing properties of the chambers were found to be good - the spread in time of the chamber response with respect to the RD5 trigger is about 5 ns. The properties of the chambers make them a suitable device to be used in the CMS experiment as the basis of the muon trigger.

2. The prototype of the triggering device.

A prototype device for triggering on the high energy muons in the RD5 experiment was tested at CERN during the RD5 June run. The tests performed in 1994 covered a wider selection of beam momenta than last year. The device uses programmable ALTERA 7128 arrays and makes its decisions based on the patterns of hits registered in four RPC chambers. Depending on the hit pattern, the trigger provides an approximate value of the muon momentum starting from 10 GeV/c. The trigger efficiency is about 99% (see Fig.2).

1.17 Color Collective Phenomena at the Early Stage of Ultrarelativistic Heavy-Ion Collisions [1]

by St.Mrówczyński

Hard and semihard processes lead to a copious production of partons at the early stage of ultrarelativistic heavy-ion collisions. Since the parton momentum distribution is strongly anisotropic, the system can be unstable with respect to specific plasma modes. Using the transport equations of the quark-gluon plasma, conditions of instability have been found and the characteristic time of its development has been estimated. Next the screening of the static chromoelectric field in the nonequilibrium plasma has been studied. Importance of the phenomena for heavy-ion collisions at RHIC and LHC has been critically discussed.

[1] St.Mrówczyński, Phys.Rev. C49 (1994) 2191

1.18 Wigner Functional Approach to Quantum Field Dynamics [1]

by St.Mrówczyński

We have introduced the Wigner functional representing a quantum field in terms of the field amplitudes and their conjugate momenta. The equation of motion for the functional of a scalar field has been derived and the relevance of solutions of the classical field equations to the time evolution of the quantum field has been pointed out. The equation of motion of the Wigner functional has the familiar form of a transport equation. We discussed the field in thermodynamical equilibrium and found the explicit solution of the equations of motion for the so-called slow "rollover" phase transition. Finally, we have briefly discussed the approximate methods for the evaluation of the Wigner functional that may be used to numerically simulate the initial value problem.

[1] St.Mrówczyński and B.Mueller, Phys.Rev. D50 (1994) 7542

1.19 WA 98 - Large Acceptance Hadron and Photon Spectrometer

by T.Siemiarczuk for the WA 98 Collaboration

The aim the experiment (Fig.1) is the high statistics study of photons, neutral hadrons and charged particles, and their correlations in Pb-Pb collisions at 160 GeV/A. The photons are measured by a 10,000 module Lead Glass Spectrometer yielding high precision data on π^0 and η at midrapidity (with transverse momenta 0.3 GeV/c<p_t<4.5 GeV/c for π^0 and 1.5 GeV/c<p_t<4.0 GeV/c for η covering the "thermal" as well as the "hard scattering" regime beyond 3 GeV/c) and determination of the thermal and direct photon to π^0 ratio. The pad preshower Photon Multiplicity Detector allows, by comparing with the charged particle multiplicity measurement, to determine the photon enrichment in an event or event class. The charged particle setup contains a Multistep Avalanche Chamber tracking system with Silicon Drift Chambers to measure the multiplicities and the momenta, and a Time-of-Flight System for particle identification. This allows us to correlate electromagnetic and charged hadronic data within event classes, yields high statistics transverse momentum spectra of identifield hadrons as well as Bose-Einstein correlation data. Energy flow measurements are available with mid rapidity (3.7<η<5.5) and zero-degree calorimetry.

In November 1994, the new CERN facility supplied its first lead ion beams. With lead beams, the more compact nuclear concentrations of matter will improve the chances of seeing the long-awaited quark-gluon plasma. Some millions of events have been measured in our first run with the lead beam at 160 AGeV incident on the lead, the niobium and the nickel targets in a search for photons issuing from the early part of the collision and with a goal to study whether the properties of the hadrons produced in the dense medium are altered.

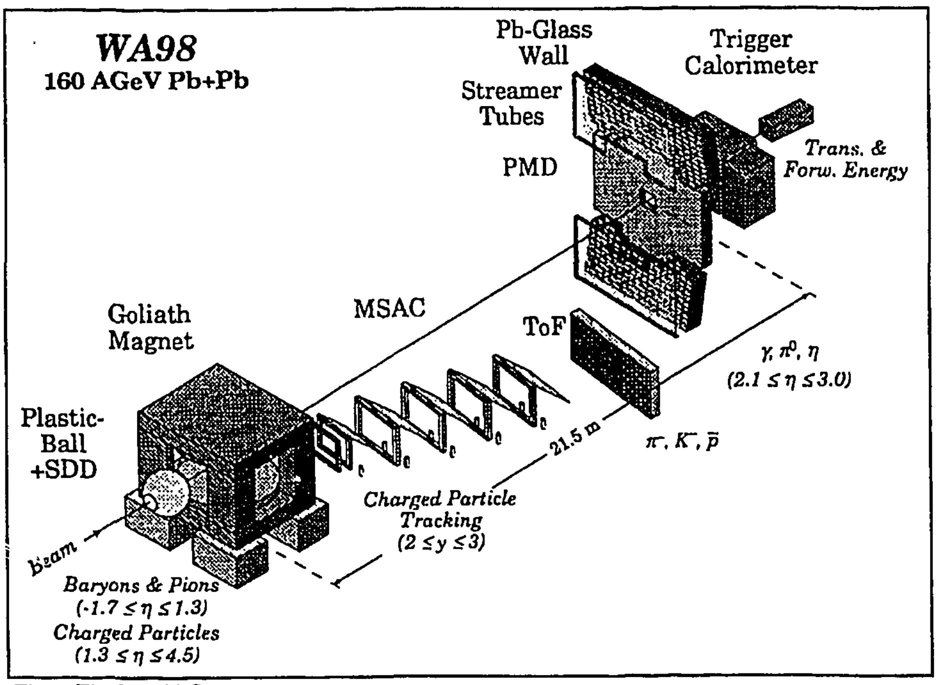

Fig.1. The WA 98 Spectrometer

Figure Details:

- Plastic Ball + Si-Drift Detector (SDD)
- Vertex Magnet (GOLIATH)
- ToF-Spectrometer
- Photon Multiplicity Detector (PMD)
- Multi Step Avalanche Chambers (MSAC's) + Padchamber
- Pb-Glass Spectrometer
- Hadron Calorimeter (MIRAC)
- Zero-Degree Čerenkov Detector
- Zero-Degree Calorimeter

1.20 WA 93 - Spectrometer for Correlations between Photons and Hadrons

T.Siemiarczuk for the WA 93 Collaboration

The experiment combines two essential means of quark diagnosis: the measurement of photon production rates relative to charged particles or π^0's, and the measurement of transverse momenta of charged and neutral particles and their correlations. The experimental setup consists of highly segmented lead glass arrays (3780 modules) at a distance of 9 m from the target covering the range 2<y<3. The detector allows us to reconstruct the transverse momentum of π^0's and η's. A preshower detector that can be operated in a hadron-blind mode complements the photon measurement in the range 3<y<5.5. The detector yields the number of photons and, to a limited extent, also information on the total electromagnetic transverse energy. Charged particle tracking is achieved by a set of newly developed multistep avalanche chambers read out by CCD cameras downstream of the GOLIATH vertex magnet. Bose-Einstein correlations allow source size measurements up to 20 fm. The coverage is 4<y<4 for two field settings of BxL=1 and 2 Tm. Events of high energy density (central collisions) are selected by triggering on high E_t or low energy deposition at zero degree.

We have carried out the first event-by-event measurement of relative production of charged particles and photons in S+Au collisions at 200 AGeV/c with the WA 93 detector at the CERN SPS.

The charged particles and photons were detected simultaneously in pseudorapidity range $2.9 \leq \eta \leq 3.5$ with full azimuthal coverage. The charged particles were detected in a circular Silicon Drift Detector (SDD) [1] placed at a distance of 146 mm downstream of the target. The photons were measured by the Photon Multiplicity Detector (PMD) [2] situated 22.5 m from the target.

Preliminary results for the asymmetry parameter, $(N\gamma - N_{ch})/(N\gamma + N_{ch})$, are shown in the figure for central and peripheral events. The data set is being examined for particular events with unusually large content of photons or charged particles.

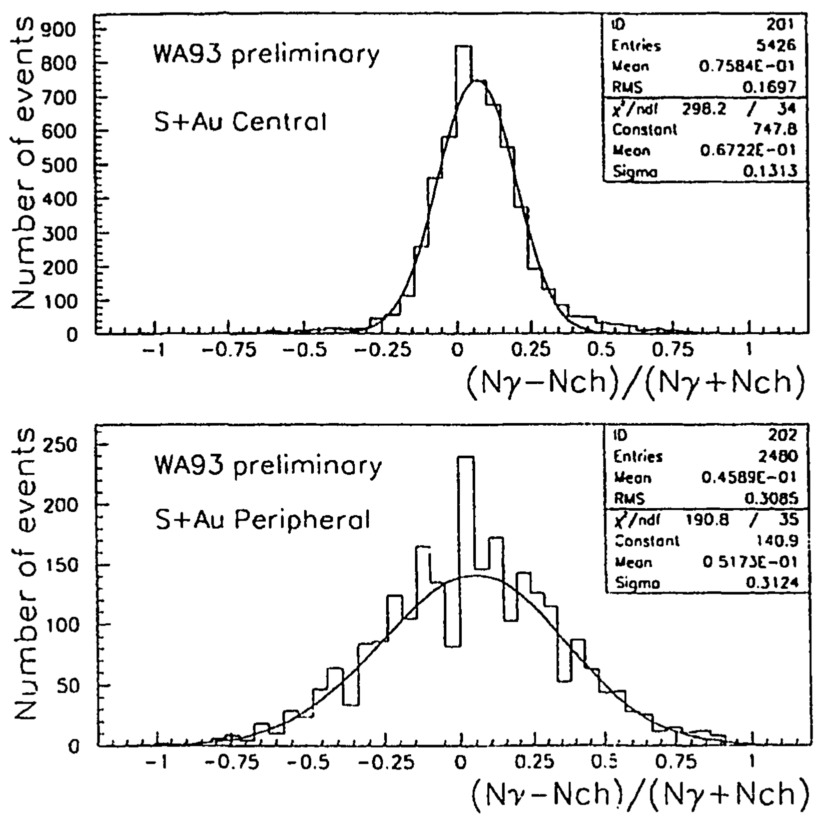

Fig.1.

The presence of such events is predicted [3] to be a signature of the formation of the disoriented chiral condensate, and may be related to the production of Centauro or anti-Centauro events observed in cosmic ray experiments, or it may signal the formation of the quark-gluon plasma.

We have examined the azimuthal substructure in photon emission in a S+Au collision at 200AGeV. In central collisions, since there is no preferred direction, one expects the final state particles to be uniformly distributed in the azimuthal plane. The detected photons are to a large extent the result of π^0 decay, and any asymmetry in π^0 emission should lead to asymmetry in photon angles. If the particles are emitted preferentially uniformly then we label the event "ring-like" (where the unit vectors along the direction of emission of particles resemble the spokes of a bicycle wheel). If the emission is in a limited range then we label the event "jet-like". In order to make a quantitative estimate we define two finctions:

$$S_1 = -\Sigma \ln(\delta\phi)_i \qquad S_2 = \Sigma\,(\delta\phi)_i^2$$

where $\delta\phi$ is the azimuthal angle between two consecutive photons. If the total azimuthal angle is normalized to 1, and the event multiplicity is n, then S_1 takes values nln(n) and 0 and S_2 takes values 1/n and 1 for a ring-like and jet-like event respectively.

The values of functions S_1 and S_2 have been determined for each event. It is observed that the central events have a ring-like structure. The low multiplicity events are found to have less symmetry. The data have been compared with VENUS + GEANT simulations.

Preliminary results from one-(η−) and two- (η-ϕ) dimensional analyses of two-photon correlations are obtained for the reaction of 200 A GeV S projectile with Au target. There is no evidence for correlations in the collision beyond that accounted for by the particle generator VENUS filtered through the detector simulation GEANT.

We have also measured the $<p_t>$ of photons in the WA 93 experiment using the transverse electromagnetic energy measured in the MIRAC calorimeter and the photon multiplicity measured by a high granularity preshower detector [2]. The present results, although preliminary, confirm a trend of increase of $<p_t>$ with centrality.

[1] P.Rehak et al., Nucl. Inst. and Meth. 235 (1985) 224
[2] Y.P.Viyogi et al., WA93 Collaboration, Nucl. Phys. A556c, (1994) 623
[3] J.D.Bjorken, K.K.Kowalski and C.C.Taylor, "Baked Alaska", Proc. of Les Rencontres de Physique de la Vallee d'Aoste, ed. M.Greco, Editions Frontiers (1993)

1.21 The Spin Dependent Structure Function g_1^p (x) of the Proton and a Test of the Bjorken Sum Rule

by J.Nassalski, E.Rondio, A.Sandacz, W.Wiślicki

The spin dependent structure functions of the nucleon, g_1, and g_2 can be measured in polarized deep inelastic lepton-nucleon scattering [1]. Measurements of g_1 for the proton and the neutron allow us to test a fundamental QCD sum rule, derived by Bjorken [2], and to study the internal spin structure of the nucleon. Ellis and Jaffe [3] have derived sum rules for the proton and neutron, under the assumptions that the strange sea is unpolarized and that SU(3) symmetry is valid for baryon octet decays.

In the SMC experiment performed at CERN, longitudinally polarized muons were scattered from longitudinally polarized protons and deuterons. In 1994 data were taken on the deuteron target and results from 1993 running on the proton target were analysed and published. These proton data will be discussed in this paper. They cover the kinematic range 1 GeV^2 < Q^2 < 60 GeV^2 and 0.003 < x < 0.7.

The asymmetry A_1^p is extracted from combinations of data sets taken before and after a polarization reversal. Each event is weighted with the corresponding values of virtual photon depolarisation factor D, and the dilution factor f, the fraction of the event yield protons in the target (f ≈ 0.12).

The results for A_1^p for each x bin at the respective mean Q^2 are shown in Fig. 1 and compared with measurements from SLAC experiments. The important contribution of the SMC experiment is the extention of kinematic range towards low x.

The spin structure function g_1^p was evaluated from the asymmetry A_1^p in each x bin. It was done at Q_0^2 = 10 GeV^2, which represents an average value for our data, assuming A_1 (x, Q^2) to be independent of Q^2.

After estimating the contribution from unmeasured regions the result for the first moment of g_1^p (x) at Q_0^2 = 10 GeV^2 is

$$\Gamma_1^p (Q_0^2) = \int_0^1 g_1^p (x, Q_0^2)\, dx = 0.136 \pm 0.011 \pm 0.011$$

Results for g_1^p and its first moment are given in Fig. 2. The Ellis-Jaffe sum rule, including first order QCD corrections, predicts $\Gamma_1^p = 0.176 \pm 0.006$ for $\alpha_s(10\ \mathrm{GeV}^2) = 0.23 \pm 0.02$, corresponding to $\alpha_s(M_Z^2) = 0.113 \pm 0.004$ and four quark flavors. Our measurement is two standard deviations below this value.

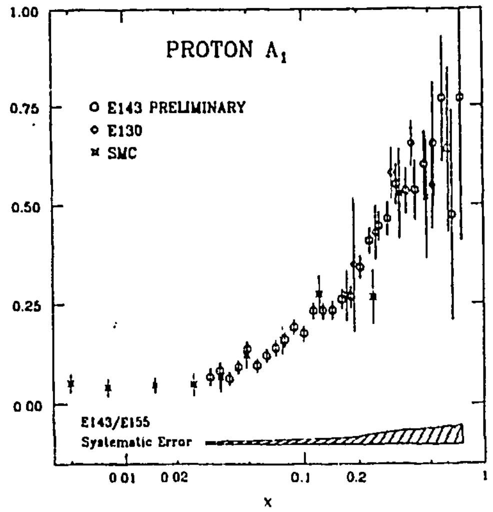

Fig.1.

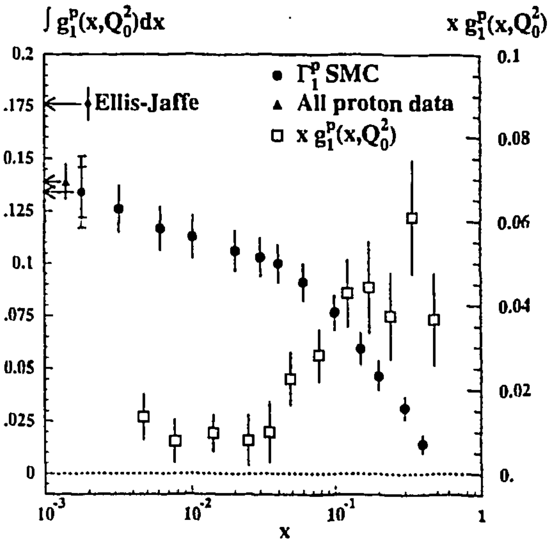

Fig.2.

The first moment Γ_1^p can be expressed in terms of the proton matrix element of the flavor singlet axial vector current a_0 [4] and the SU(3) coupling constants F and D. We obtain $a_0 = 0.18 \pm 0.08 \pm 0.08$. In the quark-proton model, a_0 is proportional to $\Delta\Sigma$ the sum of the quark spin contributions to the nucleon spin. Our result corresponds to $\Delta\Sigma = 0.22 \pm 0.10 \pm 0.10$ and $\Delta s = -0.12 \pm 0.04 \pm 0.04$. We thus find that only a small fraction of the nucleon spin is due to the helicity of the quarks, and that the strange sea is negatively polarized.

We now turn to a test of the Bjorken sum rule [2], using all available proton, neutron and deuteron data. We do this test at $Q^2 = 5$ GeV^2 in order to avoid a large Q^2 evolution. A fit to Γ_1^p, Γ_1^n and Γ_1^d, reevaluated at 5 GeV^2 under the assumption that the asymmetries A_1 are independent of Q^2, yields $\Gamma_1^p - \Gamma_1^n = 0.163 \pm 0.017$ ($Q^2 = 5$ GeV^2), where statistical and systematic errors are combined in quadrature. When one uses the available deuteron and proton data alone the result is gives $\Gamma_1^p - \Gamma_1^n = 0.204 \pm 0.029$($Q^2 = 5$ GeV^2), with a larger error due to the limited statistics in the deuteron experiment. The theoretical prediction, including perturbative QCD corrections up to third order in α_s, gives $\Gamma_1^p - \Gamma_1^n = 0.185 \pm 0.004$ (Theory)($Q^2 = 5$ GeV^2), which is in agreement with the above experimental results.

The Bjorken sum rule is now confirmed, at the one standard deviation level, to within 10 % of its theoretical value.

[1] V.W. Hughes and J. Kuti, Ann. Rev. Nucl. Part. Sci. 33(1983)611.
[2] J.D. Bjorken, Phys. Rev. 148(1966)1467; Phys. Rev. D1(1970)1376.
[3] J. Ellis and R.L. Jaffe, Phys. Rev. D9(1974)1444; D10(1974)1669.
[4] EMC, J. Ashman et al., Phys. Lett. B206(1988)364; Nucl. Phys. B328(1989)1.

1.22 WASA Experiment at Celsius

by A.Kupść, P.Marciniewski, A.Nawrot, J.Stepaniak

Cooled ion storage ring CELSIUS in Uppsala operates for four years and accelerates protons up to 1.36 GeV kinetic energy. Luminosity achieved with cluster jet target is about 10^{31}cm^{-2} s^{-1}. WASA collaboration prepares a 4π detector system for precise study of rare processes (up to pb region) in nuclear and particle physics. The first stage of the detector system (the so called PROMICE-WASA setup) has been used for two years and is devoted to the study of near threshold meson production and investigations of pd and dd reaction. It consists of a forward spectrometer (for detection of particles scattered at angles below 23 degrees) and two CsI(Na) arrays, which enable the detection of photons and hadrons emitted at large angles. The forward spectrometer consists of seven different planes of plastic hodoscopes. The angular coverage of each CsI array is 60^0 for the polar angle and 49^0 for the azimuthal angle. The cesium arrays give a resolution in energy for charged particles of about 3 % and for photons of about 8 %. The resolution in scattering angle is about 5^0.

Such resolution is sufficient for the reconstruction of neutral mesons via their decay photons, but is not good enough for study of hadronic reaction products. Therefore two new position detectors are beeing manufactured in Warsaw. In 1994 two tests of 52 modules of this detector were done at CELSIUS and further work on additional 52 modules and electronics for the detector is in progress.

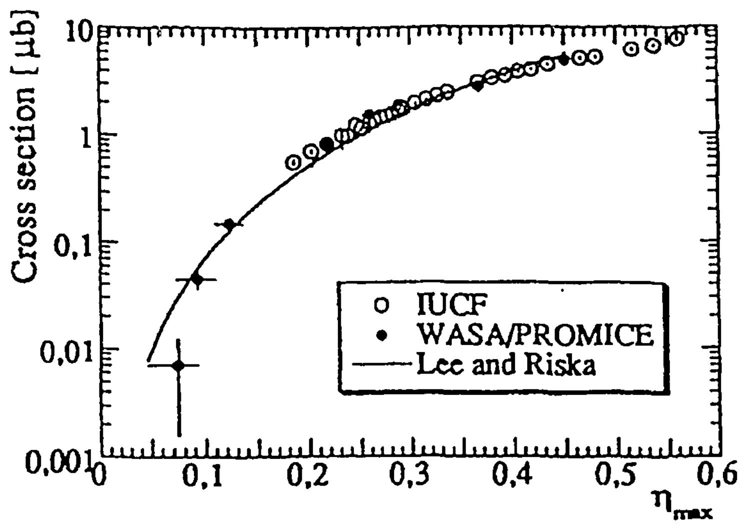

Fig.1. Cross section for the pp → ppπ^0 reaction as a function of the maximum π^0 momentum in the center of mass system in the units of the pion mass. Full points - WASA/PROMICE results. Open points - the data from the IUCF, Indiana experiment [ref.1], curve from the ref.2.

In 1994 the data were collected on proton deuteron interactions at six energies from the threshold for η production up to 1200 MeV. The main aim of this measurement is to have more information on η interaction with nucleons, and in addition we shall find out how to use p+d → p+d+η and/or p+d → ^{3}He+η as a source of tagged η's for the rare decay studies.

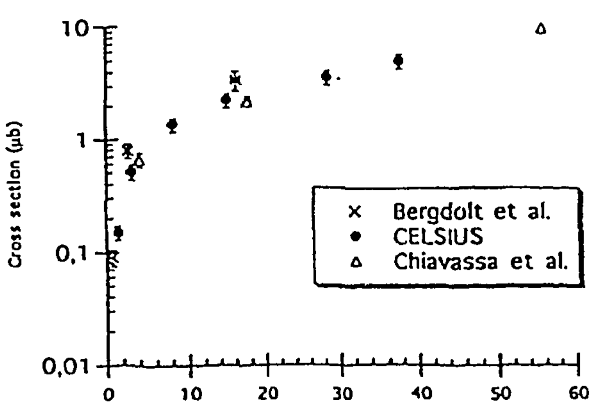

Fig. 2 Preliminary cross sections for the reaction pp → ppη as a function of the kinetic energy in the CM system (full points), compared with the results from two experiment at Saturne [ref.3]

The analysis of the previously collected data on the near threshold production of neutral pion and η meson has lead to the experimental cross sections presented in the figs 1 and 2.

The WASA/PROMICE facility at CELSIUS has the unique possibility of approaching so close to the threshold because of the good efficiency of the neutral trigger based on decay photons. The results are in satisfactory agreement with previous data in the overlapping region. It gives additional weight to the conclusion that the term with two-nucleon axial charge is of importance [Ref.2] and heavy meson exchange plays a crucial role in neutral pion production in proton-proton interactions near threshold [Ref.5].

[1] H.O. Meyer et al., Nucl. Phys. A539(1992)633
[2] T.-S.H. Lee and D.O. Riska, Phys. Rev. Lett. 70(1993)2237
[3] A.M. Bergdolt et al., Phys. Rev. D48(1993)R2969
[4] E. Chiavassa et al., Phys. Lett. B322(1994)270
[5] C.J. Horowitz et al., Phys. Rev. C49(1994)1337

2. COSMIC RAY PHYSICS

2.1 Extensive Air Showers (EAS) of High Energy Cosmic Rays (CR).

2.1.1 EAS Data Analysis and Interpretation
by J.Gawin, B.Szabelska, J.Szabelski

Analysis of data collected by Lodz EAS array was continued.
We tried to describe properties of EAS registered in the Lodz array. We used the results of EAS development simulations performed in Karlsruhe. Comparison of predictions with the results of EAS observations in the Lodz array shows that the proposed method of description is very sensitive to the assumed cosmic ray mass composition. The work was presented at the European Cosmic Ray Symposium in Balaton-Fured, Hungary.

2.1.2 Search for UHE Cosmic Ray Point Sources
by J.Zabierowski

Correct registrations were used to analyse correlation between arrival time of EAS from the direction of the Crab Nebula and the phase of the pulsar. There was no excess of showers from this direction. The analysis was performed for normal showers and 'muon defficient' showers. Phase analysis for the period of radio-pulsar has also been performed. The paper has been accepted for publication by (Journal).

2.1.3 EAS of High Energy CR - 200 GeV Muon Group Analysis
by J.Szabelski

In the frame of our collaboration with the Institute of Nuclear Research of the Russian Academy of Sciences we had three and then two more guests from Moscow and Baksan. From our side two persons stayed in Moscow and Baksan Laboratory. We continued the analysis of Russian data on high energy muons registered under the ground and the analysis of so called narrow showers registered in the ground-level array "Carpet". The latter effect has been explained as being due to high energy muon interactions in the walls of the building in which the array is placed. Two persons from SINS took part in the Inter-regional Cosmic Ray Conference in Moscow (end of June 1994) and presented talks on multiplicity distribution of muons registered in the Baksan Muon Telescope and the mass composition of the primary CR in the energy range 10^{14} - 10^{16} eV.

2.1.4 Nucleus - nucleus Interaction
by J.Szabelski

Studies of nucleus-nucleus incractions were continued. We performed simulations of EAS development for protons as the primary particles (proton - air-nucleus collisions) and for iron nuclei as the primary particles (nucleus - nucleus collisions). We predicted numbers of high energy muons in EAS for protons and for iron nuclei assuming superposition and abrasion-evaporation model of nucleus-nucleus interaction. The work was presented at the European Cosmic Ray Conference. The KfK Karlsruhe program CORSIKA has been adapted for EAS development simulations.

2.2 Experimental Techniques.

2.2.1 Participation in the WASA Experiment
by J.Zabierowski

We continued our collaboration with the Institute of Radiation Sciences in Uppsala. Since several years it has been devoted to the WASA project on the CELSIUS storage ring at Uppsala University. Various activities were devoted to the developement of the 4π vertex detector. In particular, the preliminary studies on the Light Pulser Calibration System for this detector have been made. The existing PROMICE/WASA experimental setup was used for data taking in experiments aiming at the measurements of the production cross section of π^0 and η mesons. The preliminary results were presented at the conference in Juelich and will be published soon in Physics Letters B. Some modifications and tuning of the existing Light Pulser system for the present setup were made. The design concept of the Light Pulser system and its performance were presented in Nuclear Instruments and Methods.

2.2.2 Geiger - Müller Tubes Production
by J.Gawin, R.Firkowski, S.Kowalczyk, S.Pachała, P.Sulkowski

Production of Geiger-Müller counters for the Lodz EAS array and proposed muon telescope was continued. The exchange of G-M counters in the underground hodoscope was finished.

2.2.3 Muon Telescope
by J.Szabelski

Construction of the small muon telescope and all other works connected with it has been suspended because of lack of financial support and a minimum of solar activity.

2.2.4 EAS of High Energy CR - Collaboration in Kaskade
by J.Wdowczyk, J.Zabierowski

In Kernforschungszentrum Karlsruhe (KfK) in Germany, curently the biggest in Europe cosmic ray experiment, has been under construction since 1990. Its main goal is to investigate the primary mass composition in the energy range 10^{14}-10^{17}eV. The array part will start to deliver experimental data in 1995.

In 1994 we finished the first stage of our collaboration programme, namely the participation in developement and production of several hardware and software components of the array and central calorimeter. This was possible due to financial support from KBN(grant No. 2 0962 91 01 Title: "Investigation of the mass composition of the primary cosmic radiation in the energy range 10^{14} - 10^{17} eV".. We have delivered for the experiment the full set of trigger units for the array (120 VME modules) and PC boards with software for the power supply control for the central calorimeter (40 modules).

Some preparations to the data analysis have been made, namely with the use of the CORSICA code.

2.3 Studies of CR Origin and Propagation in the Galaxy.

2.3.1 Analysis of Data from Compton Gamma Ray Observatory
by B.Szabelska, J.Szabelski

Studies of gamma rays in the frame of collaboration with NASA (project GRO-93-248) has been continued. Full set of data from the experiment EGRET onboard NASA Compton Gamma Ray Observatory has been obtained. Three seminar lectures on gamma ray astrophysics and studies of Galactic CR were given.

2.3.2 Galactic Gamma Rays
by J.Wdowczyk

Results of the EGRET experiment were used for studies of the energy spectrum of CR and CR electrons as a function of position in the Galaxy.

2.3.3 Cherenkov Observation of EAS
by J.Gawin, B.Szabelska, J.Szabelski, A.Wasilewski

Studies of EAS by observing Cherenkov radiation in collaboration with College de France and University of Perpignan have been started. The goal of experimental studies performed in France (experiments ASGAT, THEMISTOCLES and CAT) is to search for point sources of gamma rays of energy around 1 TeV. Our group takes part in the analysis of experimental results. The main problem is to discriminate photon induced EAS from more numerous ones induced by CR protons and nuclei. Several computer simulations of the observed events have been performed.

2.3.4 Highest Energy CR
by J.Wdowczyk

Studies of the origin of highest energy cosmic rays have been continued. The possibility that this component of CR comes from the big halo filled by galactic CR has been discussed. The model explains some recent observations, especially these concerning arrival directions of the highest energy EAS.

2.3.5 Studies of CR Mass Composition by Fractal Analysis
by J.Wdowczyk

Studies of the primary CR mass composition through fractal analysis have been performed. An attempt to find the mass of particles initiating cascades in the atmosphere (EAS, Pamir families) through studies of structure of these cascades at the level of observation by means of fractal analysis has been undertaken.

C. ACCELERATORS

1. ELECTRON ACCELERATORS

1.1 Summary Note on Exploitation of LIMEX-4 Accelerator for Cancer Therapy

by M.Pachan, A.Wysocka, J.Walerian, K.Zembaczyński

The clinical operation of prototype linear accelerator LIMEX-4 MeV in Oncological Centre-Ursynów is approaching its end. The machine is still on duty in daily treatment of patients, but due to a growing number of people to be treated in Radiotherapy Department there exists a tendency to replace LIMEX by a higher energy and more universal accelerator.

It should be emphasized, that the 4 MeV accelerator was designed to create a foundation for production in Poland of low-energy and comparatively non-expensive accelerators, which as a sources of X-ray photon beam, can replace with surplus in parameters, the cobalt-60 units.

Therefore in parallel to routine operation, a very careful survey of important parameters, reliability, failures and weak points has permanently been conducted, possible modifications and improvements introduced, and what is most important, the observations and recommendations for future versions of this type of accelerator have been gathered.

There is now an opinion that 20 ÷ 30 low energy accelerators can be located in Polish radiotherapy centres.

In this way the prototype has fulfilled its task.

As a summary of clinical operation results in the last few years, the following data have been collected:

Year	Number of patients	Number of irradiation field in one session
Oct. 91/92	6 058	16 953
1993	8 820	22 498
1994	3 218	9 546
$\sum$ 91-94	18 095	48 997

Having in mind that every patient comes few times (about 3) for irradiation it gives about 6 000 of new patients. With the results from previous years, altogether more than 10,000 people have been treated with LIMEX.

1.2 Extension of Studies for the Project of LIMEX-15A, New Generation Medical Accelerator. RF System

by J.Bigolas, S.Kuliński, M.Pachan

In the SINS Annual Report 1993, some initial results of feasibility study of a new medical accelerator with energy in the range 15 - 18 MeV were presented. On the basis of this study, the general technical and economical description of the whole system was completed and was enclosed to formal application for Ordered Research Project. This application was supported by the President of National Atomic Energy Agency and the Minister of Health, and directed to proper commission for detail examination.

In the frame of research activity in 1994, study on most important problems was continued, and in particular on the features of radio-frequency system.

Introduction of the separated bunching section in the accelerating structure imposes a necessity of two transmission paths for r.f. power from klystron generator to accelerating system.

The evaluated division of peak power for these two branches is as follows:

for the buncher (up to 3 MeV)	0.2 ÷ 0.6 MW constant
for main "c" section (up to 18 MeV)	4.6 MW (variable)

Fig. 1 presents a simplified diagram of r.f. system.

For maximum phase acceptance of the injected electrons, the bunching section is supplied with constant r.f. power, and the main section with variable power depending on the requested energy of the electron beam. Typically, this energy should be selected in the range 6-15 MeV (with option 18 MeV).

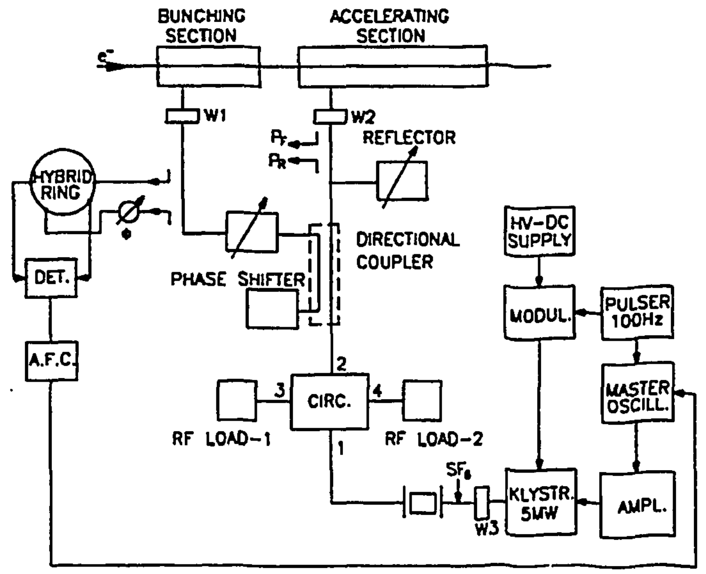

Fig.1. LIMEX 15 r.f. System

As a source of r.f. power in S band, serves of klystron amplifier of 5 MW peak power in 4 - 5 μs pulses. This power is transmitted through rectangular waveguide, filled with insulation gas SF_6, under a pressure of 1.8 bar. The pressure sensor switches off the klystron power supply if the pressure falls below the critical value. In the waveguide the ferrite circulator is included to protect the klystron against excessive level of reflected wave. The klystron amplifier is excited from the master oscillator with frequency stability in the range $5 \cdot 10^{-6}$ and an intermediate amplifier with output power around 200 W. To ensure most suitable operation conditions, the klystron supplied from pulse modulator is working with constant output power. The necessary division of power between the bunching section and the main accelerating section is performed with a directional coupler interconnected in the main waveguide.

Both parts of the accelerating structure are tuned to the same frequency and kept constant by precise temperature control. During the operation Automatic Frequency Control (AFC) is necessary and uses the error signal from phase sensitive hybrid ring connected with r.f. transmission line to the buncher. The AFC system is correcting in a small range the operating frequency of the master oscillator. Experimental stand for model measurements of r.f. system is in preparation.

1.3 Accelerating System for Linear Electron Accelerators for Energies up to 25 MeV

by S.Kuliński, J.Bigolas, M.Pachan

Till now we have mastered in Poland the design of linear electron accelerators of energies up (10 ÷ 12) MeV. However many applications equire energies above 20 MeV, with a possibility of output energy variation in rather wide limits. The most important of these applications are: cancer therapy, isotopes production (e.g. Iodine-123), accelerators for Free Electron Lasers (FEL), accelerators generating X-rays and neutron beams for radiography and structural investigations.

Taking into account these wide and important applications, and also rather high price of accelerating structures for such accelerators (being above hundred thousand dollars) the Department of Acceleration Physics has decided to undertake the work of designing and building a family of accelerating systems suitable for accelerators to the above mentioned applications. The main elements of the accelerating system are: electron gun and accelerating structure

1. Electron Gun

Hitherto we have used in linear electron accelerators diode guns. Taking into account that the new systems should be more suitable and flexible with respect to the required parameters and their variations we find it necessary to elaborate the triode gun in which the parameters such as current intensity, pulse duration, rise time etc, are controlled by the potential of the additional grid.

The principal parameters of the gun for most of the applications with the exception of FEL will be the following:

Maximum beam current - hundreds of miliampers, Voltage V_g = (50 ÷ 100)kV, pulse duration t_i = (2 ÷ 4) μsec with possible short rise time, repetition frequency f_{rep} = (1 ÷ 300)Hz, regulated pulse delay with respect to RF pulse for acceleration, up to 1 μs.

2. Accelerating structure

The accelerating structure is composed of a chain of elementary resonant cells or cavities having the same resonant frequency. With the exception of the first few cells, whose lengths increase monotonically together with the velocity of electrons, all the other are identical. We will use the standing wave (SW) biperiodic type of structure working in the $\pi/2$ mode. The structure is biperiodic, since it is composed of the set of alternating bigger accelerating cells and smaller coupling cells. The mode is $\pi/2$ since the RF phase change between the adjacent cells is $\pi/2$. The advantage of SW, $\pi/2$ structure is high shunt impedance Z_{sh} characteristic for SW structure and high group velocity, due to $\pi/2$ mode, characteristic for the travelling wave structures.

The RF power supply to the SW structure is divided into two parts $P = P_{ac} + P_b$, where $P_{ac} = V^2/Z$ creates the voltage V necessary for the acceleration ($Z = Z_{sh}L$ is the total shunt impedance of the structure with the length L), and $P_b = V \cdot I$ is the power of electron beam.Usually $P_{ac} > P_b$, or even $P_{ac} \gg P_b$, then $P \approx P_{ac}$ and the RF power is proportional to the square of electron energy V. For instance, P_{max}/P_{min} will be about 11 for electron energies 6 to 20 MeV and about 17.5 for 6 to 25 MeV. Such large RF power variations are undesirable and often difficult to perform during normal functioning of a klystron.

Another difficulty which should be solved in accelerators with variable energy is the dependence of the phase acceptance of the accelerating structure on the electron energy i.e. on the electric field level in the structure. Usually the initial part of the structure with variable cells lengths is optimized to accept a possible large band of input phases for a given output energy. For other energies (field levels) the phase acceptance decreases quickly, e.g. the structure designed for energies (6 $\div$ 20)MeV and optimized for the maximum phase acceptance at 11 MeV accepts about 50% of all phases in the vicinity of 11 MeV, and only about 10% at 6 and 20 MeV.

The solution to both of above problems is to divide the structure into two parts: a buncher and main accelerator. The buncher will be a short section with variable length cells optimized for large phase acceptance. Here the field level can be kept constant (separate power input). The main accelerator has uniform cells. Since energy increase is proportional to $E_m \cos\varphi$, the output energy can be varied changing both field level E_m and the phase φ.

Preliminary calculations of the electron dynamics have been done for the following division of the structure: buncher 6 $\div$ 7 cells with variable lengths followed by (23 $\div$ 24) uniform cells.

The result of the calculations was, that it is possible to find a solution which guarantees a phase acceptance of the order of 50% and more for wide variation of final energy with a sufficiently small energy dispersion of the order of $\pm$ 5%.

Such optimization of accelerating system with an output energy 25 MeV or higher, can be used to design and building accelerators for many above mentioned important applications.

1.4 Modernization and Exploitation of Low-Energy Electron Accelerator EAK 400/100 Operating with Bent Crystal X-ray Spectrometer

by W.Drabik, R.Kielsznia, P.Kapla, W.Straś

The EAK 400/100 electron accelerator, which in 1993 had been adopted for operation with bent crystal spectrometer, was upgraded during 1994.

Modernization was performed in two ways:

- installation of a new oil-free vacuum system
- improving of electron gun design

The new vacuum system consists of Drytel-100 pump with a pumping speed of 27 l/s and turbomolecular 5900-type pump with a pumping speed of 800 l/s (both manufactured by Alcatel). Drytel-100 incorporates an oil-free membrane pump and molecular drag pump (MDP).The membrane pump provides start evacuation from atmosphere to mid range vacuum level (10 mbar). After that the MDP takes over supplying clean vacuum up to a level of 10^{-6} Torr.

In the system the Drytel-100 is used for backing of turbomolecular pump ensuring high vacuum.

The system ensured the vacuum up to $3x10^{-6}$ Torr for long time operation of the EAK 400/100 and enabled work in the range 150-300 keV without breakdowns in the accelerating structure.

The electron gun was improved by replacing cathode node; the new one consisting of lanthanum hexaboride as an emitter and pyrolytic graphite as a heater. Diagram of the cathode node is presented in figure 1, whereas heating power-voltage characteristic is shown in figure 2. The previously checked life-time of the node is over 1000 hours.

During 1994 EAK 400/100 has been operating for experiment with bent crystal spectrometer for about 750 hours.

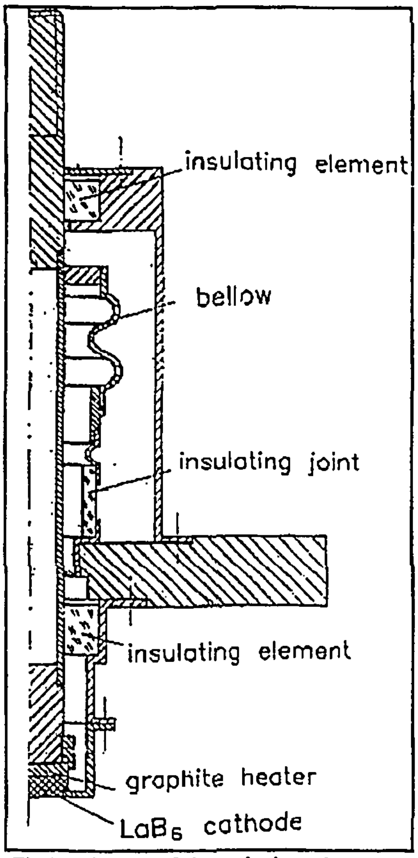

Fig.1. Diagram of the cathode node

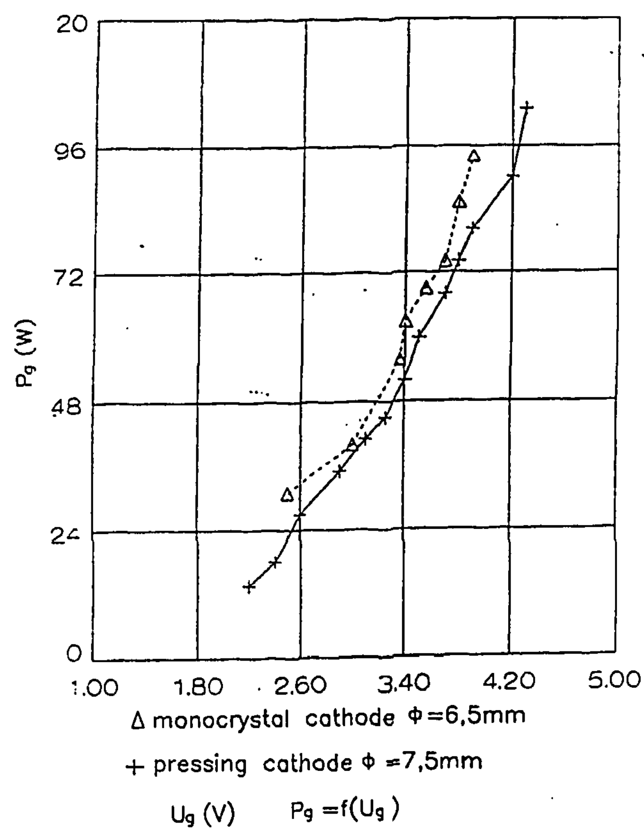

Fig.2. Heating power-voltage characteristic

1.5 Summary of the Project: "Electron Accelerator 800 keV/0.4-1 MW for Purification of Flue Gases from SO_2 and NO_x"*)

by W.Drabik, A.Jerzykiewicz, R.Kiełsznia, K.Kocięcka, J.Witkowski

On the base of technological and technical requirements the following parameters were assumed:

- electron beam energy: 800 keV
- electron beam current: 250 mA max.
- output voltage ripple: < 5%
- efficiency: > 90%
- main insulation: SF_6 gas
- time rating: continuous (6000-8000 hrs/year)
- reliability and simplicity of operation

The system is energized from the 3-phase/6kV mains. The main subsystems are 6 kV distributor, 6kV/1-12kV regulating transformer, 12 kV regulator, 800 kV/400 kW power supply unit and two 200 kW accelerating heads.

Voltage regulation is performed by changing of stopped rotor position to stator windings. Voltage unit forms 30-stage magnetically-coupled cascaded bridge rectifier. The magnetic circuit is composed of three iron columns joined together at the bottom and top by an iron yoke; the magnetic core is grounded. Primary windings are connected in delta configuration. Each secondary coil triplet feeds a three phase bridge rectifier. The power needed for supplying two electron guns is taken from two additional windings at - 800 kV potential level. SF_6 gas and epoxy resin are used as main insulation materials. The power is transmitted to accelerating heads by means of two h.v. cables or bus-ducts.

Accelerating head, insulated with SF_6, is composed of Pierce-type electron gun, electrostatic multi-gap accelerating structure, focusing and scanning coils, scanning horn and output window with titanium foil. Main task during the project was computer simulation and experimental verification realizing of the work on simplified models, as a preparatory design work of a functional prototype.

The following problems were simulated numerically:
- transient states in the system consisting of supply unit, transmission line and accelerating head.
- electric fields in insulating subsystems of supply unit
- electric fields of bus-duct configuration
- electron trajectories, charge density and current density in electron optics system of the accelerator
- focusing of the beam by solenoidal magnetic field
- heat transient states and temperature distribution of titanium foil during transmission of scanned electron beam
- analysis of the air cooling coefficient and amount of heat possible to take away from the foil.

Experimental verification was carried out on the following models using test stands:
- model of 800 kV/0.5 A bus-duct insulated with SF_6 and epoxy
- model of one multiplying section of supply unit
- model of 25 kV/250 mA electron gun with LaB_6 emitter and pyrolytic graphite heater
- model of accelerating tube segment with shielding electrodes
- model of output system
- test stands for testing of coils, rectifiers, varistors, spark gaps and accelerating segment with direct, alternating and impulse voltage
- test stand for testing of bus-duct with 1000 kV
- test stand for testing of generation, transmission and extraction of electron beam
- test stand for measuring of air cooling coefficient

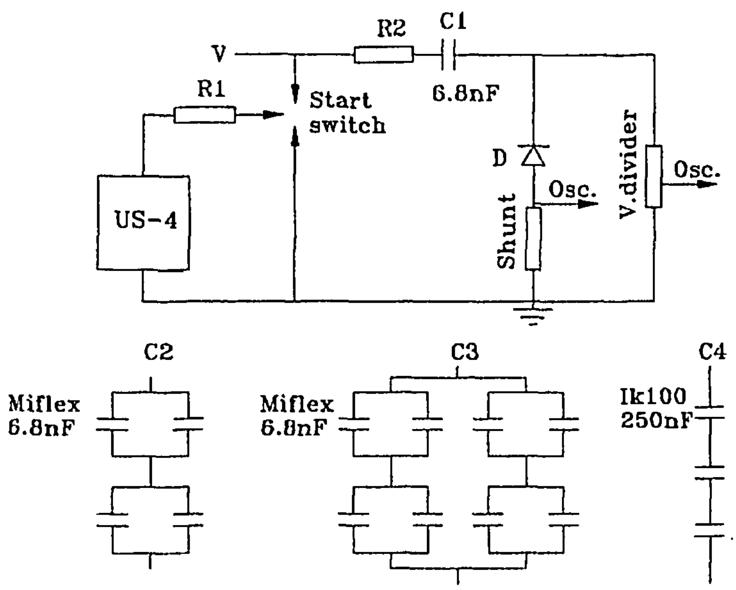

Fig. 1. Scheme of circuit for testing of diode current loading.

Special emphasis was put on the analysis of reasons and effects of fast transients (30-40 ns) in the system during operation and on the choice of most suitable protection against overvoltages and overcurrents caused by them. From numerical calculations with PSpice programs it turns out that the h.v. diodes are most endangered elements, so avalanche diodes from several manufacturers were tested with respect to overvoltages and overcurrents. Figures 1 and 2 show schematic diagrams of test voltage and current test stands for the examination, whereas figures 3 and 4 some of the results.

Metal-oxide varistors and special construction spark gaps were considered as protection elements and their effectiveness was measured.

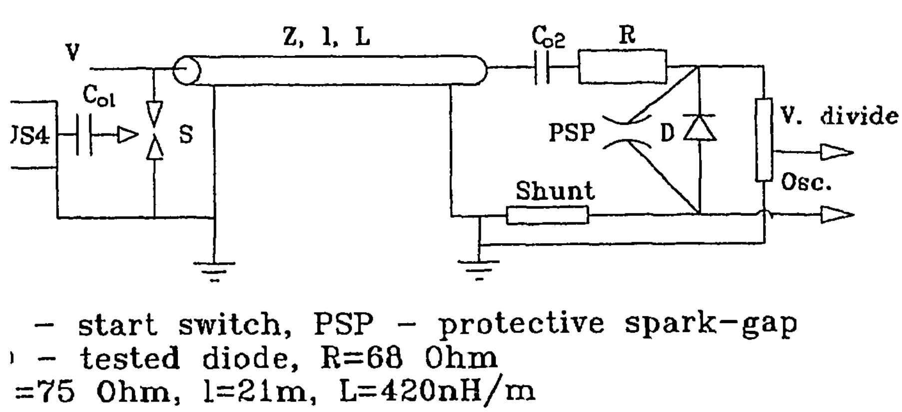

Fig. 2. Scheme of circuit for diode testing

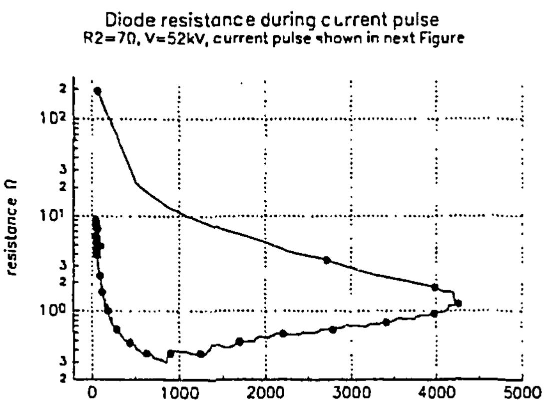

Fig. 3.

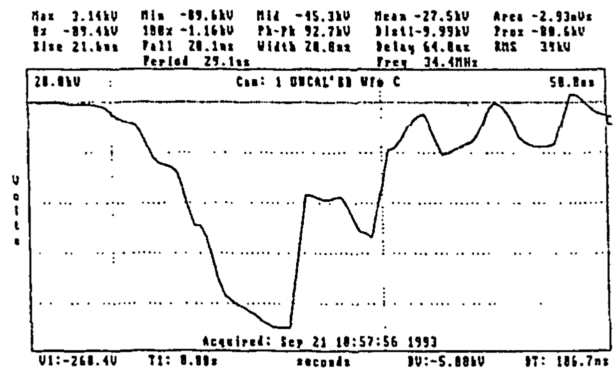

Voltage during breakdown withstand tests of diode 0.4A. 80kV

Fig. 4.

Technical data and experience acquired during realization of the project give overall picture of behaviour of the system in the steady-state conditions as well as in transients states. This theoretical and experimental knowledge creates the foundation for further development and undertaking a technical design of prototype accelerator.

*) The project was supported by Polish State Committee for Scientific Research - project no 2 0985 91 01.

1.6 Electron Linear Accelerator FEL for Spectroscopy of Muonic Hydrogen

by S.Kuliński, J.Bigolas, M.Pachan

The short muon life time and the high accuracy required in measurement of the energy difference between levels of muonic hydrogen, having at the same time a reasonable event rate, set a number of severe requirements on the radiation source needed for experiment. Analysis of the problem made in the ENEA Institute at Frascati [1] has shown that the optimum solution is Free Electron Laser (FEL) excited by a linear electron accelerator. The principal parameters of such an accelerator should be as follows:

Output energy	-	5.5 MeV
Pulse current (macro-bunch)	-	0.45 A
Pulse duration	-	2 μsec
Peak current (micro-bunch)	-	40 A
Micro-bunch duration (FWH M)	-	3.7 ps
Pulse repetition frequency	-	200 Hz
Injection energy	-	70 - 100 keV
Electron gun	-	Pierce, Triode
Accelerating system	-	standing wave $\pi/2$, S-band (f = 2998 MHz)
RF power source	-	pulse klystron

On the request of the ENEA Instituite the Department of Accelerator Physics of Soltan Institute made a preliminary project of the accelerator fulfilling the above requirements. The main parts of the system are:

100 keV gun, RF chopper, prebuncher, 5.5 MeV standing wave $\pi/2$ - biperiodic S-band accelerating structure, focusing elements and steering.

The Gun: type - Pierce, triode, pulse duration 2 μs, energy Wg = 100 keV, energy dispersion $\Delta Wg/Wg = 10^{-3}$, current $(1 \div 1.5)$A, emittance $\epsilon \approx \pi \cdot 10^{-5}$ m rad. Cathode (dispenser) diameter $D_K \approx 6$ mm.

The chopper: To avoid the beam loading of the system by electrons which will be outside the phase acceptance of the accelerating structure, it can be necessary to eliminate those electrons by a chopper. An RF cavity oscillating in the deflecting TE_{102} mode is proposed.

The prebuncher: is necessary to increase the peak current of the bunch decreasing simultaneously the energy and phase dispersion at the exit of the linear accelerator which follows the prebuncher. The preliminary calculations have given the following results for the prebuncher parameters: bunching

parameter $B_p = \pi D V_{PB}/(V_0 \lambda \beta_0) = (1.45 \div 1.55)$ where $D \approx 25$ cm drift space, $V_{PB} \approx 10$ kV prebuncher voltage, $V_0 \approx 100$ kV gun voltage, $c\beta_0$ - electron velocity corresponding to V_0, prebuncher gap $g = 0.1\ \lambda = 1$ cm. For these values the band of input phases $\Delta\phi_i \approx 150^0$ is squeezed to $\Delta\phi_{out} \approx 25^0$.
Accelerating structure: type - standing wave biperiodic, mode $\pi/2$, frequency $f = 2998$ MHz, number of cavities 10+2 halves, length $L \approx 54$ cm, shunt impedance $Z_{sh} \approx 70$ MΩ/m, unloaded quality factor $Q_0 \approx 12000$.
Filling time and beam loading
The filling time is given by

$$\tau = \frac{2Q_0}{\omega(1+\beta)}$$

where $\omega = 2\pi f$, and β is the coupling constant. For $Q_0 = 12\,000$, $\beta = 1$, and $f = 3 \cdot 10^9$Hz, $\tau = 0.64\ \mu$sec

To have shorter filling time-necessary for the experiment with muonic hydrogen one should have larger β. On the other hand to avoid the large energy dispersion caused by the heavy beam loading one should precisely choose the coupling β and the moment of beam injection to the structure. The right time to turn the beam on, is

$$t_b = \tau \ln \frac{2\beta^{1/2}(Z_{sh}LP)^{1/2}}{iZ_{sh}L}$$

Taking: $\beta = 3$, input power $P = 3.4$ MW, $i = 0.45$ A, we get $\tau = 0.32\ \mu$sec, $t_b = 0.27\ \mu$sec, $V = 5.56$ MV, these values are close to the required [1,2]. The power supply will be the (6-7) MW klystron.

[1] F.Ciocci at al. Compact Waveguide FEL for Spectroscopy of Muonic Hydrogen - Report ENEA
[2] F.Della Valle et al. Measurement of the 3D-3P Transition in Muonic Hydrogen - Report ENEA

1.7 Emittance Measurements in Electron Guns
by J.Pszona, J.Olszewski, M.Śliwa

Beam monitoring plays a great role in designs of high energy and high power accelerators. Most frequently used controlling systems assume beam current and beam emittance monitoring. Current losses as well as emittance growth, both are unwanted processes which should be avoided during the beam acceleration. To compare the quality of guns, measurements of emittance are necessary during their upgrading and tests.

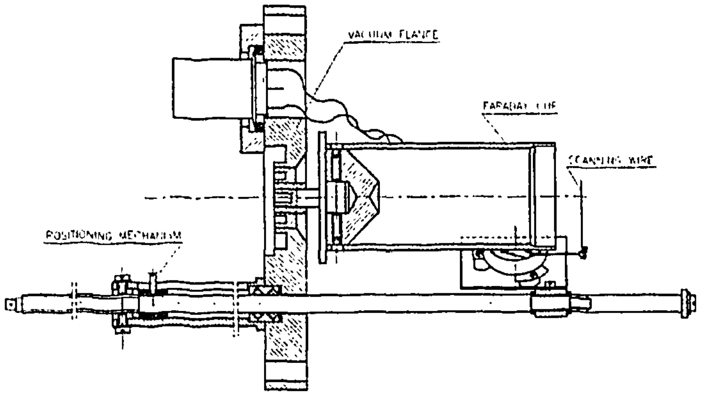

Fig.1. Emittance measurement system

To measure a particle position and angle distribution in a beam, a special two-scanner measuring system has been designed and constructed. Side view of the system is shown in fig.1. It consists of a vacuum flange, a Faraday cup, scanners and mechanics. The vacuum flange is sealed to the experimental chamber by an O-ring seal. The Faraday cup situated behind the scanners is made of copper and has 40mm diameter and 100 mm length. It permits the control of the gun working region. Mechanical construction enables the movement of the scanning plane in 75 mm range, giving complete information about the behaviour of the beam in the drift region. The scanner's construction is based on electromagnetic mechanisms of microampere meters. These mechanisms are steered by 7-bit digital to analog converters (fig.2). The signal from the converter moves the scanning wire through the examined distance in 128 steps. The position of a wire is displayed on a 3 digit display and is registered on XY recorder. The construction of electronics allows us to work in one-step - manual mode, which is very useful during the calibration of the scanners. During profile measurements the scanning is automatic with regulated frequency of steps. The signal from scanning wire is registered in Y-channel of XY recorder. As the signal could be as small as 10^{-9} A, a special electrometric, low bias, current to voltage converter has been used in the signal path. During the first tests of the system a triode electron gun characteristics has been measured. Beam profiles which have been plotted gave a value of emittance $4\cdot\pi\cdot10^{-4}$[m·rad]. Further steps in testing the gun will show what improvement of beam quality could be possible.

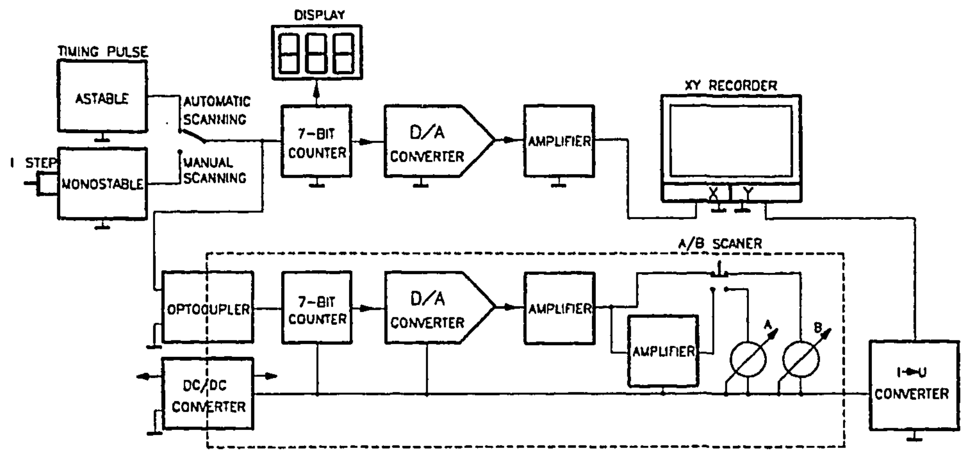

Fig.2. Scanner's electronics

1.8 Heating Effect of Output Window in High Power Electron Accelerator

by I.Zychor, M.Rabiński

The heating of a beam output window in a high power d.c. electron linear accelerator is one of the most important processes which have to be taken into account in a design of such an accelerator. The heating is a result of electron interaction with matter followed by an absorption of energy in a metallic foil used as a window.

In the case of a "thin" window, which thickness is small in comparison with the range of incident electrons, the multiple Coulomb scattering is observed together with other processes of less importance. The SHOWME Monte Carlo code [1] is used to simulate the transport of electrons, positrons and photons through matter. All basic interactions of primary and secondary particles are taken into account.

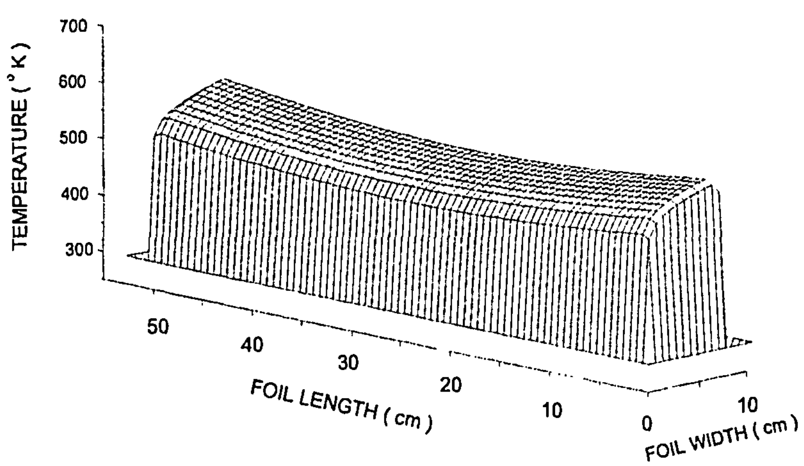

Fig.1. The temperature distribution in a 50 μm titanium foil calculated for 800 keV electrons

An 800 keV electron beam was assumed to penetrate a 50 μm titanium foil. The 800 keV electron range in titanium is equal to 0.49 g/cm^2. The beam is incident on the titanium foil in the following way: it is parallel to the primary beam direction in the foil centre and its angle of incidence increases monotically up to 30° at a distance of 3 cm from the foil centre. The energy absorption coefficient calculated by use of the SHOWME code for the beam described above is equal to 0.045 ± 0.004.

A mathematical model of the thermal phenomena is given by the two-dimensional conduction equation. During the foil irradiation the outside surface of the window is cooled down by the air blowing from a nozzle situated side-on along the window edge. Efficiency of this type of cooling is given by a semi-empirical formula describing the distance dependence of a coefficient in Newton's law of conductance. The energy radiation from both foil surfaces is described by the Stefan-Boltzmann law. Boundary conditions are determined by a given temperature of the foil supporting frame.

Computations of the temperature distribution in the accelerator window have been carried out with TFIELD code [2] for several materials of foil. Results for the titanium window are shown in Fig.1. The main characteristic of the calculated temperature distribution is a nonsymmetric thermal field introduced by the applied cooling technique.

[1] I.Zychor, "Applications of Monte Carlo Method to Electron and Photon Transport", SINS Report 3/X (1994)

[2] M.Rabiński et al., "Numerical Method of Solving Two-Dimensional Heat-Conduction Equation", INR Report 1917/XXIV/PP/A (1981)

1.9 Monte Carlo Simulations of Irregular Radiation Fields in Radiotherapy

by I.Zychor

A typical electron beam defining system consists of scattering foils, adjustable collimators and an electron applicator. The scattering metal foils flatten the radiation field of medical accelerators. The adjustable collimators shield a patient from secondary radiation. The electron applicator produces radiation fields with demanded shapes and protects surrounding healthy tissues.

The Monte Carlo simulation allows to see the effects of different parts of the beam defining system on the final dose distribution. The simulation geometry is shown in Figure 1. The 18 MeV monoenergetic, monodirectional electron beam (so called "pencil beam") is perpendicularly incident on the water phantom. The full simulation includes all components of the beam defining system which either cross the beam or are used to define its edge. Parts of the supporting assembly which came close to the geometric edge of the beam were not included. Some of the details of the beam defining system are given below.

In Figure 2 the Monte Carlo calculated relative isodose contours for an 18 MeV electron pencil beam in water are shown for the tube aluminum applicator with a cut-out in a shape of letter I which is 12 cm high, with bottom and top parts 9 cm long and 4 cm thick. The electron applicator height is 2.5 cm. The isodose contours are calculated for a setup consisting of the scattering foil and electron applicator, both described above. The scattering foil is placed 30 cm from a vacuum window and the applicator - 90 cm from it. The distance between the vacuum window and the water phantom surface is 96 cm. The shown isodoses are for the fourth 1 cm thick layer lying 4 cm below the water phantom surface. The calculated isodoses follow the shape of the electron applicator.

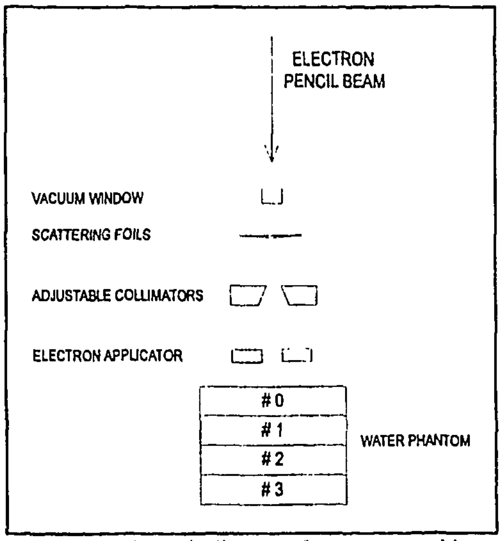

Fig.1. The schematic diagram of geometry used in calculations

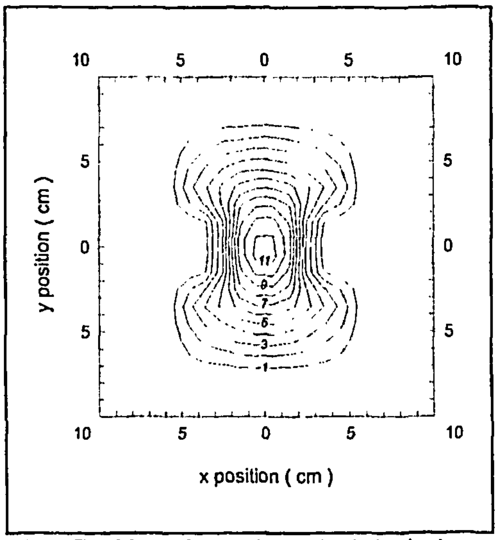

Fig.1. The Monte Carlo calculated relative isodose contours for an 18 MeV electron pencil beam for a beam defining system described in a text

The calculations were performed on the CONVEX C-3210 computer at the Soltan Institute for Nuclear Studies at Świerk. One million particle histories were simulated in calculations. The average calculation time taken per one incident electron depended on the setup geometry. For the case presented here it was 0.024 seconds. The calculations were made on the 1 cm x 1 cm mesh.

The presented Monte Carlo calculations are helpful in a better understanding of phenomena occurring when the electron beam passes through the matter and they could be used for designing of beam defining systems [1].

[1] I. Zychor, "The Application of Monte Carlo Method to Electron and Photon Transport", SINS Report-3/X (1994)

1.10 Preliminary Results of Beam Acceleration in the SC Linac LISA at LNF Frascati

by M.Castellano[1)], M.Ferrario[1)], M.Minestrini[1)], P.Pattari[1)], F.Tazzioli[1)], L.Catani[1)], S.Tazzari[1)], S.Kuliński

The construction of the superconducting (SC), radiofrequency (RF) electron linac LISA [1] at Frascati INFN Laboratories was completed at the end of 1993 and its commissioning was carried out in the first half of 1994. The project started in 1989 as a test machine for technologies related to linear colliders. Originally an FEL program was also launched as a useful application and a test of the beam quality. The room temperature 1 MeV injector had been completed two years before [2] and beam transport tests had already been performed, obtaining 0.5 mA in several millisecond pulses at the entrance of the SC linac, after the achromatic 180^0 degrees arc. The energy spread was about 2%, consistent with theoretical predictions.

Acceleration through all four cavities was first achieved in a two week shift in March 94. The cavities were driven with 40 ms RF pulses and 1 Hz repetition rate, so as to obtain high peak field values without overloading the refrigerator, even with relatively low Q values of the order of several 10^8 at (3.5 ÷ 4) MV/m.

The average current of 0.5 mA was accelerated to 20 MeV with an rms energy spread of $4 \cdot 10^{-3}$. Considerable fluctuations in transverse position and peak current were present and at least partly attributed to residual fluctuations of the injector RF parameters, especially phases, and to the SC cavities voltage fluctuations, particularly those of cavity no 1 - the first encountered by the 1 MeV beam.

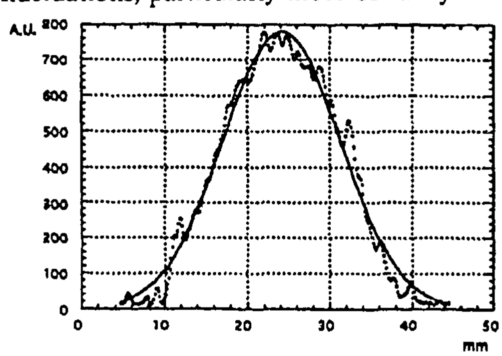

Fig.1. Beam energy spectrum (1.8 mm = 1‰)

As for the injector, a campaign of improvement of the control and stabilisation circuitry is in progress. Improved stability of the voltage and phase of the forward RF wave feeding the capture section have already allowed to transport 2 mA through the 1 MeV and practically without losses.

Vibrations of SC cavities are still a problem. The stability seems to improve as the pressure in the liquid helium bath is increased. At present, the maximum attainable pressure is, however, limited to 1.4 bar absolute by the safety valves that protect cavities against deformation [3].

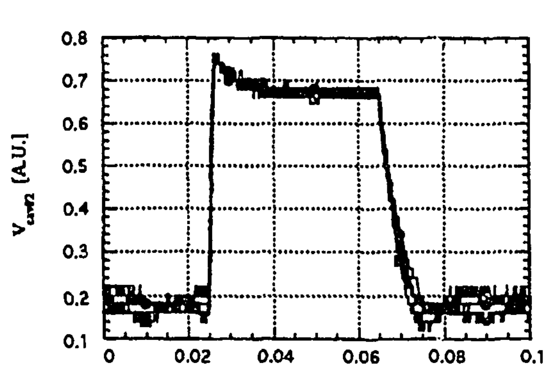

Fig.2. Waveform evolution in quiet cavity

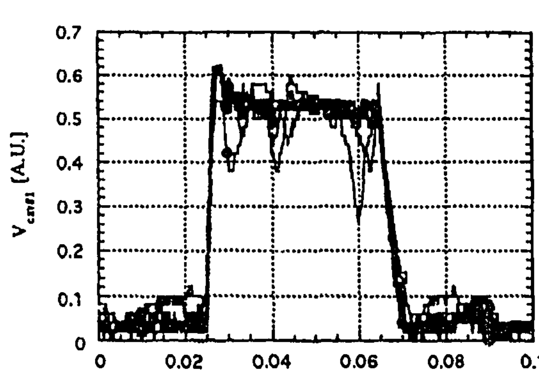

Fig.3. Waveform evolution in vibrating cavity

[1] M.Castellano et al. "Status of the LISA Superconducting Linac Project", in Proc. of Particle Accelerator Conference, San Francisco, USA, May 1991.

[2] A. Aragona et al. "1 MeV Capture Section for LISA Injector", Proc. of the EPAC 90 Conference Nice, June 1990.

[3] Proc. of the EPAC 94 Conference, London, June 1994.

[1] Istituto Nazionale di Fisica Nucleare, Frascati, Italy

1.11 Higher Order Mode Power Deposition in the Superconducting RF Accelerating Cavities of LEP Collider*)

by E.Pławski

To rise the energy of the LEP collider to its design value of 90 GeV per beam a total of 192 superconducting (SC) accelerating cavities is being actually produced at CERN [1]. These cavities will boost the old RF accelerating system composed of 120 conventional room temperature cavities. The majority of the cavities is built in Nb sputter coated Cu technology. At a temperature of 4.5 K the RF power lost in one 4-cell cavity to excite 6 MV/m of fundamental mode is about 100 W and it has to be removed by boiling helium. The cavities are assembled in cryo-modules of 4 cavities each using bellow-shaped interconnections. The beam ports of cryo-modules have the form of conical section (taper) which brings down the large bore of cavity end to a standard beam tube. The frequency of fundamental (accelerating) mode is 352.21 MHz and higher order TM_{0n} type modes have cut off frequencies 1.1 GHz at the taper beginning and 2.2 GHz at the taper end.

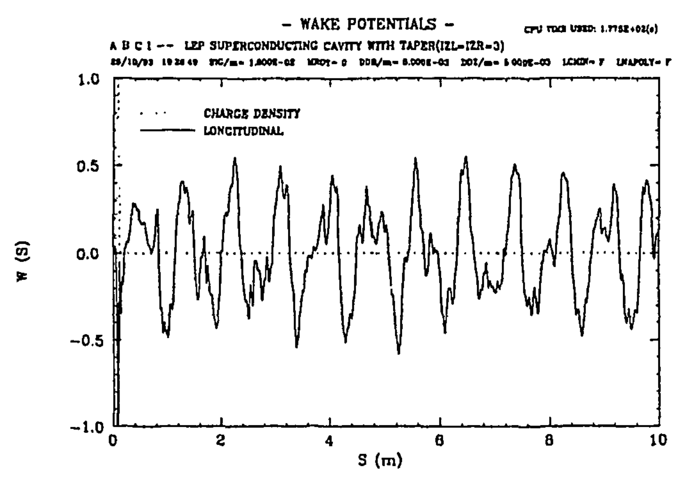

Fig.1. Longitudinal wake left by 1.6 cm gaussian bunch in 4-cell SC cavity

A bunch of charged particles passing the accelerating cavities and interconnections induces both longitudinal and transverse-deflecting fields. The kinetic energy lost by a bunch is transferred to electromagnetic energy within the volume of the cavity, the frequency spectrum of the exited parasitic modes depending on the bunch length and the cavity geometry. Amongst the parasitic modes, for a small beam deviation from the axis, only the TM_{0n} and TM_{1n} are of interest as withdrawing a sizable amount of energy and being responsible for beam instabilities respectively. To minimize these effects, these modes have to be sufficiently dumped. Various types of higher order mode (HOM) couplers [2] or absorbers are under development to remove effectively the energy deposited into the above modes.

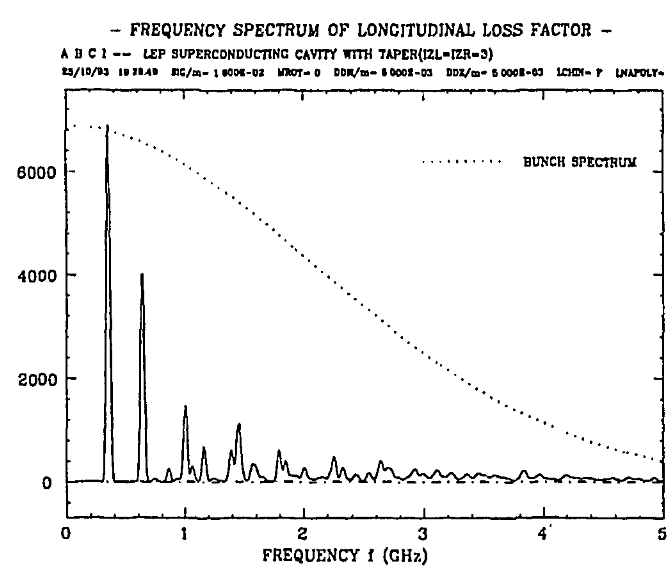

Fig.2. Real part of FFT of wake of Fig.1

A parameter of particular concern for practical realisation of such damping schemes is the total generated HOM power and its spectral distribution. In our case it was calculated by a numerical solution of the Maxwell's equations in the time domain. For this purpose code ABCI [3] treating the more general problem of transverse and longitudinal wake potentials was used. From the calculated wakes the coupling impedances are found. The frequency spectrum of longitudinal loss factor is then obtained as a product of the real part of longitudinal impedance and bunch spectral power density factor $\exp(-(\omega\sigma/c)^2)$.

The actual LEP1 (45 GeV per beam) beam intensities are achieved by the use of all installed wiggler magnets maximizing the bunch length to a value of about 2 cm rms [4]. As a consequence of energy upgrading to 90 GeV per beam (LEP2) the bunch length may go down even below 1 cm. This will increase the losses and automatically increase the HOM power to be extracted from the RF cavities.

The longitudinal wake potentials, impedances and loss factors were calculated for different bunch lengths down to 0.5 cm rms [5], the shape of SC cavities, interconnections and tapers taken as the boundary conditions.

The example of longitudinal wake left in the cavity and corresponding real part of impedance is shown in Fig.1 and Fig.2.

In Fig.3 the differences of loss factor for different bunch lengths are illustrated.

For LEP beam intensity of 0.75 mA average per bunch, and 4 bunches per each of electron and positron circulating beam the HOM power deposited in different frequency ranges is illustrated in Table 1.

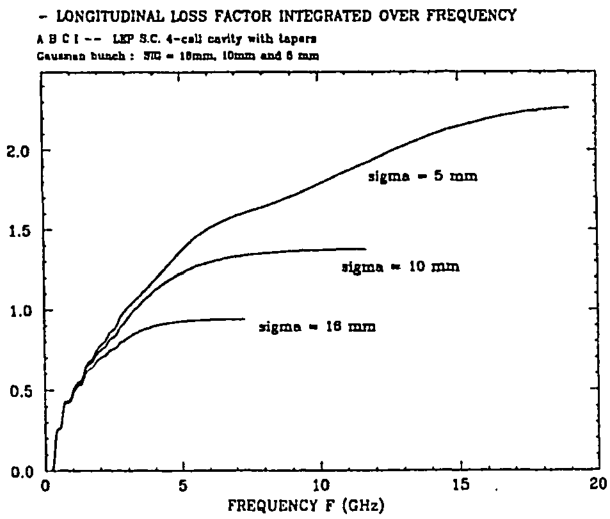

Fig.3. The integral of energy loss factor vs frequency

Table 1.

Bunch length rms (cm)	Total HOM power per module (W)	Power per coupler for f < 2.2 GHz (W)	Power per module above 2.2 GHz (W)
1.6	1000	95	240
1.0	1460	105	620
0.5	2690	108	1830

The powers were calculated for 1 cryo-module comprising 4 cavities, 5 interconnections and 2 tapers. Each SC cavity is equipped with 2 HOM couplers, a total of 8 couplers per cryo-module. The power in the first frequency range can be completely extracted by HOM couplers since their external Q is 5 order of magnitude smaller then the Q_0 of modes in this frequency range. It is expected that also the energy going into the region 1.1 ÷ 2.2 GHz will be extracted so efficiently that significant additional cooling power consumption is avoided [6,7]. Above 2.2 GHz longitudinal cavity modes may excite the propagating TM_{01} waveguide mode in the beam line. This mode will be there absorbed by special ferrite absorbers which are under development.

[1] G.Cavallari et al. Status of the RF Superconductivity of CERN AT/93
[2] E.Haebel Particle Accelerators vol. 40 (1992)
[3] Y.H.Chin CERN, SL/93-24(AP)
[4] J.M.Jovett CERN SL/93-24(AP)
[5] E.Haebel, E.Pławski, CERN LEP Note 94-19 (SL)
[6] Ph.Lebrun CERN AT/94-08 (CR)
[7] E.Haebel CERN, SL-DI 94-06, p.429-436

*) This work was done during scientific stay at CERN

1.12 Quality Assurance Program on Stereotactic Radiosurgery: Test of PLATO Radiosurgery Treatment Planning*)

by A.Wysocka

Three-dimensional treatment planning system (PLATO) was used to calculate the isodose distributions for linac-based various radiosurgical techniques:single stationary beam irradiation, complete rotational irradiation, convergent beam irradiations (CBI). This system was verified experimentally with 15 MV X-ray narrow beams following the treatment planning test program suggested by G.Hartmann and I.Ermakov [1].

To measure the dose and the dose distribution the film dosimetry in a solid spherical and cubic tissue-equivalent phantoms was used.

The phantom consisted of a number of 1 cm thick RW-3 slabs shaped into a sphere with a 16 cm diameter. The film could be placed between two parts of the sphere in such a way that different displacements of the film plane from the centre of the sphere were obtained. All measurements for CBI were performed each in a transverse (x-y), coronal (x-z) and sagittal (y-z) planes.

In each test a comparison of measured and calculated data were obtained for the three beams formed with collimators of 5, 10, and 20 mm in diameter.

Inaccuracy of measurements is estimated to be 5%. Such an inaccuracy induces corresponding errors in the definition of position, depending however on the level of the dose taken for the comparison. Above the 50% dose level where the gradients of dose distribution are of the order 10% per mm, a 5% error in the measured value of the dose corresponds to a displacement of 0.5 mm between the measured and the real isodose curve.

For the single stationary beam irradiation a comparison between measured and calculated: (a) depths at 80%, 70% and 50% of the dose and (b) displacements from central axis at 50%, 10% and 5% of the dose was done. The reference depth was 30 mm. For the (a) and (b) cases all differences were below 0.5 mm and 0.1 mm, respectively.

In the complete rotational irradiation technique one may use continuous or incremented change of azimuthal angle. The isodose contours dependence on the angle incrementation was tested. The deviations from the circular form less than 0.3 mm and 5 mm for isodose contours above and below 50% of nominal dose were observed respectively, once the angle increment was up to 10^0. With an angle increment much higher (20^0), the observed deviation from the circular contours were too large (>10 mm).

At the same time, a comparison of diameters of measured and calculated isodose contours were performed for this type of irradiation.

The 80% and 20% levels were compared with the computed isodose contours in the central transverse plane, at an angle increment Δ of 10^0.

It was possible to obtain an agreement between measured and computed diameters better than 0.3 mm and 10.0 mm for dose levels above and below 50% of nominal dose respectively.

The measurements of dose profiles performed with CBI irradiations were aiming to check the accuracy of the calculated dose distributions. Measured and calculated beam profile widths were compared along X, Y and Z stereotactic coordinates, centred at the target point. The profile widths were compared at different isodose levels. The technique of six arcs with 140^0 per arc was used in all CBI irradiations. A target point irradiated with 30 Gy was placed: (a) in the centre, (b) 2 cm and (c) 6 cm from the centre of the spherical phantom. Measured and calculated profile widths differed less than 0.5 mm, 1.0 mm and 10.0 mm for 80%, 50%, and 20% dose levels, respectively.

Finally the test of monitor units was performed. It confirmed that monitor units provided by the treatment planning for each arc of a CBI and a given dose accumulated in the target point agree to 3% with the absolute value of the dose measured at the target point in the phantom.

A conclusion can be drawn that calculated and measured results compare well for all the tested quantities.

[1] G.Hartmann et al."A Quality Assurance Program on Stereotactic Radiosurgery" 1994, (in press)

*) This work was done in DKFZ-Heidelberg and supported by CEC

1.13 Tissue-Phantom Ratio TPR, Beam Profiles and Relative Output Factors of Small Circular 15 MV X-ray Beams for Radiosurgery*)

by A.Wysocka

Radiosurgery refers to high-dose irradiation of a limited volume of tissue, generally in a single fraction. Acceptance of a new technique in radiotherapy, such as linear accelerator based radiosurgery, requires a precise dosimetry. In the Department the of Radiology of German Cancer Research Centre in Heidelberg the following characteristics of the small fields were determined:(a) relative output factors, (b) dose profiles (off-axis factors), and (c) central axis attenuation on the beams (tissue-phantom ratio (TPR) and percentage depth dose).

The 15 MV X-ray beam from Mevatron was formed using additional cylindrical collimators of 5, 10 and 20 mm in diameter.

In order to measure dose and dose distributions the diamond detector in a water phantom (Welhöfer) and the therapy verification film Kodak X-Omat V in a solid and cubic tissue-equivalent phantom (PTW Freiburg) were used.

The relative output factors for the beam formed with collimators of 5, 10 and 20 mm in diameter were 0.69; 0.89; and 0.99 respectively.

The percentage depth dose (PDD) values for a 15 MV X-ray beams formed with collimators of 5, 10 and 20 mm in diameter were measured.

The measurements of the collimator scatter correction factor $S_c(r)$ and the total scatter correction factor $S_{c,s}(r)$ for small fields (collimator diameters: 5÷20 mm) were performed according to [1]; see fig.1.

The results of these measurements were used for the determination of the phantom scatter correction factor $S_p(r)$, and the tissue-phantom ratio TPR (d,r_d) by the relation:

$$TPR(d,r_d) = \left(\frac{P(d,r,f)}{P(d_0,r,f)}\right)\left(\frac{f+d}{f+d_0}\right)^2\left(\frac{S_p(r_{d0})}{S_p(r_d)}\right)$$

Figure 2 shows a comparison of measured TPR (d,r_d) with TPR (d,r_d) calculated from depth dose with and without correction factor. The estimation of the error in the TPR determination was done and appropriate beam model required for small field treatment planning was determined.

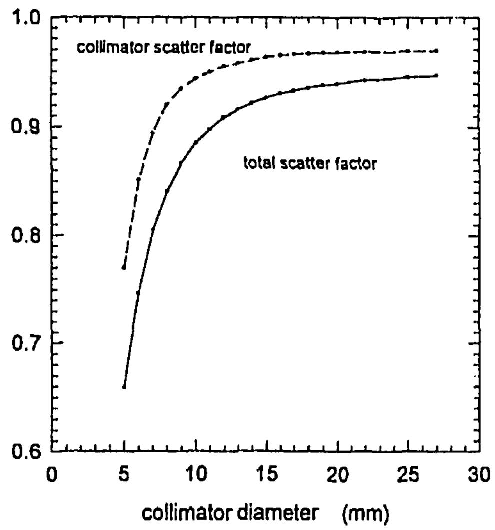

Fig.1. Scatter correction factors as a function of collimator diameters

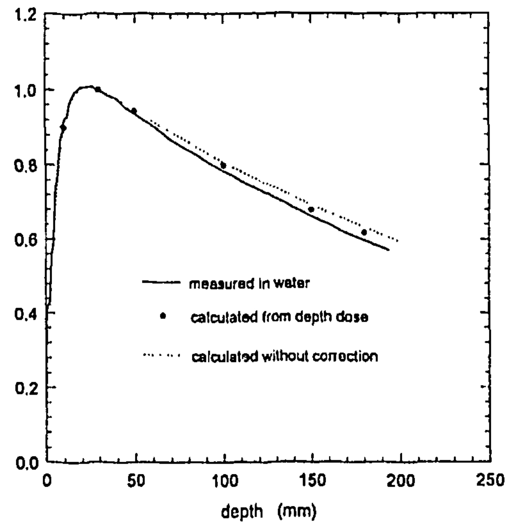

Fig.2. TPR values of 15 MV X-ray beam for 5 mm collimator diameter

The purpose of this work - to give basic input data for the radiosurgery treatment planning program was fulfilled.

[1] F.M.Khan et al. Med.Phys. 7(3), May/June 1980

*) This work was supported by CEC grant.

1.14 Medical Electron Accelerator CO-LINE

by B.Cisowska, E.Jankowski, L.Kotulski

Since December 1994 the accelerator has been operated in the Regional Oncological Centre, Łódź. It has passed perfomance tests according to international standard IEC 976 and technical report IEC 977. The accelerator parameters are listed below (according to the IEC 977).

X-ray wedge filters:

Design.	Max. irradiat. field	Wedge filter angle	Related isodose value	Wedge filter factor
15^0 (fig.1.)	20x20 cm	20^0	67.1%	78%
30^0	15x20 cm	33^0	65.0%	70%
45^0	10x20 cm	47^0	63.0%	70%
60^0 (fig.2.)	10x20 cm	57^0	63.6%	55%

Dose monitoring system.

Range of absorbed dose over which the standard is met - 0 to 10 Gy.
Range of absorbed dose rates over which the standard is met - 0.5 - 2 Gy/min.

Reproducibility: 0.16%, tolerance 0.5%
Proportionality: 1.2%, tolerance 2%
Dependence of the shape of the radiation field: 1.2%
Stability after high absorbed dose delivered: 0.2%, tolerance 2%
Stability throughout the week: 0.8%, tolerance 2%
X-radiation.
Nominal X-ray energy 4 MeV.
Penetrative quality: 5.50 cm. Max. deviation 1.8%, tolerance 3%
Quality index: 0.626
Flatness of square X-ray fields: 108.7%
Symmetry of square X-ray fields: 102.2%, tolerance 103% - fig.3.
Maximum ratio of absorbed dose: 105.5%, tolerance 107%.
Depth of dose max. for 10x10 cm radiation field: 1.1 cm - fig.4.

Penumbra of radiation fields:

radiation field	5x5 cm	10x10 cm	30x30 cm
penumbra /mm/	8.1	8.7	12.3

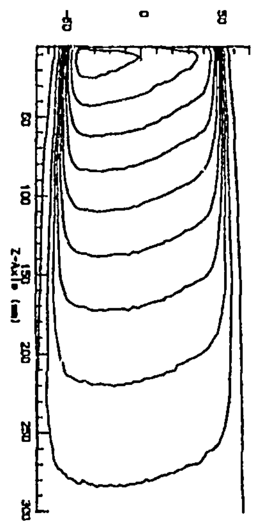

CO - LINE 10x10 FSD 80cm WA15°

Fig.1.

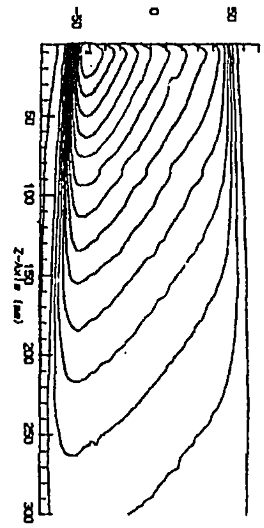

CO - LINE 10x10 FSD 80cm WA60°

Fig.2.

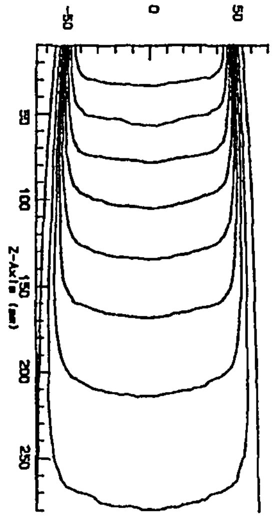

CO-LINE 10x10 FSD 80cm

Fig.3.

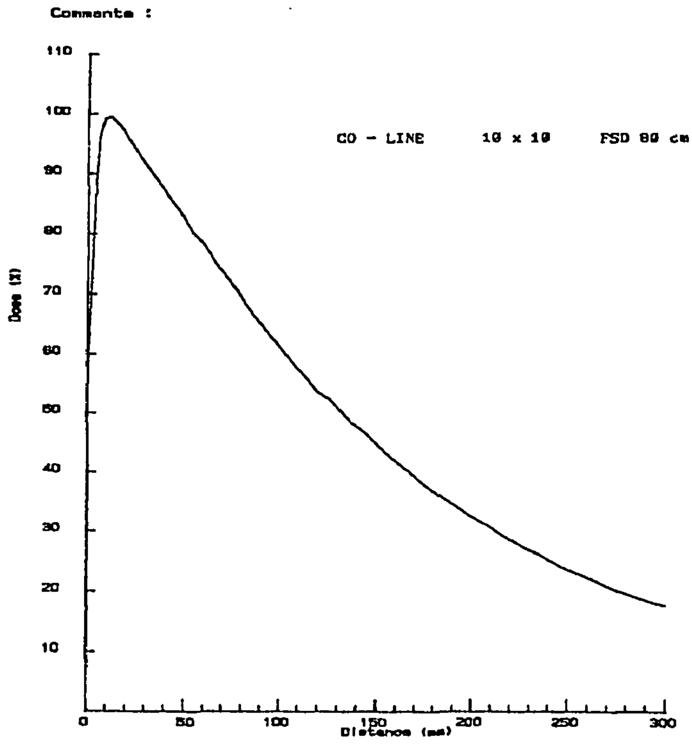

Fig.4.

1.15 POLKAM 15 - Therapeutic Table with Direct Current Power Transmission System

by J.Kuczyński, A.Kuciak, Z.Kuciak

Direct current power driving system has been designed and constructed by ZDAJ to provide continuous and precise displacements of moving parts of the therapeutic table. Solution is based on thyrystor converter with phase control ensured inverter operation. Functional block diagram of all power driving system is shown in fig. 1.

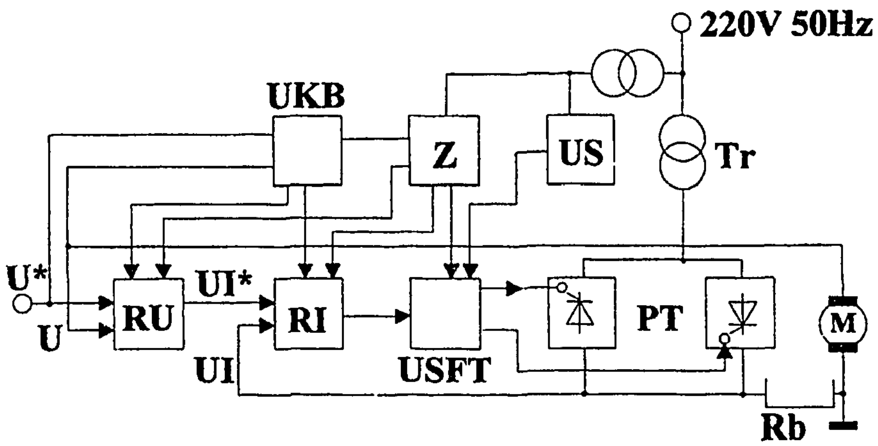

Fig.1.

Functional blocks:

- thyrystor converter	- PT	- comparator and interlocking units	- UKB
- voltage regulator	- RU	- motor	- M
- armature current regulator	- RI	- transformer	- Tr
- phase control unit	- USFT	- measure dropping resistor	- Rb
- phase lock unit	- Us	- stabilized voltage supply	- Z

Application of the electromagnetic clutches and brakes enables both automatic and manual control. Two consoles, located on both sides of the table, ensure a convenient control of the drivers.

2. PROTON AND ION ACCELERATORS

2.1 C-30 Cyclotron Upgrading in 1994

by J.Wojtkowska, J.Lorkiewicz, T.Kozłowski, E.Pławski, R.Morozowicz, W.Pencillo, A.Grajda

In 1994 the C-30 isochronous cyclotron at Soltan Institute for Nuclear Studies was used for basic research in low-energy nuclear physics. Two research projects concerning 1) study of the neutron-rich nuclei from the region of symmetric fission, produced in an uranium target bombarded by 25 MeV protons and 2) study of the charged particles spectra and angular distributions from the proton induced reactions, were continued [1]. The overall operation time of the machine in 1994 was close to 300 hours.

To improve the operational characteristics of the machine itself, the following changes were made:

- a new stripper foil driving system was constructed
- the radioactive contamination of the system components was partially reduced
- the life-time of the internal, PIG-type H^-ion sources, was considerably increased

In order to obtain a proton beam, H^- beam acceleration is followed by stripping on an aluminum foil. The external proton beam transmission depends on the stripper position with respect to the axis of the following ion guide. So far only the radial position (the distance from the machine centre) of the stripper was varied and the proton beam exit coordinates were dependent on the beam energy. Additional trajectory corrections using external steering magnets were only partially successful and the final beam intensity and quality was severely reduced. To correct this effect a new driving system for the stripper was developed, which permits to change its position in both, radial and azimuthal directions. The stripper is moved using two step-motors with a remote-control system.

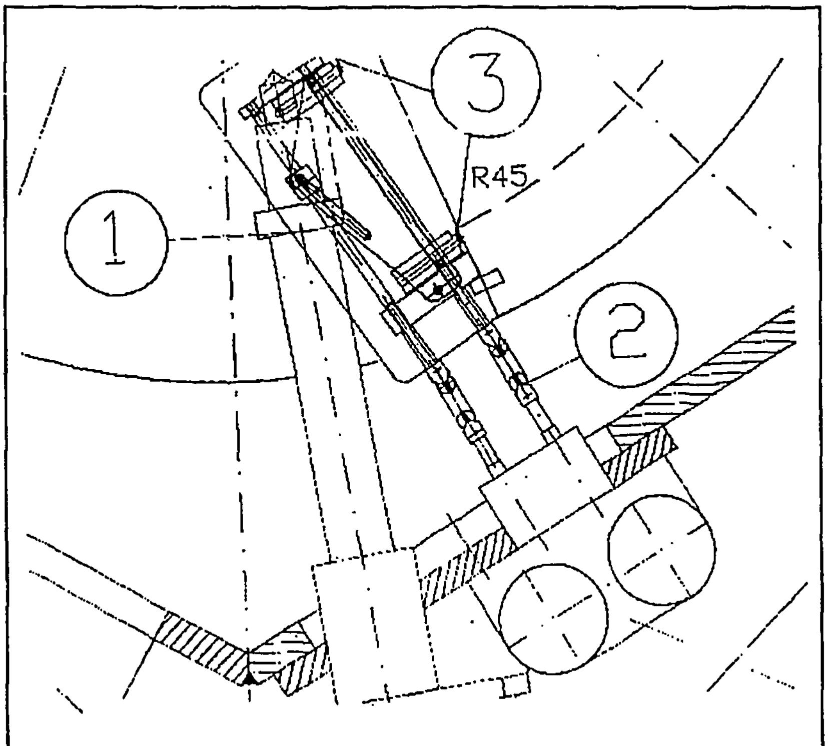

Fig.1. The C-30 beam extraction region

The radioactive contamination of the ion guide, internal ion sources and vacuum chamber was due to ^{56}Co isotope production in components made of stainless steel. New ion guide and ion source with components of aluminum alloy were installed. Works on a vacuum chamber radiation shield have begun.

The PIG-type ion sources continuous operation time was limited by sputtering of tantalum cathodes by heavy ions produced by ionization of gas impurities. To cope with this a new gas feeding system was constructed with a water absorber and a palladium filter. The operation time was increased from the typical 25 up to over 70 hours.

[1] J.Lorkiewicz, J.Wojtkowska, E.Pławski, A.Piotrowski, Z.Preibisz, T.Kozłowski, J.Rondio, "Upgrading Programme of the C-30 Cyclotron at Swierk and its Use for Experimental Physics, Proc. Fourth European Particle Accelerator Conference, London, June 1994

2.2 Construction and Preliminary Tests of the External H^- Ion Source for the C-30 Synchronous Cyclotron

by J.Lorkiewicz, T.Ołdakowski, E.Pławski, H.Wojnarowski, A.Stępiński, W.Pencińło

The extracted beam intensity of C-30 cyclotron is currently limited by the operating parameters of internal H^-, PIG-type ion sources.

The limiting parameters are:

- the H_2 pressure in the source discharge
- RF dee voltage amplitude

The high H^-density in the discharge plasma calls for high pressure which in turn leads to the stripping in the process of acceleration. The least energetic protons give rise to excessive radiation hazard.

The good extraction efficiency of H^- ions from thermal plasma calls for the very high RF dee voltage; this, due to the RF break-downs, limits the RF pulse duty ratio to the value of 0.2.

The way to overcome these limitations is the injection of H^- ions of energy 18 keV to flue centre of the cyclotron from the external source. An external, miniature multicusp H^- ion source was designed and developed within last years. It consists of a small (33 mm in diameter) plasma chamber surrounded by 12 rows of permanent magnets arranged in the line-cusp configuration. The construction of the source started in 1993 and was continued in 1994. The following components of the prototype source were completed in 1994:

- the supporting structure for ferrite or samanium-cobalt permanent magnets with a distilled-water cooling system, which can absorb up to 3 kW of a heat flux from discharge chamber. The discharge chamber average temperature should be kept below 600 K.
- the back flange of the plasma chamber with cathodes of thoriated tungsten filaments and a water cooling system,
- the supporting structure for extraction electrode with a cooling system.

The prototype source was completed in 1994 and the preliminary tests were done. The source was attached to the beam injection system and its working parameters were measured. The total current from the source was measured using a Faraday cup placed 40 cm from the emission hole. Transverse magnetic field was generated in the extraction region, in order to reduce the electron current to the cup. The obtained source operation parameters are listed below:

- filament current	40 A
- arc current/voltage	10 A/150 V,
- gas flow rate	4 ccm/min STP,
- emission hole diameter	5 mm,
- H^- current	about 1.2 mA

The source optimization will be continued. The ion beam intensity is supposed to increase after replacing the ferrite magnets by samarium-cobalt ones. So far the arc current and vacuum pumping speed couldn't be increased due to financial restrictions.

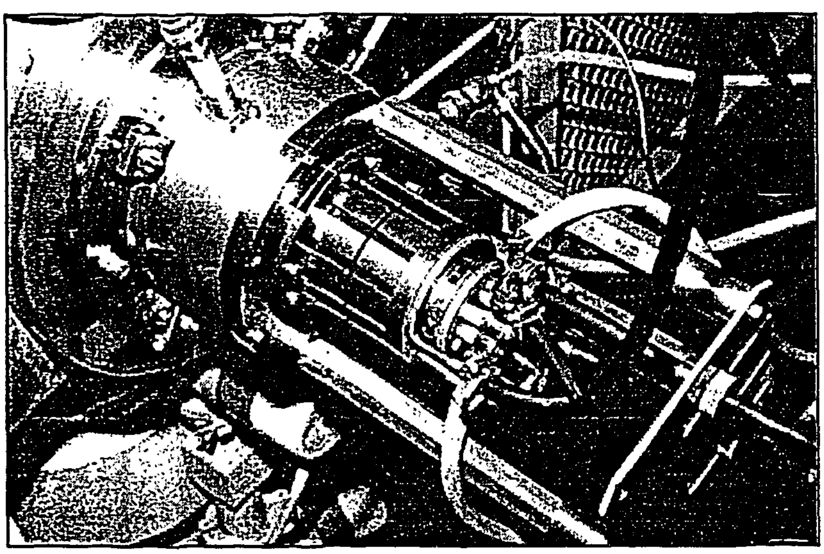

Fig.1. Present status of the multicusp H^- ion source

2.3 U-200 Cyclotron RF Accelerating System

by S.Getka, B.Daniel, R.Morozowicz, W.Pencilło, E.Pławski

In the 1994 the U-200P heavy ion isochronous cyclotron located in Warsaw University was officially put into operation. To facilitate the start-up procedure the even-harmonic mode of operation was initially adopted. The dees of RF panel resonators were galvanically coupled in the centre of the machine forming thus $\lambda/2$ like structure and this structure was exited from one RF power source by means of the inductive coupling to one resonator. The resonant frequency of the structure was kept constant by the Automatic Frequency Control (AFC) module actuating two tuning trimmers located in resonators. In this mode of operation the Ne^{+2} accelerated on 4-th harmonic was chosen as a "test" particle to verify the reliability of the system components.

To reach full operational capability of the RF accelerating system (the odd and even mode of operation) the additional AFC module was added, the resonators were decoupled and the system of Automatic Phase Control (APC) between the dee voltages was incorporated. The APC system shown in Fig.1 has the full phase range of regulation $\pm 150^0$ and dynamic range of $\pm 30^0$. It can stabilize the relative phase shift between the dee voltages to less than 0.2^0 and has the cut-off frequency ~ 500 Hz. These parameters were verified using precision vector HP 8753C Network Analyzer.

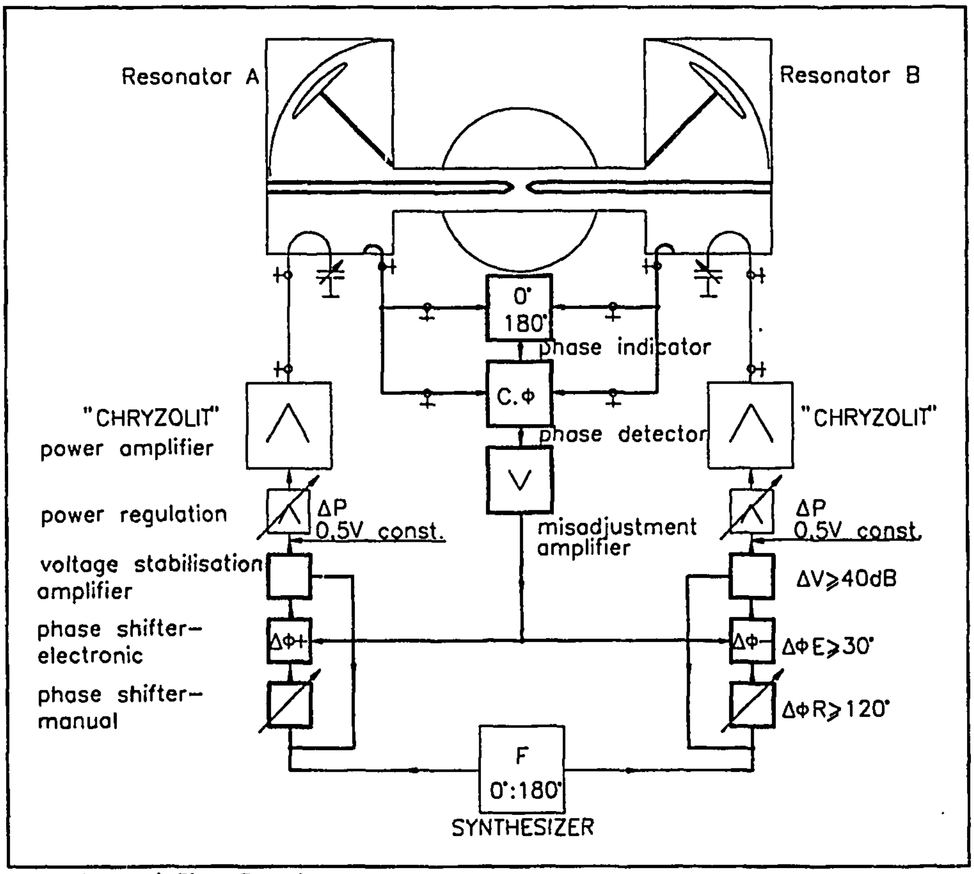

Fig.1. Automatic Phase Control system

2.4 The 0° Facility in the COSY Accelerator*)

by I.Zychor, O.W.B.Schult[1)]

The COSY (COoler SYnchrotron) accelerator complex in Jülich consists of several ion sources, the isochronous cyclotron, a 100 m long injection beam line, the COSY ring with a circumference of 184 m and extraction beam lines to the external experiments. It will provide proton beams with energies from 40 MeV to 2.5 GeV. The COSY ring is made up of two 40 m long straight sections (which act as telescope with 1:1 imaging, giving either a 1π or 2π phase advance) and of two 52 m long arc sections with a mirror symmetry.

Because of high luminosity at internal targets the COSY accelerator is an ideal tool for the investigations of the subthreshold production of K^+ mesons [1]. As the internal targets are very thin they produce much less background and secondary reactions than thick targets in external experiments. A magnetic spectrometer is necessary for the separation of the ejectiles from the circulating COSY beam and for the determination of their momenta.

The 0° Facility consists of a magnetic device, the internal target and a special vacuum and support system. The magnetic device comprises three dipole magnets: the first dipole D1 deflects the beam out of its direction in the straight section, the second D2 serves as a separator and spectrometer while the third dipole D3 brings the beam back into its original track. This 0° Facility allows measurements mainly under forward angles down to 0° where the cross sections are largest. Some details of the 0° Facility and the COSY ring are shown in Figure 1. The main conditions which an internal target place should fulfil are as follows: enough space (7 m) to install the 0° Facility, small β function values at the target place, the phase advance equal to 1π or 2π, keeping the symmetry of the COSY ring.

The first concept was to place the 0° Facility at the TP1 position in the COSY ring because of the favourable beam parameters and the possibility to locate and optimize experimental installations in the 6.3 m long free part of the telescopic straight section around this target place [2]. The disadvantage of using the TP1 place is a fact that this place is not in a symmetry point of COSY.

The alternative possibility is to use the target place TP2 in the centre of a straight section and this conception is now under study by use of the MAD code [3]. The MAD (Methodical Accelerator Design) program is a general purpose tool for a design of synchrotrons and a study of charged particle optics in alternating gradient accelerators and beam lines. The code handles very large and small accelerators. Features of the code include linear lattice parameter calculation, linear lattice matching, survey calculations, particle tracking, chromatic effects and resonances. The first calculations made for the TP2 target place indicate that it is possible to fulfil conditions mentioned above for the 1π mode.

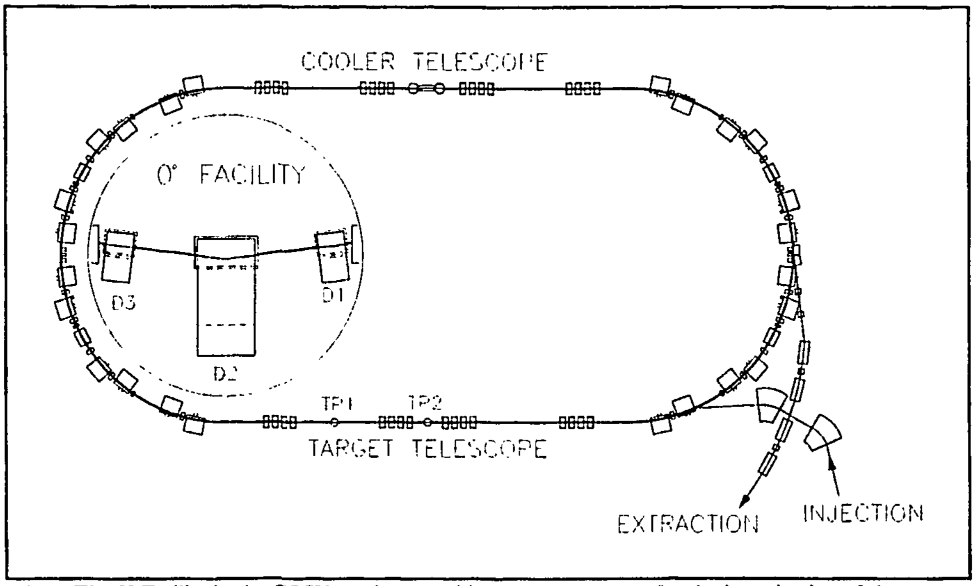

Fig.1. The 0° Facility in the COSY accelerator with the detector setup for the investigation of the K^+ meson production

[1] W. Borgs et al., "Study of the Subthreshold K^+ Production with a 0° Facility at TP2 in COSY", COSY Proposal #18 (1991)
[2] O.W.B. Schult et al., Physica Scripta 48 (1993) 47
[3] H. Grote and F.Ch. Iselin, "The MAD Program", CERN/SL/90-13 (AP)

* This work was supported by the TEMPUS project
[1] Institut für Kernphysik, Forschungzentrum Jülich, D-52425, Germany

D. ELECTRONICS AND DETECTORS

1. NUCLEAR ELECTRONICS

1.1 Pulse-Shape Discrimination for Particle Identification in 4π Silicon Balls

by G.Pausch[1], W.Bohne[2], A.Buscettti[3], G.DeAngelis[3], G.DePoli[3], H.Grawe[2], D.Hilscher[2], M.Moszyński, G.Röschert[2], R.Schubart[4], D.Wolski, R.Zanon[3]

The efforts to exploit pulse-shape discrimination (PSD) for identification of charged particles in planar Si detectors [1] have been continued, stimulated by the proposal to build a 4π Si-ball for charged particle detection as an ancillary detector for EUROBALL [2]. In a test experiment carried out at ISL (VICKSI) in Berlin we irradiated Si detectors manufactured for the Berlin Si-Ball BSB [3] and for the Legnaro ΔE-E Si-Ball ISIS [4] i) with light charged particles produced in fusion-evaporation reactions (150 MeV ^{36}Ar + Ni) and ii) with heavier fragments produced by 510 MeV ^{36}Ar projectiles in mixed targets consisting of C, Ni, Ag, and Au (Table 1). All detectors were operated in the rear-side injection mode [5].

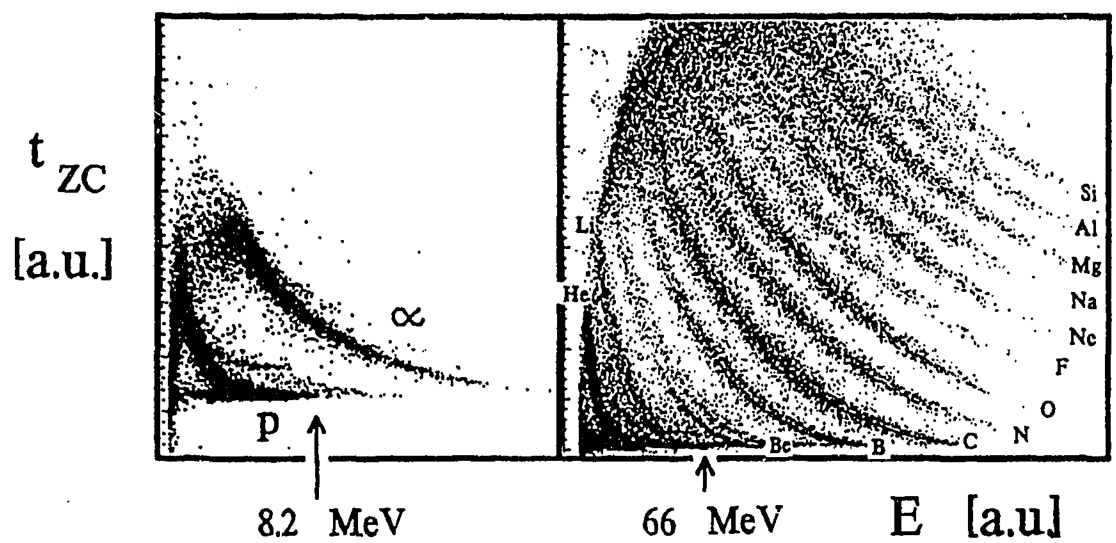

Fig.1 Scatterplots of the zero-crossing time t_{ZC} (y axis) versus energy deposition E (x axix) obtained with a PSD scheme similar to [6]:
a) p/α discrimination (reation 150 MeV ^{36}Ar+Ni, det. 3 at θ_{lab}=110°, bias 80 V)
b) Heavy ion identification (510 MeV ^{36}Ar+{C+Ni+Au}, det. 4 at 25°, bias 80 V)

The most important results can be summarized as follows:

1) Excellent resolution was obtained with a PSD scheme similar to the zero-crossing technique which is well known from n/γ discrimination with scintillation detectors [6]: Two subsequent differentiations ($\tau_{RC} \approx$ 100...200ns) of the charge signal provide a bipolar pulse. The zero-crossing time t_{ZC} is measured relative to a rise-time compensated constant-fraction timing of the bipolar pulse. No external time reference is necessary.

2) Best particle resolution was found with a detector bias slightly above the voltage for total depletion (fig.1), i.e. if low-energy ions are stopped in a region of very weak electric field (increased rise-time and pulse-shape differences [5]. However, the huge rise-time variation which supports PSD means a non-linear energy calibration due to the ballistic deficit (fig.2). If precise energy information is of interest one needs spectroscopy amplifiers (SPA) with ballistic deficit correction (BDC) [7].

3)The 500 μm Eurisys detectors show excellent resolution for p/α discrimination as well as for heavy-ion identification (fig.1). This is consistent with previous experience from detector tests [1] and experiments with the BSB.

4) There is no doubt that the concept of a Si-Ball with PSD is feasible.

Table 1. Si detectors used in the test experiment

Det. No.	Detector Type	Manufacturer	Thickness [μm]	Recomm. Bias [V]	Particle Resolution
1	ISIS "ΔE" [a]	Micron Semiconductor	130	22	moderate
2	ISIS "E" [a]	Micron Semiconductor	1000	123	no
3	BSB Type C [b]	Eurisys Measurements	500	70	excellent
4	BSB Type C [b]	Eurisys Measurements	500	70	excellent

[a] $\approx$ 1000 mm^2, transmission mount, used in rear-side injection mode
[b] $\approx$ 750 mm^2, glued with the high-field (front) side onto a 630μm ceramics backing

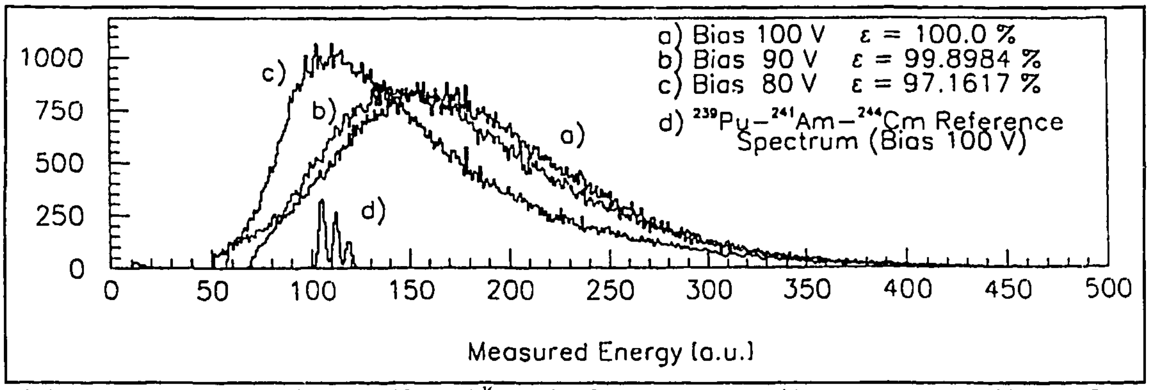

Fig.2 Energy spectra of α particles from 150 MeV ^{36}Ar+Ni at θ_{lab}=110° measured with a spectroscopy amplifier (τ=0,5 μs) for detector 3 with bias voltages of a) 100 V, b) 90 V, c) 80 V. The ballistic deficit due to larger rise times of the charge signal at lower bias shifts the measured amplitudes (parameter E) to lower values and causes a non-linear energy calibration. Nevertheless the counting efficiency ϵ for α particles stays nearly constant.

[1] G.Pausch et al., Nucl. Instr. and Meth. A349(1994)281, and refs. therein
[2] H.Grawe et. al., Proposal for a 4π Silicon Ball for EUROBAL, July 1994
[3] W.Bohne et al., Annual Reports HMI-B 497(1992)92, and HMI-B 507(1993)79
[4] G.DeAngelis, EUROBALL LCP det. Meeting, Bordeaux, May 1994 (slide report)
[5] G.Pausch et. al., Nucl. Instr. and Meth. A337(1994)573

[1] FZ Rossendorf, Institut für Kern- und Hadronenphysik, FRG
[2] Hahn-Meitner-Institut Berlin, Bereich Festkörperphysik, FRG
[3] Istituto Nazionale di Fisica Nucleare Legnaro, Italy
[4] Universität Göttingen, FRG

1.2 Comparison of n-γ Discrimination by Zero-Crossing and Digital Charge Comparison Methods[*]

by D.Wolski, M.Moszyński, T.Ludziejewski, A.Johnson[1], W.Klamra[1], Ö.Skeppstedt[2]

A comparative study of the n-γ discrimination done by the digital charge comparison and zero-crossing methods was carried out for a 130 mm in diameter and 130 mm high BC501A liquid scintillator coupled to a 130 mm diameter XP4512B photomultiplier. The high quality of the tested detector was reflected in a photoelectron yield of 2300$\pm$100 phe/MeV and excellent n-γ discrimination properties with energy discrimination thresholds corresponding to very low neutron (or electron) energies. The superiority of the Z/C method was demonstrated for the n-γ discrimination method alone, as well as, for the simultaneous separation by the pulse shape discrimination and the time-of-flight methods down to about 30 keV recoil electron energy (see fig.1). The digital charge comparison method fails for a large dynamic range of energy and its separation is weakly improved by time-of-flight method for low energies.

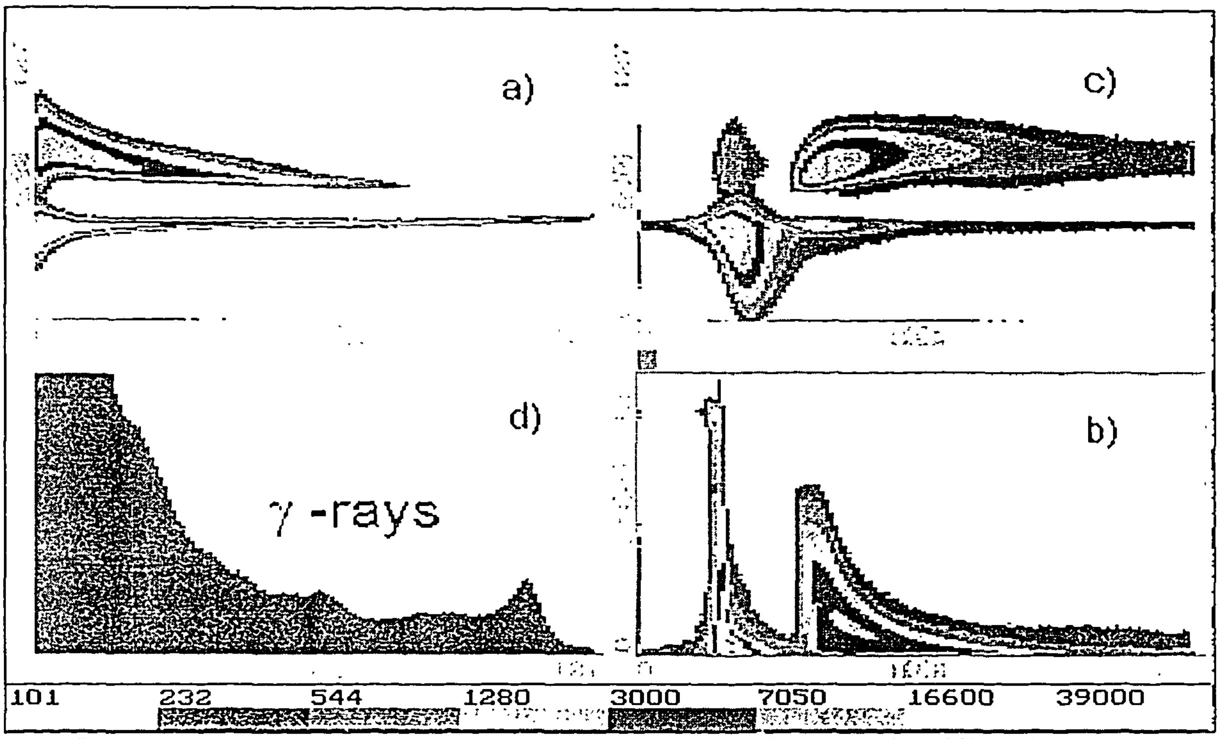

Fig.1. The n-γ discrimination by simultanous measurements of the zero-crossing time and the time-of-flight. The zero-crossing time distribution versus energy (a). The time-of-flight versus energy (b). The zero-crossing time versus the time-of-flight (c). The energy spectrum of γ-rays selected by the zero-crossing method (d). Note that the analysis of the 2D spectrum of the zero-crossing versus the time-of-flight allows to select very clearly both the neutron and γ-events. The time calibration for both spectra is: 1 channel = 0.8 ns.

[1] D.Wolski, M.Moszyński, T.Ludziejewski, A.Johnson, W.Klamra, Ö.Skeppstedt, submitted to Nucl. Instr. and Meth.

*) This work was suppotred by State Commitee for Scintific Research (Grant Nr 2P 302 096 07)

1.3 Advantages and Limitations of LSO Scintillator in Nuclear Physics Experiments*)

by M.Moszyński, T.Ludziejewski, K.Moszyńska, D.Wolski, W.Klamra[1], E.Devitsin[2], V.Kozlov[2]

The aim of this work was to study the basic properties of the LSO crystal in detection of γ-rays and α-particles. The light yield, the light pulse shape and the properties of this new crystal in the energy and time spectroscopy were studied to discuss the capabilities and limitation of LSO crystal in experiments in nuclear physics.

All the studies were carried out for three LSO samples with the dimensions of 15x15x1.5 mm^3, 10x10x2 mm^3 and 5x4x14.5 mm^3. The last sample was undenvent by additional annealing in order to improve its optical and scintillation properties. The LSO crystals were grown at the Lebedev Physical Institute in Moscow. The concentration of Ce in the studied LSO samples was equal to 0.22 %. For the measurements with γ-rays the crystals were coated with a teflon tape, while for α-particles the uncoated crystals and the crystals coated with a 3.3 μm thick aluminised mylar foil were used. The tested LSO crystals showed a strong day light afterglow. It was thus necessary to keep them in darkness at least 24 hours to eliminate the afterglow.

All the measurements were carried out using the Philips XP2020Q photomultiplier with the radiant photocathode sensitivity of 74 mA/W at 400 nm and with the Hamamatsu S3590-03 and S2744-03 photodiodes with the typical quantum efficiency of 50 % at 420 nm.

The light yield expressed in terms of the number of photoelectrons was found to be equal to 4200±200 phe/MeV, as measured with the XP2020Q photomultiplier comparing the scintillation spectrum to that of the single photoelectron pulse height spectrum. Thus it is roughly by factor of two lower as compared to small NaI(Tl) scintillators. The observed difference in relation to the earlier published data of Melcher et al [1] seems to be mainly associated with the fact that the light yield was previously determined in the DC mode based on the emission spectra of both scintillators. The number of electron-hole pairs of 18500±900 e-h/MeV measured with the S3590-03 photodiode seems to be too high if assuming that the emission spectrum of the LSO is around its peak at 420 nm. The analysis of the data suggests that the emission band at 460 nm [2], extended into longer wavelengths up to about 600 nm, is responsible for the observed excess of e-h pairs.

The light pulse shape of the LSO measured by the single photon method exhibited a pure exponential decay with a time constant of 46.6±2 ns for both γ-rays and α-particles, see fig.1. The absence of the faster component of 12 ns, observed in the previous study [1], in all the samples of LSO has to be pointed out.

The energy resolution of 10 % and 14.6 % for the 662 keV γ-rays from ^{137}Cs source were obtained for the photomultiplier and photodiode, respectively, and thus comparable to those observed by Melcher et al [1,3]. A α/γ ratio of the light yield of 0.15 was found for the α-particles of 5 to 9 MeV energy using radioactive sources, see fig. 2. This value suggests a strong quenching of the light for light charged particles which may limit a potential application of LSO as particle detector.

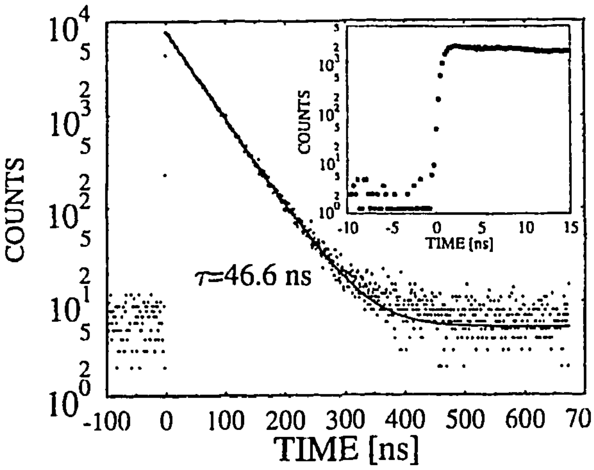

Fig. 1 Decay time spectrum of the LSO crystal induced by gamma rays from ^{137}Cs source

The time resolution study were carried out with the LSO crystal coupled to the XP2020Q photomultiplier and using a small NE111 plastic coupled to the XP2020UR photomultiplier as a reference. A time resolution of 180 ps was observed for ^{60}Co γ-rays at 1 MeV threshold and 400 ps for 100 keV threshold. The contribution of the reference counter was equal to 70 ps. Note that the time resolution of a 2.5 cm x 1 cm BaF_2 crystal measured in this same conditions at 1 MeV threshold was equal to 120 ps, see fig. 3.

The study confirmed a number of advantages of the LSO crystal for nuclear physics experiments, however, for a small size samples. For larger volumes the natural radioactivity of the LSO crystal, about 300 counts/s/cm^3, limits possible applications. The high number of e-h pairs produced in the photodiodes makes LSO attractive for small compact scintillation probes.

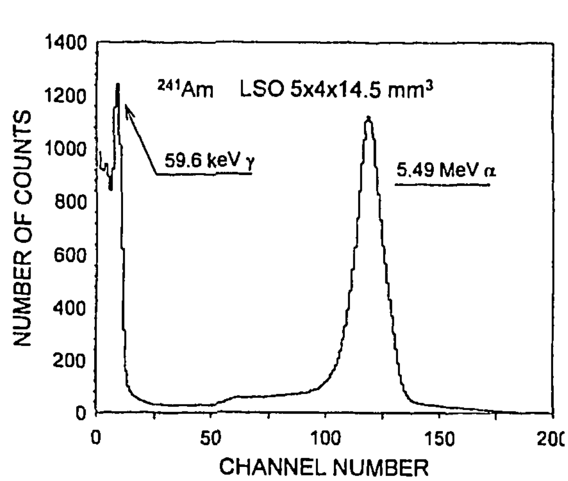

Fig.2. The energy spectrum of the 5,49 MeV α and 59,6 keV γ-line from a ^{241}Am source measured with the LSO crystal coupled to XP2020Q photomultiplier.

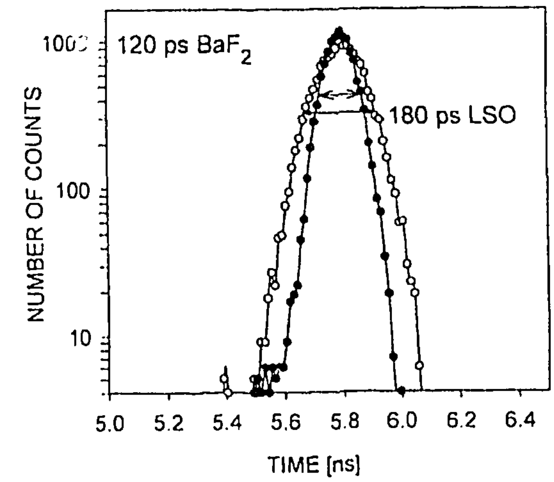

Fig.3 The comparison of time spectra measured with LSO and BaF_2 crystals for ^{60}Co γ-rays at 1 MeV threshold

[1]. C.L.Melcher and J.S.Schweitzer, IEEE Trans. Nucl Sci. NS39(1992)212.
[2]. H.Suzuki, T.A.Tombrello, C.L.Melcher and J.S.Schweitzer, IEEE Trans. Nucl Sci. NS40(1993)380.
[3]. C.L.Melcher, IEEE-NS Conference Record 1992.

1) Royal Institute of Technology, Department of Physics, Frescati, S-104 05 Stockholm, Sweden
2) Lebedev Physical Institute, Leninsky pr. 53, 117924 Moscow, Russia

*) This work was suppotred by State Commitee for Scintific Research (Grant Nr 2P 302 096 07)

1.4 Electronic Equipment for NA49 Experiment at CERN

by A.Chłopik

Multiple electronic equipment has been developed and tested for use in Slow Control and Laser Control of NA49 Experiment at CERN in collaboration with Institute of Experimantal Physics of Warsaw University and CERN. The following CAMAC modules have been prepared for Slow Control:

- Gas Chambers Control,
- NIM Clock Generator,
- Quad High Voltage.

The following modules have been developed for Laser Control:

- Triple High Voltage,
- Laser Valves Control,
- Laser Signal Converters.

The purpose of Gas Chambers Control Unit is to receive analog signals from Gas Chamnbers and to convert them into NIM standard signals. These signals control the mixture of gases in the chambers. There are four signal channels on each board. Fifteen of such units have been produced so far.

NIM Clock Generator CAMAC modules are used to trigger other electronics in Slow Control of NA49 Experiment. At the output of a unit an asynchronous square wave of NIM standard levels is generated. This signal can be gated from the CAMAC Bus using standard commands. Four of such modules have been produced so far.

Quad High Voltage CAMAC unit is used to set high voltage on Gas Chambers. Each module has four outputs. The output voltages are controled from CAMAC Bus with 16-bit digit value. They can be changed in the range from 50V to 1,7kV. Four of such modules have been produced so far.

Triple High Voltage module is based on Quad High Voltage module. It is purposed to control crystal dimensions in NA49 Experiment which can position the lasers very precisely (with 100μm resolution). There are three outputs. The output voltages can be changed with 16-bit digit value sent via CAMAC Bus in the range from about -50V to +250V.

The lasers are positioned roughly with the Laser Valves Control CAMAC Unit. Each laser table is connected to two valves. One of the valves turns the table to the left and another turns it to the right. To switch the valve on a power of 6W has to be delivered. Thus each of the output is able to give current of 0,5A with 12V. The CAMAC commands open or close the valves which works independently.

The lately produced module is a NIM unit for converting laser signals to NIM levels and NIM levels to laser signals. A laser signal is a square wave with logical levels of 0V and 15V. There are four converters: laser-to-NIM-non-inverting, laser-to-NIM-inverting, NIM-to-laser-no-inverting and NIM-to-laser-inverting.

1.5 ARIADNA: New Developments for C-30 Cyclotron

by Z.Guzik

New designs and develompents were done for C-30 Cyclotron. The software support for Monitoring and Control System ARIADNA was restructured and enhanced. The remote Process Controller 'node' works now under control of MULTIX real-time kernel. A lot of new system utilities were added. The optoisolated data link between the node and IBM PC based server is conducted via two layer (transport and message) Z-LINK protocol. The autobatching mechanism was adopted and an on-line status reporting on the entire apparatus is provided.

The *beam profile* monitoring system was integrated into ARIADNA node. This monitoring system is based on two-dimensional wire chamber. Works concerning main magnet magnetic field stabilisation are under preparation.

1.6 Evaluation of a Possibility of the DC Swept Beam Detection by an Electromagnetic Induction Method

by M.Uzdowski, W.Drabik

The swept dc beam in a high power linear accelerator produces alternating magnetic field which may be used for a beam position detection inside the tube of the accelerator. Theoretical calculations and the measurements on the simulated tube have been made. The results of calculations are shown in fig.1 and fig.2.

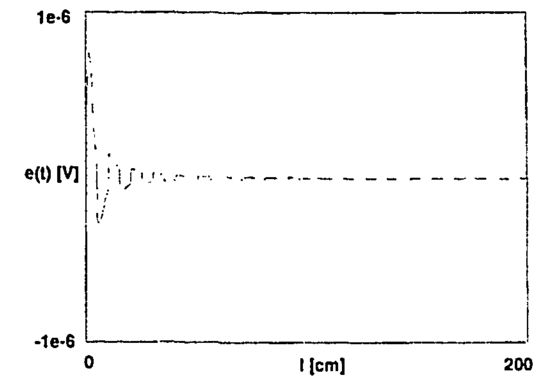

Fig.1. "X" coil electromotive force

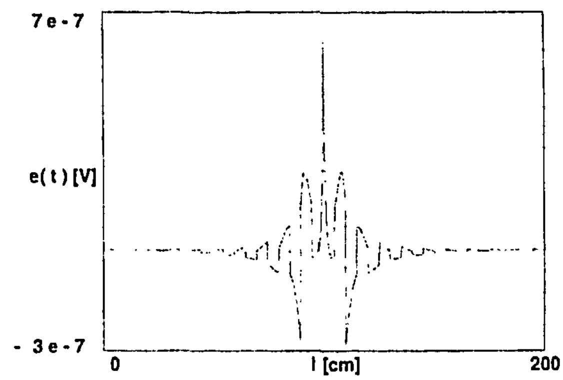

Fig.2. "Y" coil electromotive force

It was assumed that the beam is swept in the plane perpendicular to the foil closing the tube. Calculations were made for one-turn coil 2x2 cm.

A simulating system has been built. The beam was simulated by the current flowing in 9 parallel wires placed in distances of 10/9 cm. The sweeping of the beam was simulated by switching the current from one wire to another. The parameters of the coil were: n=30.000, R=5,1kΩ, C=292 nF, L=86,6H without a core or 463,6 H with a core. Results in fig.3 show that the method may be useful for monitoring and corrections of the trajectory of the swept beam but the optimum coil and special electric amplifing system should be used.

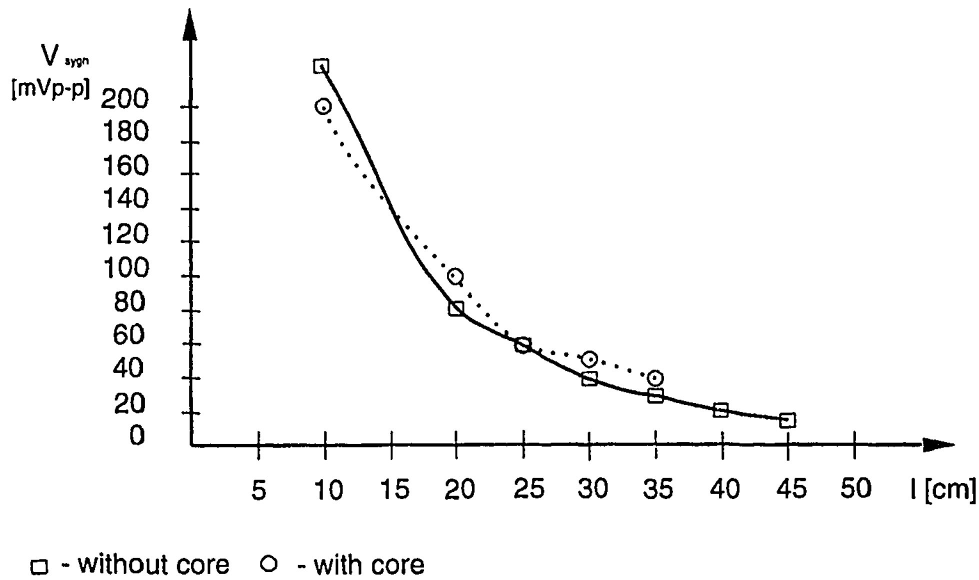

Fig.3. Coil electromotive force versus distance (experimental results)

1.7 A New Pulse Stretcher for Spectroscopy ADC's

by Z.Kulka, S.Borsuk

A new feedback pulse stretcher has been designed for different types of the successive - approximation spectroscopy ADC's built around commercially available ADC chips with 0 to +5 input voltage range and ± 12V power voltage supplies.

A simplified diagram of the new pulse stretcher is shown in fig.1. Similarly to the other circuits [1-3] this one contains: strobed peak detect and hold circuit, optically coupled peak detector and bootstrapped input gate. The strobed operation quarantees the power dissipation balance of the stretcher input stage (T1,T2) and clamps the input node of T1 to the diode - transistor (not shown) bootstrap which monitors the stretcher output. As result, the integral non-linearity errors can be reduced. Peak detection through the optical coupler isolates the memory capacitor C1 from back-induced digital noise.

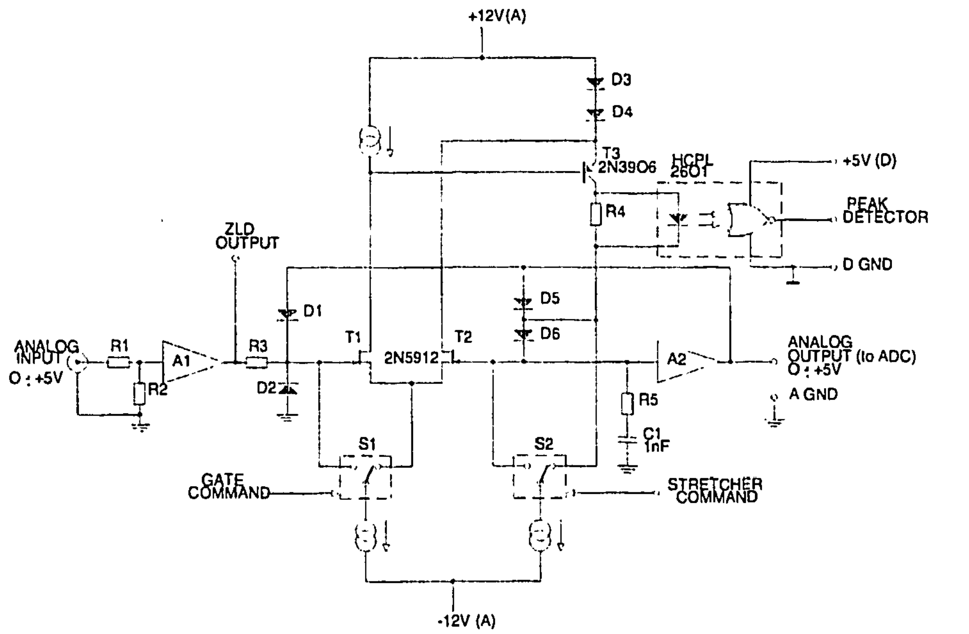

Fig.1 Simplified diagram of the pulse peak stretcher

[1] P.Casoli, P.Marancsi, Nucl. Instr. and Meth., 166(1979)299

[2] S.Borsuk, Z.Kulka, SINS-2085/P-III/E/B (1989)

[3] EG and G ORTEC, Spectroscopy ADC model AD 413

2. SEMICONDUCTOR DETECTORS

2.1 X-ray detection efficiency of Si/Li and HRSi detectors

by W.Czarnacki, B.Sawicka, T.Sworobowicz, G.Hahn, A.Kotlarski

In the previous report a possibility of manufacturing the HRSi silicon detecting structures suitable for high-resolution X-ray spectrometry was reported; HRSi denotes that the material for the structure is the high-resistivity silicon rather than the lithium-compensated silicon. In order to examine such structures more closely, the efficiency of X-ray radiation detection of the HRSi detectors has been measured and compared to that of the Si/Li ones. The measurements were taken at 5.9 keV (Fe^{55} source). For that purpose the following items have been manufactured, assembled and set up:

- 5 Si/Li detecting structures with active thicknesses from 3 to 4.5 mm, active area appx. 28 sq.mm, capacitance from 1.2 to 1.4 pF and breakdown voltage above 1000V;
- 8 HRSi detecting structures with active thicknesses from 3 to 3.5 mm, active area appx. 28 sq.mm, capacitance from 1.5 to 2 pF and breakdown voltage above 1000V (p-type material, 20 kΩ·cm and 50 kΩ·cm resistivity);
- LN_2 cryostat and charge sensitive preamplifier with cooled first stage of amplification;
- scanning setup with Fe^{55} source, Pb collimator of a beam diameter of 0.2 mm and micropositioning stage.

The selected structures were placed in the same cryostat; the operating parameters of the structure and the charge preamplifier were individually optimized. The resulting energy resolution was from 170 to 180 eV FWHM for Si/Li detectors, and from 190 to 200 eV FWHM for HRSi ones. The detection efficiency was measured radially for points 0.2 mm apart at several bias voltages: for 2 Si/Li detectors the bias voltages were 100, 300 and 500 V; for one of the HRSi detector -- 600, 700 and 1000V; for the other HRSi detector -- 300, 400 and 500 V. It has been found that the detection efficiency for the HRSi detector made of 20 kΩ·cm material depends distinctly on the bias voltage, as opposed to the efficiency for all other tested detectors. However, there always exists a bias voltage for which the detection efficiency may be regarded as constant within the statistical error. The results are being prepared for publication.

2.2 Application of microelectronic techniques to semiconductor spectrometric detectors (joint effort with IET Warsaw)

by E.Belcarz, W.Czarnacki, M.Pilch[1], T.Sworobowicz

Application of technologies of microelectronics industry (e.g. silicon planar technology) may bring about better control of parameters of silicon spectrometric detectors, as well as pave a way to the development of advanced types of silicon radiation detectors (strip, multielement etc.). To assess the usefulness of technologies attainable in IET Warsaw, the following steps have been performed:

- Designing, manufacturing and testing a series of detecting p-n structures made on 380 μm thick wafers of n-type silicon of resistivity appx. 1 kΩ·cm; the active area of structures was a circle with 12 mm diameter.
- Selecting 6 structures with leakage currents below 0.5 μA at 20 V bias.
- Determining the energy resolution of the structures for α particles of 8.778 MeV energy; it ranged from 45 to 120 keV FWHM.

The obtained energy resolutions were 2 to 6 times worse than those attainable with the state-of-the-art technology; it means that the currently developed structures may be applied only to the detection of charged particles. Application of microelectronic industry technologies for other types of detectors (including spectrometric ones) requires a controlling of many material and technological parameters, which remain out of control at the present time.

[1] Institute of Electron Technology, Warsaw

2.3 Portable X-Ray Spectrometer with Silicon Thermoelectrically-Cooled Detector

by W.Czarnacki, M.Słapa and M.Traczyk

The technology of low-leakage Si(Li) detectors immune to ambient was investigated. The technology was studied on structures of several cm^2 area. The obtained leakage at room temperature was at a level of about 8 nA/($cm^2 \cdot 100 \mu m$). Using this technology, cylindrical Si(Li) structures of 7 mm^2 area and 3 mm thickness have been manufactured. The surface stabilization was made by means of suitable silicon resins. The leakage currents amounted to 25-35 nA at +20°C, and dropped down to 1.5-8 nA after cooling down to -20°C. However, they changed after several cycles of cooling down and warming up. The work on surface stabilization is being continued.

2.4 Personal Silicon Doserate Meter

by M.Słapa and M.Traczyk

Silicon photodiodes have been tested as detectors for X- and γ-ray radiation dosimeters. The analysis of the influence of noise [1], detector temperature, and of the shape of spectra generated by the photodiodes at several incident radiation energies on dosemeter parameters has been performed. The model describing the collection of injection charge generated in the photodiode active region has been proposed [2]. The number of pulses and the total charge generated by the photodiode in response to unit dose has been measured as a function of X- and γ-ray radiation energy. The dependence of the dosemeter sensitivity on the radiation energy has been related to photodiode parameters and to the applied algorithm of the data computation. It has been shown that for photodiodes with a depletion layer below about 60 μm, the number of counts is a better measure of the dose, whereas for the photodiodes with the layer thicker than about 200 μm it is rather the total ionization charge.

A model of a personal dosemeter with silicon photodiode has been developed. The analog part of the model is designed in bipolar discrete technology, the digital part -- with the use of a low-power microprocessor. The measurements taken with the model fully confirmed the project specifications. The dosemeter operates in the energy range 50 keV - 1.5 MeV at the nonlinearity of the sensitivity less than 20%.

The research on photodiodes indicates that the 20 keV energy threshold should be attainable; such low level is an important requirement in applications in radiation protection.

Modern silicon photodiodes together with microelectronic circuits available in 90' made it possible to design a new generation of dosimeters, the so called EPDs (electronic personal dosemeters). Thanks to the built-in memory and microprocessor data processing such EPDs can not only warn about a temporary radiation hazard, but also accumulate data on the history of irradiation. The obtained results indicate that the presently applied passive personal dosimeters (films and thermoluminescence dosimeters) may soon be replaced by the EPDs.

[1] M.Traczyk, M.Słapa: Commercially Manufactured Photodiodes in Detection of Low-Energy X- and Gamma-Ray Radiation, accepted for publication in Nukleonika

[2] M.Słapa and M.Traczyk: Silicon Photodiodes Response to Interactions of x- and γ-ray Radiation with the Diode Base, to be published in Nuclear Instruments and Methods

E. PLASMA PHYSICS

1. THEORY AND COMPUTATIONAL PHYSICS

1.1 Kadomtsev-Petviashvili Soliton Decay and Interactions

by E.Infeld, A.Senatorski, A.A.Skorupski

Solitons described by one variant of the Kadomtsev-Petviashvili equation (KPI), which arises in various weakly dispersive media (two-component plasma, neutral fluids and solid state) were examined both numerically and theoretically. Numerical simulations were performed to examine the time evolution of the line soliton (x dependent only and propagating in the x direction) which at $t=0$ was modulated in the y direction by a cosine function with some amplitude δ. Three different types of behaviour were found:

(i) For infinitesional values of δ ($=0.016$) the modulated line soliton decays into a smaller line soliton and an array of two-dimensional solitons ("lumps") [1,2].

(ii) For small but noticeable δ ($=0.04$) a decay of type (i) is followed by emission of a second array of lumps. Both arrays are approximately of the same size, and so propagate with approximately the same speed (no interaction of lumps).

(iii) For large values of δ ($=0.4$) the scenario is somewhat similar to (ii) but the lumps emitted later are larger in size and so faster than those emitted first. The faster lumps catch up with, interact with, and overtake the slower ones. An interesting feature, not encountered in other soliton interactions, is a shift in y by half a wavelength of the modulation, see Fig. 1 [3]. A similar shift in y could also be observed when an array of lumps was scattered by a line soliton, if parameters were chosen appropriately. The appearance of the shift in y in some situations was examined and explained theoretically [3].

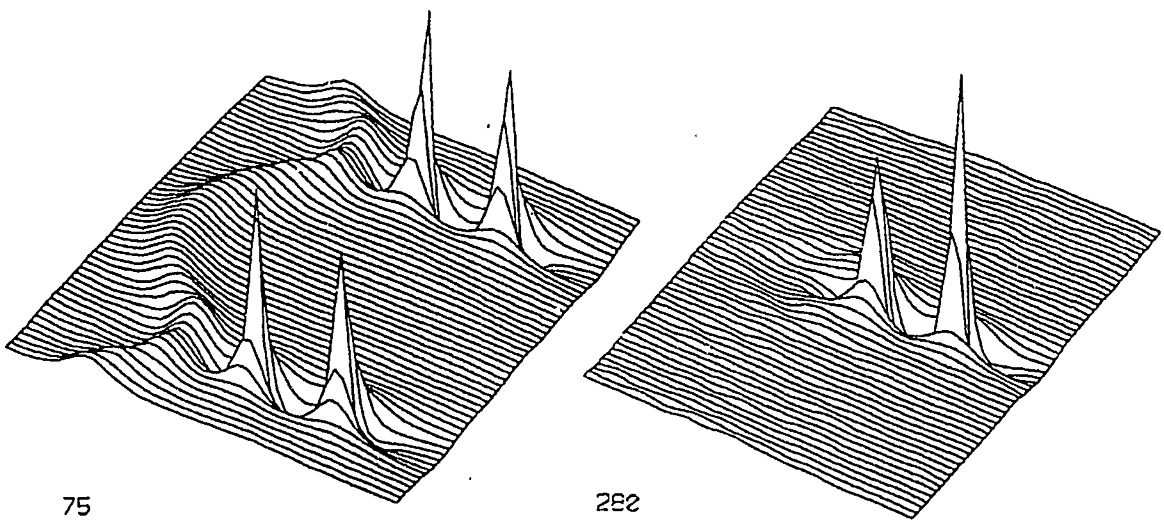

Fig.1a. Members of two arrays of lumps before interaction. Fig.1b. A member of two arrays of lumps after interaction.

[1] E.Infeld, A.Senatorski, A.A.Skorupski, Phys.Rev.Letters 71 (1994) 1345
[2] D.E.Pelinovskii, Y.A.Stepanyants, ZhETF 104 (1993) 3387
[3] E.Infeld, A.Senatorski, A.A.Skorupski, Phys. Rev. E, in press

1.2 Painlevé Test when the Solution has no Poles; Analysis of an Equation Governing a System of Interacting Dipoles

by P.Goldstein, E.Infeld, H.Zorski[1]

The "Painlevé test" is applied to an equation describing a system of finite-size dipoles interacting via electrostatic forces. The test requires modification because the solution does not have poles. General remarks on performing the test in such cases extend our understanding of the problem.

[1] Institute of Fundamental Technological Research

1.3 Isothermic Surfaces in E^3 as Solution surfaces

by J.Cieśliński, P.Goldstein, A.Sym

We show that the theory of isothermic surface in E^3 - one of the oldest branches of differential geometry - can be reformulated within the modern theory of completely integrable (soliton) systems. This enables one to study the geometry of isothermic surfaces in E^3 by means of powerful spectral methods available in the soliton theory. Also the associated non-linear system is interesting in itself since it displays some unconventional soliton features and, physically, could be applied in the theory of infinitesimal deformations of membranes.

1.4 Development of the GRAD-1D Computer Code for the Description of a Tokamak Plasma by Means of Grad's Higher Expansion Approach

by M.Rabiński

The description of a tokamak edge plasma with the fluid approach overestimates transport coefficients (heat conductivities and longitudinal viscosities) in regions where validity of the hydrodynamic approximation is violated. In such a case heat fluxes are not determined by local temperature gradients, but they depend nonlocally on profiles of plasma parameters.

Over the past few years, a more sophisticated model of the transport coefficients [1] has been used in the BOUND_1D package of one-dimensional codes. Plasma transport has been described by the two-fluid model with viscous stresses and heat fluxes treated as independent variables. Equations for the nonlocal transport coefficients have been derived in the frame of the 21-moment Grad approximation, thin contradistiction to the commonly applied 5-moment approach.

Recently, the BOUND_1D code has been developed into the GRAD_1D [2]. The main aim of the new program is to facilitate comparative studies of introducing a particular Grad approximation. It is justified to assume that such studies may show the the significance of introducing new terms and equations, when passing to a higher stage of Grad's expansion. This analysis will create a basis for the selection of the most effective theoretical formalism relevant to transport phenomena in an edge plasma.

During the next year, a direct visualization of numerical solutions and a program manual should be prepared.

[1] Rabiński M.: Edge Plasma Transport in Grad Approach, 18th Europ. Conf. on Controlled Fusion and Plasma Physics, Berlin 1991, vol 15C, part III, 33-36.
[2] Rabiński M.: GRAD_1D Package of Programs for Modelling of Edge Plasma in a Tokamak (in Polish) Proc. 3rd General Meeting of Polish Nuclear Society, Warsaw 1994.

1.5 Description of Radiation- and Excitation-Processes in Hydrogen Atom by a Classical Approach

by M.Gryziński, and M.Kowalski

Light emitted from atoms has the form of photons carrying energy and angular momentum, created during the jumping of an electron between excited atomic states, according to the formula: $E_{n'n}=hc/\lambda_{n'n}=h/T_{n'n}=U_i(1/n'^2-1/n^2)$, $L_{n'n}=\hbar$, where U_i - ionization potential.

Such a loss of energy and angular momentum by an excited atomic electron has been calculated classically by solving the set of electron motion equations, under the assumption that there exists a radiation-resistance force [1] ($F_r = m_e \Gamma v$), proportional to the velocity of the electron (v), where Γ denotes the resistance constant. Consequently,

$$\frac{dE}{dt} = \vec{F}_r \cdot \vec{v}, \qquad \frac{d\vec{L}}{dt} = \vec{r} \times \vec{F}_r$$

where $E = mv^2 - e^2/r$ is the energy of the electron in a hydrogen atom.

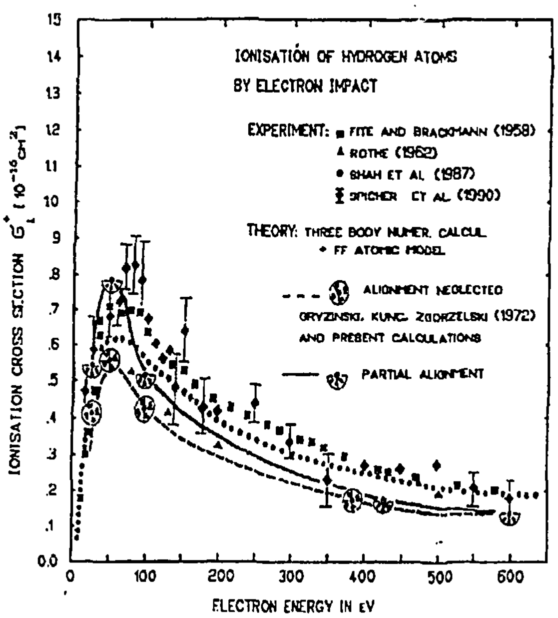

Fig.1. e^-+H ionization

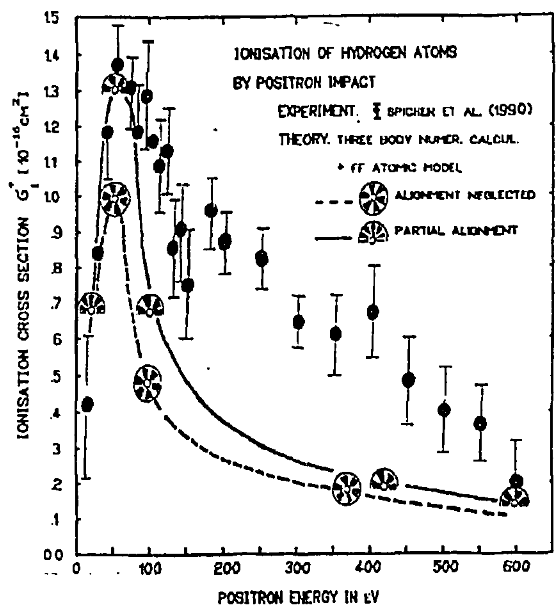

Fig.2. e^++H ionization

From the relations given above it is easy to calculate that the electron looses angular momentum according to the formula: $L = L_0 \exp(-\Gamma t)$. This makes possible it to define the resistance-radiation parameter between (n') and (n) atomic states as: $\Gamma_{n'n} = (E_{n'} - E_n) \cdot \ln(L_{n'}/L_n)/h$. As a result, it has been shown that an electron looses energy equal to $E_{n'n}$, and angular momentum $L_{n'n} = \hbar$. It means that the calculations describe correctly the emission of photons from a Hydrogen atom. Additionally, it has been found that the times of electron transitions ($t_{n,n}$) were equal to the experimental emission periods of photons ($T_{n'n}$), e.g.: $t_{21} = 2.85 T_{Bohr} \approx T_{21} = 2.7 T_{Bohr}$ or $t_{32} = 14.408 T_{Bohr} = T_{32} = 14.408 T_B$.

Solving classical three-body equations for the $e^{\pm}$+H ionization process, on the basis of a classical quasi free-fall atomic model [2], and assuming an alignment of the electron orbit in a projectile field, there good agreement of calculated ionization cross sections with experimental ones [3] has been obtained, for various energies of the projectiles, as shown in Figs.1 and 2. Details were given in a paper accepted for publication [4].

[1] J.D.Jackson, Classical Electrodynamics, (California Univ.1974).
[2] M.Gryziński, Phys. Rev. Lett. 14 (1965) 1059.
[3] G.Spicher at al. Phys. Rev. Lett 64 (1990) 1019.
[4] M.Gryziński, M.Kowalski, Alignment of hydrogen atoms in $e^+$and e^- ionizing collisions, Phys. Letters A (in press).

2. EXPERIMENT

2.1 Time- and Space-Resolved Studies of X-Rays Emitted from "Hot-Spots" in Correlation with Electron- and Ion-Streams from MAJA-PF Device

by L.Jakubowski, M.Sadowski. and J.Żebrowski

In studies performed with the MAJA-PF facility particular attention has been paid to measurements of the spatial distribution of hot-spots formed inside a pinch column and their temporal correlations with other phenomena. For this purpose, use was made of a special equipment designed for observations of hot-spot behavior within chosen regions (appr. 8 mm in dia.) of a dense plasma at distances of 10 and 30 mm from the inner electrode front. Simultaneously, the whole region of the pinch column was observed by means of a pinhole camera equipped with a 10-μm-thick Be-foil filter.

Soft and hard X-rays emitted from the whole pinch region were also registered with scintillation detectors shielded with appropriate metal foils.

In research on the MAJA-PF facility, particular efforts have been devoted to measurement of the spatial distribution of the "hot spots" inside a pinch column and their time correlation with other phenomena.

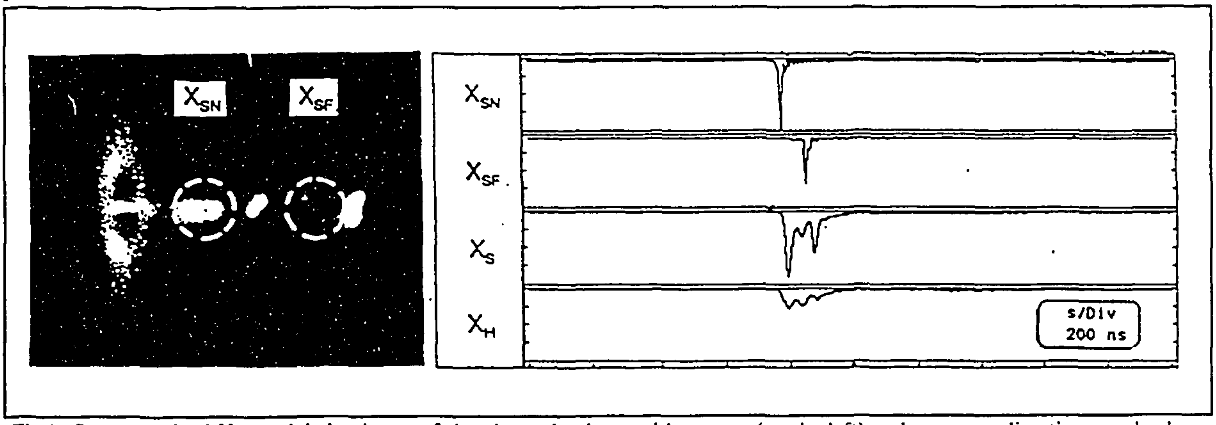

Fig.1. Space-resolved X-ray pinhole picture of the electrode plate and hot-spots (on the left) and corresponding time-resolved signals from soft and hard X-rays (on the right).

It has been observed that hot-spots, as formed within the pinch column, can exist for about 7-10ns. In general the hot-spots, which are produced at larger distances from the electrode ends, appear 70-100 ns later than those produced close to the electrodes, as shown in Fig.1. This observation suggests that the considered hot-spots are probably formed successively as the current sheath collapses at the z-axis. It has been estimated that an apparent velocity of the collapsing current sheath along the z-axis can amount to 2×10^7 cm/s.

Time-resolved signals of fast electron pulses have been obtained with Čerenkov-type detectors made of thin diamond radiators, which enable us to lower the threshold energy level down to about 50 keV. It has been found that such electron pulses last from 30 to 50 ns and they seem not to be correlated with the hot-spots appearance. Some detailed results of these studies have already been presented at conferences (Montpelier [1] and Foz de Iguaçu [2]).

[1] M.Sadowski, J.Baranowski, L.Jakubowski, S.Kienle, H.Schmidt, E.Składnik-Sadowska, J.Żebrowski: Diagnostics of X-Ray Emission from PF-Type Facilities and its Time Correlation with Particle Pulses, Proc. 21th EPS Conf. Fusion and Plasma Phys., Montpelier 1994, Part III, pp.1320-1323.

[2] L.Jakubowski, M.Sadowski, J.Żebrowski: Studies of X-Rays, Hot-Spots and E-Beams with High-Current PF-Type Discharges; Proc. Int. Conf. of Plasma Phys., Foz do Iguaçu 1994, p.306.

2.2 Complex Studies on Temporal Correlations of Emission of Charged Particles, Neutrons, and X-Rays from PF-360 Facility

by M.Sadowski, J.Żebrowski, and L.Jakubowski

At the beginning of 1994 the PF-360 facility was renovated and some parts of a current pulse generator were modernized tests were also performed with the optimization of fluid resistors which protect individual sections of the condenser bank.

During the first semester we carried out detailed studies (started in the previous year) of the influence of an additional amount of argon puffed into the focus region with a high-pressure fast acting gas-valve. In these studies, particular attention was paid to time-integrated observations of X-rays, which were performed by means of pinhole cameras with different magnification, as well as to time-resolved measurements of the X-ray emission, which were carried out with scintillator-pmt sets. We also performed measurements of ion emission characteristics by means of miniature scintillation detectors placed on walls of the vacuum chamber and coupled optically with fast photomultipliers. Some results of those studies, which in a part were carried out within a framework of the collaboration with the IPF in Stuttgart, have been presented at the 21st EPS Conference in Montpelier [1]. General conclusions concerning the X-ray and electron emission from the PF-360 facility, have been presented (together with recent results from the MAJA-PF facility) at conferences in London [2] and Foz de Iguaçu [3]. Some selected experimental results have also been included in an invited lecture given at the PSAE Symposium in Warsaw [4].

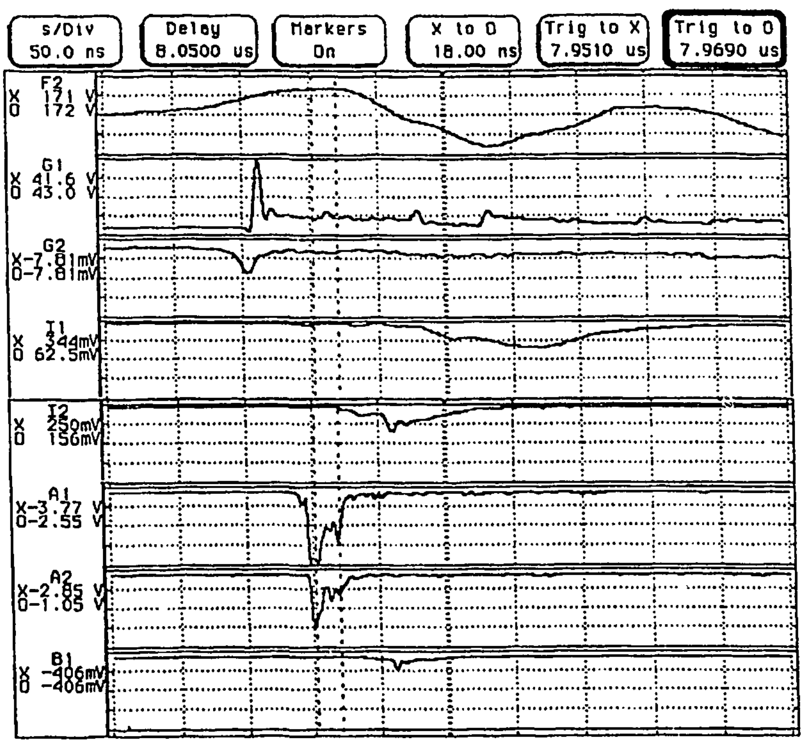

Fig.1. Typical waveforms from a single shot performed with the PF-360 facility operated at po=4.1 hPa D2, U_o=32 kV, W_o=141 kJ, Yn=1.49x10^{10}. The traces correspond to: U - voltage, dI/dt - current derivative, Yn - hard X-rays and neutrons, E_D & E_P - electron signals from diamond (D) and plastic (P) Čerenkov radiators, I_{im} & I_{io} - ion signals from 2 detectors with (m) and without (o) magnetic field.

Recent results of these measurements, which were partly carried out within the framework of a collaboration with a team of physicists from IPF-Stuttgart, have been presented at the 21-st EPS Conference in Montpelier.

After removal of the pulse gas valve and a replacement of the inner electrode front-plate by a new one (with a central 71-mm-dia. hole) we installed an EET-1 system designed for time-resolved studies of the electron beam emission. That system it made possible to register the Čerenkov radiation emitted from different radiators placed behind the main collector plate. An ion pinhole camera with time-resolving equipment was also installed. By means of these diagnostic tools several series of correlation measurements were performed with the use of a 12 channel digital oscilloscope of the HP 16500/16501 type. We registered waveforms of U(t), I(t), and dI/dt, three VR signals obtained from 3 selected regions placed close to the electrode ends, as well as signals from the neutron probe, and electron-induced signals from diamond and plastic radiators. Two ion signals obtained from 2 miniature scintillation detectors placed inside the ion pinhole camera were measured. The application of different filters and an additional magnetic field enabled as to obtain reference signals, and the use of an elongated drift tube increased the spatial resolution. It was possible to obtain interesting experimental data, as shown in Fig.1, but for final conclusions it is necessary to perform more detailed correlation measurements.

The diagnostic methods developed for studies of X-rays, fast electrons, and ions, which were used in the MAJA-PF and PF-360 facilities, have also been presented at the "Atom in Service with Man and Civilization" Exposition during the PNS Meeting in Warsaw [5].

[1] M.Sadowski, J.Baranowski, L.Jakubowski, S.Kienle, H.Schmidt, E.Składnik-Sadowska, J.Żebrowski: Diagnostics of X-Ray Emission from PF-Type Facilities and its Time Correlation with Particle Pulses, Proc. 21th EPS Conf. Fusion and Plasma Phys., Montpelier 1994, Part III, pp.1320-1323.

[2] M.Sadowski, J.Żebrowski, E.M.Al.Mashhadani: Time-Integrated and Time-Resolved Measurements of X-Rays and Charged Particles from PF-360 Facility; AIP Conf. Proceedings 299 -Dense Z-Pinches, (AIP, New York 1994) 244-250.

[3] L.Jakubowski, M.Sadowski, J.Żebrowski: Studies of X-Rays, Hot-Spots and E-Beams with High-Current PF-Type Discharges; Proc. Int. Conf. of Plasma Phys., Foz do Iguaçu (Brasil 1994), p.306.

[4] M.Sadowski: Non-linear Electromagnetic Phenomena in High-Current Discharges of the PF-Type (in Polish); Proc. of 3rd National Symposium on "Applications of Electromagnetism in Modern Techniques and Technologies", Łańcut 1994.

[5] L.Jakubowski, M.Sadowski, J.Żebrowski: Methods of Measurements of X-rays and Fast Ion- and Electron-Streams from Plasma-Focus Devices in which occur Nuclear Fusion Reactions (in Polish); Proc. of 3rd General Assembly of Polish Nuclear Society, Warsaw 1994.

2.3 Elaboration of Results from the Last Series of Experiments with the POSEIDON Facility; Collaboration with IPF in Stuttgart

by M.Sadowski, L.Jakubowski, E.Składnik-Sadowska, J.Stanisławski, A.Szydłowski, and H.Schmidt[1)]

Within the framework of the scientific collaboration with the Institut für Plasmaforschung (IPF) in Stuttgart, Germany. We wrote performed final proofs of two papers on Plasma-Focus with additional gas targets produced by the gas-puffing in the POSEIDON facility [1-2].

During a one-month scientific stay in Stuttgart Professor M.Sadowski and Dr. H.Schmidt analyzed results of the last series of measurements, which were carried out by the IPJ team delegated previously to perform experimental studies at POSEIDON. These studies concerned discharges realized with the additional injection of considerable amounts of various heavy-gas admixtures (in particular of Ar and N_2). The analysis concerned measurements of voltage- and current-waveforms, ultrafast photos made with a high-speed streak camera, frame pictures taken with a fast high voltage diode, and framing Schilieren-type pictures obtained with an optical system equipped with a N_2 pulse laser with 1 ns exposition. We also analyzed signals induced by fast electron teams in the Čerenkov-type detectors, and time correlations of current peculiarities (from dI/dt traces) with signals corresponding to maximum compression (so-called r_{min} signals), X-ray pulses, as well as electron- and neutron-pulses. Also investigated were mean values of the neutron yield as a function of experimental conditions.

It has been demonstrated that under determined geometrical energetic- and gaseous-conditions the average neutron yield at the D_2 gas puffing can be increased even by 80%. It has also been shown that a gaseous target (formed by puffing along the z-axis) can change considerably dynamics and the structure of the collapsing current sheath and the formed pinch column. We elaborated a fast draft of a paper on the influence of additional gas targets on dynamics and other characteristics of the compression phase in the PF-type discharges.

[1] H.Schmidt, M.Sadowski, L.Jakubowski, E.Składnik-Sadowska and J.Stanisławski: Gas-Puff Target Experiments with POSEIDON Plasma Facility: Plasma Phys. and Contr. Fusion 36 (1994)13-24.

[2] H.Schmidt, L.Jakubowski, M.Sadowski, E.Składnik-Sadowska, J.Stanisławski, and A.Szydłowski, Annular Gas Puff Target Experiments with POSEIDON Plasma Focus, AIP Conference Proceedings 299 - Dense Z-Pinches (AIP, New York 1994) 340-347.

[1)] IPF-Stuttgart

2.4 Participation in Plasma Experiments with the PF-1000 Facility; Collaboration with IFPiLM in Warsaw

by M.Sadowski, A.Szydłowski, and PF-1000 Team (IFPiLM)

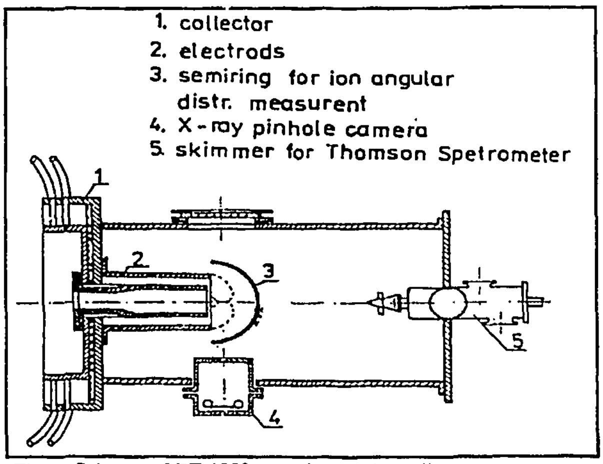

Fig.1. Scheme of PF-1000 experiment: 1 - collector, 2 - electrodes, 3 - semiring with ion detectors, 4 - X-ray pinhole camera, 5 - ion pinhole camera

In January 1994 we started the first experiments with the PF1000 facility, which was put into operation in the Institute of Plasma Physics and Laser Microfusion. The experiments performed in 1994 were only a preliminary phase of exploitation tests with that facility. A charging voltage was limited to 20 kV, and the tests were carried out within an experimental chamber filled with hydrogen instead of deuterium. The applied electrodes had too small dimensions for future experiments to be performed with high energetics.

During 1994, several diagnostic methods were tested, as shown in Fig.1. Using an X-ray pinhole camera we took pictures of the plasma-focus column. We also took VR pictures of the plasma-focus region by means of a high-speed smear camera as well as with an ultra-fast-frame camera equipped with an image converter. Strong pulses of X-rays and neutrons were registered with a scintillation probe. Total neutron yields were measured with silver- and indium-activation counters. On the basis of a series of PF shots with deuterium filling, it was found that the average neutron yield for non-optimized discharges at 200 kJ was about 10^9.

Within the frame of a bilateral collaboration (between the IPJ and IFPiLM) some Dept. P-V staff participated in all PF-1000 experiments. They were responsible in particular for diagnostics of fast ions emitted from PF discharges. They designed and assembled equipment for various ion measurements [1]. Using solid-state nuclear track detectors, placed upon a special semi-circular support inside the experimental chamber (at the distance of 30 cm from the electrode ends), an angular distribution of fast ions (mostly protons) emitted from the plasma-focus region was determined, as shown in Fig.2. Using an ion pinhole camera with track detectors, placed at a distance of about 200 cm from the electrode outlet, pictures were also taken of fast ion beams emitted along the z-axis. Results of these preliminary measurements will be presented at 2nd National Symposium PLASMA'95 in June 1995.

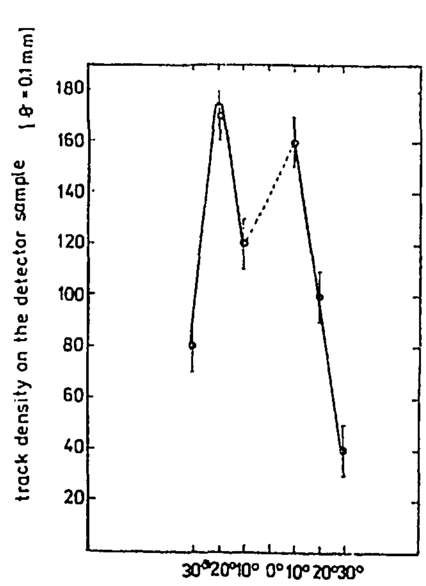

Fig.2. Angular distribution of fast ions (mostly protons) emitted from PF-1000 facility

[1] M.Sadowski, A.Szydłowski, Technical Documentation of Parts for Diagnostic Equipment (in Polish), Inter. Report (Dept. P-V IPJ, Świerk 1994), - unregistered.

2.5 Studies of Mass- and Energy-Spectra of Ions and Neutral Particles Emitted from IONOTRON-93 Device

by J.Baranowski, and E.Skladnik-Sadowska

The IONOTRON-93 device is a small facility (I_{max} = 250 kA, U_0 = 30 kV, E = 11 kJ) designed mainly for basic studies of plasma - ion beams, as well as, electron and neutral-beams. In 1994 studies were performed with deuterium filling at various values of time delays τ. The most important results can be summarized as follows:

1. A time-integrated mass- and energy-spectrum of ions, emitted from a deuterium plasma along the symmetry axis demonstrates that N^{1+} ions and N_2^{1+} molecules are present in the plasma stream in large amounts for discharges with $\tau = 180\ \mu s$.
2. The ion current density as measured on the symmetry axis and at 15^0 to the z-axis, shows that ion current densities amount to several or several dozen A/cm^2 and they depend strongly on a time delay τ. The measurements have been performed with a Faraday cup equipped with additional (active) grids.
3. Time-resolved measurements of neutral streams emitted along the z-axis (as performed with a charge exchange cell, an additional stationary electric field, and a Faraday cup) have shown that neutrals are probably emitted at the same time as high energy ions.

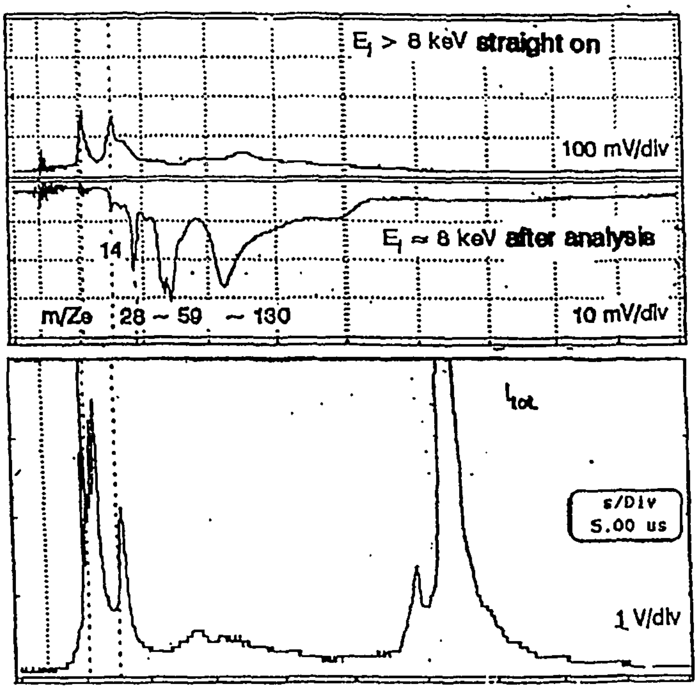

Fig.1. Time - resolved ion current signals for $\tau = 180\ \mu s$. Ion current signal "straight on" - E_i>8 keV, and ion signals after analyses - Eii=8keV (upper). The total ion current signal before analyses (lower).

4. The time-resolved mass- and energy-spectra of ions with an electrostatic analyzer equipped with an ion - electron converter and a Faraday cup. Those measurements have shown that ions with kinetic energy $E_i > 8$ keV are probably emitted during the maximum the main current. Some of examples of time-resolved traces are shown in Fig.1. The most important results of studies in operation have been presented in two papers [1-2].

[1] J.Baranowski, W.Komar, E.Składnik-Sadowska, Diagnostics of Ions within High Intensity Plasma Streams, Proc. 21 EPS Conf. on Controlled Fusion and Plasma Physics, (Montpellier 1994).

[2] J.Baranowski, E.Składnik-Sadowska, Mass-Energy Measurements of Ions within Intensity Plasma Stream, Proc. of 3rd General Assembly Polish Nuclear Society, Warsaw 1994.

2.6 Measurements of Plasma-Ion Beam Power Deposited on Target in the IONOTRON Device as a Function of Time

by W.Komar, J.Stanisławski, J.Langner, J.Piekoszewski, J.Białoskórski

The method relies upon the observation of changes in intensity of thermal radiation (within the IR range) emitted by a silicon target which is exposed to pulsed plasma beams. To measure the IR radiation intensity, use is made of a semiconductor photodetector. Since silicon is semitransparent in the IR spectral range, the radiation emitted from hot areas of a silicon wafer can be observed behind the target. In the experiment the silicon wafer serves simultaneously as a target converting the kinetic energy of plasma beams into thermal radiation, and as a shield for the detector.

A special measuring device has been constructed to register the IR radiation intensity simultaneously by means of three IR detectors (operating within different wavelength ranges) and to measure time-integrated plasma beam energy density with four calorimeters. The measurements have been performed at the modified SOWA-400 facility. The measuring device with the detectors and the silicon target has been placed on the z-axis of the system, at a distance of 0.5÷1 m from the electrode ends.

In order to combine the IR radiation intensity (determined from detector signals) with a temperature distribution inside the target, a theoretical model has been developed. In this model the self-absorption of radiation within the target (including its dependence on local temperature) as well as multiple reflections from target surfaces have been taken into account. Calculations based on this model have been performed taking into account (as a starting point) temperature distributions determined with the use of the MELT program, within the framework of the cooperation with Dept. P-IX.

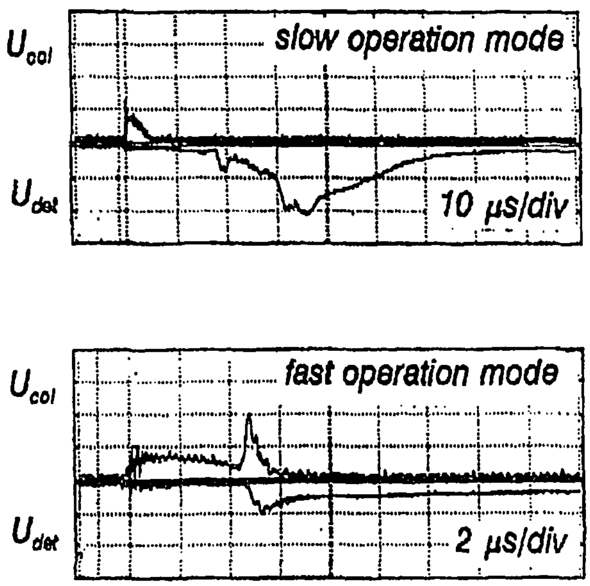

Fig.1. Typical waveforms of collector voltage (upper lines) and IR detector signals (lower lines).

A detailed analysis of the model has been performed in order to determine limits of the proposed method. It was found that for high power plasma beams (of surface density above 0.5 MW/cm^2), when the temperature of the target surface is close to the melting point, the detectors receive the IR radiation emitted mainly from a micrometer layer of the target with a temperature of about 1200 K because of the strong self-absorption in hot areas of the target and a small value of the Planck factor in cold areas. Therefore, when the power density of a plasma beam is high, results of IR radiation measurements can hardly be interpreted.

A preliminary analysis of experimental results has shown that at the distance of 1 m from the electrode ends, the power density of a plasma beam ranges from 0.1 MW/cm^2 (for a slow operation mode) to 1 MW/cm^2 (for fast operation mode).

2.7 Calibration of Nuclear Track Detectors of the CR-39 and PM-355 Types by Monoenergetic Deuterons and α-Particles

by M.Sadowski, E.M.Al-Mashhadani, A.Szydłowski, T.Czyżewski, L.Głowacka, M.Jaskóła, C.Rolfs[1] and M.Wieluński[1]

Solid-state nuclear track detectors (SSNIDs) have for many years been used in plasma research mostly for diagnostics of fast ions. About 10 years ago we developed a new type of such detectors, which was denoted as the CR-39 plastic. Since about 5 years, another improved plastic called the PM-355 type has also been available. The CR-39 and PM-355 plastics are very useful for electrons of light ions and they are often applied in various plasma experiments.

Taking into account applications of SSNIDs for studies carried out in Dept. P-V, and a lack of accurate calibration data, it was decided to investigate the sensitivity of these detectors within the energy range 0.2-4.5 MeV. The main aim of the calibration measurements was to determine dimensions of tracks (produced by light ions in the detector) as a function of ion energy, its electrical charge, and conditions of the etching. Such calibration characteristics facilitate an analysis of experimental data and they make possible e.g. the identification of ions on the basis of their tracks.

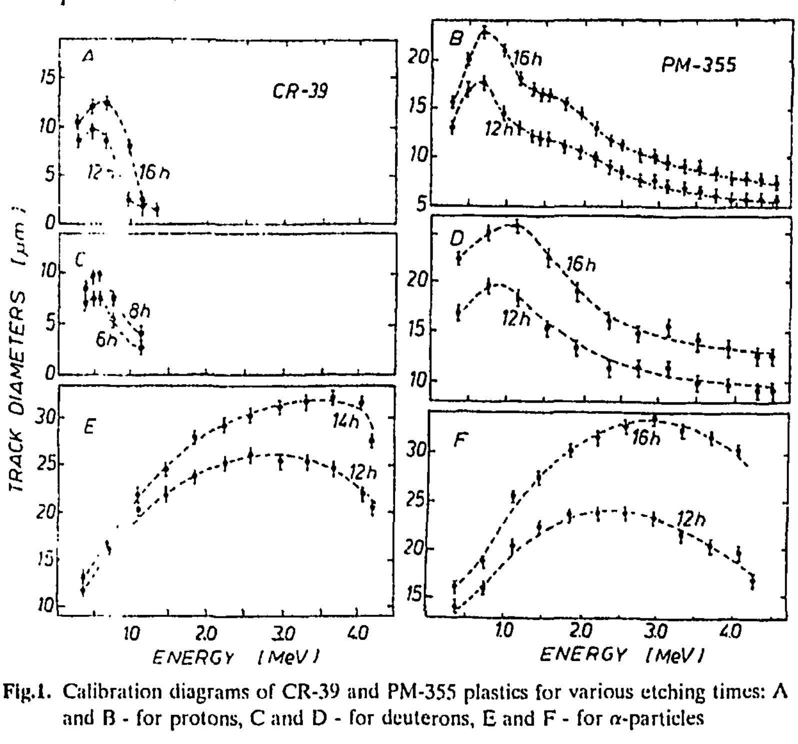

Fig.1. Calibration diagrams of CR-39 and PM-355 plastics for various etching times: A and B - for protons, C and D - for deuterons, E and F - for α-particles

To perform the calibration, monoenergetic ion beams from two accelerators were used. Samples of the detectors were exposed to the ion beams of energy ranging from 0.4 to 4.6 MeV in 0.2 MeV steps. The first measurements with monoenergetic protons were completed in 1993, and the results were presented in two papers published in 1994 [1-2]. The second stage of studies, which comprised the calibration of CR-39 and PM-355 plastics with monoenergetic deuterons and α-particles, was described in two other papers [3-4]. Except for the ions, the irradiation and etching procedures were the same as those described before [1].

The calibration diagrams are shown in Fig.1. The most important results can be summarized as follows. The PM-355 plastic demonstrates tracks of larger diameters and it can be used for protons and deuterons within a wider energy range than the CR-39 plastic. The calibration curves have distinct maxima at given ion energy values, above which the track diameters decrease monotonically, It is therefore possible within the determined energy range to estimate an ion energy on the basis of the track diameter.

[1] M.Sadowski, E.M.Al-Mashhadani, A.Szydlowski, T.Czyżewski, L.Głowacka, M.Jaskóła, and A.Wieluński: Investigation on the Response of CR-39 and PM-355 Track Detectors to Fast Protons in the Energy Range 0.2-4.5 MeV; Nucl. Inst. and Meth. in Phys. Res. B86(1994)311-316.

[2] E.M.Al-Mashhadani, M.Sadowski, A.Szydłowski; Measurements of Fusion Produced Protons with Modern Nuclear Track Detectors; Fizika Plazmy 20, 2(1994)196-198.

[3] M.Sadowski, et al.; Comparison of Responses of CR-39 and PM-355 Track Detectors to Fast Protons, Deuterons and He-Jons within Energy Range 0.2-4.5MeV; Radiation Measurements (in press).

[4] M.Sadowski, E.M.Al-Mashhadani, A.Szydlowski, T.Czyżewski, L.Głowacka, M.Jaskóła, C.Rolfs, and M.Wieluński; Comparison of Responses of CR-39 and PM-355 Track Detectors; Proc. 17th Intern. Conf. on Nuclear Tracks in Solids (Dubna, 1994), p.153.

[1] Ruhr University

2.8 Investigation of the Melting of a Silicon Target Surface Bombarded by a Plasma Beam, Using Refraction Index Changes[*]

by J.Appelt, W.Komar

A starting point of the proposed method is the fact that values of the refraction index (and in consequence those of the reflection coefficient) of silicon in a solid and a liquid state are considerably different. The method relies on observations of intensity changes in a laser beam reflected from the target surface. This method has already been applied to study on silicon melting by a intense laser beam [1].

In experiments performed in 1994 a possibility of applying this method to investigate of the target melting with an intense plasma beam was studied. A silicon target, which was placed inside a plasma focus device (PF046) at the distance of about 0.5 m from electrode ends, has been irradiated with an auxiliary laser beam from a He-Ne-laser. The intensity of light reflected from the target surface bombarded by a plasma beam,as obtained from the PF-046 device, has been measured by means of a photomultiplier equipped with a set of filters and diaphragms.

In the experiments described above it was found that the detection of a liquid phase appearance on the target surface was impossible because of other effects (e.g. a metal deposition), which cause serious permanent changes in the reflecting properties of the silicon surface.

[1] M. von Allmen. Laser and Electron Beam Processing of Materials, 6, Academic Press, 1980.

[*] Work supported by the State Committee for Scientific Research (Poland) under contract No 919/2/91

3. TECHNOLOGY

3.1 Construction of a Modified Model System for Data Acquisition and its Laboratory Tests; Collaboration with NIIEFA in St.Petersburg

by M.Bielik

Within the framework of the task mentioned above we performed technological studies of various applications of FO-SY-TS (Fiber Optic Separation for Variable Transients Transmission System). As a result we designed a new Fiber-Optic ON-OFF unit, which makes possible switching circuits, including those at high potential. The developed ON-OFF unit operates in a controlled mode, i.e. a control signal is transmitted back through the second optical cable and it is confirmed only when a switching order (ON or OFF) is realized. A transmission unit of the FO-ON-OFF unit has been equipped with a connector for PC controller. An electrical scheme of the unit has been shown in Fig.1.

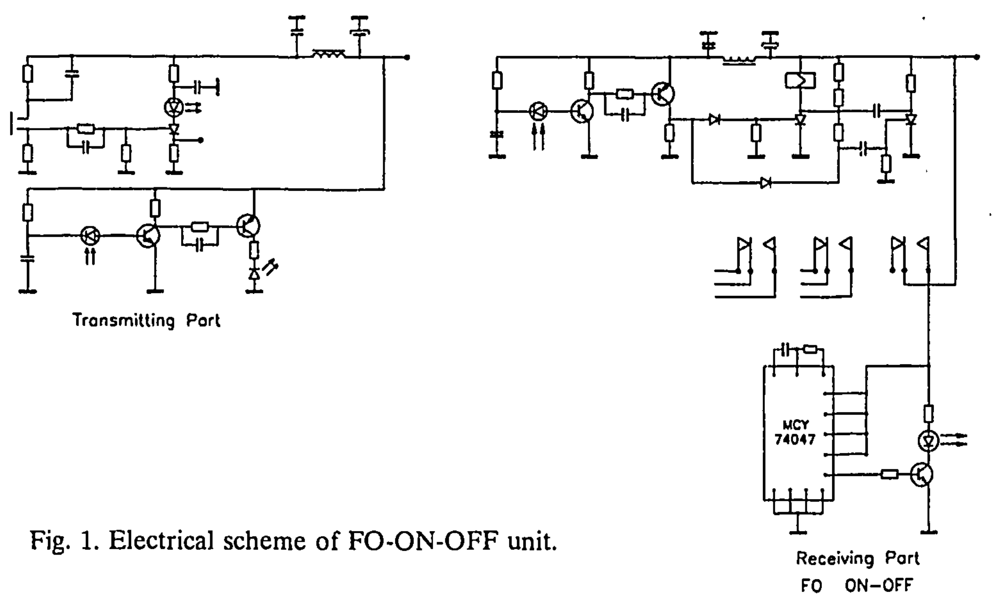

Fig. 1. Electrical scheme of FO-ON-OFF unit.

The FO-ON-OFF together with the FO-SV-TS unit, which was developed before [1] make possible the design and assembling of miniature systems for controlling high voltage pulse generators. They can perform the following program:

- Switching ON and OFF of a HV generator	FO-ON-OFF
- Switching OFF the crowbars (with confirmation)	FO-ON-OFF
- Switching ON and OFF various HV sources	FO-ON-OFF
- Switching OFF a charging unit at chosen voltage	SV-FO-TS
- Switching the pressure of air in spark gaps	FO-ON-OFF
- Continuous measurements of pressures	SV-FO-TS
- Measurements of charging voltages at HV sources	SV-FO-TS

Both units (FO-SV-TS and FO-ON-OFF) have been tested in the High-Voltage Laboratory at the Institute of Plasma Physics and Laser Microfusion in Warsaw. Results of tests will be presented at the 17th Symposium on Plasma Physics and Technology, to be held in Prague in June 1995.

The FO-ON-OFF developed unit will also be used in the pulse supply system of an electron gun in the LAE-10 electron accelerator. This system has been constructed for the Institute of Nuclear Chemistry and Technology in Warsaw.

[1] M.Bielik, Data Acquisition System for Slow Variable Transients with Fiber Optic Separation, Proc. 17th Symp. on Fusion Technology (SOFT, Rome 1993), vol. 2, pp.993-996.

3.2 Modification of Data Acquisition System for Probe Array and Adaptation of IONOTRON Generator for Studies of DPE Process

by K.Czaus

In order to improve the operation of the IONOTRON-SW30 device and to apply it for the DPE technology, the electrical strength of the main HV parts of the IONOTRON generator has been improved by about 50%. Within the framework of this work the construction of the main current collector and of precollectors, as well as that of a spark-switch in the condenser bank units, have been modified. It has been proved that IONOTRON-SW30 can be used for DPE technological material research.

Within the framework of the modernization of the data acquisition system for calorimetric measurements, a new USM-1 control unit has been designed and assembled. The unit makes possible automatic measurements and it is coupled with a control unit of the IONOTRON-SW30 facility by means of the OR-1 opto-electronic receivers and optical cables which ensure galvanic isolation.

3.3 Modification of a Steel Surface by Means of the PF-046 Device

by J.Appelt

Over the past few years the possibility of surface modification of materials with carbon ions (atoms) has been analyzed. In the case of construction steel an intermediate layer containing carbon atoms, of a thickness ranging from several to above a dozen micrometers, can change surface properties, e.g. increasing the microhardness. Several series of Plasma Focus discharges have been carried out for a wide range of hydrogen pressures, using a graphite insert in the front plate of the center electrode. We performed irradiation of the 18HGT steel samples designed for carburizing, but it has not shown a required increase in the surface hardness. Therefore, other kinds of steel (structure and composition giving promise of with a positive result of the experiment) have been used. In particular, the 4H13 stainless steel (hardenable) has been implanted. The samples have been prepared for consecutive measurements of the microhardness and carbon distribution.

3.4 Analysis of Material Sample Irradiation within PF-360 and POSEIDON Facilities. Collaboration with IPF, Stuttgart

by J.Langner, J.Piekoszewski, H.Schmidt[1], and Team of Trento University (Italy)

The main aim of work undertaken in 1993 was to verify the possibility of the application of a large facility of the Plasma-Focus type for the formation of thin layers with high hardness (e.g. Titanium Nitride) on various substrates.

In 1994, the main task was to perform an analysis of material samples irradiated previously within the PF-360 facility in Świerk and within the POSEIDON facility in Stuttgart. The preliminary analysis comprised on evaluation of the state of the surface, uniformity, and color of the samples. The microscopic examination revealed a high degree of damage in surfaces of most samples (numerous craters, "orange peel", microdroplets of deposited metal). The uniformity of the irradiated materials was also unsatisfactory. A change of color was used as the main criterion of the evaluation. A gold color, which is characteristic for TiN layers, was observed only for 20% of the examined sample population. Using such criteria the best sample was selected, and after that it was investigated by means of X-ray diffractomery.

The investigations performed on one half of the surface of the selected sample at the Institute of Nuclear Chemistry and Technology in Warsaw, did not reveal the presence of Titanium Nitride. The measurements performed using a more sensitive Phillips diffractometer within the framework of a collaboration with Trento University, Italy revealed a trace amount of TiN on the second half of the sample. The distribution and intensity of the CuK_α lines are similar to those for a powdered material. It means that there is no preferential orientation of crystallites, unlike in the case of other PVD methods. In summary it can be concluded that large PF-type facilities, in spite of the ability to synthesize TiN, are not suitable for the forming of homogeneous coatings over large area surfaces.

[1] IPF - Stuttgart

3.5 The Use of Metallic Plasma Pulses in Formation in Thin Coatings on the Melted Surface of the Substrates

by J.Langner, J.Stanisławski, J.Piekoszewski

The work is aimed at the verification of the feasibility of the new process in which the ions and vapor of a metal, generated by Pulsed Metal Vapor Vacuum Arc (PMVVA) type of source delivered to the substrate both: the coating material and the heat sufficient to melt its near- surface layer. The experiment is based on the technique developed at SINS and referred to as Pulse Implantation Doping (PID) in which the plasma pulses are generated exclusively of the working gas injected externally in to the interelectrode space. In the present version, the additional source of metallic plasma PMVVA in PID facility - IONOTRON is installed. The appropriate synchronization of IONOTRON-PMVVA action makes it possible to accomplish the process in which the stream of metallic plasma impinges on the melted surface of the processed material. Since the processes induced in this way have a transient character, the formation of the metastable phases and alloys, nonexisting in thermodynamic equilibrium state is possible. In the course of the present phase of this work the PMVVA source was designed, installed and put into operation. Experiments on the formation of Al, Cu and Ti on various substrates are in progress.

3.6 Deposition by Pulsed Erosion: Formation of Chromium and Titanium layers on various substrates

by J.Piekoszewski, J.Langner, K.Czaus, M.Traczyk, Z.Werner

A set of Ti and Cr electrodes has been prepared. Conditions of the DPE process which enable a deposition of layers on surfaces as large as 20 sq.cm have been preliminarily established. In a series of experiments, the dependence of DPE efficiency on the discharge delay time $\Delta\tau$ has been determined for Cr and Ti and for two working gases (Ar and N). 1H18N9T steel was used as the substrate. Then, two sets of Ti layer depositions on SW18 steel have been performed in conditions giving the maximum deposition efficiency; one set for 5 pulses, the other for 50 pulses. In the former case the Ti layer was intended to be a transition layer in the steel/Ti/TiN structure; in the latter one -- as a material to be transformed into TiN in a separate nitriding process.

It turned out however -- contrary to the expectations -- that the amount of Titanium deposited in both cases differs only slightly. In order to examine the influence of the substrate material on the Ti DPE efficiency, another set of experiments has been conducted. The process was carried out simultaneously on Cu, SW18 and Al_2O_3 substrates. After each pulse two parameters were controlled: change in the sample weight and the relative amount of Titanium as seen by X-ray fluorescence analysis (X-ray tube with Ag anode at 15 kV potential and with beryllium window); the latter measurements were taken for Cu and Al_2O_3 substrates. It turned out that successive pulses almost regularly cause an increase of mass in the case of Cu samples, but a decrease in the case of other substrates; the amount of Titanium increases in all cases. Additionally, on Al_2O_3 substrates there appears a smoothed, highly adhesive and electrically conductive layer.

The results concerning mass variation agree qualitatively with computer simulation of thermodynamics of the DPE process, reported separately. A practical conclusion can be drawn from the above experiments: in order to avoid mass decrease in the case of metallic substrates (and related disadvantageous microgeometrical effects), one has to adjust the process parameters individually for each kind of such substrates in such a way, that the melting of the near-surface layer takes place without an excessive evaporation of the substrate material. Surface conditions of ceramic materials processed by the DPE are a separate problem, which is very interesting from both scientific and practical point of view.

3.7 Computer Simulation of Thermal Evolution in Selected Targets Irradiated by Intense Plasma Pulses

by R.Baranowski[1)], J.Białoskórski, J.Langner, J.Piekoszewski, Z.Werner

A series of numerical calculations modelling the thermal evolution of a flat target irradiated by an intense plasma pulse of Gaussian power distribution have been performed for about 100 sets of input parameters. The calculations were based on the MELT program developed by UMCS Lublin University; the program takes into account the phase transitions of the target material (melting and recrystallization). The varied parameters were: width (at the half maximum) of the irradiating pulse, total pulse energy and target material data. The computations were made for conditions typically encountered in presently conducted experiments with practically used targets: copper, steel, alundum and silicon.

The results confirm qualitatively some intuitively expected effects of such irradiations:

- At the fixed pulse energy and pulse length, the surface temperature of the target increases and the depth of recrystallization decreases with lowering the thermal conductivity of the target material;
- Pulses of 4 - 5 J/cm² energy density and assumed durations of 200...500 ns FWHM heat up the target up to the temperature at which evaporation of the material starts to play an important role. This phenomenon is distinct in the case of alundum, should be negligible in the case of copper, whereas in the case of steel, evaporation depends very critically on the total energy and on the duration of the pulse.
- The dependence of the depth to which the target melts on the pulse energy is the more steep, the lesser is the heat of melting of the material. It means that the dependence is much more steeper in metals (low heat of melting) than in ceramics (high heat of melting). Therefore, controlling the melted depth in metals is much more difficult than in other materials.

[1] The Institute of Physics, UMCS University

3.8 Construction of a Marx-600kV Pulse Generator with Modernized 2IC8 Spark-Gaps; Study and Analysis of their Operation within this Generator

by J.Witkowski, and R.Mirowski

On the basis of the GU-600 HV-generator constructed previously [1], we designed and a assembled a new model of four-stage Marx generator. In each stage of the new generator we used two IK100/0,4μF-type capacitors and one modernized switching spark-gap of the 2IC8w type. Resistors for the formation of a front time and half value time were composed of TWO60-type resistors.

The new Marx-600kV generator is designed for generation of HV pulses with a normalized shape, and these with a shorter rise-time (rising linearly). Therefore the generator can be used for the testing of break-down strength of various electrical devices and equipment designed for the overvoltage protection.

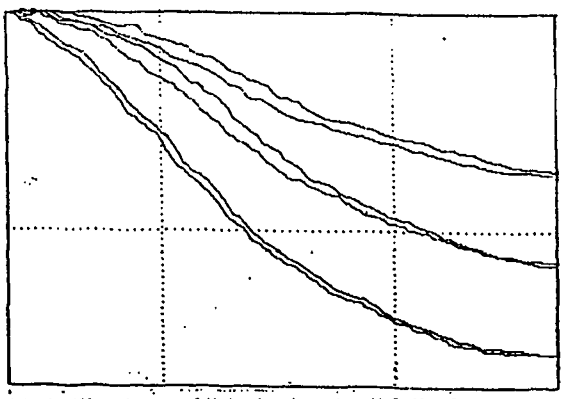

Fig.1. Waveforms of lightning impulse (1.2/50), fronts, as registered for different charging voltages: 10, 15 and 20 kV, respectively. Scale: 82 kV/div, 0.5 μs/div.

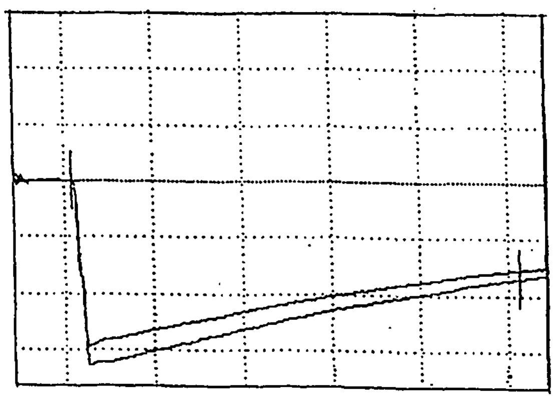

Fig.2. Waveforms of lightning impulse (1.2/50), as registered for two different charging voltages: 10 and 15 kV. Scale: 32.8 kV/div, 10 μs/div

On the basis of the performed tests it has been shown that the generator operates with a small (nanosecond) jitter time within the voltage range from 0.5 to 0.8 U_n. Due to the application of the modernized 2IC8w spark-gaps an irregular operation of the generator was eliminated. This was observed inGU-600 and GU-2400 generators constructed before, and was connected with some difficulties in the triggering of the 2IC8 spark-gaps.

Within the framework of technological HV research, the generator was tested for pulses with the maximum amplitude up to 360 kV (the value limited by measuring dividers). New measuring dividers for higher voltages are to be constructed in 1995.

3.9 Equipment for Testing and Protection of Medium-Voltage Devices from Overvoltages Induced by Steep Pulses; Preliminary Studies

by K.Kocięcka

Pulse alternating electromagnetic fields create high hazards for electric systems because they can cause sharp rising overvoltages.

The most hazardous pulses are those with a risetime and voltage collapse time below 1μs. The main sources of such overvoltages are transient states, and in some cases nuclear explosions. High-altitude EMP explosions have the largest range of effects. In laboratories special HV generators for the formation of steep voltage pulses are designed and constructed. They are used for testing of electrical devices and protection equipment.

A protecting system should reduce the maximum amplitude of overvoltages to a level of the with- stand voltage for a protected device. Any protecting device should work in a reliable and regular way under determined conditions. As overvoltage protectors are often used:

- gas arresters,
- chopping spark-gaps,
- lightning arresters composed with SiC resistors or ZnO varistors, and semiconductor rectifiers.

All the devices mentioned above can be used in parallel connections with the protected devices. When the protection level is insufficient these devices can be used simultaneously in a cascade system.

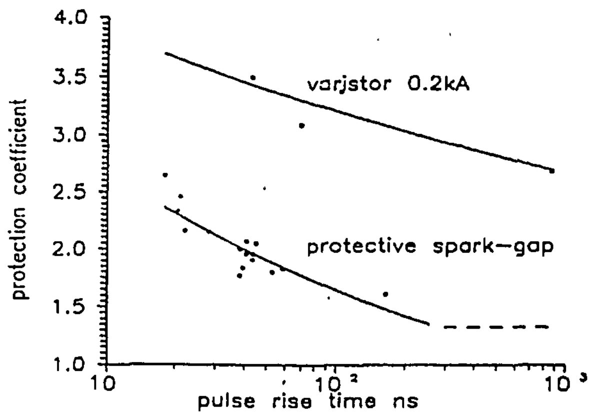

Fig.1. Comparison of varistor and spark-gap protection characteristics

In 1994 at Dept. P-V there we performed preliminary tests of spark-gaps and ZnO varistors as overvoltage protectors from steep overvoltages which appear during the operation of an 800kV/1MW accelerator supply-unit [1].

It has been shown that a spark-gap with a quasi-homogeneous electric field and the additional ionization in the case of steep voltage pulses provides a protection level almost twice as lower than that achieved with varistors [2], as shown in Fig.1.

[1] W.Drabik, A.Jerzykiewicz, K.Kocięcka, J.Witkowski, Design Study of Ecological Accelerator, 4th European Particle Accelerator Conf. EPAC'94 (London 1994).

[2] A.Jerzykiewicz, W.Drabik, K.Kocięcka, J.Witkowski, Protection Characteristics of Varistors Made of Metal Oxides for Voltage Pulses with Steep Front (in Polish), Tech. Review No 5(1994)102-106.

VI. PUBLICATIONS, PATENTS, SEMINARS, RESEARCH PROJECTS

a. PUBLICATIONS, CONFERENCE PROCEEDINGS, CONTRIBUTIONS

1. L-SUBSHELL IONIZATION OF RARE EARTH ELEMENTS BY CARBON ION BOMBARDMENT.
J.Braziewicz, J.Semaniak, **T.Czyżewski, L.Głowacka, M.Jaskóła**, M.Haller, R.Karschnick, W.Kretschmer, D.Trautmann
J. Phys. B: At. Mol. Opt. Phys. 27 (1994) 1535

2. L-SUBSHELL IONIZATION BY ^{14}N IONS.
J.Braziewicz, J.Semaniak, **T.Czyżewski, L.Głowacka**, M.Haller, **M.Jaskóła**, R.Karschnick, A.P.Kobzev, M.Pajek, W.Kretschmer, D.Trautmann
Nucl. Instr. and Meth. B86 (1994) 185

3. ^{208}Pb STATES HOMOLOGOUS TO THE 1.484 MeV, 11/2 STATE OF ^{205}Tl.
P.Guazzoni, **M.Jaskóła**, L.Zetta, G.Graw, R.Hertenberger, D.Hofer, P.Schiemenz, U.Atzrott, R.Neu, G.Staudt
Phys. Rev. C 49 (1994) 2784

4. TESTING AlCuMg-ALLOYS REFERENCE MATERIALS USING THE PIXE METHOD
J.Lipiński, **T.Czyżewski, L.Głowacka, M.Jaskóła**, J.Gałązka
Nukleonika 39 (1994) 101

5. PREEQUILIBRIUM SPIN EFFECTS IN FESHBACH-KERMAN-KOONIN AND EXCITON MODELS AND APPLICATION TO HIGH-SPIN ISOMER PRODUCTION
M.B.Chadwick, P.G.Young, P.Oblozinski, **A.Marcinkowski**
Phys. Rev. C49 (1994) 2885

6. CROSS SECTIONS FOR (n,p) REACTION ON RUTHENIUM ISOTOPES IN TERMS OF THE NOVEL MULTISTEP COMPOUND REACTION MODEL
D.Kielan, A.Marcinkowski
Acta Phys. Pol. B25 (1994) 1219

7. GRADUAL ABSORPTION OF FAST NEUTRONS IN NIOBIUM.
A.Marcinkowski, D.Kielan
Nucl. Phys. A578 (1994) 168

8. AN INTERPRETATION OF THE ^{56}Fe(n,p)^{56}Mn EXCITATION FUNCTION.
J.Rondio, B.Mariański, A.Korman
Acta Phys. Pol. B25 (1994) 841

9. SELF ORGANIZATION IN THE NUCLEAR SYSTEM: II. FORMATION OF A NEW ORDER.
W.Iskra, M.Müller, I.Rotter
J. Phys. G20 (1994) 775

10. SELF ORGANIZATION AND DISORDER IN AN OPEN QUANTUM SYSTEM.
M.Müller, I.Rotter, **W.Iskra**
Acta Physica Polonica B25 (1994) 711

11. J DEPENDENCE IN ^{12}C(^{6}Li, ^{3}He).
K.W.Kemper, P.L.Kerr, A.J.Mendez, E.G.Myers, E.L.Reber, **K.Rusek**, G.Tungate
Phys. Lett. B321 (1994) 183

12. INTERACTION OF ALIGNED ^{23}Na WITH ^{206}Pb AT THE COULOMB BARRIER: QUASIELASTIC SCATTERING, FUSION AND FISSION.
H.Reich, K.Becker, M.Detje, W.Korsch, H.Leucker, **Z.Moroz, K.Rusek**, H.G.Völk, W.Widdra, D.Fick
Nucl. Phys. A576 (1994) 409

13. ^{208}Pb(^{7}Li,^{6}Li)^{209}Pb REACTION AT 33 MeV AND ITS EFFECT ON ELASTIC SCATTERING.
K.Rusek et al.
Nucl. Phys. A575 (1994) 412

14. CLUSTER-FOLDING ANALYSIS OF ^{6}Li+^{26}Mg SCATTERING AT 60 MeV.
K.Rusek, N.M.Clarke, R.P.Ward
Phys. Rev. C50 (1994) 2010

15. COLLECTIVE EXPANSION IN CENTRAL Au + Au COLLISIONS
W.C.Hsi, ..., **B.Zwięgliński**
Phys. Rev. Lett. 73 (1994) 3367

16. EVALUATION OF ATOMIC DISPLACEMENT IN ION IMPLANTED GaAs.
J.Kaczanowski, A.Turos, K.Gärtner, T.Bachman, W.Wesch
Nucl. Instr. and Meth. B85 (1994) 607

17. CHANNELING STUDIES OF OXYGEN SUBLATTICES IN OXIDE SINGLE CRYSTALS.
A.Turos, O.Meyer, **L.Nowicki**, J.Remmel, M.Wieluński
Nucl. Instr. and Meth. B85 (1994) 448

18. TEMPERATURE DEPENDENT DECHANNELING OF 1.4 MeV He^+ AND OPTICAL NEAR-EDGE ABSORPTION IN B^+ IMPLANTED GaP.
W.Wesch, E.Wendler, **J.Kaczanowski**, **A.Turos**
Nucl. Instr. and Meth. B85 (1994) 533

19. CLOSE ENCOUNTER PROCESSES IN MONTE CARLO SIMULATIONS OF ION CHANNELING
A.Dygo, W.N.Lennard, I.V.Mitchell
Nucl. Instr. and Meth. B90 (1994) 142

20. AZIMUTHALLY AVERAGED BACKSCATTERING YIELD NEAR THE <100> AXIS IN Si
A.Dygo, W.N.Lennard, I.V.Mitchell, J.P.Smulders
Nucl. Instr. and Meth. B90 (1994) 161

21. RANDOM SPECTRUM FOR THE CHANNELING-BACKSCATTERING TECHNIQUE: A ROTATING AXIAL-DIP STUDY.
A.Dygo, W.N.Lennard, I.V.Mitchell, P.J.M.Smulders
Nucl. Instr. and Meth. B84 (1994) 23

22. ENERGY LOSS DISTRIBUTIONS FOR 625 keV H^+ IONS IN Si SINGLE CRYSTAL.
A.Dygo, M.A.Boshart, M.W.Grant, L.E.Seiberling
Nucl. Instr. and Meth. B93 (1994) 117

23. *POLYGONIZATION OF SINGLE CRYSTALS OF THE FLUORITE-TYPE OXIDE UO_2 DUE TO HIGH DOSE ION* IMPLANTATION.
Hj. Matzke, **A. Turos**, G. Linker
Nucl. Instr. and Meth. B91 (1994) 294

24. CHANNELING ON ROUGH SURFACES
A.Barcz, **S.Kwiatkowski**, **R.Sidor**, **A.Turos**
Appl. Phys. A49 (1994)

25. RADIAL PATTERN OF NUCLEAR DECAY PROCESSES.
W.Iskra, M.Müller, I.Rotter
Preprint FZR-39, May 1994, Phys. Rev.C (in press)

26. IMPACT PARAMETER AND REACTION PLANE DETERMINATION FOR Au + Au COLLISIONS AT E/A = 400 MeV.
G.J.Kunde, .., **B.Zwięgliński**
GSI Report GSI-94-46, Nucl. Phys. A (in press)

27. FRAGMENT FLOW AND THE MULTIFRAGMENTATION PHASE SPACE
G.J.Kunde, ..., **B.Zwięgliński**
Phys. Rev. Lett. (in press)

28. ENERGY-LOSS DISTRIBUTIONS FOR 2.5 MeV He^+ IONS INCIDENT ON Si SINGLE CRYSTAL
M.A.Boshart, **A.Dygo**, L.E.Seiberling
Phys. Rev. A (in press)

29. Δ DECAY AND ABSORPTION IN NUCLEI.
S.Rousteau, ..., **P.Zupranski**
Proc. XXXII International Winter Meeting on Nuclear Physics, Bormio, Italy, Jan. 24-28, 1994, Universita Degli Studi di Milano, Ricerca Scientifica ed Educazione Permanente, Suppl. N. 97, p. 447

30. ODNO- I DVUKHSTUPENCHATYE PRIYAMYE PEREDACHI KLASTEROV V REAKTSYAKH (d,HI) I (α, HI) NA LEGKIKH YADRAKH
A.T.Rudchik, ... **L.Głowacka**, **J.Turkiewicz**, et al.
Proc. Int. Conf. on Nuclear Spectroscopy and Nuclear Structure, St. Petersburg, May 17-20, 1994, p.231

31. DOORWAY STATES OR GRADUAL ABSORPTION.
A.Marcinkowski
Proc. Int. Conf. on Nuclear Data for Science and Technology, Gatlinburg (USA), May 9-13 1994, (to be published by the APS)

32. SÄTIGUNG DER RIESENRESONANZSTÄRKE IM BEREICH SEHR HOHER NIVEAUDICHTE.
W.Iskra, M.Müller, I.Rotter
Verhandlungen der Deutschen Physikalischen Gesellschaft, Frühjahrstagung München 1994, Physik der Hadronen und Kerne, p.1807

33. ZEITSKALEN IN KERNREAKTIONEN
W.Iskra, M.Müller, I.Rotter
Verhandlungen der Deutschen Physikalischen Gesellschaft, Frühjahrstagung München 1994, Physik der Hadronen und Kerne, p.1812

34. STRUKTUREN IN WIRKUNGSQUERSCHNITTEN - WIDERSPIELUNG DES TRAPPINGS?
E.Sobeslavsky, W.Cassing, F.M.Dittes, W.Iskra, I.Rotter
Verhandlungen der Deutschen Physikalischen Gesellschaft, Frühjahrstagung München 1994, Physik der Hadronen und Kerne, p. 1814

35. THE HOMOLOGY CONCEPT AS A SPECTROSCOPIC TOOL
U.Atzrott, ..., **M.Jaskola, J.Tropilo**
Verhandlungen der Deutschen Physikalischen Gesellschaft, Frühjahrstagung München 1994, Physik der Hadronen und Kerne, p. 1816

36. CLUSTER-FOLDING ANALYSIS OF ^{6}Li+^{26}Mg SCATTERING AT 60 MeV.
K.Rusek et al.
IOP Annual Congress, Brighton 11.04.-14.04.1994, p. 32

37. STUDY OF THE THRESHOLD ANOMALY IN THE SCATTERING OF POLARIZED ^{7}Li FROM ^{208}Pb.
I.Martel-Bravo, ..., **K.Rusek**, et al.
IOP Annual Congress, Brighton 11.04.-14.04.1994, p. 33

38. STUDY OF THE THRESHOLD ANOMALY IN THE SCATTERING OF POLARIZED ^{7}Li FROM ^{208}Pb.
I.Martel-Bravo, ..., **K.Rusek**, et al.
Proc. V International La Rabida Summer School, La Rabida, Spain, July 1994

39. CLUSTER FOLDING STUDY OF POLARIZED ^{7}Li SCATTERING FROM ^{208}Pb
K.Rusek, et al.
"Clusters in Nuclear Structure and Dynamics", Strasbourg, September 1994

40. POLARIZED ^{7}Li STUDIES AT THE NUCLEAR STRUCTURE FACILITY, DARESBURY
R.P.Ward, ..., **K.Rusek**, et al.
Int. Symposium on High Energy Spin Physics and Polarization Phenomena in Nuclear Physics Bloomington, September 1994

41. STUDY OF THE THRESHOLD ANOMALY IN THE SCATTERING OF POLARIZED ^{7}Li FROM ^{208}Pb
I.Martel-Bravo, ..., **K.Rusek**, et al.
Int. Symposium on High Energy Spin Physics and Polarization Phenomena in Nuclear Physics Bloomington, September 1994

42. DOUBLE-FOLDED F.R. DWBA ANALYSIS OF THE ^{90}Zr($\vec{p}$,α)^{87}Y REACTION
U.Atzrott, ..., **M. Jaskola**, et al.
Int. Symposium on High Energy Spin Physics and Polarization Phenomena in Nuc. Phys. Bloomington, September 1994, 214

43. SPECTROSCOPY OF ^{88}Y BY MEANS OF THE ^{91}Zr($\vec{p}$,α)^{88}Y REACTION AT 22 MeV
L.Zetta, ..., **M.Jaskola, J.Tropilo**, et al.
Int. Symposium on High Energy Spin Physics and Polarization Phenomena in Nuc. Phys. Bloomington, September 1994, 216

44. STUDY OF THE ^{206}Bi($\vec{p}$,α)^{206}Pb REACTION AT 22 MeV
L.Zetta, ..., **M.Jaskola**, et al.
Int. Symposium on High Energy Spin Physics and Polarization Phenomena in Nuc. Phys. Bloomington, September 1994, 218

45. SPECTROSCOPY OF ^{87,88}Y BY MEANS OF THE ^{90,91}Zr(p,α)^{87,88}Y REACTIONS AT 22 MeV
U.Atzrott, ..., **M.Jaskola, J.Tropilo**, et al.
LXXX Congressso Nazionale Societa Italiana di Fisica, Lecce, Sept. 26 - Oct. 1 , 1994, p.48

46. ANALYSING POWERS AND CROSS SECTIONS FOR ^{6}Li + ^{12}C SCATTERING AT 50 MeV
P.L.Kerr, ..., **K.Rusek**, et al.
Fall Meeting of the American Physical Society, 266-29 October 1994

47. J DEPENDENCE IN ^{12}C(^{6}Li, ^{3}H)^{15}N AT E(^{6}Li=50 MeV)"
K.W.Kemper, ..., **K.Rusek**, et al.
Fall Meeting of the American Physical Society, 266-29 October 1994

48. COLLECTIVE EXPANSION IN CENTRAL Au + Au COLLISIONS
W.C.Hsi, ..., **B.Zwięgliński**, et al.
MSU National Superconducting Cyclotron Laboratory Annual Report 1993, p. 23-26

49. MULTIFRAGMENTATION IN CENTRAL COLLISIONS
M.B.Tsang, ..., **B.Zwięgliński**, et al.
Proc. of the XXXI International Winter Meeting on Nuclear Physics, Bormio, Italy, January 25-29, 1993 ed. I. Iori, Ricerca Scientifica ed Educazione Permanente, suppl. 96 (1993) 84

50. MULTIFRAGMENTATION IN CENTRAL COLLISIONS
M.B.Tsang, ..., **B.Zwięgliński**, et al.
Proc. of the IX Winter Workshop on Nuclear Dynamics, Key West, Florida, Jan. 30 - Feb. 6, 1993, ed. B.Back, W.Bauer, J.Harris (World Scientific Publishing, 1993), p. 144.

51. FUSION AND DEEP-INELASTIC PROCESSES IN THE COLLISIONS OF ^{14}N WITH LIGHT NUCLEI
O.Yu.Goryunov, A.V.Mokhnach, O.A.Ponkratenko, A.A.Shvedov, E.I.Koschy, Yu.G.Mashkarov, **L.Głowacka, J.Turkiewicz**
Proc. 5th Int. Conf. on Nucleus-Nucleus Collisions, Taormina, Italy, May 30 - June 4, 1994, p.183

52. MULTIPLE N-SHELL IONIZATION INDUCED BY 0.4 - 2.0 MeV/amu C AND N IONS
J.Semaniak, J.Braziewicz, M.Pajek, **T.Czyżewski**, **L.Głowacka**, **M.Jaskóła**, W.Kretschmer, M.Haller, R.Karschnick, D.Trautmann
13th Int. Conf. on the Application of Accelerators in Research & Industry, November 1994, Denton, Texas, USA, PA11

53. M-SHELL X-RAY PRODUCTION BY C AND N IONS
J.Semaniak, J.Braziewicz, M.Pajek, **T.Czyżewski**, **L.Głowacka**, **M.Jaskóła**, W.Kretschmer, M.Haller, R.Karschnick, D.Trautmann
13th Int. Conf. on the Application of Accelerators in Research & Industry, November 1994, Denton, Texas, USA, PA12

54. X-RAY FLUORESCENCE ANALYSIS OF CELTIC GLASSES
J.Braziewicz, J.Semaniak, M.Pajek, **M.Jaskóła**
13th Int. Conf. on the Application of Accelerators in Research & Industry, November 1994, Denton, Texas, USA, PB69

55. STUDY OF ARSENIC EVOLUTION DURING RTA OF Au BASED OHMIC CONTACTS TO GaAs.
A.Piotrowska, ..., **S.Kwiatkowski**
Proc. MRS Spring Meeting, San Francisco, April 1994

56. RAPID THERMAL NITRIDATION OF TUNGSTEN-CAPPED SHALLOW OHMIC CONTACT TO GaAs
E.Kamińska, ..., **S.Kwiatkowski**
Proc. MRS Spring Meeting, San Francisco, April 1994

57. EXCITATION OF A QUANTAL GAS IN Q TIME-DEPENDENT POTENTIAL
J.Błocki, F.Brut, W.J.Świątecki
Acta Phys. Polonica B25 (1994) 637

58. EXCITATION OF QUANTAL AND A CLASSICAL GAS; A TIME-DEPENDENT POTENTAL
J.Błocki, F.Brut, W.J.Świątecki
Lawrence Belkeley Laboratory preprint LBL-36026 (1994)

59. NEUTRON RESONANCE PARAMETERS AND THERMAL-NEUTRON CAPTURE BY ^{43}Ca
M.C.Maxon, J.A.Harvey, S.Raman, J.E.Lynn, **W.Ratyński**
Phys. Rev. C48 (1993) 553

60. TOWARDS THE SOLUTION OF THE NUCLEON SPIN PROBLEM
Z.Moroz
Acta Phys.Polonica B25 (1994) 601

61. EXCITATION FUNCTION FOR ^{178}W PRODUCTION IN THE ^{181}Ta(p,4n)^{178}W REACTION OVER PROTON ENERGY RANGE 28.8-71.8 MeV
N.G.Zaitsewa, **E.Rurarz**, V.A.Khalkin, V.I.Stegailov, and L.M.Popinenkova
Radiochimica Acta 64(1994)1-6

62. PRODUCTION CROSS SECTIONS AND YIELDS OF LONG LIVED ^{44}Ti FROM 100 MeV PROTON BOMBARDMENT OF VANADIUM
N.G.Zaitseva, **E.Rurarz**, M.B.Tchikalov, M.Vobecky, V.A.Khalkin, L.M.Popienkowa
Radiochimica Acta 65(1994)157

63. PRODUCTION OF ^{67}Cu FROM NATURAL AND ENRICHED ZINC SAMPLES USING 14 MeV NEUTRONS
M.Matul, **S.Mikołajewski**, **J.Piętka**, **E.Rurarz**, T.Kempisty
Nukleonika 39(1994)63

64. PROCEEDINGS OF "XXIII MAZURAIAN LAKES SUMMER SCHOOL"
Ed. **Z.Sujkowski**, J.Skalski
Acta Phys. Polonica B vol.25 N° 3 - 4(1994)

65. HARD PHOTON INTENSITY INTERFEROMETRY IN HEAVY ION REACTION
M.Margues, ..., **Z.Sujkowski**, et al.
Phys. Rev. Lett. 73(1994)34

66. THE ANGULAR-MOMENTUM DEPENCENCE OF THE GIANT DIPOLE RESONANCE IN ^{154}Dy
R.F.Noorman, ..., **Z.Sujkowski**, et al.
Nuc. Phys. A574 (1994) 501

67. DI-LEPTON YIELD FROM THE DECAY OF EXCITED ^{28}Si STATES
J.C.Bacelar, **A.Buda**, A.Bałanda,..., **Z.Sujkowski** et al.
Nucl. Phys. A569 (1994) 101c-110c

68. HIGHLY CONVERTED TRANSITIONS IN THE QUASI-CONTINUUM OF ^{143}Eu
M.Palacz, **Z.Sujkowski**, A.Atac, M.Piiparinen, et al.
Nucl. Phys. A578 (1994) 225

69. IMPACT PARAMETER DEPENDENCE OF HARD PHOTON PRODUCTION IN INTERMEDIATE ENERGY HEAVY-ION COLLISIONS
G.Martinez,..., **Z.Sujkowski**, et al.
Phys. Lett. B334 (1994) 23

70. L-SHELL IONIZATION PROBABILITIES IN NEAR CENTRAL HEAVY ION - ATOM COLISIONS
T.Ludziejewski, P.Rymuza, Z.Sujkowski, M.Carlen, J.Cl.Dousse, **J.Hoszowska**, J.Kern, Ch.Rheme
Acta Phys. Pol. B25 (1994) 699

71. M-SHELL IONIZATION RESULTING FROM NEAR-CENTRAL COLLISIONS OF MID-Z ATOMS WITH 5.5 MeV/AMU OXYGEN IONS
M.Carlen, B.Boschung, J.Cl.Dousse, Z.Halabuka, **J.Hoszowska**, J.Kern, Ch.Rheme, M.Polasik, **P.Rymuza, Z.Sujkowski**
Phys. Rev. A49 (1994) 2524

72. X-RAY EMISSION FROM VERY-HEAVY H- AND HE-LIKE IONS IN COLLISIONS WITH GASEOUS AND SOLID TARGETS
Th.Stöhlker, ..., **P.Rymuza** et al.
Nucl. Instr. Meth. B87 (1994) 64

73. CHARGE STATES AND ENERGY LOSS OF RELATIVISTIC HEAVY IONS IN MATTER
C.Scheidenberger, H.Geissel, Th.Stöhlker, H.Folger, H.Irnich, C.Kozhuharov, A.Magel, P.H.Mokler, R.Moshammer, G.Münzenberg, F.Nickel, M.Pfützner, **P.Rymuza**, W.Schwab, J.Ullrich B.Voss
Nucl. Instr. Meth. B90 (1994) 36

74. STRUCTURE OF VERY HEAVY FEW-ELECTRON IONS - NEW RESULTS FROM THE HEAVY ION STORAGE RING, ESR
P.H.Mokler, Th.Stöhlker, C.Kozhuharov, R.Moshammer, **P.Rymuza**, F.Bosch, T.Kandler
Phys. Scripta T51 (1994) 28

75. EXPERIMENTAL N=3 LEVEL LIFETIMES OF NA LIKE HEAVY IONS IN THE REALM OF MASSIVE RELATIVISTIC EFFECTS
E.Träbert, ..., **P.Rymuza** et al.
Phys. Lett. A188 (1994) 355

76. L-SUBSHELL RESOLVED PHOTON ANGULAR DISTRIBUTION OF RADIATIVE ELECTRON CAPTURE INTO HE-LIKE URANIUM
Th. Stöhlker, ..., **P.Rymuza** et al.
Phys. Rev. Lett. 73 (1994) 3520

77. SOME RECENT RESULTS ON NEUTRON DECAY OF ^{208}Pb EXCITED TO ENERGIES IN THE 14 TO 25 MeV RANGE
D.Chmielewska, A.M.van den Berg, Y.Blumenfeld, N.Alamanos, F.Auger, J.Blomgren, et al.
Nucl. Phys. A 569(1994)383c

78. NEUTRON DECAY OF THE EXCITATION-ENERGY REGION UP TO 60 MeV, EXCITED BY HEAVY ION SCATTERING, (I) ^{208}Pb
A.M.van den Berg, **D.Chmielewska**, et al.
Nucl. Phys. A578 (1994) 238

79. NEUTRON DECAY OF THE EXCITATION-ENERGY REGION UP TO 60 MeV, EXCITED BY HEAVY-ION SCATTERING, (II) ^{90}Zr and ^{124}Sn
J.Blomgren, ..., **D.Chmielewska**, et al.
Nucl. Phys. A578 (1994) 267

80. NEUTRON DECAY OF DEEP-HOLE STATES POPULATED BY THE ^{208}Pb (^{3}He,a) ^{207}Pb REACTION AT 202 MeV
P.-O.Soderman, ..., **D.Chmielewska** et al.
Nucl. Phys. A576 (1994) 215

81. LINE WIDTHS OF PHOTO INDUCED L X-RAY OF URANIUM
J.Hoszowska, J.-Cl.Dousse, Ch.Rhëme
Phys. Rev. A50 (1994) 123

82. DESCRIPTION OF NO_x REMOVAL FROM EXHAUST GASES IN E-BEAM PROCESS BY THE LINEAV APPROXIMATION
J.Boużyk, M.Sowiński
SINS Report No 7/II/1994, Otwock-Świerk

83. TIME SCALES OF FUSION-FISSION REACTIONS CALCULATED FROM PRESCISSION NEUTRON MULTIPLICITIES
K.Siwek-Wilczyńska, **J.Wilczyński**, R.H.Siemssen, H.W.Wilschut,
Proceedings of the Fifth International Conf. on Nucleus-Nucleus Collisions, Taormina, Italy, 1994
Nucl. Phys. A (in press)

84. MISSING MOMENTUM VECTOR IN THE ^{197}Au(^{20}Ne; F_1, F_2, PLF) REACTION AT 15 MeV/u
A.Wieloch, J.Brzychczyk, K.Grotowski, H.K.W.Leegte, S.Micek, P.Pawłowski, R.Planeta, R.H.Siemssen, Z.Sosin, H.W.Wilschut, K.Siwek-Wilczyńska, **J.Wilczyński**
Nucl. Phys. A (in press)

85. RADIATIVE ELECTRON CAPTURE STUDIED IN RELATIVISTIC HEAVY-ION ATOM COLLISIONS
Th.Stohlker, C.Kozhuharov, P.H.Mokler, A.Warczak, F.Bosch, H.Geissel, R.Moshammer, C.Scheidenberger, J.Eichler, A.Ichihara, T.Shirai, **P.Rymuza**,
Phys. Rev. A (in press)

86. DOPPLER-SHIFT ASSISTED FAST ION SPECTROSCOPY: A CASE STUDY FOR X-RAY EMISSION FROM 277 MeV/U Pb^{81+} IONS
P.H.Mokler, Th.Stohlker, C.Kozhuharov, R.Moshammer, **P.Rymuza**, Z.Stachura, A.Warczak
J. Phys. B (in press)

87. TIME SCALES OF FUSION-FISSION REACTIONS CALCULATED FROM PRECISSION NEUTRON MULTIPLICITIES[b)]
K.Siwek-Wilczyńska, **J.Wilczyński**, R.H.Siemssen, H.W.Wilschut
Proc. of the Fifth Int. Conf. on nucleus-nucleus Collisions
Taormina, Italy, May 30 - June 4, 1994

88. BREATHING MODE IN FINITE NUCLEI AND THE EQUATION OF STATE OF NUCLEAR MATTER[b)]
Z.Sujkowski
Proc. of the Conf.: New Nuclear Snucture Phenomena in the Vicinity of a Closed Shell, Stockholm-Uppsala, Aug.30-Sep.3, 1994

89. RADIATIVE ELECTRON CAPTURE IN RELATIVISTIC HEAVY-ION ATOM COLLISIONS
Th.Stohlker, ..., **P.Rymuza**, et al.
7th Int. Conf. on the Physics of Highly Charged Ions, Austria, Vienna, Sept. 19 - 23, 1994

90. RESONANT TRANSFER AND EXCITATION INVESTIGATED VIA X-RAY EMISSION IN U^{90+}→C COLLISIONS.
T.Kandler, ..., **P.Rymuza**, et al.
7th Int. Conf. on the Physics of Highly Charged Ions, Austria, Vienna, Sept. 19 - 23, 1994

91. RESONANT TRANSFER EXCITATION DETERMINED VIA X-RAY EMISSION IN U^{90+} →C-COLLISIONS[b)]
T.Kandeler, ..., **P.Rymuza**, et al.
7th Int. Conf. on the Physics of Highly Charged Ions, Austria, Vienna, Sept. 19 - 23, 1994

92. LIFETIME MEASUREMENTS OF THE HIGH-SPIN STATES IN N=106 NUCLEI: ^{183}Ir AND ^{182}Os
R.Kaczarowski, U.Garg, R.Lehmkuhl, S.Naguleswaran, B.Prause, G.Smith, J.C.Walpe
BAPS 39(1994)1419

93. GIANT RESONANCES AND THE COMPRESSIBILITY OF NUCLEAR MATTER[b)]
Z.Sujkowski
7th Int. Conf. on Nuclear Reaction Mechanisms, Italy, Varenna, June 15-20, 1994

94. NEUTRON DECAY OF EXCITED IN $_{208}$Pb IN THE GDR REGION AND ABOVE[b)]
D.Chmielewska
7th Int. Conf. on Nuclear Reaction Mechanisms, Varenna, June15-20, 1994

95. EXCITATION OF QUANTAL AND A CLASSICAL GAS A TIME-DEPENDENT POTENTIAL[b)]
J.Błocki
Proc. of the Fourth KINR International School, Fourth Int. Conf. on Nuclear Physic, Kiev, Aug. 1994

96. A PROTON INTRUDER BAND IN ^{113}In[b)]
S.Naguleswaran, ..., **R.Kaczarowski**
Conf. on Phys. From Large γ-ray Detector Arrays, Berkeley, California, USA, Aug. 2-6,1994

97. LONGITUDINAL AND TRANSVERSE K-SHELL IONIZATION OF TA ATOM IN COLLISIONS WITH REALATIVISTIC NE IONS[b)]
P.Rymuza, et al.
7th Int. Conf. on the Physics of Higly Charged Ions, Vienna, Austria, Sept. 1994

98. GROUND STATE EXCITATION OF H- AND HE-LIKE BI PROJECTILES OBSERVED IN COLLISIONS WITH LOW-Z TARGETS[b)]
Th.Stohlker, ..., **P.Rymuza**, et al.
7th Int. Conf. on the Physics of Highly Charged Ions, Vienna, Austria, Sept. 1994

99. CHARGE STATES AND ENERGY LOSS OF RELATIVISTIC HEAVY IONS IN MATTER[b)]
C.Scheidenberger, ..., **P.Rymuza**, et al.
7th Int. Conf. on the Physics of Highly Charged Ions, Vienna, Austria, Sept. 1994

100. LENBENSDAUERMESSUNGEN AN WENIG-ELEKTRONEN-IONEN SCHWERER ELEMENTE[b)]
E.Trabert, ..., **P.Rymuza**, et al.
15 Arbeitstagung uber Energiereiche Atome Stopen, Riezlem, Austria, Jan. 1994

101. RESONANTER ELEKTRONENEINFANG, GEMESSEN UBER DIE RONTGENEMISSION IN U^{90+} → C-STOSSEN[b)]
T.Kandler, ..., **P.Rymuza**, et al.
15 Arbeitstagung uber Energiereiche Atome Stopen, Riezlem, Austria, Jan. 1994

102. RADIATIVE DECAY OF DOUBLE K-SHELL VACANCIES IN MEDIUM-HEAVY ATOMS IONIZED BY $^{4}HE^{++}$ IONS
B.Boschung, ..., **T.Ludziejewski**, **P.Rymuza**, **Z.Sujkowski**
15 Arbeitstagung uber Energiereiche Atome Stopen, Riezlem, Austria, Jan. 1994

103. IDENTIFICATION OF DIFFERENT REACTION CHANNELS OF HIGH ENERGY NEUTRONS IN LIQUID SCINTILLATORS BY THE PULSE SHAPE DISCRIMINATION METHOD
M.Moszyński, G.J.Costa, et al.
Nucl. Instr. and Meth. A343 (1994) 563

104. PROPERTIES OF YAG SCINTILLATOR
M.Moszyński, T.Ludziejewski, D.Wolski, W.Klamra and L.O.Norlin
Nucl. Instr. and Meth. A345 (1994) 461

105. STUDY OF n-γ DISCRIMINATION WITH NE213 and BC501A LIQUID SCINTILLATORS
M.Moszyński, G.J.Costa, G.Guillaume, B.Heusch, A.Huck and S.Mouatassim
Nucl. Instr. and Meth. A350 (1994) 226

106. THE LIGHT YIELD RESPONSE OF A NE213 SCINTILLATOR TO CHARGED PARTICLES RESULTING FROM NEUTRON INTERACTIONS
S.Mouatassim, G.J.Costa, G.Guillaume, B.Heusch and **M.Moszyński**
Nucl. Instr. and Meth. (in press)

107. ADVANTAGES AND LIMITATIONS OF A LSO SCINTILLATOR IN NUCLEAR PHYSICS EXPERIMENTS
T.Ludziejewski, K.Moszyńska, M.Moszyński, D.Wolski, W.Klamra, L.O.Norlin, E.Devitsin and V.Kozlov
Submitted to IEEE Trans. Nucl, Sci.

108. COMPARISON OF n-γ DISCRIMINATION BY ZERO-CROSSING AND DIGITAL CHARGE COMPARISON METHODS
D.Wolski, M.Moszyński, T.Ludziejewski, A.Johnson, W.Klamra and Oe.Skeppstedt
Nucl. Instr. and Meth. (in press)

109. BALLISTIC DEFICIT CORRECTION METHODS FOR LARGE Ge DETECTORS - HIGH COUNTING RATE STUDY
G.Duchene and **M.Moszyński**
Nucl. Instr. and Meth. (in press)

110. NEUTRON DETECTOR ARRAY FOR EUROBALL
M.Moszyński, D.Wolski
EUROBALL Neutron Detector Subgroup Meeting, Germany, Köln, Aug. 22-28, 1994

111. COMPARISON OF n-γ DISCRIMINATION BY ZERO-CROSSING AND DIGITAL CHARGE COMPARISON METHODS
M.Moszyński, D.Wolski,
EUROBALL User Meeting, France, Starbourg, Sept. 19-23, 1994

112. ADVANTAGES AND LIMITATIONS OF LSO SCINTILLATORS IN NUCLEAR PHYSICS EXPERIMENTS
M.Moszyński, T.Ludziejewski, K.Moszyńska, D.Wolski, W.Klamra, L.O.Norlin, E.Devitsin and V.Kozlov
Nuclear Science Symposium 1994, Norfolk, USA, Oct.30 - Nov.5

113. ARIADNA MONITORING AND CONTROL SYSTEM FOR C-30 CYKLOTRON
Z.Guzik
Conf. "ESONE - Real Time Data 94", Dubna, Russia, June 1994

114. ONE-BIT A/D and D/A CONVERTERS (in Polish)
M.Nadachowski
Radioelektronik Audio-Hi-Fi-Video 1,3(1994)15

115. DIGITAL RESISTANCE METERS (in Polish)
M.Nadachowski
Radioelektronik Audio-Hi-Fi-Video 4(1994)15

116. GAMMA RADIATION - AN ENEMY OR A FRIEND? (in Polish)
M.Nadachowski
Radioelektronik Audio-Hi-Fi-Video 12(1994) supplement 21

117. FLUKE POWER METERS (in Polish)
M.Nadachowski
Radioelektronik Audio-Hi-Fi-Video 11(1994)11

118. MICROPROCESSOR SYSTEM BUS - 8-BIT AND 16-BIT DATA (MULTIBUS I) PART 1: FUNCTIONAL DESCRIPTION WITH ELECTRICAL AND TIMING SPECIFICATION.
T.Jamrógiewicz, M.Kazubek, **R.Trechciński, M.Rybka**
Polish Standard PN-IEC 796-1

119. MICROPROCESSOR SYSTEM BUS - 8-BIT AND 16-BIT DATA (MULTIBUS I) PART 3: MECHANICAL AND PIN DESCRIPTIONS FOR THE EUROCARD WITH PIN AND SOCKET (INDIRECT) CONNECTORS.
T.Jamrógiewicz, M.Kazubek, **R.Trechciński, M.Rybka**
Polish Standard PN-IEC 796-3

120. TERMINOLOGY RELATED TO MICROPROCESSORS
Z.Jędrzejczyk, **R.Trechciński, M.Rybka**
Polish Standard PN-IEC 824

121. AN APPROACH TO EXPERIMENTAL MICRODOSIMETRY AT THE NANOMETER SCALE
S.Pszona and R.Gajewski
Radiation Protection Dosimetry, 52(1994)427

122. ELECTRONIC GUIDE FOR NUCLEAR CROSS-SECTIONS
V.S.Barashenkov, **A.Polański**
Preprint JINR, E-2-94-417, Dubna, 1994

123. GAMMA-RAY BUILDUP FACTORS IN AIR ABOVE A PLANE SOURCE ON AIR-GROUND INTERFACE
K.Wincel
8th International Conference on Radiation Shielding, Arlington, USA, April 24-27, 1994

124. NEUTRON MONITORING IN THE NATURAL ENVIRONMENT
S.Pszona
25th International Symposium Radiation Protection Physics, Dresden, Germany, Sept. 26-30, 1994

125. LOW-LEVEL NEUTRON MONITORING
S.Pszona
Int. Workshop on Advances in Radiation Measurements, Chalk River, Canada, October 2-5, 1994

126. NANODOSIMETRY WITH "JET COUNTER" DEVICE
S.Pszona
CEC Contractors Meeting, Legnaro, Italy, Nov. 2-4, 1994

127. GAS-PUFF TARGET EXPERIMENTS WITH POSEIDON PLASMA-FOCUS FACILITY;
H.Schmidt, **M.Sadowski, L.Jakubowski, E.Skladnik-Sadowska, and J.Stanisławski**
Plasma Phys. and Contr. Fusion 36 (1994) 13-24.

128. ALIGNMENT OF HYDROGEN ATOMS IN E+ AND E- IONISING COLLISION;
M.Gryziński, M.Kowalski
Phys. Lett. A (in press)

129. INVESTIGATION ON THE RESPONSE OF CR-39 AND PM-355 TRACK DETECTORS TO FAST PROTONS IN THE ENERGY RANGE 0.2-4.5.MEV;
M.Sadowski, E.M.Al-Mashhadani, **A.Szydłowski, T.Czyżewski, L.Głowacka, M.Jaskóła**, and A.Wieluński:
Nucl. Inst. and Methods in Phys. Research B86(1994)311-316.

130. MEASUREMENTS OF FUSION-PRODUCED PROTONS WITH MODERN NUCLEAR TRACK DETECTORS;
E.Al-Mashhadani, **M.Sadowski, A.Szydłowski**;
Fizika Plazmy vol. 20, No 2, 1994(169-198)

131. COMPARISON OF RESPONSES OF CR-39 AND PM-355 TRACK DETECTORS TO FAST PROTONS, DEUTERONS, AND HE-IONS WITHIN ENERGY RANGE 0.2-4.5 MeV;
M.Sadowski, E.M.Al-Mashhadani, A.Szydłowski, T.Czyżewski, L.Głowacka, M.Jaskóła, C.Rolfs, M.Wieluński:
Radiation Measurements (in press)

132. PROTECTION CHARACTERISTICS OF VARISTORS MADE OF METAL OXIDES FOR VOLTAGE PULSES WITH STEEP FRONT (in Polish);
A.Jerzykiewicz, **W.Drabik, K.Kocięcka, J.Witkowski**:
Technical Review, No 70(1994)102-106.

133. DEPARTMENT OF THERMONUCLEAR RESEARCH ANNUAL REPORT 1993,
M.Sadowski, and **W.Pawłowicz**
REPORT SINS-2/V, OINTEA, Otwock-Świerk, 1994

134. BIANNUAL REPORT 1992-1993 ON PLASMA RESEARCH AND APPLICATION IN POLAND;
E.Infeld, M.Sadowski
Rep. of Plasma Phys. Section of Phys. Com., Polish Academy of Sciences, CBK, Warsaw, June 1994.

135. PLASMA FACILITIES, MEASURING EQUIPMENT, AND HIGH-VOLTAGE SYSTEMS FOR BASIC RESEARCH AND TECHNOLOGY;
M.Sadowski, W.Pawlowicz
IPJ Report SINS-4/V, OINTEA, Otwock-Świerk, 1994

136. ANNULAR GAS PUFF TARGET EXPERIMENTS WITH POSEIDON PLASMA FOCUS;
H.Schmidt, **L.Jakubowski, M.Sadowski, E.Skladnik-Sadowska, J.Stanisławski, A.Szydłowski**
AIP Conference Proceedings 299 - Dense Z-Pinches, AIP, New York (1994)340-347

137. DIAGNOSTICS OF X-RAY EMISSION FROM PF-TYPE FACILITIES AND ITS TIME CORRELATION WITH PARTICLE PULSES;
M.Sadowski, J.Baranowski, L.Jakubowski, S.Kienle, H.Schmidt, **E.Skladnik-Sadowska, J.Żebrowski**
Proc.21th EPS Conf. Contr. Fusion and Plasma Physics (Montpelier, 1994), Part III, pp. 1320-1323.

138. STUDIES OF X-RAYS, HOT-SPOTS AND E-BEAMS WITH HIGH-CURRENT PF-TYPE DISCHARGES;
L.Jakubowski, M.Sadowski, J.Żebrowski
Proc. Intern. Conf. of Plasma Physics, Foz do Iquacu (Brasil 1994), p.306.

139. TIME-INTEGRATED AND TIME-RESOLVED MEASUREMENTS OF X-RAYS AND CHARGED PARTICLES FROM PF-360 FACILITY
AIP Conference Proceedings 299 - Dense Z-Pinches, (AIP, New York 1994)

140. NONLINEAR ELECTROMAGNETIC PHENOMENA IN HIGH-CURRENT DISCHARGES OF THE PF TYPE (in Polish);
L.Jakubowski, M.Sadowski, J.Żebrowski
Proc. of 3rd National Symposium on "Applications of Electromagnetism in Modern Techniques and Technologies", Łańcut 1994.

141. METHODS OF MEASUREMENTS OF X-RAYS AND FAST ION- AND ELECTRON-STREAMS FROM PLASMA-FOCUS DEVICES IN WHICH OCCUR NUCLEAR FUSION REACTIONS (in Polish)
M.Sadowski
Proc. of 3rd general meeting of Polish Nucleonics Society, Warsaw 1994

142. DIAGNOSTICS OF IONS WITHIN HIGH INTENSITY PLASMA STREAMS;
J.Baranowski, W.Komar, E.Składnik-Sadowska
Proc. 21 EPS Conf. on Controlled Fusion and Plasma Physics, Montpellier 1994

143. MASS- AND ENERGY-MEASUREMENTS OF IONS WITHIN INTENSE PLASMA STREAM (in Polish);
J.Baranowski, E.Składnik-Sadowska
Proc. 3rd General Meeting of Polish Nucleonics Society, Warsaw 1994

144. GRAD_1D PACKAGE OF PROGRAMS FOR MODELLING OF EXTERNAL PLASMA REGIONS IN TOKAMAK (in Polish);
M.Rabiński
Proc. 3rd General Meeting of Polish Nucleonics Society, Warsaw 1994

145. COMPARISON OF RESPONSES OF CR-39 AND PM-355 TRACK DETECTORS TO FAST PROTONS, DEUTERONS, AND HE-IONS WITHIN ENERGY RANGE 0.2-4.5 MeV
M.Sadowski, E.M.Al-Mashhadani, A.Szydłowski, T.Czyżewski, L.Głowacka, M.Jaskóła, C.Rolfs, M.Wieluński
Proc.17th Intern. Conf. on Nuclear Tracks in Solids, p. 153, Dubna, 1994.

146. ROLE OF THE ATOMIC MODEL IN ATOMIC COLLISION THEORY:
M.Gryziński
Invited talk given at XIII th Inter. Conference on "Applications of Accelerators i Research and Industry", Denton, USA, 1994.

147. PRODUCTION RATE AND DECAY LIFETIME MESUREMENTS OF B_s^0 MESONS AT LEP USING D_S AND F MESONS
P.Abreu, R.Gokieli, M.Górski, R.Sosnowski, M.Szczekowski, M.Szeptycka, P.Szymański, P.Zalewski et al.
Z. Phys. C61 (1994) 407

148. INTERFERENCE OF NEUTRAL KAONS IN HADRONIC DECAYS OF Z^0
P.Abreu, R.Gokieli, M.Górski, R.Sosnowski, M.Szczekowski, M.Szeptycka, P.Szymański, P.Zalewski et al.
Phys. Let. B323 (1994) 242

149. STUDY OF HARD SCATTERING PROCESSES IN MULTI HADRON PRODUCTION FROM $\gamma\gamma$ COLLISIONS AT LEP
R.Gokieli, M.Górski, R.Sosnowski, M.Szczekowski, M.Szeptycka, P.Szymański, P.Zalewski
Z. Phys. C62 (1994) 357

150. MEASUREMENT OF THE LINE SHAPE OF THE Z^0 AND DETERMINATION OF THE ELECTROWEAK PARAMETERS FROM ITS HADRONIC AND LEPTONIC DECAYS
P.Abreu, R.Gokieli, M.Górski, R.Sosnowski, M.Szczekowski, M.Szeptycka, P.Szymański, P.Zalewski et al.
Nucl. Phys. B417 (1994) 3

151. IMPROVED MEASUREMENT OF CROSS-SECTIONS AND ASYMETRIES AT THE Z^0 RESONANCE
P.Abreu, R.Gokieli, M.Górski, R.Sosnowski, M.Szczekowski, M.Szeptycka, P.Szymański, P.Zalewski et al.
Nucl. Phys. B418 (1994) 403-430

152. MEASUREMENT OF THE $e^+e^- \rightarrow \gamma\gamma(\gamma)$ CROSS SECTION AT LEP ENERGIES
P.Abreu, R.Gokieli, M.Górski, R.Sosnowski, M.Szczekowski, M.Szeptycka, P.Szymański, P.Zalewski et al.
Phys. Let. B327 (1994) 386

153. SEARCH FOR THE STANDARD MODEL HIGGS BOSON IN Z^0 DECAYS
P.Abreu, R.Gokieli, M.Górski, R.Sosnowski, M.Szczekowski, M.Szeptycka, P.Szymański, P.Zalewski et al.
Nucl. Phys. B421 (1994) 3-40

154. MEASUREMENT OF THE B_0 - ANTI B_0 MIXING PARAMETER IN DELPHI
P.Abreu, R.Gokieli, M.Górski, R.Sosnowski, M.Szczekowski, M.Szeptycka, P.Szymański, P.Zalewski et al.
Phys. Let. B332 (1994) 488

155. INVARIANT MASS DEPENDENCE OF PARTICLE CORRELATIONS IN HADRONIC FINAL STATES FROM THE DECAY OF Z^0
P.Abreu, R.Gokieli, M.Górski, R.Sosnowski, M.Szczekowski, M.Szeptycka, P.Szymański, P.Zalewski et al.
CERN-PPE-94-02, Z. Physik C63 (1994) 17-28

156. A MEASUREMENT OF THE B_s^0 MESON MASS
P.Abreu, **R.Gokieli, M.Górski, R.Sosnowski, M.Szczekowski, M.Szeptycka, P.Szymański, P.Zalewski** et al.
CERN-PPE-94-22, Phys. Let. B324 (1994) 500-508

157. A PRECISION MEASUREMENT OF THE AVERAGE LIFETIME OF B HADRONS
P.Abreu, **R.Gokieli, M.Górski, R.Sosnowski, M.Szczekowski, M.Szeptycka, P.Szymański, P.Zalewski** et al.
CERN-PPE-94-24, Z. Phys. C63 (1994) 3-16

158. CHARGED KAON PRODUCTION IN τ DECAYS AT LEP
P.Abreu, **R.Gokieli, M.Górski, R.Sosnowski, M.Szczekowski, M.Szeptycka, P.Szymański, P.Zalewski** et al.
CERN-PPE-94-88, Phys. Let. B334 (1994) 435-449

159. MEASUREMENT OF TIME DEPENDENT B_d^0 - ANTI - B_d^0 MIXING
P.Abreu, **R.Gokieli, M.Górski, R.Sosnowski, M.Szczekowski, M.Szeptycka, P.Szymański, P.Zalewski** et al.
CERN-PPE-94-132, Phys. Lett. B338 (1994) 409-420

160. ANODE WIRE AGEING IN PROPORTIONAL COUNTERS
A.Algari, **M.Szeptycka**, et al.
Nucl. Instr. Meth. 338 (1994) 348

161. PHOTON MULTIPLICITY MEASUREMENTS IN NUCLEUS-NUCLEUS COLLISIONS AT 200 AGeV
Y.P.Viyogi, **T.Siemiarczuk, G.Stefanek**, et al.
Nucl. Phys. A566 (1994) 623

162. MEASUREMENT OF THE SPIN DEPENDENT STRUCTURE FUNCTION $g_1(x)$ OF THE PROTON
SMC; D.Adams, **J.Nassalski, E.Rondio, A.Sandacz, M.Szleper, W.Wiślicki**, et al.
DAPNIA-94-04, Phys.Lett. B329 (1994) 399

163. COMBINED ANALYSIS OF WORLD DATA ON NUCLEON SPIN STRUCTURE FUNCTIONS
SMC; B.Adeva, **J.Nassalski, E.Rondio, A.Sandacz, M.Szleper, W.Wiślicki**, et al.
CERN-PPE-93-206, Phys. Lett. B320 (1994) 400

164. MEASUREMENT OF THE DEUTERON POLARIZATION IN A LARGE TARGET
SMC; B.Adeva, **J.Nassalski, E.Rondio, A.Sandacz, M.Szleper, W.Wiślicki**, et al.
CERN-PPE-94-54, Submitted to Nucl. Instrum. Methods A343 (1994) 363

165. MEASUREMENT OF THE SPIN DEPENDENT STRUCTURE FUNCTION $g_1(x)$ OF THE DEUTERON
SMC; B.Adeva, **J.Nassalski, E.Rondio, A.Sandacz, M.Szleper, W.Wiślicki**, et al.
CERN-PPE-93-47, Phys. Lett. B302 (1993) 533

166. REEVALUATION OF THE GOTTFRIED SUM
NMC; P.Amaudruz, **J.Nassalski, E.Rondio, A.Sandacz, M.Szleper, W.Wiślicki**, et al.
CERN-PPE/94-32, revised ver. of CERN-PPE-93-117, Rapid Comm. in Phys. Rev. D50 (1994) 1

167. MEASUREMENT OF DEUTERON POLARISATION IN A LARGE TARGET
SMC; B.Adeva, **J.Nassalski, E.Rondio, A.Sandacz, W.Wislicki**, et al.
CERN-PPE/94-34, March 1994, Nucl. Instr. Meth. A349 (1994) 334

168. QUASIELASTIC J/ψ MUOPRODUCTION FROM HYDROGEN, DEUTERIUM, CARBON AND TIN
NMC; M.Arneodo, **J.Nassalski, E.Rondio, A.Sandacz, M.Szleper**, at al.
Phys. Lett. B332 (1994) 195

169. SPIN ASYMMETRY IN MUON-PROTON DEEP INELASTIC SCATTERING ON A TRANSVERSALY - POLARISED TARGET
SMC; B.Adeva, **J.Nassalski, E.Rondio, A.Sandacz, W.Wislicki**, et al.
CERN-PPE/94-116, July 1993, Phys.Lett. B336 (1994) 125

170. EXCLUSIVE ρ^0 AND ϕ MUOPRODUCTION AT LARGE Q^2
NMC; M.Arneodo, **J.Nassalski, E.Rondio, A.Sandacz, M.Szleper**, at al.
CERN-PPE/94-146, September 1994, Nucl. Phys. B429 (1994) 503

171. TOWARDS A RELATIVISTIC TRANSPORT THEORY OF NUCLEAR MATTER
S.Mrówczyński and U.Heinz
Ann. Phys. 229 (1994) 1

172. COLOR COLLECTIVE PHENOMENA AT THE EARLY STAGE OF ULTRARELATIVISTIC HEAVY-ION COLLISIONS
S.Mrówczyński
Phys. Rev. C49 (1994) 2191

173. NONEQUILIBRIUM QUARK-GLUON PLASMA FROM THE INITIAL STAGE OF ULTRARELTIVISTIC HEAVY-ION COLLISIONS
S.Mrówczyński
Nucl. Phys. A566 (1994) 399c.

174. COLOR COLLECTIVE PHENOMENA AT THE EARLY STAGE OF ULTRARELATIVISTIC HEAVY-ION COLLISIONS
S.Mrówczyński
Proc. of Worshop "Pre-Equilibrium Parton Dynamics" Berkeley, 1993, ed. Xin-Nian Wang, LBL-34831, Berkeley, 1994.

175. PROMPT BREAKUP VERSUS SQUENTIAL DECAYS
S.Mrówczyński
Proc. of XXI-st Int. Workshop on Gross Properties of Nuclei and Nuclei Excitations, Hirschegg, ed. H.Feldmeier, Darmstadt, 1994.

176. AN INVESTIGATION OF INTERMITTENCY IN PROTON-GOLD, OXYGEN-GOLD, SULPHUR-GOLD AND SULPHUR-SULPHUR COLLISIONS AT 200 GeV PER NUCLEON
J.Bächler, **H.Białkowska**, et al.
Z. Phys. C61 (1994) 551

177. CHARGED PARTICLE SPECTRA IN CENTRAL S - S COLLISIONS AT 200 GeV PER NUCLEON
J.Bächler, **H.Białkowska**, et al.
Phys. Rev. Letters 72 (1994) 1419

178. STRANGE PARTICLE PRODUCTION IN NUCLEAR COLLISIONS AT 200 GeV PER NUCLEON
J.Bächler, **H.Białkowska**, et al.
Z. Phys. C64 (1994) 195

179. THE NA49 DATA ACQUISITION SYSTEM
T.Alber, **H.Białkowska**, et al.
IEEE Transactions on Nuclear Science 41 (1994) 30

180. TRANSVERS MOMENTUM COMPENSATION IN $\pi^{+}p$ INTERACTIONS AT 250 GeV/c
EHS/NA22 Collaboration;
N.M.Agababyan, **H.Białkowska**, **J.Stepaniak**, et al.
Z. f. Phys. C64 (1994) 381-389

181. TRANSVERSE MOMENTUM DEPENDENCE OF BOSE-EINSTEIN CORRELATIONS IN 200 AGeV/c S + A COLLISIONS
T.Alber, **H.Białkowska**, et al.
Phys. Rev. Letters, (in press)

182. PATTERN COMPARATOR TRIGGER (PACT) FOR THE MUON SYSTEM OF THE CMS EXPERIMENT
Andlinger, **M. Górski**, **M. Szeptycka**, et al.
Nuclear Instr. and Methods, (in press)

183. MEASUREMENT OF THE B^0 - ANTI B^0 MIXING USING THE AVERAGE ELECTRIC CHARGE OF HADRON JETS IN Z^0 DECAYS
P.Abreu, **R.Gokieli**, **M.Górski**, **R.Sosnowski**, **M.Szczekowski**, **M.Szeptycka**, **P.Szymański**, **P.Zalewski** et al.
CERN-PPE-93-220, Phys. Let. B, (in press)

184. RECENT RESULTS OF THE FORWARD RICH IMAGING CHERENKOV DETECTOR OF THE DELPHI EXPERIMENT AT LEP
W.Adam, **R.Gokieli**, **M.Górski**, **R.Sosnowski**, **M.Szczekowski**, **M.Szeptycka**, **P.Szymański**, **P.Zalewski** et al.
IEEE Transactions on Nuclear Science (in press)

185. SEARCH FOR PAIR PRODUCED HEAVY SCALARS IN Z^0 DECAYS
P.Abreu,**R.Gokieli**, **M.Górski**, **R.Sosnowski**, **M.Szczekowski**, **M.Szeptycka**, **P.Szymański**, **P.Zalewski** et al.
CERN-PPE-94-83, Z. Phys. C (in press)

186. PERFORMANCE OF THE HPC CALORIMETER IN DELPHI
A.De Min, **R.Sosnowski**, **M.Szczekowski**, **M.Szeptycka**, **P.Szymański**, et al.
Nucl. Inst. and Meth. (in press)

187. A STUDY OF RADIATIVE MUON PAIR EVENTS AT Z^0 ENERGIES AND LIMITS ON AN ADITIONAL Z' GAUGE BOSON
P.Abreu, **R.Gokieli**, **M.Górski**, **R.Sosnowski**, **M.Szczekowski**, **M.Szeptycka**, **P.Szymański**, **P.Zalewski** et al.
CERN-PPE-94-121, Z. Phys. C, (in press)

188. J/ψ PRODUCTION IN THE HADRONIC DECAYS OF THE Z^0
P.Abreu, **R.Gokieli**, **M.Górski**, **R.Sosnowski**, **M.Szczekowski**, **M.Szeptycka**, **P.Szymański**, **P.Zalewski** et al.
ERN-PPE-099, Phys. Let. C, (in press)

189. MEASUREMENT OF THE γ (B ANTI - B) / γ (HADRON) BRANCING RATIO OF THE Z BY DOUBLE HEMISPHERA TAGGING
P.Abreu, **R.Gokieli**, **M.Górski**, **R.Sosnowski**, **M.Szczekowski**, **M.Szeptycka**, **P.Szymański**, **P.Zalewski** et al.
CERN-PPE-94-131, Aug. 1994, Z. Phys. C, (in press)

190. PRODUCTION CHARACTERISTICS OF K^0 AND LIGHT MESON RESONANCES IN HADRONIC DECAYS OF THE Z^0
P.Abreu, **R.Gokieli**, **M.Górski**, **R.Sosnowski**, **M.Szczekowski**, **M.Szeptycka**, **P.Szymański**, **P.Zalewski** et al.
CERN-PPE-94-130, Aug. 1994, Z. Phys. C, (in press)

191. IS BOUND ${}^4_\Sigma He$ FORMED IN K^- - MESON CAPTURE FROM REST IN LIQUID HELIUM : II
R.H.Dalitz, **A.Deloff**
Nuclear Physics A, (in press)

192. WIGNER FUNCTIONAL APPROACH TO QUANTUM FIELDS DYNAMICS
S. Mrówczyński, B. Mueller
Phys. Rev. (in press)

193. COMPARISON OF ENERGY FLOWS IN DEEP INELASTIC SCATTERING EVENTS WITH AND WITHOUT A LARGE RAPIDITY GAP
ZEUS Collaboration; M.Derrick, **M.Adamus**, et al.
DESY-94-117, July 1994, 17pp Phys. Lett. B338 (1994) 483-496

194. OBSERVATION OF JET PRODUCTION IN DEEP INELASTIC SCATTERING WITH A LARGE RAPIDITY GAP AT HERA
ZEUS Collaboration; M.Derrick, **M.Adamus**, et al.
DESY-94-063, Apr. 1994, 17pp Phys. Lett. B332 (1994) 228-243

195. MEASUREMENT OF TOTAL AND PARTIAL PHOTON PROTON CROSS-SECTIONS AT 180 GeV CENTER OF MASS ENERGY
ZEUS Collaboration; M.Derrick, **M.Adamus**, et al.
DESY-94-032, March 1994, 43pp Z. Phys. C63 (1994) 391-408

196. OBSERVATION OF DIRECT PROCESSES IN PHOTOPRODUCTION AT HERA
ZEUS Collaboration; M.Derrick, **M.Adamus**, et al.
DESY-93-151, Nov. 1993, 43pp Phys. Lett. B322 (1994) 287-300

197. TRANSVERSE MOMENTUM DEPENDENCE OF BOSE-EINSTEIN CORRELATIONS IN 200 GeV A S + A COLLISIONS
R.Morse, **H.Białkowska**, et al.
LBL-36062, VC-414, 1994

198. CASCADES OF NUCLEAR INTERACTIONS IN LIQUID HYDROGEN
A.S.Gaitinov, **W.Wiślicki**, **T.Siemiarczuk**, et al.
JINR-E1-94-201

199. STATUS REPORT ON WA93/WA98
M.M.Aggarwal, **T.Siemiarczuk**, **G.Stefanek**, **L.Tykarski**,
CERN-SPSLC, May 24, 1994

200. OBSERVATION OF TWO ENHANCEMENTS IN M(π^-pp) IN THE REACTION pd $\rightarrow$ π^-ppp AT 1 GeV
A.Deloff, **T.Siemiarczuk**
SINS/VI, 1994

201. CASCADES OF NUCLEAR INTERACTIONS IN LIQUID HYDROGEN
A.Gaitinow, **T.Siemiarczuk**, **W.Wiślicki**,
ZIBJ E1-94-201, 1994

202. THE RESOLUTION OF THE LINEAR SILICON DRIFT DETECTOR STUDIED BY A COMPUTATIONAL MODEL
M.Kozłowski, **T.Siemiarczuk**, **G.Stefanek**, L.Tykarski
CERN/ALICE SIL/94-10, 1994

203. UPPER CROSS SECTION LIMIT FOR DIBARYON PRODUCTION FROM pd $\rightarrow$ npp ACTION AT 1 Gev
A.Kupść
Uppsala University WASA 2/94

204. OBSERVATION OF HARD SCATTERING IN PHOTOPRODUCTION EVENTS WITH A LARGE RAPIDITY GAP AT HERA
ZEUS Collaboration; M.Derrick, **M.Adamus**, et al.
DESY-94-210, Nov. 1994, 14pp.

205. EXTRACTION OF THE GLUON DENSITY OF THE PROTON AT SMALL x
ZEUS Collaboration; M.Derrick, **M.Adamus**, et al.
DESY-94-192, Oct. 1994, 13pp.

206. INCLUSIVE JET DIFFERENTIAL CROSS-SECTIONS IN PHOTOPRODUCTION AT HERA
ZEUS Collaboration; M.Derrick, **M.Adamus**, et al.
DESY-94-176, Oct. 1994, 19pp.

207. SEARCH FOR EXCITED FERMIONS IN ELECTRON-PROTON COLLISIONS AT HERA
ZEUS Collaboration; M.Derrick, **M.Adamus**, et al.
DESY-94-175, Oct. 1994, 45pp.

208. MEASUREMENT OF THE PROTON STRUCTURE FUNCTION F2 FROM THE 1993 HERA DATA
ZEUS Collaboration; M.Derrick, **M.Adamus**, et al.
DESY-94-143, Aug. 1994, 43pp.

209. PHYSICS WITH WASA AND PROMICE
H.Calen, **A.Kupść**, **A.Nawrot**, **J.Stepaniak**, et al.
Physics with GeV Particle Beams, Jülich, Aug. 22-25, 1994, (in press in conference proceedings)

210. SEARCH FOR DIBARYONS IN pd --> npp REACTION AT CELSIUS
A.Kupść
Physics with GeV Particle Beams, Jülich, Aug. 22-25, 1994, (in press in conference proceedings)

211. NEW RESULTS ON THE GOTTFRIED SUM AND $\bar{d} \neq \bar{u}$ IN THE NUCLEON SEA
J.Nassalski
International Symposium on Spin-Isospin Responces and Weak Processes in Hadrons and Nuclei, Osaka, Japan, March 8-10, 1994, (in press in conference proceedings)

212. RESULTS ON THE SPIN DISTRIBUTION OF VALENCE AND SEA QUARKS IN THE NUCLEON
J.Nassalski
27th Int. Conf. on High Energy Phys., Glasgow, July 20-27, 1994, (in press in conference proceedings)

213. POLARIZATION OF VALENCE AND SEA QUARKS IN THE PROTON
W.Wislicki
29th Rencontres de Moriond QCD and Hight Energy Hadronic Inteıactions, Meribel les Allues, March 20-25, 1994, (in press, Editions Frontieres, 1994)

214. EXCLUSIVE ϱ^0 AND ϕ MUOPRODUCTION AT LARGE Q^2
A.Sandacz
Int. Conf. "Heart of the Matter", Blois, France, June 19-25, 1994, (in press in conference proceedings)

215. EXCLUSIVE ϱ^0 AND ϕ MUOPRODUCTION AT LARGE Q^2
A.Sandacz
27th Int. Conf. on High Energy Phys., Glasgow, July 20-27, 1994, (in press in conference proceedings)

216. STRUCTURE FUNCTIONS AND THE GOTTFRIED SUM FROM NMC DATA
E.Rondio
V Conf. on the Intersections of Particle and Nuc. Phys., St Petersburg, Florida, May 31 - June 6, 1994, (in press in conference proceedings)

217. PROMPT BREAKUP VERSUS SQUENTIAL DECAYS
S.Mrówczyński
XXI-st Int. Workshop on Gross Properties of Nuclei and Nuclei Excitations, Hirschegg, 1994, (in press in conf. proceedings)

218. THE SPIN STRUCTURE FUNCTIONS - EXPERIMENT
J.Nassalski
Educational Workshop on Basics of the Hadron Structure, Warsaw, April 24-26, 1994

219. REVIEV OF EXPERIMENTAL DATA ON STRUCTURE FUNCTIONS
E.Rondio
Educational Workshop on Basics of the Hadron Structure, Warsaw, April 24-26, 1994

220. DIFFRACTIVE LEPTOPRODUCTION OF VECTOR MESONS
A.Sandacz
Educational Workshop on Basics of the Hadron Structure, Warsaw, April 24-26, 1994

221. MASS COMPOSITION OF PRIMARY COSMIC RAYS IN THE RANGE 10^{14}-10^{17}eV:
J.Wdowczyk
Journal of Physics G: Nuclear and Particle Physics, 20(1994)1001

222. COSMIC RAYS ANISOTROPIES AT VERY HIGH ENERGIES EXPECTED FOR NEW MODELS OF THE GALACTIC MAGNETIC FIELD
M.Giller, J.L.Osborne, **J.Wdowczyk**, M.Zielińska
J. Phys. G. 20(1994)1649

223. MASS COMPOSITION OF PRIMARY COSMIC RAYS AT ENERGY 10^{14}-10^{16} eV.
HIGH MULTIPLICITY MUON GROUPS OF ENERGY > 0.25 TeV.
A.V.Voevodsky, V.B.Petkov, A.M. Semenov, A.L.Tsyabuk, A.E.Chudakov, **J.Szabelski**
Izviestia RAN, seria fizitcheskaya 58(1994) 127-129

224. HIGH POWER LED PULSER FOR GAIN MONITORING IN A MULTICOUNTER EXPERIMENT
J.Zabierowski
Nucl. Instr. and Meth. A338 (1994) 577-581

225. A MEASUREMENT OF THE PHASE DISTRIBUTION OF THE EXTENSIVE AIR SHOWERS FROM THE DIRECTION OF THE CRAB NEBULA
M.Giller, W.Miller, A.Wozniak, **J.Zabierowski.**
Astroparticle Physics, (in press)

226. THE TRIGGER ELECTRONICS FOR THE ARRAY PART OF THE KASCADE EXTENSIVE AIR SHOWER EXPERIMENT
J.Zabierowski, H.O.Klages, H.Schieler
Nucl. Instr. and Meth. (in press)

227. THE TRIGGER UNIT FOR THE DETECTOR ARRAY OF THE KASCADE EXPERIMENT
J.Zabierowski, H.O.Klages, H.Schieler
KfK Report 5373, June 1994

228. THE WASA AND PROMICE PROJECTS
D.Akimov,...**J.Zabierowski** et al.
TSL Progress Report 1992-1993, pp. 77- 87, Uppsala University, TSL, 1994

229. GALACTIC GAMMA RAYS FROM THE INVERSE COMPTON PROCESS
M.Giller, **J.Wdowczyk**, A.W.Wolfendale, L.Zhang
J. Phys. G, (in press)

230. SPECTRAL CHANGES FOR LOCAL COSMIC RAYS. I. THE PROTON COMPONENT
L.J.Fathooni, M.Giller, **J.Wdowczyk**, A.W.Wolfendale, L.Zhang
J. Phys. G, (in press)

231. APPLICATIONS OF THE FRACTAL METHOD TO INVESTIGATION OF MASS OF THE PRIMARY PARTICLES.
J.Wdowczyk, M.Samorski, J.Kempa
Izv. Akad. Nauk. 58(1994)58, (in Russian)

232. PROPAGATION OF GAMMA RAYS THROUGH THE UNIVERSE
J.Wdowczyk
Vulcano Workshop, May 1994

233. PICTURE OF HIGH ENERGY HADRON-HADRON INTERACTIONS DEDUCED FROM COSMIC RAY OBSERVATIONS
J.Wdowczyk
Inter-regional Cosmic Ray Conference, Moscow, June 1994

234. HIGH MULTIPLICITY MUON GROUPS OF ENERGY > 0.25 TeV.
A.V.Voevodsky, V.B.Petkov, A.M.Semenov, A.L.Tsyabuk, A.E.Chudakov, **J.Szabelski**
Inter-regional Cosmic Ray Conference, Moscow, June 29, 1994

235. PHYSICS WITH WASA AND PROMICE
D.Akimov,... **J.Zabierowski** et al.
International Conference on Physics with GeV - Particle Beams, Juelich, Germany, Aug. 22-25, 1994

236. CAN FRACTAL ANALYSIS HELP TO DISTINGUISH BETWEEN GAMMA AND NUCLEUS INITIATED SHOWERS?
J.Kempa, M.Samorski, **J.Wdowczyk**
Proceedings of the XVI Kazimierz Meeting on Elementary Particle Physics, 1994, 473

237. FRACTAL STUDIES OF PARTICLE DENSITY DISTRIBUTIONS IN EXTENSIVE AIR SHOWERS AND GAMMA-RAY FAMILIES.
A.Dudarewicz, J.Kempa, M.Samorski, **J.Wdowczyk**, A.Woźniak
8-th Int. Symposium on Very High Energy Cosmic-Ray Interactions, Tokyo, July 1994, (in press)

238. MASS COMPOSITION OF PRIMARY COSMIC RAYS IN THE ENERGY RANGE 10^{14} eV -10^{16} eV.
J.Kempa, **J.Wdowczyk**
8-th Int. Symposium on Very High Energy Cosmic-Ray Interactions, Tokyo, July 1994, (in press)

239. ULTRA HIGH ENERGY COSMIC RAYS: A BRIEF STATUS REVIEW.
J.Wdowczyk, A.W.Wolfendale
Institute for Cosmic Ray Research (ICRR), University of Tokyo, January, 1994, 1

240. DETERMINATION OF PRIMARY COSMIC RAY COMPOSITION FROM X-RAY CHAMBER DATA
J.Wdowczyk
XIV European Cosmic Ray Symposium, Balaton Füred, August-September 1994

241. VERIFICATION OF SIMULATED EAS PROPERTIES IN LODZ EAS ARRAY
J.Gawin, **B.Szabelska**, **J.Szabelski**, T.Wibig
XIV European Cosmic Ray Symposium, Balaton Füred, August-September 1994

242. HIGH ENERGY MUON PRODUCTION IN IRON GENERATED EAS FOR SUPERPOSITION AND FRAGMENTATION MODELS
J.N.Capdevielle, **J.Szabelski**
XIV European Cosmic Ray Symposium, Balaton Füred, August-September 1994

243. PHYSICS OF Λ AND Σ HYPERNUCLEI"
J.Dąbrowski
Acta Physica Polonica B25 (1994) 575-587

244. A SIMPLE MICROSCOPIC THEORY OF THE OPTICAL POTENTIAL FOR HEAVY-ION SCATTERING
J.Dąbrowski
Acta Physica Polonica B25 (1994) 659-664

245. ON THE Σ HYPERNUCLEAR STATES
J. Dąbrowski, **J. Rożynek**
Phys. Lett. 323B (1994) 99-102

246. POSSIBLE S.P. NATURE OF THE Σ HYPERNUCLEAR STATES
J.Dąbrowski, **J.Rożynek**
Nucl. Phys. (in press)

247. NUCLEAR MATTER APPROACH TO THE HEAVY-ION OPTICAL POTENTIAL
J.Dąbrowski
Condensed Matter Theories, Vol.9, Ed. J.W.Clark, K.A.Shoaib, A.Sadiq, Nova Science Publish., Commack, NY, 1994, pp. 317-330

248. ON POSSIBLE S.P.NATURE OF THE Σ HYPERNUCLEAR STATES PRODUCED IN THE (K^-, π) REACTION
J.Dąbrowski, J.Rożynek
Izv. V.U.Z. Fizika, (in press)

249. THE RELATIVISTIC MEAN FIELD MODEL OF THE EMC EFFECT
J.Rożynek
in Many Body Physics, World Scientific 1994

250. RECENT THEORETICAL RESULTS ON HALF-LIVES OF DEFORMED SUPERHEAVY NUCLEI
R.Smolańczuk, J.Skalski, A.Sobiczewski,
Proc. Int. Symp. on Nuclear Physics II, Tours (France) 1994, (in press)

251. INVISIBLE RADIOACTIVITY (in polish)
A.Sobiczewski,
Postępy Fizyki, 45 (1994) 497

252. PROPERTIES AND DECAY OF ACTINIDE AND TRANS-ACTINIDE NUCLEI
A.Sobiczewski, R.Smolańczuk, J.Skalski
Proc. Int. Conf. "Actinides-93", Santa Fe, USA, 1993

253. HALF-LIVES PREDICTED FOR ISOTOPES OF HASSIUM
R.Smolańczuk, J.Skalski, A.Sobiczewski
GSI Scientific Report 1993 (Report GSI 94-1, Darmstadt 1994) p.80

254. DISCOVERY OF HEAVIEST ELEMENTS
A.Hrynkiewicz, **A.Sobiczewski**
Postępy Fizyki 45(1994)111

255. ON THE INTERACTION OF SOLITONS WITH FLOATING BODIES
E.Infeld, T.Lenkowska, JMT Thompson FRS
Nonlinear World 1 (1994) 63-71

256. POTENTIAL FUNCTIONS FOR FLOATING BODIES
E.Infeld, JMT Thompson FRS,
J. Technical Phys., 35 (1994) 319-340

257. DECAY OF KADOMTSEV-PETVIASHVILI SOLITONS
E.Infeld, A.Senatorski, A.A.Skorupski
Phys. Rev. Letters, 72(1994)1345-47

258. ON THE INTEGRABILITY OF THE INHOMOGENEOUS HEISENBERG FERROMAGNET MODEL: EXAMINATION OF A NEW TEST
J.Cieśliński, **P.Goldstein**, A.Sym
J. Phys. A: Math. Gen. 27 (1994) 1645-1664

259. VIBRATIONAL COUPLING IN FLOATING BODIES
E.Infeld, JMT Thompson FRS
J. Technical Physics 36,

260. NUMERICAL SIMULATIONS OF KADOMTSEV-PETVIASHVILI SOLITON INTERACTIONS
E.Infeld, A.Senatorski, A.A.Skorupski
Phys. Rev. E, (in press)

261. ISOTHERMIC SURFACES IN E^3 AS SOLITON SURFACES
J.Cieśliński, **P.Goldstein**, A.Sym
Preprint UW IFT/15/94; submitted for publication Phys. Letters A

262. NEUTRON HALO IN HEAVY NUCLEI FROM ANTIPROTON ABSORPTION
P.Lubiński, ... **J.Skalski, R.Smolańczuk, S.Wycech**, D.Hilscher, D.Polster, and H.Rossner, et al.
Phys. Rev. Lett. 73 (1994) 3199

263. SUPERDEFORMED BAND WITH A UNIQUE DECAY PATTERN: POSSIBLE EVIDENCE FOR OCTUPOLE VIBRATION IN ^{190}Hg
B.Crowell, ... **J.Skalski**, et al.
Phys. Lett. B333(1994)320

264. DIPOLE MOMENTS OF VERY DEFORMED NUCLEI
J.Skalski
Phys. Rev. C49(1994)2011

265. OCTUPOLE EXCITATIONS IN LIGHT XENON AND BARIUM NUCLEI
P.H.Heenen, **J.Skalski**, P.Bonche and H.Flocard
Phys. Rev. C50(1994)802

266. EXCITATION OF A QUANTAL AND A CLASSICAL GAS IN A TIME-DEPENDENT POTENTIAL
J.Błocki, F.Brut, **J.Skalski**, W.Świątecki
preprint LBL-36206, to appear in Proc. of KINR Int.Conf. on Nuclear Physics, Kiev, Ukraine, 1994

267. SPONTANEOUS FISSION HALF LIVES OF DEFORMED SUPERHEAVY NUCLEI
R.Smolańczuk, J.Skalski, A.Sobiczewski
preprint GSI-94-77, submitted to Phys. Rev. C

268. HIGH ACCURACY MASS DETERMINATION OF CESIUM AND BARIUM ISOTOPES
H.Stolzenberg, G.Bollen, H.J.Kluge, T.Otto, G.Savard, L.Shweikhard, R.B.Moore, G.Ronleau, J.Szerypo, **Z.Patyk**
Nucl. Phys. A, (in press)

269. SHELL CORRECTION AND STABILITY OF HEAVY AND SUPERHEAVY NUCLEI
P.Rozmej, **R.Smolańczuk, A.Sobiczewski**
Proc. 4th Int. KINR School on Nuclear Physics, Kiev (Ukraine) 1994, (in press)

270. COLLINEAR ASYMPTOTIC DYNAMICS FOR MASSIVE PARTICLES REGGEIZATION AND EIKONALIZATION
J.Boguszyński, H.Dahmen, R.Kretschmer, **L.Łukaszuk, L.Szymanowski**
preprint Univ. of Siegen, SI 94-15, Zeit. f.Physik A, (in press)

271. EFFECTIVE ACTION FOR MULTI-REGGE PROCESSES IN QCD
R.Kirschner, L.Lipatov, **L.Szymanowski**
Nucl. Phys. B425 (1994) 579

272. SYMMETRY PROPERTIES OF THE EFFECTIVE ACTION FOR HIGH-ENERGY QCD
R.Kirschner, L.Lipatov, **L.Szymanowski**
Phys. Rv. D, (in press)

273. HYDRODYNAMICAL BEAM JETS IN HIGH ENERGY HADRONIC COLLISIONS
U.Ornik, R.M.Weiner, **G.Wilk**
Nucl. Phys. A566 (1994) 469c-472c

274. FLUCTUATIONS OF CROSS SECTIONS SEEN IN COSMIC RAY DATA?
G.Wilk, Z.Włodarczyk
Phys. Rev. D50 (1994) 2318-2320

275. FINAL STATE INTERACTIONS IN BOSE-EINSTEIN CORRELATIONS AND SOURCE FUNCTIONS
M.Biyajima, T.Mizoguchi, **G.Wilk**,
SULDP-1994-5; Z. Phys. C, (in press)

276. HADRONIZATION AND INELASTICITIES
F.O.Duraes, F.S.Navarra, **G.Wilk**
IFUSP/P-1103 (1994) preprint; Phys. Rev. D, (in press)

277. BOSE-EINSTEIN CORRELATIONS OF K-MESONS AND THEIR PRODUCTION MECHANISM IN S+ Pb REACTIONS
M.Biyajima, T.Mizoguchi, Y.Nakata, **G.Wilk**,
Prog. Theor. Phys. (in press)

278. A UNIFIED CONFORMAL MODEL FOR FUNDAMENTAL INTERACTIONS WITHOUT DYNAMICAL HIGGS FIELD
M.Pawłowski, R.Rączka,
Foundation of Physics 24(1994)1305

279. CONFORMAL SPACE-TIMES - THE ARENAS OF PHYSICS AND COSMOLOGY
A.O.Barut, P.Budinich, J.Niederle, **R.Rączka**
Foundation of Physics 24, November 1994

280. AN ANALYSIS OF MEAN LIFE TIME OF UNSTABLE ELEMENTARY PARTICLES
J.Bogdanowicz, M.Pindor, **R.Rączka**
Preprint ILAS/EP-3/1994, Trieste, Foundations of Physics 25, No 6, (in press)

281. MASS GENERATION INT HE SM WITHOUT DYNAMICAL HIGGS FIELD
M.Pawłowski, R.Rączka
preprint ILAS 2/94, hep-ph 9403303

282. HIGH ENERGY BEHAVIOUR OF TOTAL CROSS SECTIONS IN WEAK INTERACTIONS
R.Rączka, M.Pindor, C.Wetterich
Z. Phys. C61 (1993) 125

283. PROCEEDINGS OF THE FIRST GERMAN-POLISH SYMPOSIUM "PARTICLE AND FIELDS"
H.D.Doebner, **M.Pawłowski, R.Rączka**
World Scientific, Singapore 1994

284. A NEW EQUATION FOR DIPOLE CHAINS
E.Infeld
Fifth International Conference on Hyperbolic Problems, June 94, Stony Brook , USA

285. AN EQUATION FOR PROTEIN
E.Infeld, H.Zorski
STAMM 94, Lisbona, July 1994

286. AN EQUATION FOR PROTEIN DYNAMICS
E.Infeld, H.Zorski
30th Polish Conference on Mechanics, Zakopane, August 1994

287. A MODEL FOR MAGNETIZED TURBULENT PLASMA IN THE AURORAL ACCELERATION REGION
P.Goldstein, G.Rostoker, J.C.Samson
International Workshop on Space Plasmas, Feb. 28 - March 2, 1994

288. POSSIBLE S.P.NATURE OF THE Σ HYPERNUCLEAR STATES
J.Dąbrowski, J.Rożynek
International Conference on Hypernuclear and Strange Particle Physics, Vancouver, July 4-8, 1994

289. COATING DEPOSITION BY HIGH INTENSITY PULSED ION BEAM EROSION
J.Langner, J.Piekoszewski, C.Pochrybniak, F.Rosatelli, S.Rizzo, **J.Kuciński**, A.Miotello, L.Guzman and L.Moro
Surface Modific. Technologies VII, ed.T.S.Sudarshan, K.Ishizaki, M.Tukata, K.Kamata, The Inst. of Materials, VII 807 (1994)

290. DEPOSITION BY PULSED EROSION OF NICKEL AND ALUMINUM ON COPPER
J.Langner, J.Piekoszewski, C.Pochrybniak, F.Rosatelli, S.Rizzo, J.Kuciński, A.Miotello, L.Guzman and P.Lazzeri
Surface and Coating Technology, 66 (1994) 300

291. STABILITY OF THE PASSIVE STATE OF AL-MO SPUTTER-DEPOSITED GLASSY METALS
M.Janik-Czachor, A.Wołowik, **Z.Werner**
Corrosion Science, Vol. 36 (1994) No 11 pp 1921-1930

292. BREAK-DOWN OF PASSIVITY OF AL-MO GLASSY METALS
M.Janik-Czachor, A.Wołowik, **Z.Werner**
accepted for publication in *Material Science Forum*

293. SURFACE MODIFICATION OF MATERIALS BY PULSED ION BEAMS
J.Piekoszewski, J.Langner, L.Waliś, **Z.Werner, C.Pochrybniak, K.Czaus**, A.Ciurapiński and **J.Białoskórski**
accepted for publication in Nukleonika

294. COMMERCIALLY MANUFACTURED PHOTODIODES IN DETECTION OF LOW-ENERGY X- AND GAMMA-RAY RADIATION
M.Traczyk, M.Słapa
accepted for publication in Nukleonika

295. PULSE IMPLANTING DOPING: THE SINGLE STEP METHOD OF FORMING THE PHOTOVOLTAIC JUNCTIONS
J.Piekoszewski, Z.Werner, C.Pochrybniak, J.Langner, J.Białoskórski, P.Konarski
to be published in Electron Technology

296. SILICON PHOTODIODES RESPONSE TO INTERACTIONS OF X- AND γ-RAY RADIATION WITH THE DIODE BASE
M.Słapa and **M.Traczyk**
to be published in Nuclear Instruments and Methods

297. BREAK-DOWN OF PASSIVITY OF AL-MO GLASSY METALS
M.Janik-Czachor, A.Wołowik, **Z.Werner**
XVIIth International Symposium on Passivity, Clausthal-Zellerfeld, Niemcy, August 22-26, 1994.

298. TECHNOLOGICAL APPLICATION OF THE PULSED PLASMA BEAMS
J.Piekoszewski, J.Langner, Z.Werner, K.Czaus, C.Pochrybniak
I Polish Scientific Conference "Modern Surface Engineering Technologies" Łódź-Spała, September 20-23, 1994.

299. APPLICATION OF THERMOELECTRIC COOLERS IN SEMICONDUCTOR IONIZING RADIATION DETECTORS
M.Słapa, M.Traczyk, W.Czarnacki
Conference Proceedings "Thermoelectricity in Medicine and Engineering" Warsaw, Oct. 12, 1994.

300. MAGNETIC BOTTLE CONFIGURATION TO COAT 1.3 GHZ COPPER CAVITIES WITH A NB SPUTTERED FILM
M.Ferrario, **S.Kulinski**, M.Minestrini, S.Tazzari
Nucl. Instr. and Methods A343 (1994)

301. ANALYSIS OF OPTICAL TRANSITION RADIATION EMITTED BY A 1 MEV ELECTRON BEAM AND ITS POSSIBLE USE AS A DIAGNOSTIC TOOL
M.Castellano, M.Ferario, **S.Kuliński**, M.Minestrini, P.Patteri, F.Tazzioli, L.Catani, L.Gregorini, S.Tazzari
Nuclear Instruments and Methods (in press)

302. THE DOUBLE WINDOW FOR ELECTRON BEAM INJECTION INTO THE FLUE GAS PROCESS VESSEL
A.G.Chmielewski, Z.Zimek, P.Pańta, **W.Drabik**
Radiation Physics and Chemistry (in press)

303. THE APPLICATION OF MONTE CARLO METHOD TO ELECTRON AND PHOTON TRANSPORT
I.Zychor
Report SINS 3/X, 1994 (in Polish)

304. ELECTRON GUN DESIGN FOR HIGH-CURRENT D.C.ELECTRON ACCELERATOR
W.Drabik, R.Kiełsznia, P.Kapla, W.Straś
Report SINS 8/X, 1994 (in Polish)

305. INFLUENCE OF THE BEAM BUNCH LENGTH ON THE HOM POWER DEPOSITION IN THE SC LEP CAVITIES
E.Haebel, **E.Pławski**
CERN LEP2 Note 94-19, October 1994

306. EARLY RESULTS OF BEAM ACCELERATION TESTS IN THE SC LINAC LISA
M.Castellano, **S.Kuliński**
Proc. of EPAC 94 Conference, London, June 1994

307. THE "LILLYPUT" - MOBILE ELECTRON LINEAR ACCELERATOR FOR RADIOGRAPHY AND ITS USE IN TESTING OF CIVIL ENGINEERING OBJECTS
J.Bigolas, S.Kuliński, M.Pachan
Proc. of EPAC 94 Conference, London, June 1994

308. 4kW, 25 keV POWER ELECTRON SOURCE FOR STUDIES OF THERMAL BEAM EFFECTS
J.Bigolas, M.Pachan, E.Pławski, J.Pszona, A.Wysocka,
Proc. of EPAC 94 Conference, London, June 1994

309. UPGRADING PROGRAM OF THE C-30 CYCLOTRON AT ŚWIERK AND ITS USE FOR EXPERIMENTAL PHYSICS
J.Lorkiewicz, J.Wojtkowska, E.Pławski, A.Piotrowski, Z.Preibisz, T.Kozłowski, J.Rondio,
Proc. of EPAC 94 Conference, London, June 1994

310. APPLICATIONS OF THE MONTE CARLO CODE FOR RADIATION TRANSPORT SIMULATION FOR USE IN RADIOTHERAPY
I.Zychor
Proc. of EPAC 94 Conference, London, June 1994

311. DESIGN STUDY ON ECOLOGICAL ACCELERATOR
W.Drabik, A.Jerzykiewicz, K.Kocięcka, J.Witkowski
Proc. of EPAC 94 Conference, London, June 1994

312. FIRST OPERATIONAL EXPERIENCE WITH THE RF SYSTEM OF THE LNS SUPERCONDUCTING CYCLOTRON
C.Pagani..., **J.Sura**, et al.
Proc. of EPAC 94 Conference, London, June 1994

313. TOWARDS THE ACCELERATION OF THE FIRST BEAM BY THE INFN SUPERCONDUCTING CYCLOTRON
L.Calabretta..., **J.Sura**, et al.
Proc. of EPAC 94 Conference, London, June 1994

b. PATENTS

1. "Nitrogen laser electrode system."
W.Nawrot; SINS, P-V
Patent No P-291262

2. "The self-acting control system of gas pressure in switching spark-gaps."
M.Bielik; SINS, P-V
File No PEW-1/94

c. SEMINARS AT OTHER INSTITUTES

Possibility of ^{123}I Production Using Warsaw Cyclotron[a]
E.Rurarz, Jan. 5, Warsaw University

Relation of B(E2, $2^+ \rightarrow 0^+$ Values and E2+ Energies in Even-Even Nuclei from the 50<Z<82 Shell High-spin Stidies of Nuclei around ^{180}Os[b]
R.Kaczarowski, Jan. 19, IKP KFA, Julich, Germany

Doorway States or Gradual Absorption[a]
A. Marcinkowski, Feb. 25, Warsaw University

Approximations of the WKB Type and their Applications[a]
A.A. Skorupski, March 9, Institute of Fundamental Technological Research Warsaw

Photovoltaic Energetics -- Reality or Illusion?[a]
Z.Werner, March 10, IEA Świerk

Soliton dynamics
E. Infeld, March 17, Cosmic Research Centre Warsaw

Galactic Gamma Rays: Studies of CR Electron and Proton Intensities in the Galaxy[a]
J.Szabelski, April 8, Astronomical Observatory of the Jagiellonian University, Cracow

Diffractive Leptoproduction of Vector Mesons[a]
A. Sandacz, April, 8, UW, Warsaw

Polarised Lithium Beams: The Latest Results from NSF[b]
K.Rusek, April 11, Institute Of Physics Conf., Brighton, UK

Physics of Inner Shell Electrons; the Link Between Atomic and Nuclear Physics[a]
Z.Sujkowski, April 18, Warsaw University

Recent Achievements of Hot Plasma Studies[a] ;
M. Sadowski: invited lecture at the IInd General Meeting of Polish Society of Applied Electromagnetism, April 22, Warsaw

K-Shell Ionization in Asymmetric, Relativistic Ion-Atom Collisions[b]
P.Rymuza, April 27, GSI, Darmstadt, Germany

Physics of Polarized Particles in the Future[a]
Z.Moroz, April 29, Warsaw University

Analog-to-digital Converters in Nuclear Spectrometry - State of Art and Future Trends[a]
Z.Kulka, May 13, Warsaw University, Institute of Experimental Physics

Large Q^2 Diffractive Muoproduction of Vector Mesons[b]
A. Sandacz, May 17, INFN, Turyn, Italy

Neutron monitoring according to ICRP-60
S.Pszona, May 19, Seminar SOPP PTFM, Warsaw

Giant Resonances and the Compressibility of Nuclear Matter[b]
Z.Sujkowski, May 31, Rudjer Boskovic Institute, Zagreb, Croatia

Deuteron Brek-Up and Search for Dibarion in WASA Experiment[a]
A. Kupść, May, UW, Warsaw

Final State Interactions of Low Energy Eta and Pi Mesons
S.Wycech, May 20, CELSIUS Workshop, Uppsala

Some solution of Schrödinger Equation
J.Bogdanowicz, June 7, Joint Institute for Nuclear Research, Dubna, Russia

Plasma-Focus Studies within Stuttgart-Świerk Collaboration and New Trends of Plasma Reesearch in Świerk;
M. Sadowski: Invited talk at the Plasma Seminar, June 15, Institut fuer Plasmaforschung in the University of Stuttgart,

Interaction of Cosmic Ray and Cosmic Gamma Rays with Radiation Fields in the Space[b]
J.Wdowczyk, June 16, KfK Karlsruhe, Germany

Electron Accelerator for Purification of Flue Gases from SO_2 i NO_x[a]
W.Drabik, June 21, Ministry of Industry and Trade, Warsaw

Compton Gamma Ray Observatory (CGRO) and the Ratio of Electron and Proton Fluxes in the Galaxy[c]
J.Szabelski, July 12, Baksan Neutrino Observatory RAN, Russia

Applications of the Monte Carlo Code for Radiation Transport Simulation for Use in Radiotherapy[b]
I.Zychor, Aug.17, Institut für Kernphysik, Jülich, Germany

Graudal Absorption a Phenomenon Accompanying Multistep Direct Reactions[b]
A. Marcinkowski, August 26, Oxford University, UK

Measurement and Monitoring System of the Flue Gases[a]
M.Sowiński, Symposium, Aug. 27-29, Bielsko-Biała, Poland

Nuclear Interaction with Polarized $^{6,7}Li$[b]
K.Rusek, Sept. 2, Philipps Universitaet, Marburg, Germany

Exclusive ϱ^0 and ϕ Muoproduction at Large Q2[b)]
A. Sandacz, Sept. 9, Meeting of the Collaboration E665, Cracow

NMC Results on Structure Functions[b)] (new data)
E. Rondio, Sept. 9, Meeting of the Collaboration E665, Cracow

Ion Beam Microanalysis of Surface Layers[a)]
A. Turos, Sept. 15, ITME, Warsaw

Technological Applications of the Pulse Plasma Streams[a)];
Z. Werner: a talk at 1st National Scientific Conference on "Modern Technologies in Surface Engineering", Sept. 20, Łódź-Spała

Pulse-Shape Analysis of Signals from the Proportional Counters[b)]
A. Trzciński, Sept. 25-28, ALADIN Collaboration Workshop, Rathen/Dresden, Germany

A Project of the Beam-Counter with the Superior Position Resolution for the ALADIN facility at GSI[b)]
B. Zwięgliński, Sept. 25-28, ALADIN Collaboration Workshop, Rathen/Dresden, Germany

Facility for Routine Tests of High-Voltage Electroenergetic Equipment[a)] ;
K.Kocięcka-Mechanisz: a talk at the exposition on "Modern Techniques in Energetics", Sept. 27, Bielsko-Biała,

Electron accelerator for Purification of Flue Gases from SO_2 and NO_x[a)]
W.Drabik, Establishment of Information, Automatization and Professional Advancement, Sept. 28, Bielsko-Biała

New Proposals for the Location of the International Institute for Dense Magnetised Plasmas in Poland[b)]
M.Sadowski: Invited talk at the 1st Technical Sesion of the Steering Committee for ICDMP, Oct. 11, Magurele n. Bucarest

On Applications of Pulsed Plasma-Ion Beams for Modification of Solid State Surfaces[a)] ;
J. Langner: a talk at the General Plasma Seminar, Oct. 18, Warsaw

Ion Beam Interactions with Solids[a)]
A. Turos, Oct. 19, UNIPRESS, Warsaw

What's New in Semiconductor Detectors[a)]
W.Czarnacki, Oct. 21, Warsaw University

Report from the 27th International Conference on High Ecnergy Physics in Glasgow[a)], part I
R. Sosnowski, Oct., Warsaw University

Report from the International Conference on High Energy Physics in Glasgow[a)], part II
"Quantum Chromodynamics and Jet Physics"[a)]
M. Szczekowski, Oct., Warsaw University

Highest Energy Particles Observed in Nature[a)]
J.Wdowczyk, Oct., CAMK, Warsaw

Antiprotonic Molecules
S.Wycech, Nov. 8, Helsinki University, Finland

Diffractive Leptoproducion of Vector Mesons in Deep Inelastic Scattering[a)]
A. Sandacz, Nov. 9, IFJ, Cracow

Measurements at the Nucleon Spin Structure[a)]
E. Rondio, Nov. 10, IFT, Warsaw

Retrospective Look at the Beginnings of Atomic Physics[b)];
M. Gryziński: invited talk at the Seminar, Nov. 11, Physics Dept. of the Texas Christian University, Denton, USA

Generation of High Power Ion Beams and Technlogical Applications [b)]
M. Gryziński: invited talk at the Seminar, Nov. 15, Aeronautics Dept. of the Southern California University, Los Angeles

Diamagnetism of Matter and Structure of the Atom [b)];
M. Gryziński: invited talk at the Seminar, Nov. 18, Chemics Dept. of the Southern California University, Los Angeles,

Dynamical Model of the Molecular Bond [b)]
M.Gryzński: invited talk at Seminar, Nov. 21, Dept. of Chemistry of the Southern California University, Los Angeles,

Parton Distributions in the Nucleon as Determined from NMC Experiment data [a)]
E. Rondio, Nov. 23, IFJ, Cracow

Results on the Spin Dependent Structure Functions from the SMC[b)]
J.Nassalski, Nov. 27, Rutherford Appleton Laboratory, Chiltun, England

ibid.
J.Nassalski, Nov. 28, Nuclear Physics Laboratory, University of Oxford, England

ibid.
J.Nassalski, Nov. 29, University of Birmingham, England

Diffractive Muoproduction of Vector Mesons in Deep Inelastic Scattering[b]
A. Sandacz, Nov. 29, Hamburg, DESY

H-and He-like Ions of High Z Elements[a]
P.Rymuza, Nov. 30, Warsaw University

Higgs Free Model for Fundamental Interactions
R.Rączka, Nov. Warsaw University

Compressibility of Nuclear Matter in the Light of Nuclear and Astrophysical Data[a]
Z.Sujkowski, Dec. 2, Warsaw University

Development and Present Status of High-Temperature Plasma Studies in Poland[b];
M. Sadowski: Invited talk at the Plasma seminar, Dec. 5, Nuclear Fusion Institute in the Russian Scientific center "Kurchatov Institute", Moscow

Recent Results of Plasma Research at the Soltan Institute in Świerk;
M. Sadowski: invited talk at the Plasma Seminar, Dec. 6, Inst. of Spectr. of the Russian Academy of Sciences, Troick n. Moscow,

Influence of Characteristics of Two-Gap Triggered Spark-Gap on Course of Discharge within Circuits of Pulse Generators[a];
K.Kocięcka-Mechanisz: a talk at the Ph.D. defense, Dec. 21, Inst. of High Power and High Voltages, Warsaw Tech. University

Microscopic Calculations of Nuclear Masses: from Liquid-Drop Model tO Hartree-Fock-Bogolubov Approach
Z.Patyk, *Lectures series GSI-Darmstadt, Dec., Germany*

a) in Polish
b) in English
c) in Russian

d. SEMINARS AT SINS

Gamma Rays from Active Galactic Nuclei: Observations and Theory[a]
W.Bednarek, Jan. 6, SINS Łódź

Polarized ^{6}Li Beams: the Latest Results Obtained at NSF Daresbury, Part I[a]
K.Rusek, Jan. 11, SINS Warsaw

TeV Emission from Close Binaries[c]
V.Moskalenko, Institute of Nuclear Physics Moscow SU, Russia, Jan. 13, SINS Łódź

Polarized ^{6}Li Beams: the Latest Results Obtained at NSF Daresbury, Part II[a]
K.Rusek, Jan. 25, SINS Warsaw

DESY - Present and Future
H.Wiik, DESY Hamburg FRG, Jan. 26, General Seminar, SINS Świerk

Structure of ^{88}Y States Excited in the ^{91}Zr(p,α)^{88}Y Reaction[a]
J. Tropilo, Feb. 8, SINS Warsaw

Neutron of natural background[a]
S.Pszona, Feb. 16, SINS Świerk

Plans of Development of Baksan Array for EAS and Muon Groups Studies[c]
A.Siemionov, Institute of Nuclear Research of the RAS Moscow, Russia, Feb. 17, SINS Łódź

Progress in Thermonuclear Research [a]
M. Sadowski, Feb. 21, General Seminar, SINS Świerk

Trapped Resonance States and Cross Section Correlations[a]
W. Iskra, Feb. 22, SINS Warsaw

Multiplicity in pA and AA Collisions. Excess K and Λ Production[a]
J.L.Kacperski, March 3, SINS Łódź

Study of (n,α) Reactions Induced by Fast Neutron on $40 \leq A \leq 109$ Targets[a]
U. Garuska, March 8, SINS Warsaw

Diffractive Processes in Hadron Interactions[a]
D.Sobczynska, March 10, SINS Łódź

Atomic Phenomena Accompanying Relativistic Heavy Ions - Atom Collisions[a]
P.Rymuza, March 17, SINS Świerk

Halo. Method of Studies and Intensity Observed in PAMIR Experiment[a]
M.Pluta, March 17, SINS Łódź

Standard Model of Elementary Constituents of Matter and Forces
R.Sosnowski, March 21, general Seminar SINS Świerk

Study of (n,p) Reactions - Experimental Set-Up[a)]
J. Rondio, March 22, SINS Warsaw

Magnetic Spectrometer "Anomalon" - Studies of Relativistic Nuclei Fragmentation[a)]
T.Dzikowski, April 7, SINS Łódź

Gamma-ray Emission in Heavy Ion Collisions with Nuclei
M.Kicińska-Habior, Institute of Experimental Physics Warsaw University, April 11, General Seminar SINS Świerk

High Energy Photons from Open Clusters[b)]
F.Giovannelli, Instituto di Astrofisica Spaziale CNR, Italy, April 14, SINS Łódź

Inelasticity in Proton - Nucleus Interactions at Relatively Low Energy[a)]
T.Wibig, April 21, SINS Łódź

Experimental Set-Up for Precise Determination of Emission Angles of Pions from (He^3,t) Reactions[a)]
W. Augustyniak, April 26, SINS Warsaw

High energy particle interactions with shielding materials[a]
A.Polański, April 27, SINS Świerk

Origin of CR of Energy above 10^{14}eV[a)]
T.Pytlos, April 28, SINS Łódź

High Energy Physics with Cosmic Ray Experiments. Experiments on EAS Using Timing and Tracking Arrays[b)]
G.D'Ali, O.Catalano, Instituto di Fisica Cosmica e Applicazioni dell'Informatica CNR, Italy, May 9, SINS Łódź

Study of Fundamental Symmetries with Use of Polarized Beams[a)]
Z. Moroz, May 10, SINS Warsaw

"The qyasi-deuteron model: 1950-1994"
J.Levinger, Rensselaer Polytechnic Institute, Troya, N.Y. May 12, SINS, Warsaw

NASA Compton Gamma Ray Observatory - Galactic Gamma Ray Background[a)]
J.Szabelski, May 19, Sins Łódź

New Ideas in Atomic Energy
J.Bartke, Institute of Nuclear Physics, Kraków, May 23, General Seminar SINS Świerk

The Use of Magnetic Spectrometer ALADIN in Measurements of Multifragmentation of Relativistic Heavy Ions[a)]
A. Trzciński, May 24, SINS Warsaw

Atmospheric Cherenkov Detector[c)]
P.A.Antonow, Institute of Nuclear Physics, Moscow, Russia, May 26, SINS Łódź

Study of Fundamental Symmetries by Means of a Polarized Beam[a)]
Z.Moroz, May, SINS Warsaw

Measurements of Fragmentation Cross-Sections of ^{12}C and ^{16}O in Hydrogen - Analysis of Experimental Results[a)]
A.Korejwo, June 9, SINS Łódź

New Results on Multifragmentation of Relativistic Heavy Ions Obtained within the ALADIN Project[a)]
B. Zwięgliński, June 14, SINS Warsaw

Nuclear Reactions without Parameters[b)]
H. Kalka, FZ Rossendorf, RFN, Sept. 20, SINS Warsaw

Minimization of Leakage Saturation Current in Silicon Homojunctions
J.Piekoszewski, Sept. 20, SINS Świerk

Advances in X-ray Spectrometry -- Literature Survey
W.M.Szymczyk, Oct. 4, SINS Świerk

The Physics of Quasars[a)]
L.Biermann, Oct. 6, SINS Łódź

Clusters in Nuclei; Conference CLUSTER'94 in Strasbourg[a)]
K.Rusek, Oct. 11, SINS Warsaw

Development of Elektromagnetic Cascade in the Earth Magnetic Field[a)]
Sz.Karakula, Oct. 13, SINS Łódź

Order, Chaos and Atomic Nucleus[a)]
J.Błocki, Oct. 17, General Seminar SINS Świerk

Influence of Magnetic Field Inhomogeneities in Galactic Halo on the CR Energy Spectrum[a]
W.Tkaczyk, Oct. 20, SINS Łódź

Homologous States Excited in (p,α) Reactions[a]
J. Tropiło, Oct. 25, SINS Warsaw

Highest Energy Cosmic Rays[a]
J.Wdowczyk, Oct. 27, SINS Łódź

Silicon Strip Detectors Used in Experiments at CERN[a]
A. Czermak, IFJ Kraków, Nov. 8, SINS Warsaw

Phase Analysis of EAS from Direction of the Crab Nebula[a]
M.Giller, Nov. 10, SINS Łódź

The Possibilities of Neutronography
A.Czachor, Institute of Atomic Energy, Świerk, Nov. 14, General Seminar SINS Świerk

What's New in Physics of Relativistic Nuclei[a]
J.Bartke, Nov. 17, SINS Łódź

Multifragmentation in Pheripheral HI Collisions and the Search for Liquid-Gas Phase Transitions in Nuclear Matter[b]
U. Lynen, GSI Darmstadt, Germany, Nov. 22, SINS Warsaw

"On Σ hypernuclei"
T.Petridou, Aristotle University of Thessaloniki, Nov. 24, SINS Warsaw

Number of Collisions of High Energy Nucleon with Nucleous of the Target Nucleus[a]
J.Sroka, Nov. 24, SINS Łódź

Super-conducting cavities in accelerators. State of the art, outlook to the future "TESLA"
D.Proch, DESY Hamburg FRG, Nov. 28, General Seminar SINS Świerk

Hadron Interactions above 10^{14}eV Registered in X-Ray Emulsion Chambers[a]
J.L.Kacperski, Dec. 1, SINS Łódź

Variation of Cosmic Rays[c]
L.KH.Shatashvili, Intitute of Physics, Georgian AN, Dec. 8, SINS Łódź

Properties of so called "Narrow Showers"[c]
S.Cherniayev, Institute for Nuclear Research of the RAS Moscow, Russia, Dec. 15, SINS Łódź

Present and Future of the Nuclear Studies in Byelorussia
N. Shumeiko, High Energy Physics Centre Minsk, Byelorussia, Dec. 15, General Seminar SINS Świerk

Review of High Energy Particles in Super Families with Σ E$\gamma \geq 400$ TeV (PAMIR Experiment)[c]
V.S.Puczkov, Dec. 22, SINS Łódź

a) in Polish
b) in English
c) in Russian

e. LIST OF RESEARCH PROJECT (GRANTS) REALIZED BY SINS IN 1994

1. STUDY OF INNER SHELL IONIZATION IN COLLISIONS WITH HEAVY IONS
Principal Investigator: **Professor Z.Sujkowski** PhD, DSc
Grant Nr 2 0964 91 01
2. COMPUTER MEASURMENT, MONITORING AND CONTROL SYSTEM FOR FLUE GASES IRRADIATION INSTALLATION
Principal Investigator: **Assoc. Professor: S.Sowiński** PhD
Grant Nr 2 0985 91 01
3. INVESTIGATION OF PRIMARY MASS COMPOSITION AND INTERACTION OF COSMIC RAYS AT ENERGIES 10^{14} 10^{17} eV
Principal Investigator: **Professor J.Wdowczyk** PhD, DSc
Grant Nr 2 0962 91 01
4. NUCLEAR MATTER THEORY
Principal Investigator: **Professor J.Dąbrowski** PhD
Grant Nr 2 0956 91 01
5. RELATIVISTIC TRANSPORT EQUATION
Principal Investigator: **Asst.Professor S.Mrówczyński** PhD DSc
Grant Nr 2 0960 91 01
6. COLLISIONS OF RELATIVISTIC IONS - STUDY OF NUCLEAR MATTER UNDER EXTREME CONDITIONS
Principal Investigator: **Professor T.Siemiarczuk** PhD DSc
Grant Nr 2 0959 91 01
7. PARTICIPATION IN THE DELPHI EXPERIMENTAL
Principal Investigator: **Professor R.Sosnowski** PhD DSc
Grant Nr 2 0963 91 01
8. PERSONAL SILICON DESORATE METER
Principal Investigator: **Assoc.Professor M.Słapa** PhD DSc
Grant Nr 2 0953 91 01
9. CURRENT PROGRESS IN STUDY AND EXPERIMENTAL RESEARCH FOR THE PROJECT OF HIGH - POWER ELECTRON ACCELERATOR ECO/800/200 KW FOR FLUE - GAS TREATMENT
Principal Investigator: **MSc W. Drabik**
Grant Nr 2 0985 91 01
10. THEORETICAL INVESTIGATIONS OF INSTABLE NUCLEI
Principal Investigator: **Professor A.Sobiczewski** PhD DSc
Grant Nr 2 0954 91 01
11. INVESTIGATION ON SURFACE MELTING OF SELECTED MATERIALS BY MEANS OF A PLASMA STREAM FROM A PLASMA GUN
Principal Investigator: **Asst.Professor J.Appelt** PhD
Grant Nr 2 0970 91 01
12. HIGH LET RADIATION COMPONENT IN NATURAL RADIATION ENVIRONMENT
Principal Investigator: **Asst.Professor S.Pszona** PhD
Grant Nr 2 0951 91 01
13. INVESTIGATION OF NUCLEUS STRUCTURE BY 30 MeV PROTONS
Principal Investigator: **Asst.Professor Z.Preibisz** PhD
Grant Nr 2 0966 91 01
14. ORDER, CHAOS AND THE ATOMIC NUCLEUS
Principal Investigator **Asst.Professor J.Błocki** PhD, DSc
Grant Nr 2 0965 91 01
15. THEORETICAL INVESTIGATION OF WAVES AND INSTABILITIES IN PLASMAS
Principal Investigator: **Professor E.Infeld** PhD DSc
Grant Nr 2 2303 91 01
16. INVESTIGATION OF NON-EQUILIBRIUM EMISSION OF NUCLEONS AND COMPLEX PARTICLES IN FUSION- LIKE REACTIONS WITH HEAVY IONS
Principal Investigator: **Professor J.Wilczyński** PhD, DSc
Grant Nr 2 P302 211 04
17. EXOTIC ATOMS
Principal Investigator: **Professor S.Wycech** PhD, DSc
Grant Nr 2 P302 140 04
18. STUDIES OF THE Δ- RESONANCE EXCITED ON NUCLEONS OF ATOMIC NUCLEI BY THE (^{3}He,t) REACTION USING THE SATURN ACCELERATOR IN SACLAY
Principal Investigator: **Assoc.Professor P.Żuprański** PhD, DSc
Grant Nr 2 P302 04604
19. PHOTON FIELD ANALYSIS FOR AIR MONITORING OF A CONTAMINATED AREA
Principal Investigator: **MSc K.Wincel**
Grant Nr 0 S001 013 04
20. USE OF METALIC PLASMA PULSES FOR THE FORMATION OF THIN LAYERS UNDER THE CONDITIONS OF SURFACE MELTING OF THE SUBSTRATUM
Principal Investigator: **Asst.Professor J.Langner** PhD
Grant Nr 7 S201 043 05

21. STUDY OF NEW SCINTILLATING DETECTORS AND DETECTION METHODS OF NUCLEAR RADIATION
Principal Investigator: Professor M.Moszyński PhD, DSc
Grant Nr 2P 302 096 07
22. INTERACTIONS OF HIGH ENERGY PARTICLES AND IONS WITH ATOMS OF HEAVY ELEMENTS
Principal Investigator: Professor Z.Sujkowski PhD, DSc
Grant Nr 2P 302 119 07
23. THE DESIGN OF NEW-TYPE MULTICHANNEL CERENKOV DETECTORS TO ANALYSE ELECTRON FLUX FROM HIGH-TEMPERATURE PLASMA
Principal Investigator: Asst.Professor L.Jakubowski PhD
Grant Nr 2P 302 058 06
24. DETERMINATION OF THE PRIMARY COSMIC-RAY COMPOSITION ON THE BASIS OF INVESTIGATION OF THE GAMMA-RAY FACILITIES DATA
Principal Investigator: Professor J.Wdowczyk PhD, DSc
Grant Nr 2P 302 061 06
25. OPERATION AND IMPROVEMENT OF THE C-30 CYCLOTRON OF THE SOLTAN INSTITUTE FOR NUCLEAR STUDIES
Principal Investigator: Asst.Professor J.Wojtkowska PhD
Grant (SPUB) Nr 621/E-78/SPUB/P3/211/94
26. PARTICIPATION IN THE DELPHI EXPERIMENT
Principal Investigator: Professor R.Sosnowski PhD, DsC
Grant (SPUB) Nr 621/E-78/SPUB/P3/210/94
27. MEASUREMENTS OF THE NUCLEAR STRUCTURE FUNCTIONS g_1,F_2 AND R IN NMC AND SMC EXPERIMENTS
Principal Investigator: Professor J.Nassalski PhD, DSc
Grant (SPUB) Nr 621/E-78/SPUB/P3/209/94

f. LIST OF RESEARCH PROJECTS GRANTED BY INTERNATIONAL ORGANIZATIONS

1. ORDER, CHAOS AND THE ATOMIC NUCLEUS
Principal Investigator: Asst. Professor J.Błocki PhD, DSc
Maria Skłodowska-Curie Joint Fund II (USA-PL)
Grant Nr PAA/NSF-91-68
2. EXOTIC SHAPES OF NUCLEI
Principal Investigator: Assoc.Professor R.Kaczarowski PhD, DSc
Maria Skłodowska-Curie Joint Fund II (USA-PL)
Grant Nr PAA/DOE-93-153
3. GAUGE THEORIES, QUANTUM GROUPS AND GRAVITY
Principal Investigator: Professor R.Rączka PhD, DSc
Commission of the European Communities, Department of Science and Technology DG XII
Grant Nr CIPA 3510-CJ-92-3006
4. INTERACTION OF HEAVY IONS WITH LIGHT TARGET ATOMS OF CR-39 POLYCARBONATE
Principal Investigator: Asst.Professor A.Wysocka MSc
Commission of the European Communities, Department of Science and Technology DG XII
Grant Nr ERB 3510 PL 921462
5. TRANSEUROPEAN MOBILITY PROGRAMME FOR UNIVERSITY STUDENTS (TEMPUS)
Chiefs: Assoc.Professor J.Stepaniak PhD, DSc, Asst.Professor M.Pachan MSc
Contract Nr JEP-4329-92/1
6. COHERENT AND CHAOTIC PROPERTIES OF MULTIPARTICLE PRODUCTION PROCESSES IN THE INTERACTING GLUON MODEL
Principal Investigator: Assoc.Professor G.Wilk PhD, DSc
Commission of the European Communities, Department of Science and Technology DG XII
Grant Nr ERB 510 PL 923898
7. PROPERTIES OF NUCLEUS-NUCLEUS INTERACTIONS AT 10^{16}eV/u
Principal Investigator: Asst.Professor J.Szabelski PhD
Commission of the European Communities, Department of Science and Technology Grant Nr ERB35 PI 92205
8. COSMIC RAY INTENSITY IN THE GALAXY FROM STUDIES OF RELATIVE CONTRIBUTION OF ELECTRONS AND PROTONS TO GAMMA RAY EMISSIVITY
Principal Investigator: Asst.Professor J.Szabelski PhD
NASA Compton Gamma Ray Observatory
Grant Nr GRO-93-248
9. SPECIFICATION OF RADIATION QUALITY AT NANOMETER SCALE
Principal Investigator: Asst.Professor S.Pszona PhD
Grant Nr ERB CI PDCT 930407; ERB F13 PCT 920041
10. ANALYSIS OF FUNDAMENTAL PROBLEMS OF QUANTUM GAUGE FIELD THEORY AND CLASSICAL AND QUANTUM GRAVITY
Principal Investigator: Professor R.Rączka PhD, DSc
Polish-German Foundation Grant Nr 984/94/LN

VII. PhD and DSc THESES

a. PhD Theses

1. **Antoni BUDA** "Dilepton decay of Giant Resonances built on excited nuclear states."
Supervisors: Professor A. van der Woude, Professor Ziemowid Sujkowski
Rijksuniversiteit Groningen, February 25, 1994, Groningen, Holland

2. **Emad A.Al MASHHADANI** "Studies of nuclear fusion reactions products in PF-360 Facility."
Supervisor: Professor Marek Sadowski
SINS March 22, 1994

3. **Andrzej KUPŚĆ** "Study of pd → npp reaction in WASA eksperiment."
Supervisor: Assoc. Professor Joanna Stepaniak
SINS June 21, 1994

4. **Cezary POCHRYBNIAK** "Formation of the photovoltaic structures $p^{+}-n-n^{+}$ and $n^{+}-p-p^{+}$ on the single crystalline silicon wafers using Pulse Implantation Dopping method."
Supervisor: Professor Jerzy Piekoszewski
SINS September 20, 1994

5. **Piotr ZALEWSKI** "Study of the beauty baryons using lepton-proton correlations in the DELPHI detector."
Supervisor: Professor Jan Królikowski
SINS December 20, 1994

6. **Krystyna KOCIĘCKA-MECHANISZ** "Influence of properties of two-gap triggered spark-gap on development of discharge in HV pulse generators circuits."
Supervisor: Professor Zbigniew Ciok
University of Technology, Warsaw, December 21, 1994

b. DSc Theses

1. **Daniela CHLEBOWSKA** "The coupling of collective and single particle degrees of freedom in atomic nuclei."
SINS March 22, 1994

2. **Zbigniew WŁODARCZYK** "Energy dependence of inelasiticity and attenuation of cosmic ray hadrons."
SINS September 22, 1994

3. **Helena BIAŁKOWSKA** "Particle production in relativistic heavy ion collisions."
SINS December 20, 1994

VIII. VISITORS, MEETINGS, WORKSHOPS

a. List of visitors to the Soltan Institute for Nuclear Studies

	Name	Institution, country	Period
1	Ertman G.	Galileo, Bologne, Italy	Jan.25
2	Wick B.	DESY, Hamburg, FRG	Jan.25-29
3 4	Fakir Jaman	Uniroyal Trading Co., Pakistan	Feb.15-18
5	Wiberg I.	SCANDITRONIX, Uppsala, Sweden	Feb.23-24
6	Bates P.	PALAT, UK	Feb.24
7	Szlachetko A.	Juni Export Polonia, UK	Feb.24
8	Katla J.	Strongbert, FRG	Feb.24
9 10 11	Teras J. Nuutinen M. Chorowski M.	CERNTECH, Finland	March 7
12 13	Verni R. Vicinanza F.	SEA, Rome, Italy	March 8-11
14	Fischer J.	Nucl. Phys. Inst., Rež, Czech Republic	March 21-29
15	Rudchik A.	Inst. for Nucl. Research, Kiev, Ukraine	March 21-23
16	Raman S.	Oak Ridge National Laboratory, USA	March 28-31
17	Petkov V.	Institute of Nucl. Research of the Russian Academy of Sciences, Moscow	April 14-May 3
18	Huang Qinghua Qu-Xianchao	Embassy of the Chinese People's Republic in Poland	April 26
19	Simssen R.	KVI, Groningen, Holland	May 9-10
20	Levinger J.	Rensselaer Polytech. Inst., Troy, NY, USA	May 11-15
21	Barut A.O.	Univ. of Colorado, USA	May 15-17 May 19-21
22	Gezolo P.	AGA, Sweden	May 17
23	Pankov A.	Inst. of Phys., Homel Politechnic, Byelorussia	May 22-29
24 25 26 27 28 29	Huang Qitao Huang Shouzeng Huang Qinghua Sun Wanhu Liu Lishan Qu Xianchao	State Science and Technology Commission of China, Beijing, chairman of the delegation member of the delegation -"- -"- -"- -"-	May 31
30 31	Spiney G. Polini M.	CERN, Geneva, Switzerland	June 8-10
32	Stöckmann G.	Comet, FRG	June 20-24
33 34	Apara T. Ertman G.	SEA, Roma, Italy Galileo, Bologne, Italy	June 28
35	Capdeville J.N.	Univ. of Bordeaux, France	Aug.16-29
36	Svärdling L.	SCANDITRONIX, Uppsala, Sweden	Aug.16-19
37	Kretschmer R.	Univ. of Siegen, FRG	Aug.22-23
38	Wolfendale A.W.	Univ. of Durham, UK	Sept.3-4
39 40	Lieder R. Utzelmann S.	FA Jülich, FRG	Sept.4-19
41 42	Prause B. Walpe J.C.	Univ. of Notre Dame, USA	Sept.4-19
43	Pat O'Brien	Ministry of Health, UK	Sept.6
44	Kalka H.	Techn. Univ. Dresden, FRG	Sept.19-22
45	Si-Ze Yang	Inst. of Phys., Bejing, Chinese People's Republic	Oct.4-18
46	Dahmen H.D.	Univ. of Siegen, FRG	Oct.15-23
47 48	Anderberg B. Lindberg S.	SCANDITRONIX, Uppsala, Sweden	Oct.17-18
49	Lipatov L.	Inst. for Nucl. Phys., St.Petersburg, Russia	Nov.7-9
50	Shulz D.	THIELLMAN, FRG	Nov.9
51 52 53	Rudchik A. Dirnak V. Mashkarov J.	Inst. for Nucl. Research, Kiev, Ukraine	Nov.14-17

54	Sakuta S.	Inst. of Nucl. Research of the Russian Academy of Sciences, Moscow	Nov.14-17
55	Ivanyuk F.A.	Inst. for Nucl. Research, Kiev, Ukraine	Nov.17-20
56	Petridou T.	Dept. of Th. Phys., Aristotle Univ. of Thessaloniki, Greece	Nov.18-24
57	Lynen U.	GSI Darmstadt, FRG	Nov. 21-23
58	Doebner M.D.	A.Sommerfeld Inst. for Mathem. Physics, TU Clausthal, FRG	Nov.26-29
59 60	Proh D. Sekutowicz J.	DESY, Hamburg, FRG	Nov.27-30
61 62	Kubes P. Kravarik J.	Technical University, Prague, Czech Republic	Dec.1-2
63	Choffel C.	Centre de Spectrometrie Nucleaire, Orsay, France	Dec.1-6
64 65	Ertman G. Greca L.	Galileo, Bologne, Italy	Dec. 1
66	Karwowski H.	Univ. of North Carolina, Chapel Hill, USA	Dec.7-8
67 68	Tsherniajev A. Sklayrow V.V.	Inst. of Nucl. Research of the Russian Academy of Sciences, Moscow	Dec.8-30
69	Shumeiko N.	High Energy Physics Centre Minsk, Byelorussia	Dec.15
70	Hernes E.	Univ. of Zürich, Switzerland	Dec.19-20

IX. OUR VISITS ABROAD

a. Long term visits of SINS staff memebers to foreign countries

	Name	Dept.	Institution, country	Period
1	Adamus M.	P-VI	DESY, Hamburg, FRG	Contract, July 1, 1991-June 30, 1994
2	Białkowski J.	P-III	PSI, Villigen, Switzerland	Contract, Nov.6, 1992-Oct.31, 1996
3	Bieńkowski A.	P-I	DESY, Hamburg, FRG	Contract, Nov.3, 1992-Nov.3, 1995
4	Bogdanowicz J.	P-IR	JINR, Dubna, Russia	Contract, Jan.1, 1991-Dec.31, 1995
5	Buda A.	P-II	KVI, Groningen, Holland	Fellowship, Dec.19, 1988-Sept.30, 1994
6	Dygo A.	P-I	Univ.of Western Ontario, London, Canada Univ.of Florida, Gainesville, USA	Fellowship, May 5, 1991-July 31, 1994 Fellowship, Aug.6, 1993-Aug.6, 1994
7	Hoszowska J.	P-II	Univ.of Fribourg, Switzerland	Fellowship, Oct.15, 1990-Oct.1, 1995
8	Kaczanowski J.	P-I	Ritsumeikan Univ., Kita-ku, Kyoto,Japan	Fellowship, May 1-Sept.30, 1994
9	Lenartowicz J.	P-I	DESY, Hamburg, FRG	Fellowship, Apr.21, 1990-Apr.23, 1994
10	Marciniewski P.	P-VI	Uppsala Univ., Sweden	Contract, Nov.5, 1993-Apr.30, 1994
11	Nassalski J.	P-VI	CERN, Geneva, Switzerland	Contract, June 1, 1994- May 31, 1995
12	Palacz M.	P-II	Manne Siegbahn Institute of Physics, Stockholm, Sweden	Fellowship, March 3, 1993-Feb.28, 1995
13	Pławski E.	P-X	CERN, Geneva, Switzerland	Contract, Sept.5, 1993-March 31, 1994
14	Pławski T.	P-II	DESY Hamburg, FRG	Contract, Sept.7, 1994-Sept.7, 1995
15	Polański A.	P-IV	JINR, Dubna, Russia	Contract, July 4, 1994-April 4, 1995
16	Sura J.	P-X	INFN, Catania, Italy	Contract, Sept.20, 1989-Sept.30, 1995
17	Szlachciak J.	P-III	IAEA, Vienna, Austria	Contract, Nov.29, 1993-Dec.31, 1995
18	Szymański P.	P-VI	Rutherford Appleton Laboratory, Chilton, UK	Contract, Nov.1, 1993-Oct.31, 1996
19	Trzciński A.	P-I	GSI, Darmstadt, FRG	Contract, Nov.7, 1993-April 7, 1994
20	Turos A.	P-I	Nat. Centre of Research and Devel. of Materials, Brindisi, Italy	Contract, June 1, 1993-May 31, 1994
21	Wiślicki W.	P-VI	CERN, Geneva, Switzerland	Contract, Aug.28-April 30, 1995

b. Short visits of SINS staff to foreign countries

	Name	Dept.	Institution, country	Period
1	Wiślicki W.	P-VI	Yale University, USA	Jan.2-11
2	Nassalski J.	P-VI	Yale University, USA	Jan.2-11
3	Mrówczyński S.	P-VI	Univ. Regensburg, FRG Hirschegg Workshop, Austria	Jan.8-23
4	Brzozowski K.	P-VI	CERN, Geneva, Switzerland	Jan.9-Feb.23
5	Wdowczyk J.	P-VII	Univ. of Durham, UK	Jan.9-Feb.5
6	Kwiatkowski S.	P-I	Univ. Bochum, FRG	Jan.9-15
7	Wysocka A.	P-X	German Cancer Research Center, Heidelberg, FRG	Jan.15- March 15
8	Kaczarowski R.	P-II	FA, Jülich, FRG	Jan.17-21
9	Sosnowski R.	P-VI	JINR, Dubna, Russia	Jan.17-20
10	Nassalski J.	P-VI	CERN, Geneva, Switzerland	Jan.20-27
11	Zalewski P.	P-VI	CERN, Geneva, Switzerland	Jan.20-29
12	Chłopik A.	P-III	CERN, Geneva, Switzerland	Jan.22-Feb.13
13	Gokieli R.	P-VI	CERN, Geneva, Switzerland	Jan.23-30
14	Filipkowski A.	P-VI	JINR, Dubna, Russia	Jan.24-31
15	Jakubowski L.	P-V	Kurchatov Institute, Moscow, Russia	Jan.30-Feb.5
16	Łukaszuk L.	P-VIII	Univ. of London, Birkbeck College, UK	Feb.1-28
17	Kuliński S.	P-X	Int. Conf. EPAC'94, Abbingdon, UK	Feb.2-6
18 19	Stepaniak J. Kupść A.	P-VI	Uppsala Univ., Sweden	Feb.3-24
20	Rondio E.	P-VI	Uppsala Univ., Sweden	Feb.3-14
21	Kaczarowski R.	P-II	Istituto Nazionale di Fisica Nucleare, Legnaro, Italy	Feb.12-19
22	Kuliński S.	P-X	National Lab. of Frascati, Italy	Feb.14-18
23	Szeptycka M.	P-VI	Technische Hochschule, Aachen, FRG	Feb.16-20
24	Nassalski J.	P-VI	CERN, Geneva, Switzerland	Feb.16-20
25	Szczekowski M.	P-VI	CERN, Geneva, Switzerland	Feb.16-March 2
26	Górski M.	P-VI	Technische Hochschule, Aachen, FRG	Feb.16-20
27	Sandacz A.	P-VI	CERN, Geneva, Switzerland	Feb.17-20
28	Zabierowski J.	P-VII	Uppsala Univ., Sweden	Feb.18-March 20
29	Pachan M.	P-X	Nat. Lab. of Frascati, Italy	Feb.19-23
30	Gokieli R.	P-VI	CERN, Geneva, Switzerland	Feb.20-March 11
31	Kozłowski T.	P-II	PSI, Villigen, Switzerland	Feb.21-March 25
32	Sujkowski Z.	P-II	KVI, Groningen, Holland	Feb.23-27
33 34	Żuprański P. Augustyniak W.	P-I	IPN, Orsay, France	Feb.27-March 13
35	Wycech S.	P-VIII	Technische Univ., Munich, FRG	Feb.27-March 6
36	Rondio E.	P-VI	Free University, Amsterdam, Holland	Feb.28-March 21
37	Wiślicki W.	P-VI	CERN, Geneva, Switzerland	Feb.28- March 27
38	Mrówczyński S.	P-VI	Duke Univ., Durham, USA	March 1- April 30
39	Górski M.	P-VI	CMS Trigger Meeting, Bad Aussee, Austria	March 2-6
40	Iskra W.	P-I	FZ, Rossendorf, FRG	March 3-June 3
41	Nawrot A.	P-VI	Uppsala Univ., Sweden	March 4-31
42	Nassalski J.	P-VI	Osaka Univ., Japan	March 5-14
43	Szymanowski L.	P-VIII	Univ. Leipzig, FRG	March 7-19
44 45	Czyżewski T. Szydłowski A.	P-I P-V	Univ. Bochum, FRG	March 9-14
46	Trechciński R.	PNJ	ESONE Executive Committee Meeting, Zurich, Switzerland	March 10-13
47	Sosnowski R.	P-VI	CERN, Geneva, Switzerland	March 16-20
48	Sandacz A.	P-VI	Free University, Amsterdam, Holland	March 16-23
49	Szleper M.	P-VI	Inst. for High Energy Phys., Amsterdam, Holland	March 16-18

50 51 52	Langner J. Jankowicz Z. Bielik M.	P-V	Research Inst. of Electrophys. App., St.Petersburg, Russia	March 19-26
53	Rusek K.	P-I	Univ. of Birmingham, UK	March 21-April 14
54	Nassalski J.	P-VI	CERN, Geneva, Switzerland	March 28-31
55	Szleper M.	P-VI	Max Planck Inst. of Physics, Heidelberg, FRG	March 31-April 20
56	Wilk G.	P-VIII	Philipps Univ. Marburg, FRG	April 1-July 30
57	Zwięgliński B.	P-I	GSI, Darmstadt, FRG	April 4- May 1
58	Wiślicki W.	P-VI	CERN, Geneva, Switzerland	April 5-30
59	Marszał T.	P-VI	CERN, Geneva, Switzerland	April 6- May 18
60	Sosnowski P.	P-VI	CERN, Geneva, Switzerland	April 11-17
61	Rymuza P.	P-II	PSI, Villigen Switzerland GSI, Darmstadt, FRG	April 14-30
62	Ludziejewski T.	P-II	PSI, Villigen, Switzerland	April 14-25
63	Szeptycka M.	P-VI	CERN, Geneva, Switzerland	April 16-20
64	Tropiło J.	P-I	Milan Univ., Italy	April 17- July 10
65	Sujkowski Z.	P-II	PSI, Villigen, Switzerland GSI, Darmstadt, FRG	April 19-28
66	Zalewski P.	P-VI	Int. Conf."BEAUTY 94", Mont St.Michel, France	April 22-30
67	Wincel K.	P-IV	"8th Int. Conf. on Radiation Shielding", Arlington, USA	April 23-29
68	Sandacz A.	P-VI	Nat. Inst. of Nuclear Physics, Turin, Italy	April 27- June 29
69	Górski M.	P-VI	CERN, Geneva, Switzerland	May 1-18
70	Deloff A.	P-VI	Univ. of Surrey, UK	May 2- July 15
71 72	Górski M. Kuczyński J.	ZDAJ	Erkrath Hospital, FRG	May 3-4
73	Szeptycka M.	P-VI	CERN, Geneva, Switzerland	May 4-11
74	Wiślicki W.	P-VI	Inst. for High Energy Phys., Amsterdam, Holland	May 5- June 6
75	Marcinkowski A.	P-I	Int. Conf. on Nuclear Data for Science and Technology, Gatlinburg, USA	May 7-14
76	Rondio E.	P-VI	CERN, Geneva, Switzerland	May 7-20
77	Wycech S.	P-VIII	Uppsala Univ., Sweden	May 9- June 9
78	Pracz J.	ZDAJ	SEA, IRVIN, Italy	May 9-11
79 80	Jankowski J. Golla P.	ZDAJ	Ministry of Health, Moscow, Russia	May 11-13
81	Sobiczewski A.	P-VIII	GSI, Darmstadt, FRG	May 12- July 12
82	Pławski T.	P-II	Int. Conf. "Environnement", Paris, France	May 15-21
83	Duda-Głowacka L.	P-I	Int. Conf. on Nucl. Spectr. and Nucl. Structure, St.Petersburg, Russia	May 16-21
84	Sosnowski R.	P-VI	CERN, Geneva, Switzerland	May 18- July 1
85	Roś Z.	P-VI	CERN, Geneva, Switzerland	May 18- July 18
86	Jaskóła M.	NB	Milan Univ., Italy	May 18- July 10
87	Zabierowski J.	P-VII	NRC, Karlsruhe, FRG	May 23- June 22
88	Szymanowski L.	P-VIII	Univ. Leipzig, FRG	May 24- June 3
89	Chłopik A.	P-III	CERN, Geneva, Switzerland	May 25- June 24
90	Kaczarowski R.	P-II	Univ. of Notre Dame, USA, ANL Argonne, USA	May 26- June 25
91	Zwięgliński B.	P-I	5th Int. Conf. on Nucleus-Nucleus Collisions, Taormina, Italy	May 28- June 4
92	Wilczyński J.	P-II	5th Int. Conf. on Nucleus-Nucleus Collisions, Taormina, Italy	May 29- June 18
93	Skalski J.	P-VIII	LBL, Berkeley, USA	May 29- June 18
94	Błocki J.	P-II	LBL, Berkeley, USA	May 29- June 19
95	Rondio E.	P-VI	5th Conf. on the Intersections of Particle and Nucl. Phys., Saint Petersburg, USA	May 30- June 7
96 97	Chmielewska D. Sujkowski Z.	P-II	Inst. Ruder Boskovic, Zagreb, Croatia 7th Conf. on Nucl. Reaction Mechanisms, Varenna, Italy Int. Conf. on Interacting Boson Model, Padova, Italy ENEA Bologne, Italy	May 30- June 21
98	Szczekowski M.	P-VI	CERN, Geneva, Switzerland	June 3-26
99	Mysłek-Laurikainen B.	P-II	Conf."Radioecology of Peatlands", St.Petersburg, Russia	June 6-11
100	Sadowski M.	P-V	Inst. of Plasma Research, Stuttgart, FRG	June 6- July 2

101	Infeld E.	P-VIII	5th Int. Conf. on Hyperbolic Problems Theory, Stony Brook, Clarkson Univ., Potsdam, USA	June 8-30
102	Wdowczyk J.	P-VII	NRC, Karlsruhe, FRG	June 9-19
103	Gokieli R.	P-VI	CERN, Geneva, Switzerland	June 12-18
104	Rondio E.	P-VI	CERN, Geneva, Switzerland	June 13-29
105 106 107	Kotulski L. Golla P. Pracz J.	ZDAJ	SEA, Aprilia, Italy	June 14-16
108	Sosnowski R.	P-VI	CERN, Geneva, Switzerland	June 19-26
109	Szeptycka M.	P-VI	CERN, Geneva, Switzerland	June 20- July 15
110	Kupść A.	P-VI	Uppsala Univ., Sweden	June 20-July 27
111	Stepaniak J.	P-VI	Uppsala Univ., Sweden	June 20-July 16
112	Jaskóła M.	NB	Meeting on Polish-German Collaboration Berlin, FRG	June 20-23
113	Szabelski J.	P-VII	Inst. for Nuclear Research of the Russian Academy of Sciences, Moscow, Russia	June 20-July 11
114	Nawrot A.	P-VI	Uppsala Univ., Sweden	June 20-23
115	Szleper M.	P-VI	CERN, Geneva, Switzerland	June 22- July 21
116	Baranowski J.	P-V	21st Int. Conf. FUSION'94, Montpellier, France	June 23- July 1
117	Wdowczyk J.	P-VII	Inst. for Nuclear Research of the Russian Academy of Sciences, Moscow, Russia	June 25- July 2
118 119 120 121 122	Drabik W. Kuliński S. Lorkiewicz J. Pachan M. Pszona J.	P-X	Int. Conf. EPAC'94, London, UK	June 26-July 3
123 124 125	Trechciński R. Charuba J. Guzik Z.	P-NJ P-III P-III	JINR, Dubna, Russia	June 26- July 3
126 127	Pracz J. Kazimierski A.	ZDAJ	SEA, Roma, Italy	June 30- July 3
128	Marciniewski P.	P-VI	Inst. for High Energy Phys., Amsterdam, Holland	July 1-30
129	Górski M.	P-VI	CERN, Geneva, Switzerland	July 3-I
130	Dąbrowski J.	P-VIII	Conf. on Hypernuclear and Strange Particle Physics, Vancouver, Canada	July 3-10
131	Boguszyński J.	P-VIII	Int. School of Subnuclear Physics, Erice, Italy	July 3-11
132	Marszał T.	P-VI	CERN, Geneva, Switzerland	July 4- Aug. 3
133	Wdowczyk J.	P-VII	Univ. of Durham, UK	July 10-24
134 135	Augustyniak W. Żuprański P.	P-I	LNS, Saclay, France	July 10-30
136	Zalewski P.	P-VI	CERN, Geneva, Switzerland	July 17-Aug.7
137	Białkowska H.	P-VI	CERN, Geneva, Switzerland	July 18-24
138 139	Szczekowski M. Sosnowski R.	P-VI	27th Conf. on High Energy Physics, Glasgow, UK	July 19-28
140	Sandacz A.	P-VI	27th Conf. on High Energy Physics, Glasgow, UK	July 20-28
141	Infeld E.	P-VIII	Int. Symp. "STAMM 94" Lisbon, Portugal	July 23-30
142	Wilczyński J.	P-II	KVI, Groningen, Holland	July 28-Aug.26
143	Gokieli R.	P-VI	CERN, Geneva, Switzerland	July 29-Aug.29
144	Sandacz A.	P-VI	CERN, Geneva, Switzerland	July 31- Sept. 4
145	Sosnowski R.	P-VI	CERN, Geneva, Switzerland	July 31- Aug. 16
146	Zychor I.	P-X	FA, Jülich, FRG	Aug.1-Sept.1
147 148	Łukaszuk L. Boguszyński J.	P-VIII	Univ. Siegen, FRG	Aug.1-21
149	Rondio E.	P-VI	Max Planck Inst., Heidelberg, FRG	Aug.2-9
150	Marcinkowski A.	P-I	Oxford Univ., UK	Aug.7-18
151	Wycech S.	P-VIII	CERN, Geneva, Switzerland	Aug.19-30
152	Moszyński M.	P-III	Inst. of Physics, Cologne, FRG	Aug.20-25
153	Kupść A.	P-VI	Aachen Univ., FRG	Aug.20-25
154	Rondio E.	P-VI	CERN, Geneva, Switzerland	Aug.21-Sept.7
155 156	Pracz J. Golla P.	ZDAJ	SIMENS, Leipzig, FRG	Aug.22-23
157	Szydłowski A.	P-V	JINR, Dubna, Russia	Aug.23-29
158	Sobiczewski A.	P-VIII	Symposium on Nuclear Physics II, Tours, France	Aug.27-Sept.2

159	Szabelski J.	P-VII	14th European Cosmic Rays Symp., Balatonfured, Hungary	Aug.27-Sept.3
160	Wiślicki W.	P-VI	CERN, Geneva, Switzerland	Aug.28-Dec.12
161	Błocki J.	P-II	Inst. for Nuclear Research, Kiev, Ukraine	Aug.28-Sept.5
162	Sujkowski Z.	P-II	SELMA'94-New Nuclear Structure Phenomena in the Vicinity of Closed Shells, Stockholm-Uppsala, Sweden	Aug.29-Sept.4
163	Rusek K.	P-I	Int. Conf. Cluster'94, Strasbourg, France Philipps Univ., Marburg, FRG	Sept.1-10
164	Rączka R.	P-VIII	The Academy of Sciences, Prague, Czech Republic	Sept.1-4
165	Sobiczewski A.	P-VIII	Inst. for Nuclear Research, Kiev, Ukraine	Sept.2-9
166	Kulczycka E.	P-II	Univ. of Leuven, Belgium	Sept.3-9
167	Wycech S.	P-VIII	Oxford Univ., UK	Sept.4-17
168	Mrówczyński S.	P-VI	CNRS, Nantes, France	Sept.5-10
169	Szymanowski L.	P-VIII	Univ. Siegen, FRG	Sept.5-Oct.10
170	Rączka R.	P-VIII	ISAS, Triest, Italy	Sept.8-Nov.7
171	Gokieli R.	P-VI	CERN, Geneva, Switzerland	Sept.10-16
172	Nawrot A.	P-VI	Uppsala Univ. Sweden	Sept.12-Oct.7
173 174	Nadachowski M. Charuba J.	P-III	XVI Int. Symp. on Nucl. Electronics, Varna, Bulgaria	Sept.12-21
175	Nowicki L.	P-I	LAL, Orsay, France	Sept.14-Oct.14
176	Żuprański P.	P-I	8th Int. Symp. on Polarization in Nucl. Phys. "SPIN 94" Bloomington, USA	Sept.15-23
177	Szabelski J.	P-VII	Univ. Perpignan, France	Sept.15-Dec.12
178	Sandacz A.	P-VI	CERN, Geneva, Switzerland	Sept.17-Oct.6
179	Moszyński M.	P-III	EUROBALL Users Meeting, Strasbourg, France	Sept.17-22
180	Rymuza P.	P-II	Conf. HCI'94, Vienna, Austria GSI, Darmstadt, FRG	Sept.18-28
181	Wincel K.	P-IV	Inst. on Phys. and Power Engineering, Obninsk, Russia	Sept.19-25
182 183	Jankowski J. Pracz P.	ZDAJ	Conf. ESTRO, Granada, Spain	Sept.23-27
184 185	Zwięgliński B. Trzciński A.	P-I	FZ, Rossendorf, FRG ALADIN Collasonetion Meeting	Sept.24-29
186	Iskra W.	P-I	FZ, Rossendorf, FRG	Sept.25-Dec.23
187	Szczekowski M.	P-VI	CERN, Geneva, Switzerland	Sept.25-Oct.12
188	Pszona S.	P-IV	Univ. of Technology, Dresden, FRG	Sept.25-30
189	Trechciński R.	P-NJ	ISO/IEC Meeting, Stockholm, Sweden	Sept.26-Oct.2
190 191	Szczeblewski F. Charczuk M.	ZDAJ	Inst. of Oncology, Budapest, Hungary	Sept.26-30
192	Sosnowski R.	P-VI	CERN, Geneva, Switzerland	Sept.28-Oct.2
193	Rondio E.	P-VI	CERN, Geneva, Switzerland	Sept.29-Oct.26
194	Jaskóła M.	NB	Erlangen-Nürnberg Univ., FRG Univ. of Basel, Switzerland	Sept.30-Oct.14
195	Duda-Głowacka L.	P-I	Erlangen-Nürnberg Univ., FRG	Sept.30-Oct.10
196	Chłopik A.	P-III	CERN, Geneva, Switzerland	Sept.30-Nov.8
197	Boguszyński J.	P-VIII	ICTP, Triest, Italy	Oct.1-13
198	Pszona S.	P-IV	Conf."Advances in Radiation Measurements", Chalk River, Canada	Oct.2-15
199	Mrówczyński St.	P-VI	Workshop on Parton Production in the Quark-Gluon Plasma, Trento, Italy	Oct.2-15
200	Wasilewski A.	P-VII	College de France, Paris, France	Oct.8-15
201	Wdowczyk J.	P-VII	College de France, Paris, France	Oct.9-18
202	Szleper M.	P-VI	CERN, Geneva, Switzerland, Max Planck Inst., Heidelberg, FRG	Oct.9-Nov.11
203	Sadowski M.	P-V	Inst. of Physics and Technology, Bucharest, Romania	Oct.10-15
204	Skalski J.	P-VIII	University of Brussells, Belgium	Oct.11-Nov.10
205	Wysocka A.	P-X	Inst. Gustave Roussy, Villejuif, France	Oct.11-Nov.4
206	Kuliński S.	P-X	Univ. Autonomia de Barcelona, Spain	Oct.14-17
207	Gokieli R.	P-VI	CERN, Geneva, Switzerland	Oct.16-23
208	Zabierowski J.	P-VII	NRC, Karlsruhe, FRG	Oct.17-Nov.15
209	Kaczarowski R.	P-II	Univ. of Notre Dame, USA, ANL Argonne, USA	Oct.18-31
210	Patyk Z.	P-VIII	GSI, Darmstadt, FRG	Oct.20-Dec.20

211	Sobiczewski A.	P-VIII	GSI, Darmstadt, FRG	Oct.27-Dec.12
212	Jakubowski L.	P-V	Conf. on Plasma Physics, Iquacu, Brasil Univ. of Buenos Aires, Argentina	Oct.28-Nov.25
213	Pachan M.	P-X	Meeting of Intern. Consulting Group for Food Irrad, Denpasar, Indonesia	Oct.29-Nov.6
214	Moszyński M.	P-III	Nucl. Science Symp. and Medical Imaging Conf., Norfolk, USA	Oct.29-Nov.6
215	Wycech S.	P-VIII	Inst. of Theoretical Physics, Helsinki, Finland	Oct.30-Nov.30
216	Pszona S.	P-IV	INFN Legnaro, Italy	Oct.31-Nov.6
217	Rymuza P.	P-II	PSI, Villigen, Switzerland	Nov.1-8
218	Kulka Z.	P-III	Inst. für Hochenergiephysik, Vienna, Austria	Nov.1-Dec.2
219	Sujkowski Z.	P-II	PSI, Villigen, Switzerland	Nov.2-8
220	Jaskóła M.	NB	Milan Univ., Italy	Nov.2-30
221	Marciniewski P.	P-VI	Uppsala Univ., Sweden	Nov.4-Dec.3
222	Gryziński M.	P-V	Texas Christian Univ. Denton, Southern California Univ. Los Angeles, Harvard Univ. Boston, USA	Nov.6-27
223	Nawrot A.	P-VI	Uppsala Univ., Sweden	Nov.7-Dec.14
224	Żupranski P.	P-I	LNS, Saclay, France	Nov.7-18
225 226	Kulczycka E. Preibisz Z.	P-II	CERN, Geneva, Switzerland	Nov.7-13
227	Zalewski P.	P-VI	CERN, Geneva, Switzerland	Nov.8-15
228	Tucholski A.	P-II	GANIL, Caen, France	Nov.10-Dec.15
229	Kaczarowski R.	P-II	FA, Jülich, RFG	Nov.11-Dec.13
230	Rondio E.	P-VI	Univ. Trieste, Italy	Nov.11-17
231	Sosnowski R.	P-VI	DESY, Hamburg, FRG	Nov.12-18
232	Sandacz A.	P-VI	Univ. Trieste, Italy	Nov.12-16
233 234	Moszyński M. Wolski D.	P-III	Hahn-Meitner-Institute, Berlin, FRG	Nov.14-20
235 236	Pracz J. Kazimierski A.	ZDAJ	SEA, Rome, Italy	Nov.14-16
237	Zychor J.	P-X	FA, Jülich, FRG	Nov.15-Dec.16
238	Siemiarczuk T.	P-VI	CERN, Geneva, Switzerland	Nov.16-Dec.1
239	Trechciński R.	P-NJ	Inst. for High Energy Phys., ESONE, Amsterdam, Holland	Nov.17-20
240 241	Sadowski M. Langner J.	P-V	Technical Univ., Prague, Czech Republic	Nov.20-23
242	Stepaniak J.	P-VI	Uppsala Univ., Sweden	Nov.20-30
243	Zabierowski J.	P-VII	Uppsala Univ., Sweden	Nov.21- Dec.18
244	Turos A.	P-I	NRC, Karlsruhe, FRG	Nov.22- Dec.21
245	Karpio K.	P-VI	CERN, Geneva, Switzerland	Nov.24- Dec.10
246	Sandacz A.	P-VI	DESY, Hamburg, FRG	Nov.26-30
247	Kozłowski T.	P-II	PSI, Villigen, Switzerland	Nov.28- Dec.24
248	Marcinkowski A.	P-I	Oxford Univ., UK	Nov.27-Dec.4
249	Szczekowski M.	P-VI	CERN, Geneva, Switzerland	Nov.27- Dec.14
250	Szymanowski L.	P-VIII	Univ. Siegen, FRG	Nov.27- Dec.24
251 252	Gokieli R. Górski M.	P-VI	CERN, Geneva, Switzerland	Nov.30- Dec.10
253 254	Sadowski M. Jakubowski L.	P-V	Kurchatov Institute Moscow, Russia	Dec.3-7 Dec.4-17
255	Rondio E.	P-VI	Uppsala Univ., Sweden	Dec.3-18
256	Sandacz A.	P-VI	INFN, Turin, Italy	Dec.4-18
257	Mrówczyński St.	P-VI	Univ. Regensburg, FRG	Dec.4-10
258	Ratyński W.	DN	ORNL, Oak Ridge, USA	Dec.4-16
259	Sujkowski Z.	P-II	GANIL, Caen, France KVI, Groningen, Holland	Dec.5-17

X. OBITUARY

BRONISŁAW BURAS (1915-1994)

Bronisław Buras was born in Warsaw in 1915. He completed his studies at the Physics Faculty of the Warsaw University and at the Lvov University where he graduated in 1940. His diploma was confirmed in 1948 at the Warsaw University. In the period 1941-45 (Nazi occupation) he worked occasionally in Warsaw.

In 1945 Bronisław Buras started his work as a senior assistant at the Institute of Experimental Physics of the Warsaw University and continued his academic carrier as assistant professor and associate professor. In the period 1953-66 Prof. B.Buras was a senior scientist at the Solid State Physics Chair of the Institute of Experimental Physics, Warsaw University, where in 1965 he became head of the Neutron Spectroscopy Division. In 1966 this division was transformed into the Chair of Nuclear Methods in Solid State Physics and Prof. B.Buras headed it till September 30, 1969.

At that time Prof. B.Buras was working on the applications of nuclear methods, mainly neutron scatering, in solid state physics. In 1961 he employed me as assistant in his group at Warsaw University. Our collaboration lasted till his departure from Poland. In 1967 I defended my Ph.D. thesis executed under Prof. B.Buras' supervision. Our collaboration concerned mostly the time-of-flight method for determination of the crystal structure developed by B.Buras.

In the fifties Prof. B.Buras was one of the organizers of the Institute of Nuclear Research and the Center of Nuclear Research at Świerk, where he was the head of the Nuclear Physics Department (IB). Professor's activity at Świerk concerned the use of the new EWA reactor in solid state physics. This work was performed in cooperation with the Warsaw University group. This cooperation lasted till 1968.

The later events have been described by Professor Jerzy Pniewski, Director of the Institute of Experimental Physics, and Dean of the Physics Faculty at the Warsaw University, in his Autobiographic Recollections:

"The brutal overnight dismissal of Professor Buras from the Institute of Nuclear Research and prohibition of his entry to the premises of the nuclear laboratories in Świerk and the reactor facilities in particular was a blow for his Chair at the Warsaw University and of course for Buras himself. We know now very well the mechanisms and aims of the initators of the Polish "cultural revolution" of that period but it was particularly unjust that one of the creators of the Institute of Nuclear Research a person involved in the construction of the reactor and the initiator of one, of the most important research activities in the Institute was treated in this way. (In April'69 the Physics Faculty Council initiated unanimously the procedure of awarding him the title of ordinary professor. Added by I.S.). In spite of friendly care extended to him at the University, being deprived of his main experimental tool, he decided to emigrate from Poland and settle down in Denmark. There he became immediately involved in research in the Nuclear Research Facility in Risö, (and the H.C.Oersted Institute, University of Copenhagen. Added by I.S.) and for many years after represented Denmark in the scientific community".

Professor B.Buras was the author of many papers on solid state physics. They mainly concerned nuclear methods (neutron scattering, the Mössbauer effect, radiation damage) and synchrotron radiation applications in condensed matter physics. He was the author of many monographs and co-author of physics textbooks for secondary schools. Professor Buras was the teacher of many generations of students and supervised many Ph.D. theses. He was active in many international organizations such as International Atomic Energy Agency and participated in international projects such as the European Center of Synchrotron Radiation in Grenoble.

Professor Bronisław Buras was a well known scientist, eminent science organizer, distinguished academic teacher and the Nestor of polish neutronography. He died in Denmark on November 22, 1994.

Izabela Sosnowska

Institute of Experimental Physics
Warsaw University

XI. AUTHOR INDEX